DSPACE

https://dspace.org/

Post-Transvaal deformation between the Johannesburg dome and the Bushveld complex

Courtnage, Paul, Michael

1995
https://hdl.handle.net/10539/24288

Downloaded from a DSpace repository. https://dspace.org/

POST-TRANSVAAL DEFORMATION BETWEEN THE JOHANNESBURG DOME AND THE BUSHVELD COMPLEX

Paul Michael Courtnage

Degree awarded with distinction on 23 May 1996.

A dissertation submitted to the Faculty of Science, University of the Witwatersrand, for the degree of Master of Science.

Johannesburg 1995

ABSTRACT

The study of an area north of the Johannesburg Dome has revealed that the rocks of the Transvaal Supergroup have been affected by widespread deformation, as well as metamorphism to the greenschist facies. Thermal modelling suggests that the metamorphism, and hence porphyroblast growth, can probably be attributed to the thermal effects of the Bushveld Complex. Thus, textural relationships between porphyroblasts and cleavage microstructure in slates could be utilized to establish the relative timing of ductile deformation events in the area.

The earliest recognisable deformation event (D_1) produced a southerly-verging cleavage (S_1). Porphyroblast-cleavage textural relationships suggest a pre- to syn-Bushveld Complex origin for S_1. D_1 has, however, not been widely observed in the study area, and may have been heterogeneously developed. The most intense and widespread of the deformation events, the D_2 event, resulted in northerly-verging structures, which include a gently southerly-dipping cleavage (S_2), bedding sub-parallel shear zones, open to tight folds and lineations (L_2). Textural relationships between the S_2 cleavage and porphyroblasts suggest that the D_2 deformation occurred in syn- to post-Bushveld Complex times. The S_2 cleavage also shows microstructural overprinting relationships with S_1. This northerly-verging deformation (D_2) has been attributed to the emplacement of the Vredefort Dome at approximately 2025 Ma.

Pre-Bushveld Complex sills and D_2 bedding sub-parallel shear zones have been deformed by southerly-verging round-hinged folds and associated steep reverse shears in the dolomite successions of the Chuniespoort Group, whereas S_2 cleavage has been deformed by upright kink folds in the Pretoria Group slate units. This deformation (D_3) is attributed to post-Vredefort Dome subsidence of the Bushveld Complex. The northerly tilt of strata may have been contributed to by uplift of the Johannesburg Dome.

North-northeast and north-northwest trending strike-slip faults (D_4) truncate and displace earlier structures. These faults offset a syenite dyke of Pilanesberg origin, which constrains their age, or their latest reactivation, to post-Pilanesberg times.

Other ductile deformation events, in the form of east- and west-verging structures, deform D_2 bedding sub-parallel shear zones. Their exact timing with respect to the remainder of the deformation events could not, however, be accurately determined, as they are minor and extremely localised. Nonetheless, the possibility exists that the easterly-verging structures owe their origin to the approximately 1,9 Ga Kheis orogeny, whereas the westerly-verging structures may have been the result of subsidence of the Cullinan-Middelburg basin in Waterberg times.

Brittle deformation in the study area is expressed as joint sets in the dolomite and slate lithologies, as well as fractures in tufa and Recent unconsolidated soils. East-west trending tufa fractures, deformed soil, and a similarly trending joint set in slate may have a common origin, related to down-to-the-north normal faulting during the Holocene.

DECLARATION

This dissertation is my own unaided work, conducted under the supervision of Drs. R.L. Gibson and E.G. Charlesworth. It is being submitted for the degree of Master of Science at the University of the Witwatersrand, and has not previously been submitted for any degree or examination at any other University.

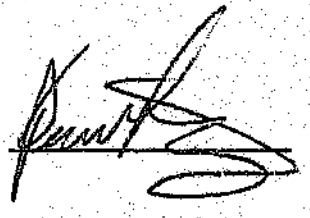

Paul M. Courtnage

15/12/1995

ACKNOWLEDGEMENTS

I would like to thank my supervisors, Drs. R.L. Gibson and E.G. Charlesworth, for their patient guidance during this research. Dr. M.A.G. Andreoli contributed to this work with discussion and advice. Ms S. Hall and Messrs. A. Mathebula and C. Mdakane are thanked for technical support. Financial support was provided in part by the Atomic Energy Corporation, the University of the Witwatersrand, and the F.R.D. core programme.

Thanks to Helen Duigan, Linda Koch and Cmdt. Kotze for organising and supplying accommodation during my field work.

Special thanks to my parents, Mike and Yvonne Courtnage, for their consistent and unquestioning support.

List of Figures

Fig. 1.1 Regional geological map of the northern Kaapvaal Craton showing the study area relative to the positions of major geological features. After S.A.C.S. (1980) and Walraven *et al.* (1990). Inset shows the position of the Kaapvaal Craton relative to the surrounding mobile belts and the Zimbabwe Craton.

Fig. 1.2 Generalised stratigraphic column for the Transvaal Supergroup. From S.A.C.S. (1980).

Fig. 2.1 Stratigraphic column of the Malmani Subgroup, Chuniespoort Group, northwest of Johannesburg in the vicinity the study area (after Eriksson and Truswell, 1973).

Fig. 2.2 Stromatolite dome developed in the Chuniespoort Group. Locality (2862,1 X; -96,8Y) (see Appendix 1 for explanation of the co-ordinate system). Looking west.

Fig. 2.3 Chert breccia with slaty matrix (SCB). Note the angularity of the clasts, their large variation in size, as well as their irregular distribution. Locality (2861,6 X;-95,0Y).

Fig. 2.4 Fountains Formation chert breccia situated on top of the Schurweberg hills. Locality (2859,0 X; -93,1 Y).

Fig. 2.5 The unconformable relationship of the Fountains Formation chert breccia with the Hennops River Formation dolomite. Locality (2857,4 X; -93,0 Y). Looking west.

Fig. 2.6 Botryoidal masses of tufa. Locality (2857,6 X; -91,8 Y).

Fig. 2.7 Tufa enclosing fragments of slate and quartzite, closely resembling conglomerate or breccia. Locality (2857,6 X; -91,8 Y).

Fig. 3.1 Photomicrograph showing north-dipping S_1, oriented oblique to bedding (S_o), being crenulated by the south-dipping S_2 cleavage. Locality 20 km west of Magaliesburg along the R509. Scale bar 0,5 mm.

Fig. 3.2 Equal area (Schmidt) net of the orientation of poles to S_2 cleavage planes (n=70) in slate units.

Fig. 3.3 Micro-scale refraction of S_2 cleavage in a sectioned slate sample. Locality (2855,1X; -92,7 Y). Scale bar 0,5mm.

Fig. 3.4 North-verging D_2 round-hinged folds in the Black Reef Quartzite Formation. Looking east. Locality (2863,1 X; -97,1 Y).

Fig. 3.5 North-verging D_2 round-hinged folds in the lower strata of the Chuniespoort Group. Looking east. Locality (2863,0 X; -95,0 Y).

Fig. 3.6 Equal area (Schmidt) stereographic representation of D_2 round-hinged folds in the Black Reef Quartzite Formation (BRQF) and the Chuniespoort Group.

Fig. 3.7 North-verging D_2 chevron folds in a slate unit of the Black Reef Quartzite Formation. Looking east. Locality (2862,8 X; -97,4 Y).

Fig. 3.8 Equal area (Schmidt) stereonet representation of the D_2 chevron folds in the Black Reef Quartzite Formation. Locality (2862,8 X; -97,4 Y).

Fig. 3.9 Monoclinal structure with steep limb developed in the Pretoria Group. Locality (2854,7 X; -91,6 Y). Looking west.

Fig. 3.10 Small-scale disharmonic recumbent folds verging northwards in a bedding sub-parallel shear zone hosted in Chuniespoort Group dolomite. Looking east. Locality (2861,7 X; -95,1 Y).

Fig. 3.11 North-verging, isoclinal, recumbently folded quartz vein in a bedding sub-parallel shear zone in Pretoria Group slate. Looking west. Locality (@857 X; -95,8 Y).

Fig. 3.12 Equal area stereonet plot of the orientations of fold hinges (n=26) and axial planes (n=15) hosted in bedding sub-parallel shear zones throughout the sequence studied. Note the consistent fold vergence, as shown by the grouping of axial plane plots.

Fig. 3.13 Micro-folded quartz vein with fold axial plane sub-parallel to S_2 cleavage in a slate horizon near the base of the Chuniespoort Group. Locality (2862,9 X; -96,8 Y). Scale bar 0,5mm.

Fig. 3.14 S-C structures (a), small-scale duplexes (b) and asymmetric disharmonic folds (c) developed in a bedding sub-parallel shear zone in the Chuniespoort Group. The orientation of the S-C structure together with northward-verging folds developed within the shear zone confirm top-to-the-north shear sense. Locality (2861,0 X; -94,5 Y). Looking west.

Fig. 3.15 Deformed ooids a) above and b) below a D_2 bedding sub-parallel shear zone in the Chuniespoort Group as a result of north-verging shear. Looking east. Locality (2861,7 X; -95,1 Y).

Fig. 3.16 Large-scale σ clast of chert showing top-to-the-north shear sense within a bedding sub-parallel shear zone in Chuniespoort Group dolomite. Locality (2861,8 X;-96,9Y). Looking west.

Fig. 3.17. Oxidised porphyroblast (arrowed) which grew pre- to syn- S_2 deformation. Sample from a slate horizon in the Chuniespoort Group. Locality (2863,2 X; -96,4 Y). Scale bar 0,5 mm

Fig. 3.18 Northerly verging micro-thrust system developed in a predominantly quartz layer. Scale bar 0,5 mm. Locality (2857,2 X; -92,5 Y).

Fig. 3.19 Flinn graph with the plots of *k-values* for deformed ooids adjacent to a bedding sub-parallel shear zone in the Chuniespoort Group.

Fig. 3.20 Quartz rodding lineations developed on thin chert laminae in the dolomite strata. Locality (2862,7 X; -95,9 Y). Looking north.

Fig. 3.21 Curved quartz rodding lineations on sub-horizontal bedding surface in the Chuniespoort Group. Pencil is pointing north. Locality (2856,2 X; -93,5Y).

Fig. 3.22 Equal area (Schmidt) stereonet representation of the orientations of quartz rodding lineations (n=67) developed outside the bedding sub-parallel shear zones.

Fig. 3.23 a) Photograph showing a stepped lineated surface over a small stromatolite dome. b) Cross-section from A-B showing top-to-the north sense of shear.

Fig. 3.24 Two sets of crenulation lineations detectable in slate horizons at the Magaliesberg locality. Looking down. South is to the top of the photograph.

Fig. 3.25 Extreme flattening of ooids, corresponding to the orientation of the south-dipping S_2 cleavage. Locality adjacent to a D_1 bedding sub-parallel shear zone in the Chuniespoort Group dolomite. Locality (2862,0 X; -95,0 Y). Looking west.

Fig. 3.26 Highly localised deformation of ooids. The strained ooids define a fabric oriented 335°\50° NE. Looking northwest. Locality (2861,4 X; -94,3 Y).Fig. 3.27 Large-scale D_3 folding in the Chuniespoort dolomite. Looking north. Locality (2860,8 X; -95,2 Y).

Fig. 3.27 Large-scale D_3 folding in the Chuniespoort dolomite. Looking north. Locality (2860,8 X; -95,2 Y).

Fig. 3.28 Orientation of D_3 fold axes (n=18) and axial planar cleavage (n=4).

Fig. 3.29 Secondary fold in dolomite and chert layers associated with the D_3 folding event in the Chuniespoort Group. Looking east. Locality (2861,2 X; -95,6 Y).

Fig. 3.30 Large-scale kink fold in Pretoria Group shales. Locality (2856,9 X; -94,5 Y). Looking southeast.

Fig. 3.31 Equal area stereonet plot of the poles to D_3 kink fold axial planes (n=25) in the Pretoria Group.

Fig. 3.32 Schematic representation (A) and stereonet (B) demonstrating how S_2 cleavage retains a constant angular relationship with bedding during kink folding.

Fig. 3.33 Equal area (Schmidt) stereonet showing rotation of S_2 cleavage and bedding in a kink fold to their original orientations. Dashed line indicates the field of S_2 poles in Fig. 3.2.

Fig. 3.34 Round-hinged fold in intercalated slate and quartzite layers in the Pretoria Group. Locality (2854,8 X; -95,1 Y). View to the west.

Fig. 3.35 Stereonet plot of the hinges of D_3 round-hinged folds (n=33) in the Pretoria Group showing their non-cylindrical nature.

Fig. 3.36 Stereonet plot of the interference fold sets at locality (2855,0 X; -92,7 Y).

Fig. 3.37 Dextral strike-slip offset of sub-vertical quartz vein adjacent to a major northerly-trending D_4 fault. Locality (2862,5 X; -97,9Y).

Fig. 3.38 Northerly trending fault in the Chuniespoort Group infilled with quartz. Locality (2856,4 X; -91,5 Y). Looking north.

Fig. 3.39 Fault breccia comprising clasts of chert (C), marble (M) and dyke material (D). Locality (2856,2 X; -92,2 Y).

Fig. 3.40 Orientation of L_2 lineations. Restoration of bedding to the horizontal suggests that they plunged horizontally or slightly south at the time of their formation.

Fig. 3.41 Rotation of D_3 folds and associated shear zones to their original orientations to account for the regional tilt of strata. Orientation of bedding is 090°/20°N.

Fig. 3.42 Rotation of D_3 kink-fold axial planes in the Pretoria Group to account for the regional tilt of strata.

Fig. 3.43 Duplex structure in a bedding sub-parallel shear zone. Locality (2857,5 X; -94,0 Y). Looking north.

Fig. 3.44 Oxidised porphyroblasts adjacent to the duplex structure shown in Fig 3.43 above.

Fig. 3.45 Easterly-dipping cleavage deforms the earlier S_2 cleavage adjacent to a reactivated D_2 bedding sub-parallel shear zone in the Pretoria Group. Scale bar 0,5 mm.

Fig. 3.46 Duplex structure similar to that in Fig. 3.46 in a slate-hosted shear zone. Locality 20 km west of Magaliesberg, along the R509. Looking north.
Scale bar 0,5mm.

Fig. 3.47 Stereographic representation of west-verging folds outside of bedding sub-parallel shear zones in the Pretoria Group.

Fig. 3.48 Easterly verging fold deforming the cleavage of a D_2 bedding sub-parallel shear zone. Looking north. Locality (2857,3 X; -94,9 Y).

Fig. 3.49 Altered porphyroblast within a D_2 bedding sub-parallel shear zone displaying possible top-to-the-east shear sense. Locality (2857,5 X;-94,0 Y). Scale bar 0,5 mm.

Fig. 3.50 Stereographic representation of joint orientations on opposite sides of a major sinistral strike-slip fault trending approximately 170°. Locality in the vicinity of (2857,2 X; -92,0Y).

Fig. 3.51 Rose diagrams representing regional joint set orientations (as determined from aerial photographs) compared with the orientation of joint sets measured from the study area.

Fig. 3.52 Cracks in unconsolidated soils oriented a) 060°, b) 100°, and c) 130°. Locality (2856,0 X; -95,6 Y).

Fig. 3.53 Comparison of the orientations of cracks in the unconsolidated soils (a) with orientations of joint sets in the adjacent slate (b), showing some correlation of orientations.

Fig. 3.54 Waterfall in more than 10 m thick unconsolidated sediments. Looking south.

Fig. 3.55 Cross-section of the waterfall in Fig. 3.54 showing the position of an inferred normal fault with downthrow to the north.

Fig. 3.56 Linear fractures in tufa trending 100°. Looking west. Locality (2857,6 X; -91,8 Y).

Fig. 3.57 Comparison of joint set data with the tufa fractures, showing some degree of coincidence. a) Prominent E-W trend of tufa "joints". b) Joints in slate adjacent to the tufa. Locality (2857,6 X; -91,8 Y).

Fig. 3.58 Waterfall defined by tufa fractures trending 100°. Looking west. Locality (2857,6 X; -91,8 Y).

Fig. 4.1 Chloritoid porphyroblast at a high angle to S_2 cleavage, displaying hour-glass zoning. Locality (2857,5 X;-94,1 Y). Scale bar 0,25 mm.

Fig. 4.2 Photomicrograph (a) and schematic representation (b) showing the intensity of cleavage increasing in close proximity to a chloritoid porphyroblast, and enveloping a wedge-shaped strain shadow of quartz on either side of it. Locality (2857,5 X;-94,1 Y). Scale bar 0,125 mm.

Fig. 4.3 Photomicrograph (a) and schematic representation (b) showing the ends of chloritoid porphyroblasts rounded and truncated by dissolution. Locality (2857,5 X;-94,1 Y). Scale bar 0,25 mm.

Fig. 4.4 Photomicrograph (a) and schematic representation (b) showing idioblastic chiastolite porphyroblast in a foliated matrix. The cleavage partially wraps, and is truncated by, the crystal. Bekker Schools locality (Fig. 1.1). Scale bar 0,5 mm.

Fig. 4.5 Photomicrograph (a) and schematic representation (b) showing two idioblastic chiastolite porphyroblasts with cleavage anastomosing, truncated and squeezed between them. Bekker Schools locality. Scale bar 0,5 mm.

Fig. 4.6 Photomicrograph (a) and schematic representation (b) showing interfering chiastolite

crystals, and variably truncated and anastomosing cleavage. Bekker Schools locality. Scale bar 0,5 mm.

Fig. 4.7 Altered and deformed porphyroblasts from within a spotted slate, Black Reef Quartzite Formation. a) East-west section showing crosses probably indicating chiastolite. b) North-south section showing the porphyroblasts deformed to lozenge shapes. Scale bar 0,5 mm. Locality (2863,1 X; -95,0 Y).

Fig. 5.1 Bushveld Complex aureole metamorphism map (modified from Saggerson and Turner, 1986). a) Unmetamorphosed lithologies. b) Albite-epidote hornfels. c) Hornblende hornfels.

Fig. 5.2 Heating of the country rock adjacent to different intrusions at different depths. D=thickness of intrusion. Distance from the contact on the x-axis given as fractions of D (after Winkler, 1979).

Fig. 6.1 Concentric arrangement of fold axes around the Vredefort Structure, from McCarthy *et al.* (1986).

Fig. 6.2 Possible extensions of D_3 fold-related shears as splays of thrusts identified from geophysical profiles (modified after Du Plessis and Levitt, 1987; and Andreoli, 1990).

List of Tables

Table 1.1 Generalized stratigraphic and geochronologic column of intracratonic basins and intrusions of the north-central Kaapvaal Craton. After Walraven (1990); S.A.C.S. (1980) and Frimmel (1994).

Table 2.1 Summary of previous work done on sills in the Bushveld Complex floor.

Table 2.2 Comparison of geochemical data of sills from the study area with published data of sills from other areas around the Bushveld Complex.

Table 3.1 Principle plane strain ratios (R) of deformed ooids adjacent to a D_2 bedding sub-parallel shear zone. Locality (2861,7 X; -95,1 Y).

Table 3.2 *K-values* determined from the principle plane strain ratios (R) of deformed ooids presented in Table 3.1.

Table 5.1 Temperatures attained at various levels in the Transvaal Supergroup due to the intrusion of the Bushveld Complex, based on the model of Winkler (1979). See Fig. 5.2. D=5000m.

Table 5.2 The values of d and r for thermal modelling, after Jaeger (1968).

Table 5.3 Temperatures attained in the Transvaal Supergroup due to the intrusion of the Bushveld Complex at various positions in space and time, based on the mathematical model of Jaeger (1950a). Initial country rock temperature assumed to be 0°C.

Table 5.4 Maximum modelled temperatures (from Table 5.3) when various geothermal gradients are taken into account.

TABLE OF CONTENTS

Abstract i

Declaration ii

Acknowledgements iii

List of figures iv

List of tables ix

CHAPTER 1 Introduction 1

1.1 General statement 1

1.2 Methodology 2

1.3 Regional geology 3

1.3.1 Pre-Transvaal history of the Kaapvaal Craton 3

a) Dominion basin 5

b) Witwatersrand basin 6

c) Ventersdorp basin 8

d) Limpopo belt 10

1.3.2 Syn-Transvaal history of the Kaapvaal Craton 11

Transvaal basin 11

1.3.3 Post-Transvaal history of the Kaapvaal Craton 18

a) Basins 18

Soutpansberg basin 18

Waterberg basin 18

Karoo basin 19

b) Orogenic events affecting the Kaapvaal Craton 19

Kheis orogeny 19

Kibaran orogeny 20

Pan-African orogeny 21

c) Vredefort Dome 22

d) Johannesburg Dome 24

e) Intrusive events 25

Bushveld Complex 25

Pilanesberg Alkaline Complex 27

Karoo igneous activity 27

CHAPTER 2 Local Stratigraphy 28

2.1 Introduction 28

2.2 Stratigraphy of the study area 28

2.2.1 Basement lithologies 28

2.2.2 Black Reef Quartzite Formation 29

2.2.3 Chuniespoort Group 30

a) Oaktree Formation 30

b) Rietfontein Formation 32

c) Tweefontein Formation 33

d) Rietspruit Formation 35

e) Zwartkrans Formation 35

f) Crocodile River Formation 36

g) Lyttelton Formation 36

h) Hennops River Formation 36

i) Fountains Formation 37

j) Remaining carbonate lithologies 37

2.2.4 Pretoria Group 39

2.2.5 Sills 40

a) Previous work 41

b) Characteristics of sills in the study area 45

c) Comparison of sills in the study area with sills from other parts of the Bushveld floor 46

2.2.6 Dykes 50

2.2.7 Recent sediments 51

CHAPTER 3 Structural Relationships 54

3.1 Introduction 54

3.1.1 Previous work 54

3.1.2 Results from this study 56

3.2 D_1 Event 57

3.3 D_2 Event 58

3.3.1 Cleavage 58

3.3.2 Folds 62

a) Black Reef Quartzite Formation and Chuniespoort Group 62

b) Pretoria Group 66

3.3.3 Bedding sub-parallel shear zones 67

a) Shear zone hosted folds 68

b) S-C fabrics 71

c) Porphyroclasts and prophyroblasts 73

d) Other structures 75

e) Strain analysis 77

3.3.4 Lineations 81

3.3.5 Deformed ooids 86

3.4 D_3 Event 88

3.4.1 Folds in the Chuniespoort Group 88

3.4.2 Folds in the Pretoria Group 92

3.5 D_4 Event 101

3.6 Effects of the Johannesburg Dome 104

3.7 Other ductile deformation 109

3.7.1 West-verging structures 109

a) Reactivated shear zones 109

b) Lineations 112

c) Folds 114

3.7.2 East-verging structures 115

3.8 Jointing and neotectonic activity 117

3.8.1 Joints 117

3.8.2 Neotectonic activity 122

a) Structures in unconsolidated soils 122

b) Structures in rufa 126

3.9 Summary 129

CHAPTER 4 Porphyroblast Microstructural Relationships 130

4.1 Introduction 130

4.2 Porphyroblast growth and cleavage relationships 131

4.2.1 Porphyroblast growth under hydrostatic stress conditions 131

4.2.2 Porphyroblast growth under directed stress conditions 134

4.3 Porphyroblasts in the study area 137

4.3.1 Chloritoid 137

4.3.2 Chiastolite 142

4.3.3 Other porphyroblasts 148

4.4 Summary 150

CHAPTER 5 Metamorphism 151

5.1 Introduction 151

5.2 Metamorphism of the Witwatersrand basin 151

5.3 Bushveld Complex related metamorphism 154

5.3.1 Eastern lobe 156

5.3.2 Western lobe 158

5.4 Intrusion-related metamorphism in the study area 161

5.4.1 Thermal modelling 161

a) Model 1 163

b) Model 2 167

c) Relevance of the thermal models to the study area 171

5.5 Metamorphism of carbonate rocks 172

5.6 Metamorphism of pelitic rocks 172

5.7 Metamorphism of sills 174

5.8 Summary 175

CHAPTER 6 Discussion 176

6.1 Introduction 176

6.2 Metamorphism 176

6.3 Deformation 177

6.3.1 D_1 event 177

Origin of the D_1 deformation 179

6.3.2 D_2 event 180

Origin of the D_2 deformation 180

6.3.3 D_3 event 185

Origin of the D_3 deformation 186

6.3.4 Uplift of the Johannesburg Dome 190

6.3.5 D_4 event 191

6.3.6 Other ductile deformation 193

a) East-verging structures 194

b) West-verging structures 194

6.3.7 Jointing and neotectonic activity 196

CHAPTER 7 Conclusions 197

References 199

Appendix 1 215

Appendix 2 216

Appendix 3 217

CHAPTER 1

INTRODUCTION

1.1 General statement

The Archaean to mid-Proterozoic sedimentary basins of the Kaapvaal Craton are host to a number of major ore deposits, among them the gold deposits of the Witwatersrand Basin and the platinum deposits of the Bushveld Complex. Since the mid-1980s, considerable attention has focussed on the effects of deformation events on, in particular, the gold deposits of the Witwatersrand Basin (e.g. Stanistreet *et al.*, 1986). An understanding of these economically important deposits is incomplete without an understanding of the deformation history of the rocks in which they are hosted. Considering the long history of the Witwatersrand basin, time-lines are necessary to constrain the relative timing of deformation events affecting the rocks. Consequently, examination of deformation events affecting the overlying Transvaal Supergroup is fundamental in determining a complete tectonic history of the Witwatersrand basin (McCarthy *et al.*, 1986; McCarthy *et al.*, 1990). Backstripping the effects of post-Transvaal deformation could provide important information pertaining to both mining and exploration ventures in the Witwatersrand basin (McCarthy *et al.*, 1986; Winter, 1987).

The current study aims primarily to identify, and to constrain, the relative ages of deformation events affecting an area of the Transvaal Supergroup using the Black Reef Quartzite Formation (at the base of the Transvaal Supergroup), and the younger intrusive events of the Bushveld Complex and the Pilanesberg Alkaline Complex, as time-lines. Study of neotectonic activity affecting Recent sediments in the area has also been undertaken, providing a tectonic history of the Transvaal Supergroup up to the Holocene. The results of

this study may contribute to the understanding of structures affecting the underlying Witwatersrand Supergroup.

1.2 Methodology

The area chosen for this study comprises a continuous N-S section through the Transvaal Supergroup, extending from its contact with the Johannesburg Dome towards the contact with the Bushveld Complex (Fig. 1.1), between latitudes 27°54' E - 27°58' E, and longitudes 25°47' S - 25°53' S. The area mapped includes a portion of the Kareebosrand Conservancy (Map 1) and Pelindaba (Map 2). Data collection entailed structural field mapping of the 5-7 km wide, approximately 14 km long area, and collection of more than 150 samples, the bulk of which were oriented. In addition to this, several important outcrops of structural and metamorphic significance near Magaliesburg (Fig. 1.1), west of the main field area, were examined. The field work was undertaken during the period July-December 1993.

Structural field mapping was undertaken using 1:10 000 orthophotographs as base maps, and aerial photographs proved useful for locating and interpreting important structures and outcrops. A basic synthesis of the tectonic evolution of the region was established during the field mapping, the results of which are presented in the enclosure (Maps 1 and 2). Subsequent microstructural study of oriented thin sections (sections were cut from oriented rock samples according to the methods outlined by Hansen (1990) aided in substantiating and refining the tectonic history. Petrographic studies and X-ray fluorescence (XRF) whole-rock analyses were used to determine the composition of sills in the study area, which were correlated with sills in other parts of the Transvaal Supergroup.

An extensive review of the available literature assisted in placing this contribution to the structural history of the Transvaal Supergroup into a framework which includes the geological events known to have affected the Kaapvaal Craton.

1.3 Regional geology

The Kaapvaal Craton of southern Africa comprises Archaean basement, consisting of granitoids and greenstones (Anhaeusser, 1973). The basement crops out extensively, and has been partially exposed in the Vredefort Dome and the Johannesburg Dome. Subsequent volcano-sedimentary deposition into successor basins which developed on the Kaapvaal Craton resulted in, amongst others, the Witwatersrand and Transvaal Supergroups. The margins of the Kaapvaal Craton are defined by approximately linear metamorphic belts on its northern, southern and western flanks (Fig. 1.1, inset), representing orogenies at different stages in the tectonic evolution of the craton. The Kaapvaal Craton itself has also been affected by tectonic and igneous events, as well as an evidently catastrophic impact event, at various stages in its history, all of which have contributed to the present-day structure of the Transvaal Supergroup rocks.

1.3.1 Pre-Transvaal history of the Kaapvaal Craton

The granitoid basement comprising much of the Kaapvaal Craton has been dated at 3170 ± 34 Ma using the U-Pb technique on samples from the Johannesburg Dome (Anhaeusser and Burger, 1982), although basement ages of more than 3200 Ma have also been reported (e.g. Robb *et al.*, 1990; Armstrong *et al.*, 1991). The Kaapvaal Craton stabilised after a major period of plutonism and thermal metamorphism approximately 3200 - 3000 Ma ago (Hunter, 1974; Robb *et al.*, 1990; Walraven *et al.*, 1990). Several basin types were developed on the Kaapvaal Craton in response to an overall Wilson Cycle in the Late Archaean, during which

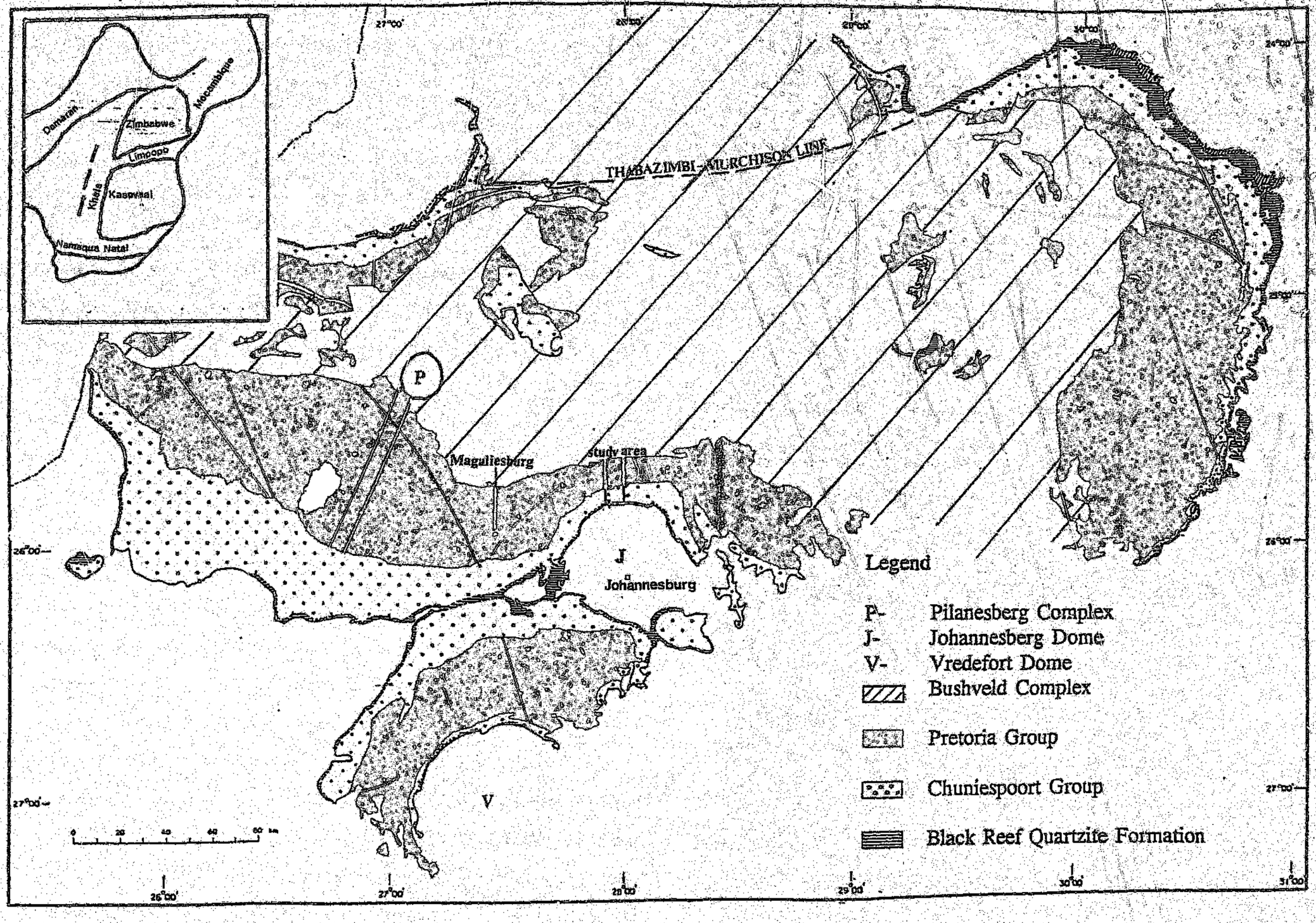

Fig. 1.1 Regional geological map of the northern Kaapvaal Craton showing the study area relative to the positions of major geological features. After S.A.C.S. (1980) and Walraven *et al.* (1990). Inset shows the position of the Kaapvaal Craton relative to the Zimbabwe Craton.

time the Limpopo Orogeny occurred (Stanistreet and McCarthy, 1991). In an attempt to evaluate the changing tectono-sedimentary conditions relevant to the formation of the Witwatersrand basin, a six-stage tectonic evolution for the Kaapvaal Craton was proposed by Stanistreet and McCarthy (1991), while Clendenin *et al.* (1988a) proposed a fully evolved, three-stage rift system for the evolution of early successor basins on the Kaapvaal Craton.

The initial stage of basin development on the Kaapvaal Craton was the establishment of a "structural framework" within the > 3,1 Ga basement (Stanistreet and McCarthy, 1991). This was provided by significant suture zones, oriented approximately ENE and NNW, which were defined by greenstone belts and their associated lineaments (Stanistreet and McCarthy, 1991). Subsequently, basins were generated on the Kaapvaal Craton which received volcanic and sedimentary deposits (e.g. Hunter, 1974; Clendenin *et al.*, 1988a and b; Walraven *et al.*, 1990; Robb *et al.*, 1990; Armstrong *et al.*, 1991).

a) Dominion basin

Following the establishment of the structural framework for the Kaapvaal Craton, an extensional failed rift basin (the Dominion basin), associated with NNE trending faults, developed (Clendenin *et al.*, 1988a; Stanistreet and McCarthy, 1991). This basin received the bimodal volcanic suites and lesser fluvial sediments of the Dominion Group (S.A. [illegible], 1980) which attain a maximum total thickness of 2200 m, and unconformably overlie the Archaean granite-greenstone basement (Bowen *et al.*, 1986; Jackson, 1991). Detrital zircons from conglomerates and zircons from volcanics within the Dominion Group date the development of the basin at approximately 3070 Ma (Table 1.1) (Robb *et al.*, 1990; Walraven *et al.*, 1990; Armstrong *et al.*, 1991).

b) Witwatersrand basin

Thermal subsidence followed the period of extension related to the development of the Dominion basin (Clendenin *et al.*, 1988a). This subsidence resulted in marine transgression into the Witwatersrand basin (Stanistreet and McCarthy, 1991), interpreted as a foreland basin yoked to an active fold and thrust belt in its hinterland (Winter, 1987). The spreading of this sea over the Kaapvaal Craton resulted in deposition of subtidal sediments of the West Rand Group (lower Witwatersrand Supergroup) which conformably overlie the Dominion Group (Stanistreet and McCarthy, 1991).

The Crown lava occurs close to the base of the Witwatersrand Supergroup stratigraphy, in the West Rand Group. This volcanic unit yielded a $^{207}Pb/^{206}Pb$ zircon age of 2914 $\pm$ 8 Ma (Armstrong, *et al.*, 1991) (Table 1.1).

The extensional conditions which prevailed during Dominion and early Witwatersrand basin development reversed to compression, and the Central Rand Group (upper Witwatersrand Supergroup) was deposited in the shrinking basin (Stanistreet and McCarthy, 1991). The shrinking basin was a result of NE-SW directed compression attributed to the subduction between and ultimate collision of the Zimbabwe and Kaapvaal Cratons, which caused the relative tectonic escape of the central part of the Kaapvaal Craton to the southeast (Stanistreet and McCarthy, 1991).

Table 1.1 Generalized stratigraphic and geochronologic column of intracratonic basins and intrusions of the north-central Kaapvaal Craton. After Walraven (1990); S.A.C.S. (1980) and Frimmel (1994).

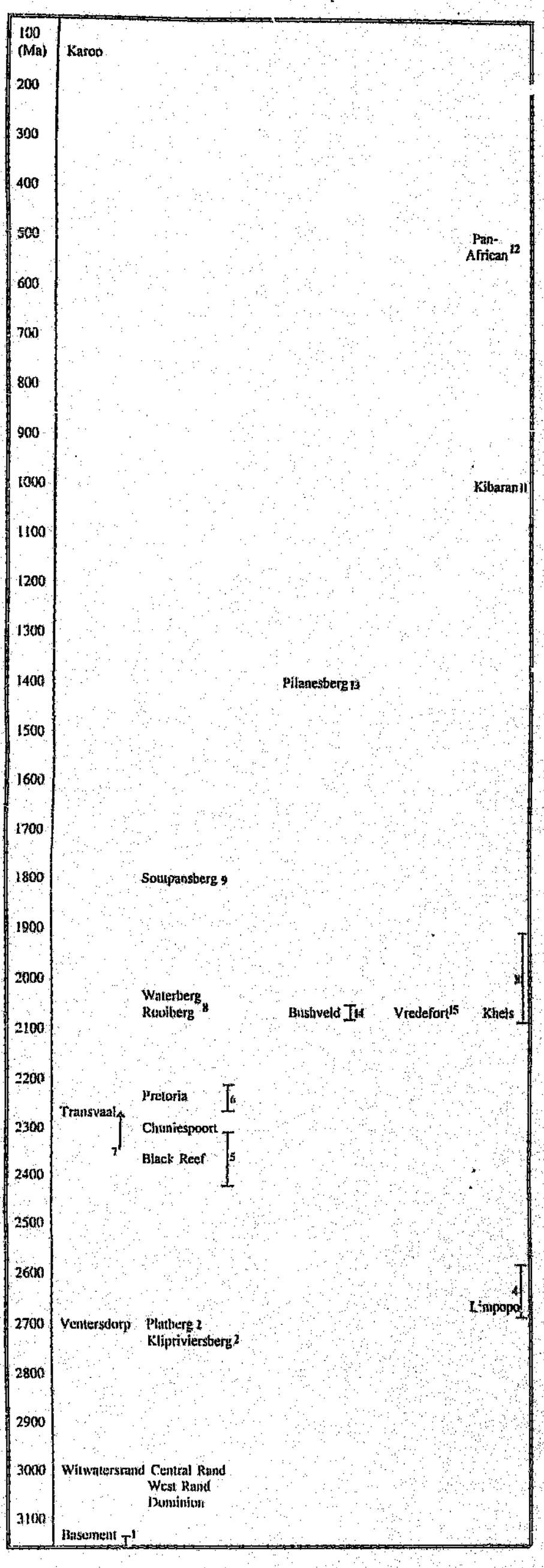

1) U-Pb Anhaeusser and Burger (1982)
2) Pb-Pb Armstrong *et al.*, (1991)
3) Pb-Pb Robb *et al.*, (1990)
4) U-Pb/ Rb-Sr Barton *et al.*, (1979); Pb-Pb Barton and van Reenen (1992a)
5) Rb-Sr Armstrong (1987)
6) Rb-Sr Burger and Coertze (1975)
7) Pb-Pb Armstrong (1987)
8) Pb-Pb Walraven and Hattingh (1993)
9) Rb-Sr Clarney *et al.*, (1990)
10) Dunne and Kruger (1991)
11) Tankard *et al.*, (1982); Matthews (1981); Martin and Hartnady (1986); Jacobs *et al.*, 1993)
12) Sacchi *et al.*, (1984)
13) Tankard *et al.*, (1982)
14) Pb-Pb, Sr-Sr Walraven *et al.*, (1990)
15) Pb-Pb Kamo *et al.*, (1995)

Ages based on $^{207}Pb\backslash^{206}Pb$ from detrital zircons collected from two reefs in the Johannesburg Subgroup of the Central Rand Group place a maximum constraint of 3007 ± 3 Ma on the age of deposition of the Johannesburg Subgroup (Robb *et al.*, 1990) (Table 1.1). A similarly determined age from detrital zircons in the Turffontein Subgroup of the Central Rand Group reveals a maximum age of 2909 ± 3 Ma for deposition of the Turffontein Subgroup (Robb, *et al.*, 1990) (Table 1.1).

The age of Witwatersrand basin development is constrained by the overlying Ventersdorp Supergroup (2714 Ma) and the underlying Dominion Group (3070 Ma) (Table 1.1) to a period of approximately 360 Ma (Robb *et al.*, 1990; Armstrong *et al.*, 1991; Robb and Meyer, 1995).

c) Ventersdorp basin

The Ventersdorp Supergroup is divided into the lower Klipriviersberg Group flood basalts, the middle Platberg Group, and the upper Bothaville and Allanridge Formations (S.A.C.S., 1980). The Klipriviersberg flood basalts are attributed to tectonic escape-related extension and oblique-slip faulting as a result of the collision of the Kaapvaal and Zimbabwe Cratons (Stanistreet and McCarthy, 1991). The basalts inundated the Witwatersrand basin, terminating sedimentation (Stanistreet and McCarthy, 1991). Changes in the stress field orientations on the Kaapvaal Craton during Klipriviersberg times are indicated by changes in the spatial distribution and orientation of successive geochemical units of the Klipriviersberg Group (Linton *et al.*, 1993). These authors established the sequence of eruption of the Klipriviersberg lavas, based on the distribution of geochemically distinct units within, and outside of, the Witwatersrand basin. The initial Klipriviersberg Group lavas erupted in the

same NE-SW directed compressive regional stress field that controlled Central Rand Group sedimentation, whereas other Klipriviersberg units may have been controlled by pre-existing fault systems (e.g. the Thabazimbi-Murchison Line, Fig. 1.1) (Linton *et al.*, 1993). Changing orientations of dyke swarms related to subsequent eruptions of Klipriviersberg lava represent changes in orientation of the regional stress field with progressive eruptions, which resulted in the sequential rotational breakout of crust in an anticlockwise direction (Linton *et al.*, 1993).

Combined data sets from Klipriviersberg lava zircon samples yield $^{207}Pb/^{206}Pb$ ages of 2714 $\pm$ 8 Ma (Table 1.1), interpreted as the date of extrusion of the Klipriviersberg lavas (Armstrong *et al.*, 1991).

Indentation of the Zimbabwe Craton into the Kaapvaal Craton finally resulted in the development of an impactogenal rift, oriented approximately perpendicular to the Limpopo orogenic belt (Section 1.3.1 *d*), into which the Platberg Group was deposited (Stanistreet and McCarthy, 1991). The Makwassie Quartz Porphyry Formation (part of the Platberg Group) yields an emplacement and crystallization age of 2709 $\pm$ 4 Ma (Table 1.1), established from combined ages obtained from $^{207}Pb\backslash^{206}Pb$ and ^{204}Pb (Armstrong *et al.*, 1991). Subsidence, tectonic activity and volcanism alternated during Bothaville and Allanridge Formation times (Clendenin *et al.*, 1988a).

d) Limpopo belt

The northern margin of the Kaapvaal Craton is separated from the Zimbabwe Craton by the ENE-WSW trending Limpopo belt (Fig. 1.1, inset). The exposed length of this belt is approximately 700 km, and its width up to 250 km. The multiply deformed and highly metamorphosed Limpopo belt comprises Archaean gneisses and metasediments divided into the Northern, Central and Southern Marginal Zones (e.g. Cox *et al.*, 1965; Coward, 1976; Watkeys, 1983). The Palala Shear Zone divides the Central Zone from the Southern Marginal Zone, while the Tuli-Sabi Shear Zone divides the Southern Marginal Zone from the Kaapvaal Craton (McCourt, 1983).

Models of Archaean continental collision between two stable cratons (the Zimbabwe and Kaapvaal Cratons) have been proposed for the origin of the late Archaean Limpopo Belt (Light, 1982; Shackleton, 1986; Roering *et al.* 1992). These models suggest a single metamorphic and deformation event which is superimposed on earlier structures. More recent work reviewed by Rollinson (1993), however, suggests that the Limpopo Belt may be better explained by accretion processes, where each zone or terrane has its own distinctive geological history. The Limpopo Belt may, therefore, not simply have been the result of a single structural and metamorphic event. The term "Limpopo orogeny" is applicable to the period of high-grade metamorphism, partial melting and igneous intrusion in the Central and Southern Marginal Zones which yields U-Pb, Rb-Sr and Pb-Pb ages of between approximately 2,7-2,6 Ga (Barton *et al.*, 1979; Barton and Van Reenen, 1992a) (Table 1.1).

Crustal thinning within and adjacent to the Limpopo belt occurred as a result of uplift of the northern margin of the Kaapvaal Craton at approximately 2050 Ma (Barton and Van Reenen,

1992b). The uplift was accommodated by motion along the Thabazimbi-Murchison Line and the Triangle Tuli-Sabi shear zone, and may be related to the tectonism that gave rise to the anorogenic Bushveld and Phalaborwa Complexes (Barton and Van Reenen, 1992b). The Thabazimbi-Murchison Line (TML) is an ENE trending structural lineament which can be traced across the Kaapvaal Craton. This structural lineament was probably initiated in the Archaean, and involved periodic strike-slip and dip-slip reactivations (Du Plessis, 1987; Martin *et al.*, 1988, 1990). The TML operated as a "transfer fault" during Ventersdorp Supergroup extension, and had a history of down-to-the-south reactivation in Chuniespoort Group times (Martin *et al.*, 1990).

1.3.2 Syn-Transvaal history of the Kaapvaal Craton

Following the indentation of the Zimbabwe Craton into the Kaapvaal Craton at approximately 2,7-2,6 Ga (Barton and Van Reenen, 1992a), gravitational collapse and erosion of the Limpopo orogenic belt led to the development of extensional rift basins and subsequent deposition of the precursors to the Transvaal basin (Clendenin *et al.*, 1988b; Stanistreet and McCarthy, 1991). Associated with this extension was a phase of thermal cooling which led to the formation of an epicontinental sea into which the Transvaal Supergroup was deposited (Clendenin *et al.*, 1988b).

Transvaal basin

The protobasinal rocks of the Transvaal Supergroup include the locally developed Wolkberg Group, Buffelsfontein Group, Godwan Formation, Groblersdal Group, Wageenbietjie Formation, and the far more extensively developed Black Reef Quartzite Formation (Eriksson and Clendenin, 1990).

The Black Reef Quartzite Formation occurs at the base of the Transvaal Supergroup (Fig. 1.2), and comprises quartzite (with lenses of grit and conglomerate) and shale (S.A.C.S., 1980) deposited in fluvial and shallow marine environments (Tankard *et al.*, 1982). Its deposition marks the period when the tectonically-thinned lithosphere was affected by post-graben thermal subsidence after the collision of the Zimbabwe Craton with the Kaapvaal Craton (Clendenin *et al.*, 1988a). The age of the Black Reef Quartzite Formation can only be approximated from data for the Vryburg Formation (a correlate of the Black Reef Quartzite Formation) in the Griqualand West basin. Based on whole-rock analyses, the Vryburg Formation has been dated at 2371 +81/ -86 Ma (Armstrong, 1987) (Table 1.1). The upper contact of the Black Reef Quartzite Formation with the overlying dolomite formations is transitional and conformable (S.A.C.S. 1980).

Extension and thermal subsidence which succeeded collision of the Kaapvaal and Zimbabwe Cratons resulted in the opening of a shallow epeiric sea (the Transvaal Sea) into which the Chuniespoort/Ghaap Group was deposited (Clendenin *et al.* 1988a, Clendenin, 1989). The epeiric Transvaal Sea covered most of the Kaapvaal Craton during Early Proterozoic times (Tankard *et al.*, 1982; Clendenin, 1989; Martin *et al.*, 1990). A shallow-water carbonate platform thus existed over most of the Kaapvaal Craton, including the Witwatersrand basin, during the Early Proterozoic (Tankard *et al.*, 1982; Clendenin, 1989).

The basin into which the Chuniespoort Group was deposited was compartmentalized and bounded by major lineaments defined by pre-existing zones of weakness (Clendenin *et al.*, 1988a). The northern margin of the basin was defined for a period by the long-lived Thabazimbi-Murchison Line (Martin *et al.*, 1988), but was subsequently overstepped (Martin

et al., 1990). The northwestern margin of the Transvaal basin was relatively active during sediment deposition while the southeastern margin was relatively passive (Eriksson, 1977; Tankard *et al.*, 1982). The basin margin activity controlled the influx of terrigenous clastic material (Tankard *et al.*, 1982). The Transvaal Sea underwent major regressions which resulted in regional unconformities characterised by quartz-arenite or chert-in-shale breccia (Clendenin, 1989; Martin *et al.*, 1990).

The Chuniespoort Group (Fig. 1.2) and its correlative, the Griqualand West Sequence, consist mainly of chemical sediments, including dolomite, limestone, chert and iron formation with minor terrigenous clastic sediments (S.A.C.S. 1980). The Chuniespoort Group, at its maximum development in the eastern and western Transvaal, consists of the lower Malmani Subgroup (divided into five groups based on chert content and algal structures), the Penge Formation, and the overlying Duitschland Formation (Fig. 1.2), which are principally chemical in composition, but which do contain some clastic material (S.A.C.S., 1980). Marginal unconformities within the Chuniespoort Group are defined by chert-in-shale breccias and quartzite lenses, which are a direct result of basinal uplift (Tankard *et al.*, 1982; Clendenin and Maske, 1986; Clendenin, 1989). The Malmani Subgroup, part of the Chuniespoort Group (Fig. 1.2), has various stromatolite markers interpreted as being formed in marginal supratidal-upper intertidal, tidal channel, mid- to lower-intertidal and subtidal areas, in environments varying from hypersaline to low salinities (Eriksson, 1977; Clendenin, 1989).

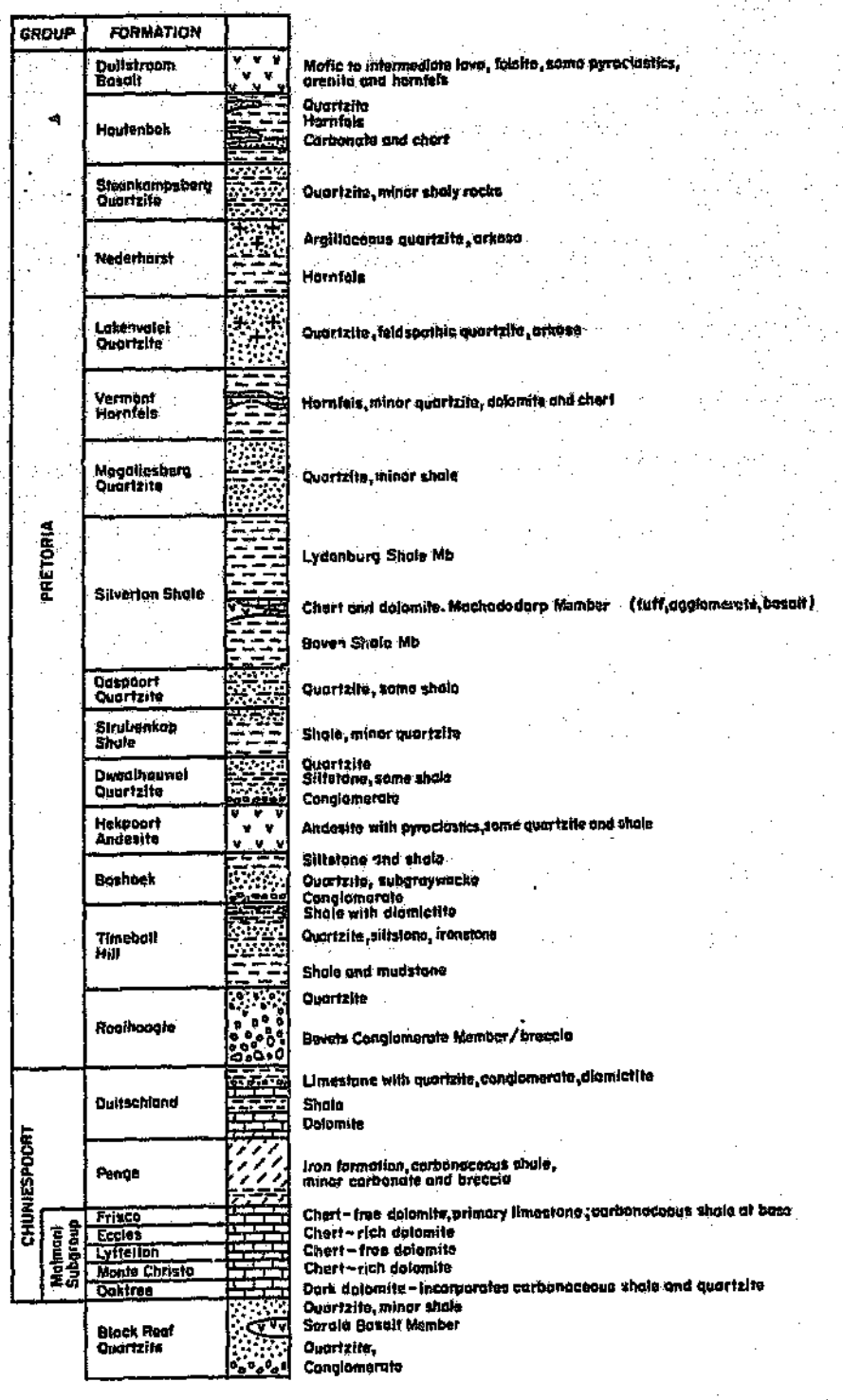

Fig. 1.2 Generalised stratigraphic column for the Transvaal Supergroup. From S.A.C.S. (1980).

The Pretoria Group overlies the Chuniespoort Group (Fig. 1.2), and is separated from it by a regional angular unconformity (Visser, 1969; S.A.C.S. 1980; Tankard *et al.*, 1982; Eriksson, 1986) characterised by a chert-shale breccia (Tankard *et al.*, 1982) resulting from a period of non-deposition and erosion (Walraven, 1981). The Pretoria Group, comprising the Rooihoogte, Timeball Hill, Boshoek, Hekpoort, Dwaalheuwel, Strubenkop, Daspoort, Silverton, Magaliesberg, Vermont, Lakenvlei, Nederhorst, Steenkampsberg, Houtenbek and Dullstroom Formations, consists mainly of shales and quartz-arenites with minor carbonates, and andesitic lavas (the Hekpoort Andesite Formation) (S.A.C.S., 1980) (Fig. 1.2). Most of the formations of the Pretoria Group are widely distributed throughout the Transvaal Supergroup, although those formations occurring above the Magaliesburg Quartzite are not found in the western portion of the Transvaal Supergroup (S.A.C.S., 1980). The Pretoria Group reaches a maximum thickness of up to 7000 m (Eriksson, 1986).

The Hekpoort Andesite Formation has been dated at 2224 $\pm$ 21 Ma (Table 1.1) based on whole-rock Rb-Sr analyses (Burger and Coertze, 1975), which is the age Walraven *et al.* (1990) accept as representative of the Pretoria Group.

An intracratonic or complex lacustrine basin environment has been postulated for the deposition of the Pretoria Group (Eriksson, 1988). Glacial, glaciolacustrine and fluvioglacial environments of deposition have been identified for the three basal units of the Pretoria Group, whereas higher up in the sequence, lacustrine or shallow basin, shallow shelf and transgressive deep water marine environments have been identified (Eriksson, 1986). Stear (1977) recognised the occurrence of estuarine deposits in conjunction with immature braided stream deposits grading into mudflat shales in the Rooiberg area. These fluvial and estuarine

facies were interpreted as part of a marginal marine environment. The volcanic units of the Pretoria Group (e.g. the Hekpoort Andesite Formation) consist of andesitic lavas, air-fall pyroclastic and lahar deposits but lack pillow structures, implying terrestrial volcanism (Eriksson, 1986).

Eriksson and Reczko (1995) divided the Pretoria Group below and above the Hekpoort Andesite Formation into the lower and upper Pretoria Group respectively. They interpreted the lower Pretoria Group as subaerial fan sediments deposited in a closed basin. The sedimentation was controlled primarily by E-W and NW-SE striking faults, possibly half-grabens, which also controlled Ventersdorp and Chuniespoort deposition. According to them, the formations overlying the Hekpoort Andesite Formation were deposited in marine basins and coastal environments followed by braid-delta / tidal-flat complexes. These overlying formations possibly formed due to thermal subsidence along faults, some of which were active during lower Pretoria Group sedimentation. The subsidence led to widespread marine transgression (Eriksson and Reczko, 1995).

Felsites of the Rooiberg Group lie discordantly above the Pretoria Group (Visser, 1969) and represent the termination of Transvaal Supergroup deposition (Tankard *et al.*, 1982). Field relationships indicate that these rhyolitic and rhyodacitic rocks are pre-Bushveld in age (Walraven *et al.*, 1990). However, Schweitzer and Hatton (1995) have shown that geochemical similarities between the felsites and the granophyres within the Bushveld Complex suggest that the Rooiberg Group was emplaced synchronously with the Bushveld Complex. This is also supported by Walraven's (in press) data.

An age for the start of Transvaal basin sedimentation has been given at approximately 2350 Ma (Table 1.1), an estimate based on whole rock Pb-Pb ages determined for the Godwan and Vryburg Formations (Armstrong, 1987). The 2241 ± 21 Rb-Sr age determined for the Hekpoort Andesite Formation in the Pretoria Group (Table 1.1) by Burger and Coertze (1973) is accepted by Walraven *et al.* (1990) as the age of clastic sedimentation of the Transvaal Supergroup. The upper age of the Transvaal Supergroup is considered to be the date of intrusion of the Bushveld Complex at approximately 2050 Ma (Walraven *et al.*, 1990). Recent single-zircon Pb evaporation age determinations (Walraven, 1995, in press) place the crystallization age of the Rooiberg Group at 2061 ± 2 Ma (Table 1.1), which defines the completion of the Transvaal Supergroup volcanic and sedimentary deposition. However, another age for the Transvaal Supergroup has recently been determined from single grain zircon $^{207}Pb/^{206}Pb$ analysis, and constrained to 2600-2450 Ma (Armstrong, pers. comm. in Frimmel, 1994a) (Table 1.1). The 2600 Ma age suggested by Clendenin *et al.* (1988b) for the formation of the Transvaal Sea corresponds well with the 2600 Ma maximum age of the Transvaal Supergroup quoted above, and suggests that the basin may have existed for close to 600 Ma (Walraven, 1995, in press).

The tensional stresses present during the formation of the Transvaal basin were still present during the early emplacement of the Bushveld Complex (Temperly, 1977). To the south of the Transvaal basin, the Johannesburg Dome was rapidly uplifted, thus resulting in simultaneous basining to the north and uplift to the south (Temperly, 1977). Regionally, the strata of the Transvaal Supergroup dip centripetally towards the Bushveld Complex (Section 1.3.5*a*), possibly as a result of subsidence following its emplacement. Northerly tilt of the southern margin of the Transvaal Supergroup may have been assisted by the emplacement

of the Johannesburg Dome (Section 1.3.5*b*) which had a history of post-Vredefort (McCarthy *et al.*, 1986), and hence post-Bushveld Complex, uplift.

1.3.3 Post-Transvaal history of the Kaapvaal Craton

a) Basins

Soutpansberg basin

The Soutpansberg Group unconformably overlies the Archaean high-grade metamorphic rocks of the Limpopo belt and the Bushveld Complex on the northern edge of the Kaapvaal Craton. The Soutpansberg Group consists of two unconformity-bounded sequences preserved in a graben and comprises predominantly quartzite with some basalt (Cheney *et al.*, 1990). It attains a maximum thickness of approximately 5500 m (Cheney *et al.*, 1990). Rb-Sr results from the basalt formations yield ages of approximately 1974-1800 Ma (Cheney *et al.*, 1990) (Table 1.1).

Waterberg basin

The dominantly fluvial Waterberg Group, regarded as mid-Proterozoic in age, attains a maximum thickness of approximately 7000 m, and is exposed in the Warmbaths and Middelburg basins (Tankard *et al.*, 1982). The sequence comprises mostly sandstone with lesser conglomerate, with locally developed trachyte and quartz porphyry. It was deposited in gently subsiding intracratonic basins and rests unconformably on the Rooiberg Group, basement rocks, the Transvaal Supergroup, and on Bushveld Granite (Tankard *et al.*, 1982). The lower age limit of the Waterberg Group is given by the Nebo Granite of the Bushveld Complex (S.A.C.S., 1980), dated at 2054,4 ± 1,8 Ma (Walraven and Hattingh, 1993) (Table 1.1). A large gap in the sedimentary record of the Kaapvaal Craton exists between the

Waterberg Group and the Karoo Supergroup.

Karoo basin

The Palaeozoic to Mid-Mesozoic Karoo basin has an areal extent of ~550 000 km^2, and thus covers approximately half of South Africa and a large portion of the Kaapvaal Craton. Karoo Supergroup sedimentation commenced in the Carboniferous Period (360-290 Ma), and consists of a wide variety of sediments with diverse origins, including glacial, marine, lacustrine and fluvial (S.A.C.S. 1980). A foreland basin model has been proposed for the Karoo (Allen *et al.*, 1986), which had a history of tectonic subsidence (Cadle *et al.*, 1990) possibly related to orogenic pulses and the changing tectonic framework of Gondwana (Tankard *et al.*, 1982). Karoo deposition ceased with the advent of widespread Jurassic (210-140 Ma) rifting and volcanism (notably the extrusion of the Drakensberg basalts) associated with the breakup of Gondwana (Tankard *et al.*, 1982; Cadle *et al.*, 1990). This was accompanied by diabase intrusions, in the form of dykes and sills, through most of the Karoo Basin (Tankard *et al.*, 1982).

b) Orogenic events affecting the Kaapvaal Craton

Kheis orogeny

The approximately 2,1-1,9 Ga Kheis belt (Duane and Kruger, 1991) (Table 1.1) extends for approximately 400 km along the western boundary of the Kaapvaal Craton (Fig. 1.1, inset). The Kheis belt may continue beneath Karoo and Kalahari cover northward into Botswana, and may be correlated with the Magondi belt of northwestern Zimbabwe (Stowe, 1989, 1990). The Kheis belt is interpreted as a thin-skinned fold and thrust belt, with crustal shortening estimated at approximately 35-55 km, which owes it origin to an Early

Proterozoic orogenic belt to the west (Stowe, 1986; Beukes and Smit, 1987). The Kheis belt has been divided into three phases of fold and thrust deformation (Stowe, 1986). Six main tectonostratigraphic thrust sheets are separated by low-angle thrusts, dipping approximately 10° west, which deform the Transvaal Supergroup rocks (Stowe, 1986; Beukes and Smit, 1987). The Bushveld Complex was intruded early in the history of, and was subsequently deformed by, the Kheis orogenic cycle (Duane and Kruger, 1991).

The boundary between the Kheis belt and the adjacent Namaqua belt is marked by sudden stratigraphic, metamorphic grade, and structural changes (Stowe, 1986). Namaqua folds deform the Kheis belt (Stowe, 1986, 1989, 1990).

Kibaran orogeny

Extensive areas of Proterozoic high grade rocks adjacent to the Kaapvaal Craton constitute the Kibaran orogenic belt, which includes the so-called Natal, Namaqualand and Mozambique provinces (Tankard *et al.*, 1982). The Natal and Namaqua provinces, which comprise supracrustal paragneisses, orthogneisses, charnockites, granitic plutons and pegmatite belts (e.g. Hartnady *et al.*, 1985), bound the Kaapvaal Craton to the south and west (Fig. 1.1). Both these terranes have a plutonic-metamorphic history isotopically dated at between approximately 1,2-0,9 Ga (Table 1.1), and are generally believed to be continuous below the Karoo cover (Nicolaysen and Burger, 1965; Hartnady *et al.*, 1985; Thomas, 1989). The cessation of the Kibaran orogeny in southern Africa corresponds to ~950 Ma mineral cooling dates (Eglington *et al.*, 1989; Cornell *et al.*, 1992; Thomas *et al.*, 1993).

The Namaqua-Natal tectonic event involved thrust-related crustal shortening (e.g. Matthews, 1981; Daly, 1988), and at approximately 1 Ga the Namaqua-Natal belt was accreted onto the southern margin of the Archaean Kaapvaal Craton (e.g. Matthews, 1986; Jacobs *et al.*, 1993). The Natal Province involved thrust and nappe dominated tectonism (Matthews, 1981), with single event subduction-obduction collision (Matthews, 1972) or repeated, relatively small-scale, accretion tectonism (Thomas, 1989). Pb-Pb single zircon dates from granites of the Natal Province have shown that crustal melting due to early arc-continent collision occurred at approximately 1090 Ma, and subsequent granites were emplaced at approximately 1050 Ma (Thomas *et al.*, 1995).

The Kibaran orogenic cycle was a major, long-lived collisional tectonic event which may originally have been continuous from the Namaqua-Natal metamorphic province in southern Africa to the similar metamorphic belts in western Dronning Maud Land, East Antarctica (e.g. Martin and Hartnady, 1986; Jacobs *et al.*, 1993).

Pan-African orogeny

The Pan-African orogeny resulted in tectonothermal overprinting in several fold belts around the margins of the Kaapvaal Craton from 600 - 450 Ma in Gondwanaland (Table 1.1). Pan-African thermal and structural overprinting affected Kibaran basement rocks of the Namaqua belt (e.g. Clifford *et al.*, 1990), Kibaran rocks of East Antarctica (Grantham *et al.*, 1991) and the Mozambique belt (Sacchi *et al.*, 1984), although not the rocks of the Natal belt (Eglington *et al.*, 1989; Thomas *et al.*, 1993).

c) Vredefort Dome

The Vredefort Dome is located approximately 120 km southwest of Johannesburg, in the geographic centre of the Witwatersrand basin (Fig. 1.1). This more or less circular structure is surrounded, on its northern and western flanks, by overturned and steeply dipping strata belonging to the Dominion Group and the Witwatersrand, Ventersdorp and Transvaal Supergroups. The southeastern sector of the structure is obscured by Karoo cover.

The Vredefort Dome has a core composed of Archaean granite gneiss, greenstone schists and amphibolite (e.g. Stepto, 1990). The diameter of the core is approximately 40 km, and the estimated original diameter of the structure may have been in the order of 190-300 km (Therriault *et al.*, 1995). Deformation of the Pretoria Group (Transvaal Supergroup) during the formation of the rim synclinorium and collar of the Vredefort Dome (Simpson, 1977) clearly implies that the Vredefort Dome formed after the deposition of the Transvaal Supergroup. Uncertainty concerning the origin of the dome has, in the past, initiated extensive debate. Prominent theories on its formation, outlined by Reimold (1993) include:

a) the result of an asteroid impact (e.g. Dietz, 1961);

b) a consequence of an internally triggered catastrophic gas explosion (e.g. Nicolaysen, 1972);

c) the end product of one or several tectonic processes including thrusting and doming (Du Toit, 1954); or

d) the result of diapiric doming (e.g. Brock and Pretorius, 1964).

A catastrophic impact origin for the Vredefort Structure is, however, almost universally accepted today (Therriault *et al.*, 1995).

Granophyre within the Vredefort Dome has been interpreted as a melt rock which formed as a direct result of the event responsible for the formation of the Dome (e.g. Walraven *et al.*, 1990). The phenomenon resulting in this Dome seems to have occurred between 1950 and 2050 Ma, as determined from zircons and micas from the granophyre (Walraven, *et al.*, 1990). SHRIMP data on zircon from the granophyre, however, place the Vredefort event at 2102 +101/-109 Ma (courtesy of W. Compston and L.O. Nicolayson, in Walraven *et al.*, 1990) while a single zircon age determination of 2002 Ma has been calculated (based on single grain zircon data presented by Walraven *et al.* (1990) (Table 1.1). More recent studies by Trieloff *et al.* (1994) place the timing of the Vredefort event at 2006 ± 17 Ma based on ^{40}Ar-^{39}Ar stepheating from pseudotachylites from the Witwatersrand goldfields. Kamo *et al.* (1995) have dated zircons in pseudotachylite from the Vredefort Structure at ca. 2024 Ma using the U-Pb technique (Table 1.1). This date has, however, been further constrained to 2025 ± 4 Ma (W.U. Reimold, pers. comm.). They interpret their result as the definitive age of the impact event which formed the Vredefort Structure.

The evidently catastrophic emplacement mechanism for the Vredefort Dome resulted in severe deformation of the Witwatersrand, Ventersdorp and Transvaal Supergroup rocks (McCarthy *et al.*, 1986; Reimold, 1993). There are various structures locally and regionally developed which are concentrically arranged around the Vredefort Dome as a result of its formation (McCarthy *et al.*, 1986). These include folds as well as normal, reverse and strike-slip faults around the northern and western margins of the Dome (Simpson, 1977; Colliston and Reimold, 1992). Simple-shear induced cleavage, folds and bedding parallel shear zones in the Witwatersrand and Transvaal Supergroup lithologies, verging out of the Witwatersrand basin, led McCarthy *et al.* (1986) to credit significant post-Transvaal compressional and

extensional deformation in the Witwatersrand basin to the formation of the Vredefort Dome.

d) Johannesburg Dome

The Johannesburg Dome, located immediately north of Johannesburg (Fig. 1.1), exposes part of the granite-greenstone basement of the region, and is unconformably overlain by the Witwatersrand and Transvaal Supergroups. This dome-like feature occupies an area of approximately 700 km^2 (Anhaeusser, 1973). The rocks comprising this structure have been dated at 3173 +9/-8 Ma, based on U-Pb zircon analysis (Anhaeusser and Burger, 1982), which is consistent with the 3120 $\pm$ 5 Ma age determined by Armstrong *et al.* (1991) for the age of the basement to the Dominion Group (Table 1.1).

The Johannesburg Dome is thought to have had a history of periodic uplift during the Proterozoic (Eriksson, 1977). The tilt of the Black Reef Quartzite Formation, the Chuniespoort Group, and the Pretoria Group off the Johannesburg Dome may have been a result of the emplacement of the dome, which constrains the doming event to post-Transvaal times (McCarthy *et al.*, 1986; Hilliard, 1994). More specifically, the doming event dispersed cleavages and reactivated structures attributed to the emplacement of the Vredefort Dome, and thus uplift of the Johannesburg Dome post-dated the Vredefort event (McCarthy *et al.*, 1986), which occurred approximately 2025 Ma ago (W.U. Reimold, pers. comm.).

Roering (1986) interpreted the Johannesburg Dome as a north-verging imbricate stack. Roering (1984; 1986) and Hilliard (1994) propose that the entire Johannesburg Dome has been affected by prominent northerly verging thrusting. However, Roering (1986) did not take into account the effects of the doming event and the subsequent tilting of the overlying

strata. Correcting for the effects of doming would restore the north-verging shear zones along the northern margin of the Johannesburg Dome to their original orientation, which is sub-vertical. Northerly-verging thrusting proposed by Roering (1984, 1986) and Hilliard (1994) may thus be inaccurate. The age of this shearing has, nonetheless, been constrained to post-Platberg, pre-Black Reef Quartzite Formation times (Roering, 1984, 1986; Roering *et al.*, 1990).

Several large-scale faults or "crush zones" (with vertical and with right-lateral wrench components), the most prominent of which trend north-east, cross-cut the Johannesburg Dome (Anhaeusser, 1973). These structures frequently extend into the lower formations of the adjacent Transvaal Supergroup (Anhaeusser, 1973).

e) Intrusive events

Several intrusive events of variable magnitude have affected the Kaapvaal Craton. The most significant of these events gave rise to the Bushveld Complex.

Bushveld Complex

The 6-9 km thick Bushveld Complex, which presently covers an area of about 65 000 km^2, is regionally discordant within the Transvaal Supergroup (S.A.C.S., 1980). The original extent of the Bushveld Complex was far greater than at present, and its southern margin may have extended at least as far as the Losberg Complex in the presently-exposed northern Witwatersrand basin (Coetzee and Kruger, 1989). The rocks of the Bushveld Complex range in composition from ultramafic to acid, and have been classified into three suites, namely, the mafic and ultramafic Rustenburg Layered Suite, the Lebowa Granite Suite and the

Rashoop Granophyre Suite (S.A.C.S. 1980). The Bushveld Complex may be related to several other intrusions, such as the Losberg Complex north of the Vredefort Dome, and the Phalaborwa Complex, both of which yield similar ages (Walraven *et al.*, 1990). The Bushveld Complex granites and basic layered rocks were emplaced between approximately 2061 ± 21 Ma, based on $^{87}Sr/^{86}Sr$ data from the basic layered rocks, and 2054 ± 4 Ma, derived from Pb-Pb whole rock analyses on the later granites (Walraven *et al.*, 1990; Walraven and Hattingh, 1993) (Table 1.1)

The magmas of the Bushveld Complex may have intruded as a result of continuous basin subsidence involving Transvaal Supergroup rocks (Sharpe and Snyman, 1980), although an impact origin for the complex has been also proposed (e.g. Elston, 1995). The basic rocks may have been emplaced as a series of pulses (Walraven, 1981), intruded into the volcano-sedimentary units of the Transvaal Supergroup at a late stage in the subsidence of this basin, possibly as a result of multi-stage conical fracturing of the crust (Sharpe *et al.*, 1981). Evidence from similar magmas beneath and within the Rustenburg Layered Suite, however, points to the synchronous emplacement of the Rooiberg felsite, granophyres, granites and mafic intrusives of the Bushveld Complex (Schweitzer and Hatton, 1995), while age data show that this magmatic activity occurred in a time-span covering only 7 Ma (Walraven, 1995, in press).

The intrusion of the Bushveld Complex resulted in deformation and metamorphism of the Transvaal Supergroup floor rocks, as well as some units of the Bushveld Complex (Sharpe and Chadwick, 1982). Several fragments of the Transvaal Supergroup are preserved within, and metamorphosed by, the Bushveld Complex (e.g. the Marble Hall and Crocodile River

Fragments) (Sharpe and Chadwick, 1982).

Pilanesberg Alkaline Complex

The Pilanesberg Alkaline Complex occurs approximately 160 km northwest of Johannesburg (Fig. 1.1), and is located within the Bushveld Complex. The roughly circular Pilanesberg Complex has a diameter of about 25 km, and has been dated at approximately 1400 Ma (Tankard *et al.*, 1982) (Table 1.1), although geochronological data point to igneous activity having occurred from Precambrian to Upper Jurassic times (Ferguson, 1973). This period of major igneous activity resulted in intrusions, pipes and irregular plugs of kimberlite and carbonatite (Ferguson, 1973), as well as basic to intermediate dyke swarms (Haughton, 1969). The syenitic and diabase dyke swarms extend from this complex on a bearing of approximately 150°, and are traceable over long distances (Haughton, 1969).

Karoo igneous activity

Fragmentation of Gondwanaland was initiated by separation of East and West Gondwanaland (Norton and Sclater, 1979), possibly as early as the late Carboniferous (Kent, 1974). From the late Triassic to the early Cretaceous a significant igneous event affected the fragmenting Gondwanaland, involving extrusion of flood basalts as well as the emplacement of dykes and sills (Eales *et al.*, 1984). The Karoo dykes display non-uniform distribution within the Karoo strata and underlying pre-Karoo rocks, and are often concentrated in prominent swarms (Eales *et al.*, 1984). It is likely that the bulk of Karoo igneous activity occurred in the lower Jurassic, although lesser igneous activity may have continued until middle and upper Jurassic times (Eales *et al.*, 1984).

CHAPTER 2

LOCAL STRATIGRAPHY

2.1 Introduction

The study area is underlain by rocks of the Transvaal Supergroup north of the Johannesburg Dome (Fig. 1.1). The Transvaal Supergroup comprises, at its base, the siliciclastic Black Reef Quartzite Formation, which is overlain by the predominantly carbonate Chuniespoort Group, and an upper clastic succession (the Pretoria Group) (Fig. 1.2). The Transvaal Supergroup in the study area unconformably rests on the basement granite-greenstone lithologies exposed in the Johannesburg Dome to the south. In the north, it is overlain by the intrusive rocks of the Bushveld Complex. The stratigraphy of the Chuniespoort Group in this area has been described, in detail, by Eriksson and Truswell (1974). In this chapter, brief descriptions of the lithologies in the study area are presented.

2.2 Stratigraphy of the study area

2.2.1 Basement lithologies

The basement rocks exposed in the Johannesburg Dome immediately south of the study area are highly weathered and outcrop is extremely limited. For this reason, no description of the basement rocks adjacent to the study area is given. Anhaeusser (1973), however, gives detailed descriptions of basement lithologies exposed in other parts of the Johannesburg Dome. The basement comprises granitoids with greenstone remnants, as well as widespread xenoliths of talcose schist, serpentinite and amphibolite. The granitoids are intrusive into the greenstone remnants, and have been classified by Anhaeusser (1973) as:

a) a tonalite-trondjhemite gneiss, which occurs mostly in the southern portion of the Johannesburg Dome;

b) relatively undeformed and unmetamorphosed granodiorite, which crops out in the southern and central areas of the Johannesburg Dome; and

c) migmatite gneiss, interpreted as the product of metamorphism of tonalite-trondjhemite gneiss, which occurs in the northern part of the Johannesburg Dome.

In the central part of the Johannesburg Dome, Maeusser (1973) also recognised a lithology that is transitional between the southern granodiorite and the northern migmatite gneiss.

2.2.2 Black Reef Quartzite Formation

In contrast to the rocks of the Johannesburg Dome, the overlying, largely clastic, Black Reef Quartzite Formation is resistant to weathering. It forms a prominent scarp, striking approximately east-west along the southern boundary of the study area, and a dip slope which is inclined approximately 20° to the north. The average thickness of the formation is approximately 10-15 m, and locally in the study area it attains a maximum thickness of approximately 30 m. The stratotype thickness of the Black Reef Quartzite Formation, west of Swartkops, is 24 m (Eriksson and Truswell, 1974).

The Black Reef Quartzite Formation in the study area comprises coarse-grained quartzite at its base, which grades upwards to finer-grained quartzite. No lenses of conglomerate, as described in S.A.C.S. (1980), were encountered in the study area, although pebble lags are sporadically developed. Cross-bedding, while not usually strikingly obvious, is nonetheless common. Ripple marks are occasionally preserved.

Overlying the basal quartzite is a dark grey slate unit, in the order of 2 - 3 m thick. A variably developed penetrative cleavage is characteristic of this slate unit. An upper quartzite layer, with similar characteristics to the basal quartzite, overlies this slate. Another 2-5 m thick, dark-grey slate unit with heterogeneously developed cleavage occupies the succeeding stratigraphic position. Intercalated with this slate are thin, massive, dolomite lenses which become progressively more abundant and more continuous upwards. The weathered surfaces of these dolomite layers are dark chocolate brown, possibly a result of high manganese content.

2.2.3 Chuniespoort Group

The majority of carbonate units in the study area lack suitable definitive features, such as marker horizons. The Oaktree, Rietfontein, Tweefontein and Fountains Formations are the only formations of the Chuniespoort Group in the study area which can be correlated with any degree of confidence to the stratotype formations of the Malmani Subgroup described by Eriksson and Truswell (1974). In addition to this, the probability exists that not all of the formations described from various type areas (Eriksson and Truswell, 1974) are developed in the study area. However, summary descriptions of the formations, in stratigraphic order (as per Eriksson and Truswell, 1974), are given below (Fig. 2.1) and correlations made, where possible, with units that occur in the study area.

a) Oaktree Formation

The exact limits of the Oaktree Formation were not clearly identified in the study area. Above the "chocolate" dolomite layers of the Black Reef Quartzite Formation, the dolomite grades to dark, greyish-brown, and then to lighter grey.

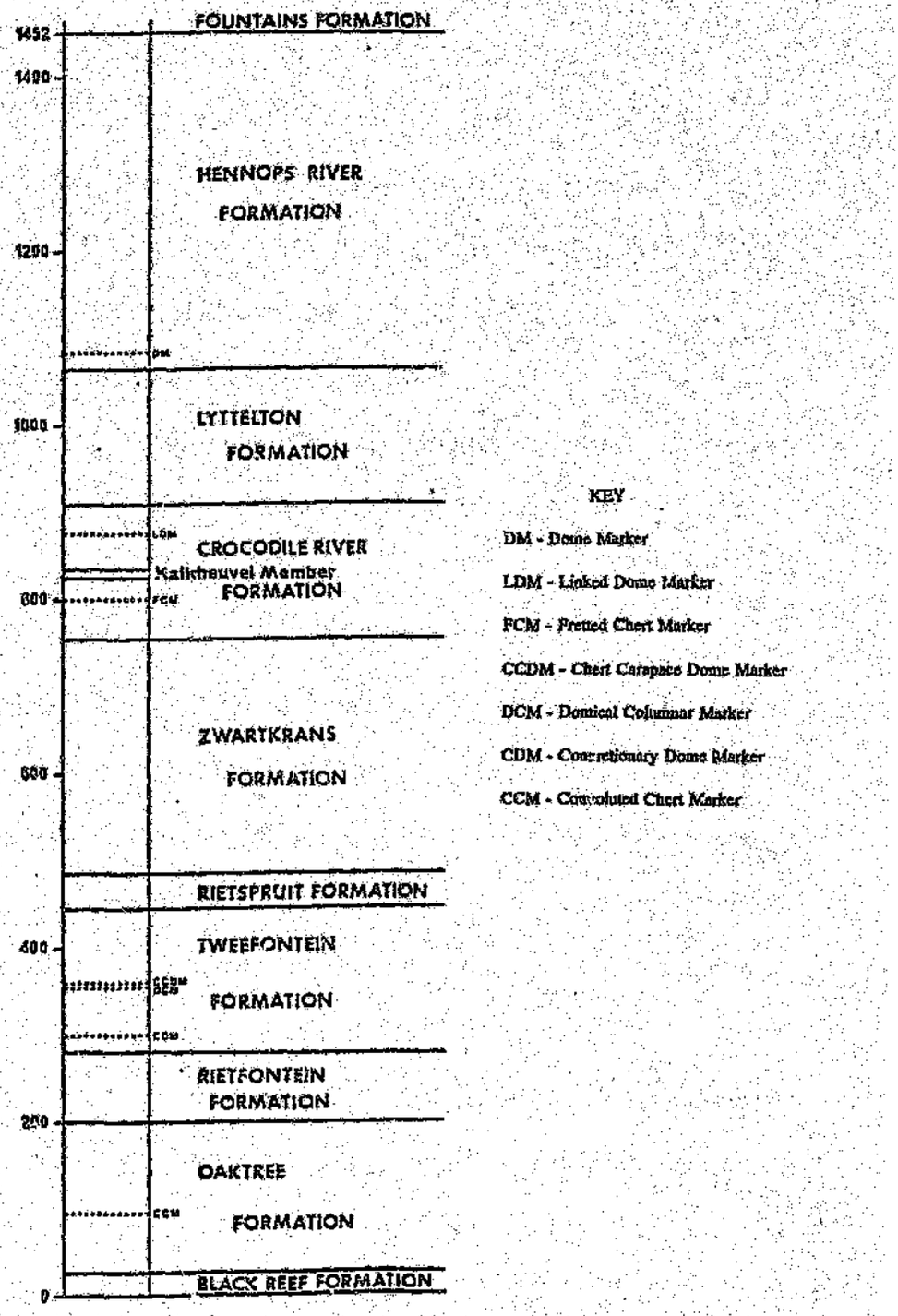

Fig. 2.1 Stratigraphic column of the Malmani Subgroup, Chuniespoort Group, northwest of Johannesburg in the vicinity the study area (after Eriksson and Truswell, 1974).

The convoluted chert marker (CCM) forms an important marker in the light-coloured dolomite of the Oaktree Formation (Fig. 2.1). In the study area it attains a thickness of 2-3 metres, and is characterised by the development of chert and convoluted stromatolite domes. The layer forms a positive relief feature, with the result that it is often traceable on aerial photographs. In the type area, Eriksson and Truswell (1974), described the CCM as convoluted with occasionally overturned domes, and having the only appreciable chert in the Oaktree Formation. Above the light grey dolomite containing the CCM is a thin layer of dark brown dolomite, which becomes lighter with increasing stratigraphic height. Macroscopic needles of tremolite are locally developed adjacent to a sill in the dark brown dolomite.

b) Rietfontein Formation

The gradational boundary between the Oaktree Formation and the overlying Rietfontein Formation is the appearance of chert (Eriksson and Truswell, 1974). The weathered surface of the dolomite overlying the CCM remains light grey, although the amount of chert present increases. The chert exists as layers up to several centimetres thick, commonly displaying preserved symmetrical ripple marks with wavelengths of the order of several centimetres. Domes with diameters usually less than 1 metre (Fig. 2.2) commonly occur but do not constitute suitable marker layers as they are not laterally persistent. Ooids (spherical calcareous accretionary bodies (Lapidus, 1987)) are abundant, although irregularly distributed, in the light grey dolomite. They usually display reverse grading, and are often deformed (Section 3.3.3).

Eriksson and Truswell (1974) described a silicified chert breccia with some shaly matrix which occupies part, or all, of the uppermost 5 m of the Rietfontein Formation. A 1-4 m

thick chert breccia with slaty matrix (Fig. 2.3) in the study area has been correlated with the chert breccia documented by Eriksson and Truswell (1974). The name "slaty chert-breccia" (SCB) was adopted for this unit in the study area. The SCB is matrix-supported, and has highly angular, unevenly distributed, unsorted, clasts of chert which vary from several millimetres to more than 20 centimetres in size. At some localities, the breccia is devoid of clasts, and resembles homogeneous fine-grained slate rather than breccia. The fine-grained matrix is characterised by a penetrative planar fabric and fractures, which possibly originated as a result of intense deformation. Examination of thin-sections shows a very fine-grained, quartz-phyllosilicate (chlorite, micas) matrix. The lateral persistence of this breccia makes it a useful marker. Compositional layering is discernible to discern, however, and bedding orientation data from this marker is characteristic pinkish-brown grass grows preferentially on the SCB.

c) Tweefontein Formation

The Tweefontein Formation, in its type-area west of Swartkops, comprises 163 m of light-grey dolomite with abundant chert, and at least three markers (Eriksson and Truswell, 1974). The stratigraphically lowest marker in the Tweefontein Formation in the study area is hosted in chert-rich grey dolomites, up to 30 metres stratigraphically above the SCB. This marker comprises relatively large domes, which often exceed one metre in height. Eriksson and Truswell (1974) term this the concretionary dome marker (CDM), which they describe as linked elongate, steep-sided domes, with approximate dimensions of 1,5 x 5 x 1 m. This important marker can be traced over long distances on aerial photographs.

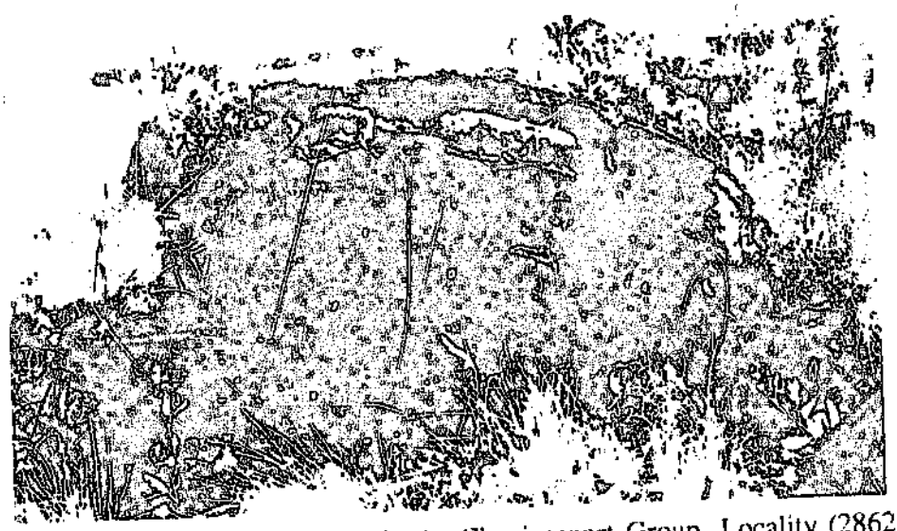

Fig. 2.2 Stromatolite dome developed in the Chuniespoort Group. Locality (2862,1 X; -96,8Y) (see Appendix 1 for explanation of the co-ordinate system). Looking west.



Fig. 2.3 Chert breccia with slaty matrix (SCB). Note the angularity of the clasts, their large variation in size, as well as their irregular distribution. Locality (2861,6 X;-95,0Y).

Several tens of metres stratigraphically above the CDM, the domical columnar marker (DCM) is developed, which consists of large stromatolite domes overlapping small columns (up to 40 cm high) which, in turn, overlie linked domes (Eriksson and Truswell, 1974). An important characteristic of the DCM is the presence of chert with a distinctive "honeycomb" texture, (or "fretted appearance" (Eriksson and Truswell, 1974)). The DCM is observed on aerial photographs, but the marker is not as extensively developed as the CDM.

In the Rietfontein Formation type-area, the chert carapace dome marker (CCDM) lies immediately above the DCM (Eriksson and Truswell, 1974). This marker constitutes flat-topped, steep-sided, large, elongate domes capped by a thick chert carapace (Eriksson and Truswell, 1974). In the study area, the CCDM occurs no more than 5 m above the CDM. The CCDM, defined by large domes and thick chert layers, is not as reliable as the other markers because of its more massive nature and lateral impersistence. Above the CCDM, a brecciated chert defines the upper limit of the Tweefontein Formation (Eriksson and Truswell, 1974).

d) Rietspruit Formation

This approximately 40 m thick formation comprises colour-banded dolomite, and is characterised by predominant columnar stromatolites and scattered quartz and calcite crystals. A silicified chert breccia defines its upper boundary (Eriksson and Truswell, 1974).

e) Zwartkrans Formation

This formation attains, in places, a thickness of up to nearly 270 m (Eriksson and Truswell, 1974). It is made up mostly of coarse, recrystallised dolomite with discontinuous chert

layers. It contains at least eight chert breccias, as well as oolitic, stromatolitic, and ripple mark layers. The upper boundary of the formation is defined by a regionally persistent chert breccia (Eriksson and Truswell, 1974).

f) Crocodile River Formation

This approximately 150 m thick formation comprises mainly dolomite with two markers - the fretted chert marker (FCM) and the linked dome marker (LDM). A series of shales, often associated with chert breccia, and stromatolite horizons are also evident. The top of this formation is marked either by a single breccia sheet, or by a series of breccia lenses in dolomite (Eriksson and Truswell, 1974).

g) Lyttelton Formation

The thickness of this formation at the type-area is 155 m, and it consists primarily of chert-free, dark dolomite with large, elongate stromatolitic mounds developed throughout the formation (Eriksson and Truswell, 1974).

h) Hennops River Formation

Much of this approximately 390 m thick formation is exposed on the scarp slope of the Schurweberg hills (between Maps 1 and 2). The Hennops River Formation comprises mostly chert-bearing light-grey dolomite. Oolites, stromatolites, a dome marker (DM), breccias and ripple marks occur at various levels of this formation (Eriksson and Truswell, 1974).

i) Fountains Formation

The Fountains Formation transgresses much of the Hennops River Formation (Eriksson and Truswell, 1974). It comprises a thick chert breccia which represents a residual accumulation of chert rubble, resulting from regional basin uplift during Chuniespoort Group times (Eriksson and Truswell, 1974). This breccia cuts back for up to 400 m through the stratigraphy, and is probably related to localised uplift (Eriksson and Truswell, 1974). The Schurweberg hills in the study area, immediately north of the Hennops River, are capped by a laterally persistent, more than 30 m thick, chert breccia (Fig. 2.4) which rests unconformably on the underlying dolomite (Fig. 2.5). This breccia is correlated with the Fountains Formation.

j) Remaining carbonate lithologies

A general description of the carbonate units in the study area that could not be correlated with to the type-area descriptions of Eriksson and Truswell (1974) is included in this section.

The dolomite lithologies of the study area are characterised by the presence of occasional concentrations of oolitic layers and lenses, abundant chert, ripple marks, and the development of small, scattered quartz and calcite crystals. North of the Schurweberg hills (Map 2), the dolomite generally possesses a grey weathered surface, although fresh surfaces are blue-grey, grading in places to pink and reddish-pink. The pink dolomite is coarsely crystalline and has poorly defined, irregular, boundaries with the grey dolomite. It is frequently found in the vicinity of fault zones. It may thus be related to localised alteration attributable to fluid flow along fault planes.



Fig. 2.4 Fountains Formation chert breccia situated on top of the Schurweberg hills. Locality (2859,0 X; -93,1 Y).

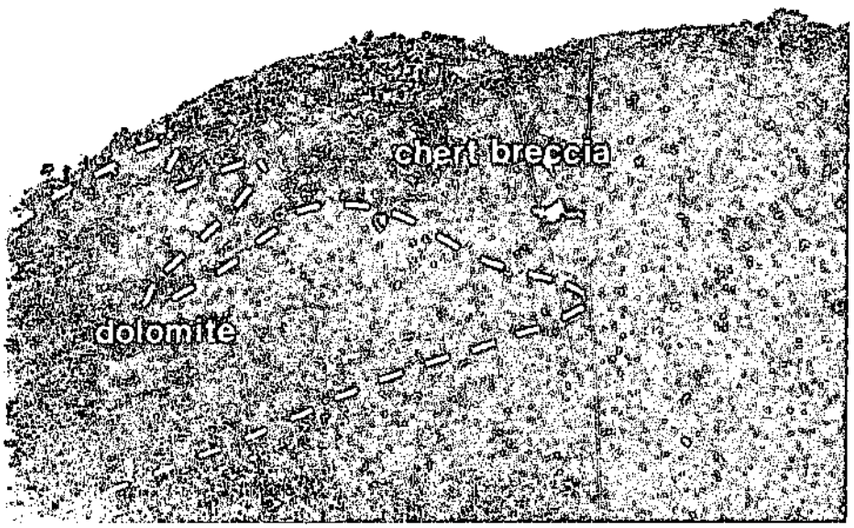

Fig. 2.5 The unconformable relationship of the Fountains Formation chert breccia with the Hennops River Formation dolomite. Locality (2857,4 X; -93,0 Y). Looking west.

In the dolomite succession, especially north of the Schurweberg hills, breccias are occasionally developed. These breccias typically comprise irregular chert, marble and dolomite clasts in a predominantly carbonate matrix. Clasts are generally sub-angular to sub-rounded, and range from millimetres to more than 10 centimetres in diameter.

A continuous band of massive chert, 3-7 metres thick and conformable with bedding, crops out a few metres below the contact of the Chuniespoort Group with the Pretoria Group. Sub-rounded, randomly orientated breccia clasts up to several centimetres in diameter occur occasionally in this unit. A bedding sub-parallel shear zone is hosted within this chert layer with a foliation so intense that the rock resembles slate.

2.2.4 Pretoria Group

In the study area, the Pretoria Group lies unconformably on the Chuniespoort Group, consistent with the relationship observed regionally (S.A.C.S. 1980). The Pretoria Group comprises essentially shale and quartzite with a prominent volcanic unit (the Hekpoort Andesite Formation), and minor conglomerate, chemical and volcanic members (S.A.C.S., 1980). The structural mapping in the Pretoria Group in the study area (i.e. up to the northern boundary of the Pelindaba property, Map 2) was largely confined to the Rooihoogte and Timeball Hill Formations (Fig. 1.2). According to S.A.C.S. (1980), these formations comprise numerous breccia, shale, conglomerate, ferruginous quartzite and diamictite units (Fig. 1.2), however, not all these units were encountered in the study area.

Slate units, which vary from grey to yellowish-brown, are by far the most abundant rock-type of the Pretoria Group in the study area. They preserve well-defined, finely-laminated

bedding, and are cross-cut regionally by a single, heterogeneously developed cleavage. In places, more than one cleavage may be present (Section 3.2).

The lowermost quartzite layers intercalated with the slate units are dark, fine grained, and reach a maximum thickness in the order of 30-40 centimetres. Higher in the stratigraphy, quartzite units are much thicker, and tend to form prominent east-west trending ridges rising several tens of metres above the surrounding countryside. These quartzite units display variable grain-size, colour, mineralogy and magnetic properties. They range from medium- to fine-grained, and vary from grey-white to reddish-brown and black. Their mineralogy ranges from almost pure orthoquartzite (for the lighter coloured units) to quartzite containing several percent magnetite and other heavy minerals (for the darker units). Trough-cross bedding structures are occasionally developed in the quartzite, but planar-cross bedding structures were not observed.

A thin layer of magnetic iron-rich mineralised breccia is situated in close proximity to a well-defined bedding sub-parallel shear zone. It is matrix-supported with angular to sub-rounded clasts varying in size from millimetres to several centimetres. The matrix comprises red, clastic material, with quartz veins and specular hematite. It is not laterally continuous, and pinches out after several hundred metres along strike.

2.2.5 Sills

Numerous sills have intruded the Transvaal Supergroup in the study area. The sills display concordant relationships with bedding and have been deformed together with the sedimentary units. Determining the origin and age of the sills thus places important constraints on the

absolute timing of deformation. For this reason, the investigation of sills in the study area has been entered into in some detail.

a) Previous work

In the Lydenburg area of the eastern Transvaal, a wide variety of mafic sills intrude the entire 12 km thick Transvaal Supergroup, increasing in frequency towards the contact with the Bushveld Complex (Sharpe, 1984). These sills may constitute up to 20 % of the total stratigraphic thickness in this area (Sharpe and Snyman, 1980). Sharpe and Snyman (1980) proposed a model for sill emplacement in the eastern Bushveld Complex where sills were emplaced during basinal subsidence prior to the intrusion of the mafic phase of the Bushveld Complex, some 8 km below the surface.

Two types of sill were identified by Willemse (1959) following studies in the eastern Transvaal (Table 2.1). The first was termed the Lydenburg type (amphibolite) sills, and the second, the Maruleng type (noritic) sills. The Lydenburg type sills were metamorphosed in the greenschist facies and were considered to represent the gabbroic parental magma of the Bushveld Complex, whereas the Maruleng type, probably originally of Lydenburg type, were interpreted as having been contaminated by the country rock. These sills attain pyroxene-hornfels facies (Willemse, 1959). Frick (1973) identified four sill types south of Willemse's working area (Table 2.1). According to him, the first group of (dioritic) sills pre-dated the Bushveld Complex. The second group of sills comprises a differentiated sequence (harzburgite - pyroxenite - norite - quartz-norite), the third comprises hybrid dolerites with metasedimentary inclusions, and the fourth, diabase.

Table 2.1 Summary of previous work done on sills in the Bushveld Complex floor.

Relative Timing	Willemse(1959)	Frick (1973)	Cawthorn et al. (1981)	Sharpe (1981)	Sharpe (1984)	Engelbrecht (1990a)
Pre-BC*	Lydenberg Type (amphibolitic) sills	Dioritic sills	Metadolerite sills	Amphibolite sills	Amphibolitized microgabbro sills (containing tremolite, hornblende, talc and serpentine)	Diabase (amphibolite) sills
Syn-BC*	Mamleng Type (noritic) sills	Differentiated, hybrid dolerite and diabase sills	Norite-Pyroxenite and hypersthene microgabbro sills		Pyroxenitic and gabbroic sills	Noritic sills
Post-BC*			? Dolerite sills?	Waterberg dolerite and gabbronorite sills		
Region	eastern Transvaal	eastern Transvaal	central Transvaal	eastern Transvaal	eastern Transvaal	western Transvaal

Note: BC = Bushveld Complex

Sharpe (1984), from extensive studies in the eastern Bushveld, identified two predominant sill types (Table 2.1). The older, pre-Bushveld sills, are distributed throughout the Transvaal Supergroup, and are altered to varying degrees by thermal and burial metamorphism (Sharpe, 1981; 1984). The pre-Bushveld Complex sills have been divided into three main classes: 1) sills containing hornblende > tremolite; 2) sills containing tremolite > hornblende; and 3) sills containing talc and serpentine. Their petrography is extremely variable, but they are characterised by amphibolitic assemblages with *no* fresh orthopyroxene. The second sill-type comprises the younger, syn-Bushveld group which is divided into pyroxenitic and gabbroic compositions, both of which are further sub-divided (Sharpe, 1984). Almost all of the syn-Bushveld sills are essentially unaltered, and contain abundant pristine or only slightly altered orthopyroxene. The syn-Bushveld sills in the eastern Transvaal preserve pristine igneous mineralogy, while the pre-Bushveld sills do not. The pre-Bushveld sills were intruded as pyroxenites and gabbros, and were metamorphosed, prior to Bushveld Complex intrusion, at albite-epidote facies, resulting in amphibolites (Sharpe, 1981). They have primarily been altered by autometamorphism (due to the close proximity of water-rich sediments (Sharpe, 1982)) during intrusion, which was later overprinted by greenschist facies burial metamorphism prior to Bushveld Complex emplacement (Sharpe, 1981). Bushveld-induced metamorphism played only a small part in their alteration (Sharpe, 1981).

In the eastern Transvaal, Sharpe (1984) also identified a later group of mafic sills. These sills have similar compositions to a set of sills intruding the Waterberg Group, identified in an earlier study by Sharpe (1981).

Cawthorn *et al.* (1981) identified four distinct ages of sills which have intruded the floor

rocks of the south-western Bushveld Complex in the central Transvaal (Table 2.1). The first comprises amphibolitised metadolerites which predate the Bushveld Complex, while another two (norite and pyroxenite, and hypersthene microgabbro) are related to the Complex, and a fourth (dolerite) shows no obvious relationship to the Bushveld Complex. Cawthorn *et al.* (1981) correlate the metadolerite sills with the Lydenburg type sills of Willemse (1959). The metadolerite sills are widespread throughout the Transvaal Supergroup, whereas the hypersthene microgabbros, norites and pyroxenites have only been located in the Pretoria Group near the contact with the Bushveld Complex (Cawthorn *et al.*, 1981). The metadolerite sills are metamorphosed whereas the main layered sequence of the Bushveld Complex is not, and as they intrude all strata of the Transvaal Supergroup, they must have been emplaced post-sedimentation but pre-emplacement of the Bushveld Complex (Cawthorn *et al.*, 1981). The metadolerites are the only sills documented by Cawthorn *et al.* (1981) that have chilled margins. Those sills associated with the Bushveld Complex typically lack chilled margins, have coarse grain sizes, are heterogeneous, and are able to melt country rock xenoliths (Cawthorn *et al.*, 1981). The sills without chill-margins were thus probably intruded into relatively hot country rocks, which facilitated slower cooling. In contrast, the metadolerites (with chill margins) must have been intruded into colder rocks (Cawthorn *et al.* 1981).

Engelbrecht (1990a), working on the Transvaal Supergroup floor rocks of the Bushveld Complex in the western Transvaal, identified two chemically similar, though petrographically distinct, tholeiitic basalt sill types, namely amphibolites (diabases) and norites (Table 2.1). The two types of sill of the Marico Hypabyssal Suite identified by Engelbrecht (1990a) are the Lydenburg type diabase of Willemse (1959), which intruded further from the contact of the Rustenburg Layered Suite (RLS), and the Maruleng type norite of Willemse (1959),

closer to the contact of the RLS. The sills intruded throughout the Transvaal Supergroup in this area, the diabases forming from norites by hydration reactions during Bushveld Complex metamorphism (Engelbrecht, 1990a). Engelbrecht (1990a) found, by comparison of geochemical data with other workers, that the diabase and norite sills adjacent to the western Bushveld Complex are chemically similar to those associated with other parts of the Bushveld Complex.

b) Characteristics of sills in the study area

Sills intruded in the mostly dolomite series of the Chuniespoort Group, especially south of the Schurweberg hills, are far more numerous than the sills intruded in the clastic sediments of the Pretoria Group in the study area. Several sills encountered in the Chuniespoort Group sediments exceed 10 m in thickness. In places, the sills crop out extensively, although their presence is more typically indicated by the presence of deep, red soils which have previously been utilised in agriculture. Most of these sills are highly weathered, making sill identification and comparisons difficult. In hand specimen, the rocks show a variation in grain size from fine- to medium-grained, often over short distances within the same sill. Grain size variations are also evident between sills. Relatively fresh sill samples have a dark grey to greenish colour in hand specimen, whereas the more altered sills are brown to buff-yellow. White feldspar, and occasionally rarer pink feldspar, is often discernable in the sills sampled.

Mineralogically, the compositions of the sills are fairly consistent. Investigation of thin sections cut from sill samples reveals more clearly their altered nature. Only one sill sampled from the study area has a primary igneous texture (Map 1, locality 2859,6 X; -94,5 Y). The

unaltered texture of this sill implies that it has probably not been affected by any major metamorphic event, and may thus be more recent than other sills encountered in the study area. The remainder of sills sampled display no primary igneous textures, and their mineralogy has been altered by metamorphism. The dominant mafic mineral observed in thin section is actinolite, probably an alteration product of clinopyroxene. Hornblende content is variable. It usually occurs as anhedral interstitial grains. Tremolite is scarce. Orthopyroxene is conspicuously absent from these sills. Plagioclase feldspar is ubiquitous in all sill thin-sections examined, although it is altered (saussuritised) to varying degrees. Quartz, white mica (muscovite), talc and carbonate minerals occur in minor amounts. Sulphides are present in varying proportions in some samples, contributing a minor percentage. Mineralogically, the sills resemble metadolerites, which may have been exposed to some significant external heat source, the most likely candidate being the Bushveld Complex.

In the study area, few sills were encountered in the rocks of the Pretoria Group. These sills vary markedly in terms of grain size, colour, thickness and distribution from those lower in the stratigraphy. The Pretoria Group sills encountered are usually no more than one metre thick and are light khaki in colour. Their homogenous, very fine-grained mineralogy precludes identification. They do not crop out extensively and field relationships are difficult to determine.

c) Comparison of sills in the study area with sills from other parts of the Bushveld floor

X-ray fluorescence geochemical analyses of sill samples from the Chuniespoort Group were undertaken in order to determine major element proportions (Appendix 2). Sampling was carried out on sills from the Chuniespoort Group rather than on sills from the Pretoria Group

as the majority of large-scale structures (notably folds and bedding sub-parallel shears) affecting the sills are best observed in the Chuniespoort Group (Sections 3.3 and 3.4), the country rock-sill contact relationships are relatively distinct, and sill outcrops are more extensive than in the lower Pretoria Group. Comparison of the geochemical data with other published sill geochemical data is presented (Table 2.2) in an attempt to establish the origin of the sills which occur in the study area.

Table 2.2 shows the published major element abundances of sills from various parts of the Bushveld Complex floor, compared with the average major element abundance of sills from the study area. The sills from the study area have similar chemical compositions to most sills analyzed by previous workers. However, the total Fe, and especially TiO_2 contents of the average sill of this study are significantly higher, and the MgO and CaO contents substantially lower, than most. These abundance differences are, nonetheless, similar to the differences between the published data. Variation in major element compositions is possibly a result of leaching and alteration, due to weathering, of sills in the study area. Hence the inference can be made that, in general, the sills hosted within the Chuniespoort Group from the study area are chemically similar to other sills occurring in the floor rocks of the Bushveld Complex.

Geochemical classification alone, however, does not categorise the sills of the study area as pre- or syn-Bushveld in age. Petrography and field relationships must also be used to constrain the origin of these sills. Cawthorn *et al.* (1981) observed that sills associated with the Bushveld Complex, i.e. the syn-Bushveld emplacement sills, lack chilled margins. They attributed this to the fact that the sills were emplaced in country-rocks with a relatively high

ambient temperature, which resulted in a slow cooling rate of the magmas.

Table 2.2 Comparison of geochemical data of sills from the study area with published data of sills from other areas around the Bushveld Complex.

	A	B	C	D	E	F	G
SiO_2	50.26	51.07	51.16	53.77	56.10	54.76	52.49
TiO_2	0.91	0.43	0.87	0.45	0.76	0.37	1.52
Al_2O_3	16.26	15.05	14.77	12.58	12.90	12.56	12.61
Fe_2O_3	1.99	9.40	10.73		1.05		12.05
FeO	6.83			9.04	8.15	8.76	
MnO	0.13	0.16	0.15	0.18	0.18	0.16	0.15
MgO	6.32	8.66	8.27	11.22	10.12	11.85	6.54
CaO	9.70	12.36	8.25	7.57	6.38	7.17	5.90
Na_2O	2.58	1.13	2.22	1.36	1.48	1.73	3.22
K_2O	1.20	0.21	0.61	0.65	1.30	0.89	1.29
P_2O_5	0.13	0.07	0.14	0.07	0.18	0.06	0.21
LOI	2.24	0.77	2.07	2.39	0.76	0.268	3.30
TOTAL	98.55	99.31	99.24	99.28	99.36	98.60	99.28

A: Lydenburg type sill (metadolerite) from the eastern Transvaal - Willemse, 1959.
B: Average composition of 14 analyses from metadolerite sill, central Transvaal - Cawthorn et al., 1981.
C: Average composition of 8 analyses of metadolerites from the eastern Transvaal - Sharpe, 1978.
D: Average composition of 17 outcrop samples of amphibolite sills, western Transvaal - Engelbrecht 1990a.
E: Marulcng type norite, eastern Transvaal - Willemse, 1959.
F: Average composition of 14 norite sill outcrop samples, western Transvaal - Engelbrecht, 1990a.
G: Average composition of 14 samples from sills in the Chuniespoort Group, present study area. See Appendix 1.

The elevated temperature of these country rocks has been ascribed to either prolonged through-flow of magma before consolidation of the sills, or regional pre-heating prior to sill emplacement (Cawthorn *et al.*, 1981). In the study area, the majority of sill contacts show chill margins, leading to the conclusion that there was little or no through-flow of magma prior to consolidation, or that the sills were emplaced in country rocks with relatively low

ambient temperatures. Therefore, they probably do not fall into the category of syn-Bushveld sills reported by Cawthorn *et al.* (1981). The fact that the sills are metamorphosed (see above) implies that they have been subjected to some heat source after their emplacement. Since they are metamorphosed and the Bushveld Complex and syn-Bushveld sills are not (Cawthorn *et al.* 1981), it is concluded that the sills of the study area belong to a pre-Bushveld suite, and that they were later altered, possibly by the emplacement of the Bushveld Complex.

The Lydenburg-type sills which occur in the Chuniespoort Group in the eastern Transvaal are mostly altered to amphibole schists, with greenschist facies mineral assemblages comprising amphiboles + quartz + saussuritised plagioclase (Willemse, 1959). They have been classified as pre-Bushveld sills by Sharpe (1981). The mineralogy of sills hosted within the Chuniespoort Group in the study area is similar to the sills described by Willemse (1959) and Sharpe (1981). Thus, the sills in the study area can confidently be correlated with the pre-Bushveld Lydenburg-type sills which occur in the eastern Transvaal.

In the study area, sills occur at intervals throughout the Chuniespoort Group, and sporadically in the Pretoria Group. Other workers studying sills associated with the Bushveld Complex identified pre-Bushveld metadolerite (amphibolite or Lydenburg type) sills throughout the Transvaal Supergroup, whereas the later, syn-Bushveld sills have only been encountered higher up in the stratigraphy, close to the contact with the Bushveld Complex (e.g. Cawthorn *et al.*, 1981; Engelbrecht, 1990a). The sills of the study area fit the distribution pattern of sills owing their origin to pre-Bushveld emplacement magmatic activity (e.g. Cawthorn *et al.*, 1981; Engelbrecht, 1990a).

2.2.6 Dykes

Dykes in the study area are poorly exposed and highly weathered, except for an approximately NNE-SSW trending dolerite dyke and a NW-SE trending syenite dyke in the southern portion of the study area (Map 1). The dolerite dyke is probably of Karoo age, whereas the syenite dyke is probably of Pilanesberg origin. The width of the dolerite dyke may exceed 10 m in places, although this is difficult to confirm due to a lack of continuous outcrop. It is medium-grained, unaltered, and shows conspicuous plagioclase phenocrystic aggregates, as well as pyroxene on fresh surfaces. A thin-section study reveals unaltered pyroxene and feldspars.

The syenite dyke attains a width of approximately 3-5m, and forms a prominent ridge up to two metres high. Its weathered surface is dark rusty-red, while fresh surfaces are dark, with relatively fine-grained plagioclase, hornblende and microcline. Both the syenite and dolerite dykes can be traced for several kilometres through the Chuniespoort Group on aerial photographs and on the ground.

Other dykes in the study area are highly weathered, usually green, and crop out only to a limited extent. Their composition, origin, and sometimes even their orientation, is ambiguous.

2.2.7 Recent sediments

Recent sediments occur sporadically throughout the study area in the form of soils and an isolated tufa deposit.

In the area south of the Hennops River (Map 1), relatively thick soils have developed from weathering of sills on flat and gently sloping areas. The valleys north of the Schurweberge hills are, for the most part, occupied by thick soils. The most important of these is a 10 m thick soil deposit which predates the youngest deformation in the area (Section 3.8.2), at locality (2856,0 X: -95,6 Y). Here, the reddish-brown soil is largely homogeneous in composition, although a slate fragment lag, probably derived from the adjacent Pretoria Group lithologies, occurs approximately 5 m from the base.

An isolated carbonate tufa deposit is located in the stream which drains westwards into the Crocodile River at locality (2857,6X; -91,8Y), near the contact of the Chuniespoort and Pretoria Groups. Tufa is a porous calcium carbonate, formed from flowing surface water (Marker, 1973). The tufa at this locality is developed as an encrustation along the stream course. It extends for more than 300 metres, is up to 20 metres wide, and is more than 2 metres thick in places. It is cream-white and has the botryoidal masses typical of tufa (Fig. 2.6). The tufa encloses fragments of slate and quartzite country rock in some places, producing a texture reminiscent of breccia or conglomerate (Fig. 2.7). Clast sizes are highly variable, and range from only a few millimetres up to approximately 10 cm in size.

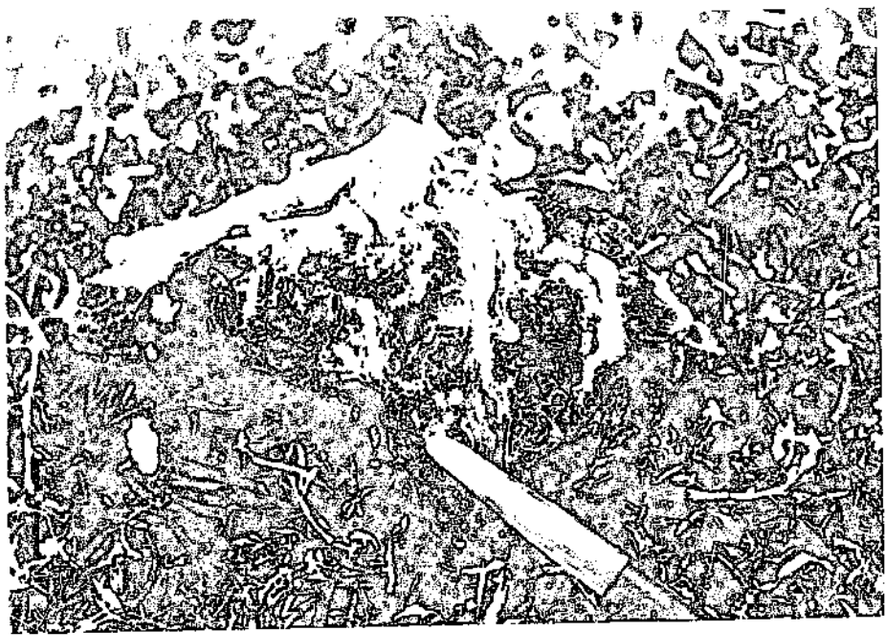

Botryoidal masses of tufa. Locality (2857.6 X; 91.8 Y)



Tufa enclosing fragments of slate and quartzite, closely resembling conglomerate or breccia. Locality (2857.6 X; 91.8 Y).

A study of tufa deposits in the Transvaal (Marker, 1973) has revealed that the maximum deposition of tufa in the region was during the Quaternary (< 2Ma). Carbon from these calcium carbonate deposits makes them suitable candidates for the C_{14} dating technique, which is limited to determining ages of less than approximately 50 000 years (Marker, 1974). Dating carried out on surface tufa and cave deposits in the Sterkfontein caves, approximately 50 kilometres southwest of the study area, reveals carbonate concretions that are approximately 48 000 years old (Marker, 1974). In the northern Transvaal, deposition of surface tufa on the rocks of the Transvaal Supergroup may have begun approximately 43 000 years ago, and continued up until at least 14 240 years ago (Marker, 1974). Other surface tufa deposits in the Northern Cape Province have been dated at approximately 36 000 years (Marker, 1974). There are, however, several tufa deposits associated with rocks of the Transvaal Supergroup which are being formed at the present day (Marker, 1973). It thus appears likely that the tufa in the study area formed within the last 48 000 years.

CHAPTER 3

STRUCTURAL RELATIONSHIPS

3.1 Introduction

3.1.1 Previous work

Structural disturbance of extensive areas of the Transvaal Supergroup and the Bushveld Complex has been documented by previous workers (e.g. McCarthy *et al.*, 1986; Andreoli, 1988, 1990). In the Black Reef Quartzite Formation along the northern margin of the Johannesburg Dome, post-Bushveld Complex age northward-verging folds, cleavage and shear zones are developed (McCarthy *et al.*, 1986). Cleavages, folding, thrusting and compressional faulting which affect the Pretoria Group extend west from Pretoria to beyond Magaliesburg (Andreoli, 1988).

Pre-Bushveld folds are developed in the Transvaal Supergroup floor rocks (e.g. Hartzer, 1995). Syn-Bushveld folds and cleavage occur both within and adjacent to the eastern lobe of the Bushveld Complex (Sharpe and Chadwick, 1982) and along the northeastern margin of the Bushveld Complex (e.g. Uken and Watkeys, 1994; 1995). Du Plessis and Levitt (1987) and Andreoli (1990) identified, from geophysical profiles near Pretoria and Rustenburg, extensive south-verging folds and thrust duplication which affect both the Transvaal Supergroup and the Bushveld Complex. Walraven (1974) reported, from geophysical profiles and field mapping, that the western Bushveld Complex and underlying Transvaal Supergroup had been gently folded into a series of large-scale NW trending open synclines and anticlines generated by NE-SW directed compression, probably of late-Bushveld age. Temperly (1977) described NNW trending faults with large displacements

which deform the Bushveld Complex as well as the Transvaal Supergroup.

Transvaal and/or post-Transvaal faulting and folding, possibly a result of compression east of the Witwatersrand basin, reactivated pre-existing structures within the Witwatersrand basin (Jansen, 1977). Westerly-verging thrusting displaced the Transvaal Supergroup adjacent to the eastern flank of the Johannesburg Dome (Temperly, 1977; Roering *et al.*, 1990; Purnell, 1994). In the Pretoria area, south-verging folds may involve the entire thickness of the Timeball Hill Formation (Temperly, 1977). The folds parallel similarly verging thrusts in this area and may thus be contemporaneous with the thrusting, indicating compression directed from north to south (Temperly 1977; Purnell, 1994).

The western margin of the Kaapvaal Craton has also been severely deformed. Thin-skinned tectonism due to the Kheis orogeny affected the Transvaal Supergroup and the Bushveld Complex in the region, producing recumbent folds and west to east directed thrust faults approximately 1,9 - 2,1 Ga ago (Stowe, 1986; Duane and Kruger, 1991).

The Johannesburg Dome is sheared near its contact with the overlying Transvaal Supergroup (Jansen, 1977). Numerous NNE and WNW trending post-Transvaal faults are also encountered both tangentially and radially to the Johannesburg Dome (Jansen, 1977). North-northeast trending strike-slip faults north of the Johannesburg Dome displace the Black Reef Quartzite Formation and the Chuniespoort Group (Anhaeusser, 1973; Hilliard, 1994).

East-northeast trending strike-slip faults of the Thabazimbi-Murchison Lineament (TML), between the Limpopo Belt and the Witwatersrand basin, have substantial post-Transvaal

displacements which continue into the basement (Roering *et al.*, 1990; Du Plessis, 1991).

3.1.2 Results from this study

Field investigations, aerial photograph examination and microstructural analysis of oriented rock samples taken in the field for this study have revealed that the Transvaal Supergroup between the Johannesburg Dome and the Bushveld Complex has been affected by several phases of deformation. This post-Transvaal deformation history has been divided into the following structural events:

1) The earliest recognisable event (D_1) resulted in a heterogeneous, southerly-verging cleavage (S_1), locally developed in the peltic units of the Pretoria Group.

2) The main deformation event (D_2) resulted in heterogeneous, northward-verging, ductile bedding sub-parallel shear zones, lineations, penetrative cleavage, small-scale folds and deformed ooids.

3) The D_3 event resulted in the formation of large-scale, open folds with associated ductile sub-vertical shear zones in the Chuniespoort Group dolomite, and mainly kink-folds in the Pretoria Group slate.

4) The D_4 event was responsible for the development of northerly-trending strike-slip faults which truncate and offset the D_2 and D_3 structures.

5) Other ductile deformation events are characterised by minor, and extremely localised, easterly and westerly verging structures. The relative timing of these two deformation events could not be precisely determined as they are never encountered interfering with one another or with later structures. They are, however, clearly superimposed on the D_2 bedding sub-parallel shear zones, and may therefore represent post-D_2 reactivations.

6) Later deformation involved the development of brittle deformation features such as joints,

possible reactivation of earlier structures, and neotectonic fault activity.

3.2 D_1 event

The most intense and widespread cleavage-forming deformation event occurred during D_2. However, at two localities west of the study area, anomalous relationships suggest the existence of an earlier D_1 cleavage-forming event. A road-cutting along the R509, 20km west of Magaliesburg town (Fig. 1.1) has S_1 cleavage intensely developed in the Pretoria Group slates. This is the only locality encountered in the study area in which the S_1 cleavage is detectable macroscopically. The (S_1) cleavage strikes, on average, between approximately 260° and 280°, and has a moderate northerly dip of up to 40°. Microscopic study reveals that the S_1 cleavage, which at this locality is defined solely by micas, is crenulated, and thus pre-dates, the south-dipping S_2 cleavage (Section 3.3.1) (Fig.3.1).

At the Bekker Schools locality, approximately 20 kilometres ENE of Magaliesburg town (Fig. 1.1), the S_1 cleavage is weakly developed in the slates of the Pretoria Group, and dips approximately 20° north. Although the S_1 cleavage is not easily detectable in hand-specimen at this locality, thin-section analysis has revealed that the cleavage is defined by the alignment of chlorite. A sample of chiastolite-bearing slate at the same locality reveals, in thin-section, the presence of moderately-developed shear cleavage (S_1), oriented sub-parallel to bedding. Porphyroblast-cleavage relationships (Section 4.3.2) indicate a pre- to syn-metamorphic timing for S_1 cleavage development, which predates the syn- to post-metamorphic timing of S_2 (Sections 4.3.1 and 4.3.2).

Field investigations and thin section analysis failed to verify the presence of the S_1 cleavage

in the remainder of the Transvaal Supergroup.



Fig. 3.1 Photomicrograph showing north-dipping S_1, oriented oblique to bedding (S_o), being crenulated by the south-dipping S_2 cleavage. Locality 20 km west of Magaliesburg along the R509. Scale bar 0,5 mm. North is to the left.

3.3 D_2 event

The D_2 event led to the development of a heterogeneous, regional cleavage, bedding sub-parallel shear zones, lineations and northerly verging fold structures throughout the study area.

3.3.1 Cleavage

The closely spaced, penetrative, S_2 cleavage is widely developed in the study area. It varies from a continuous to a discontinuous cleavage (Davis, 1984). The continuous cleavage is mostly slaty cleavage in very fine grained rock, although phyllitic cleavage and schistosity are also locally developed in close proximity to bedding sub-parallel shear zones (Section

3.3.3). The discontinuous cleavage is often a crenulation cleavage, and ranges from discrete to zonal in form (Gray, 1977). Orientation of cleavage planes is more or less consistent throughout the area, except where it has been folded by later deformation events (Section 3.4.2). S_2 cleavage strikes approximately east-west and dips shallowly (15-30°) to the south (Fig. 3.2), transecting bedding. Micro-scale cleavage refraction is occasionally revealed in thin sections where S_2 steepens as it passes from the surrounding matrix through thin quartz-rich layers (Fig. 3.3).

The S_2 cleavage has clearly crenulated the S_1 cleavage (Fig. 3.1) at the locality near Magaliesburg (Fig. 1.1). The S_2 cleavage-forming event thus post-dated D_1.

The S_2 cleavage in the study area is best developed in the slate units, although a well-developed penetrative cleavage is locally present in the carbonate lithologies. Penetrative cleavage is ubiquitous in the Pretoria Group slates, although its intensity is heterogeneous. Some slate outcrops display a pronounced penetrative cleavage, whereas others have a very poorly developed cleavage, not detectable with the naked eye. Where strongly cleaved slate units exist only as thin layers intercalated within the carbonate lithologies of the Chuniespoort Group, the cleavage is usually absent or not extensively developed in the adjacent dolomite. Cleavage thus develops more readily in the less competent, fine-grained, clastic units.

3.3.3). The discontinuous cleavage is often a crenulation cleavage, and ranges from discrete to zonal in form (Gray, 1977). Orientation of cleavage planes is more or less consistent throughout the area, except where it has been folded by later deformation events (Section 3.4.2). S_2 cleavage strikes approximately east-west and dips shallowly (15-30°) to the south (Fig. 3.2), transecting bedding. Micro-scale cleavage refraction is occasionally revealed in thin sections where S_2 steepens as it passes from the surrounding matrix through thin quartz-rich layers (Fig. 3.3).

The S_2 cleavage has clearly crenulated the S_1 cleavage (Fig. 3.1) at the locality near Magaliesburg (Fig. 1.1). The S_2 cleavage-forming event thus post-dated D_1.

The S_2 cleavage in the study area is best developed in the slate units, although a well-developed penetrative cleavage is locally present in the carbonate lithologies. Penetrative cleavage is ubiquitous in the Pretoria Group slates, although its intensity is heterogeneous. Some slate outcrops display a pronounced penetrative cleavage, whereas others have a very poorly developed cleavage, not detectable with the naked eye. Where strongly cleaved slate units exist only as thin layers intercalated within the carbonate lithologies of the Chuniespoort Group, the cleavage is usually absent or not extensively developed in the adjacent dolomite. Cleavage thus develops more readily in the less competent, fine-grained, clastic units.

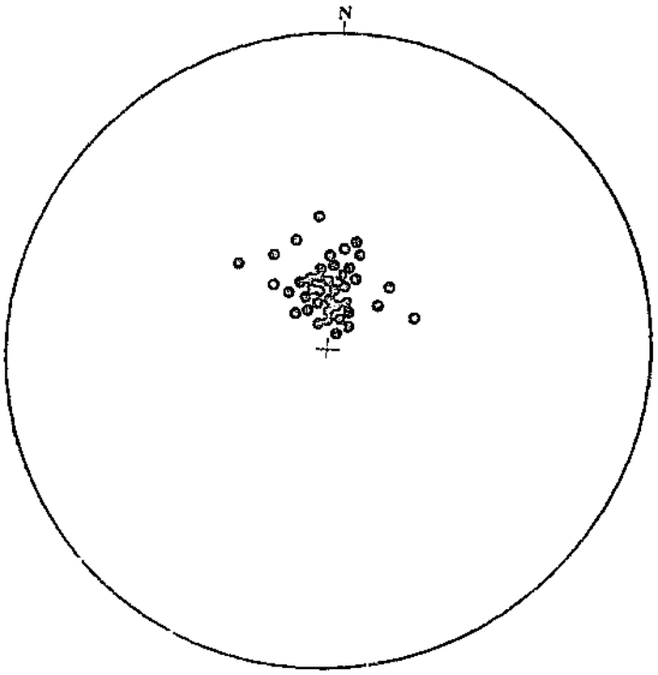

Fig. 3.2 Equal area (Schmidt) net of the orientation of poles to S_2 cleavage planes (n=40) in slate units.

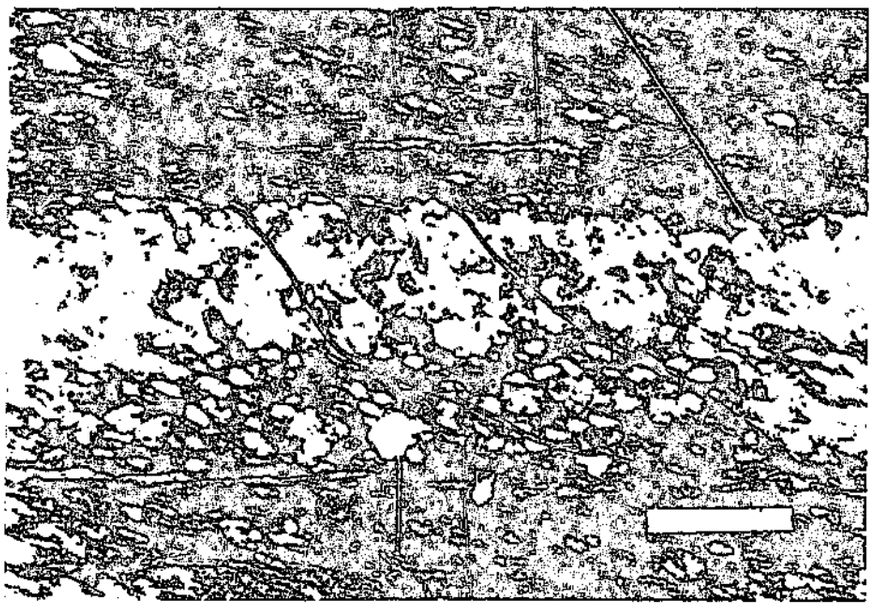

Fig. 3.3 Micro-scale refraction of S_2 cleavage in a sectioned slate sample. Locality (2855,1X; -92,7 Y). Scale bar 0,5mm.

Orientated thin sections from several localities above, within and below a D_2 bedding sub-parallel shear zone reveal a variable S_2 cleavage profile across the structures. Up to 5 metres above the bedding sub-parallel shear zones, thin sections exhibit a pronounced, although moderately intense, penetrative cleavage (S_2) dipping approximately 20-25°S. Nearer to the shear zone, cleavage orientations change slightly, dipping less steeply towards the south (approximately 10°). This cleavage also becomes more intense nearer the contact with the bedding sub-parallel shear zone. Samples within the bedding sub-parallel shear zone reveal intense deformation. The S_2 cleavage is dominant and intensely developed, and crenulations which range from zonal to discrete forms are present. Microfolded bedding planes (S_0) are generally overturned towards the north. The intensity of these folds is, however, highly variable. Inconsistencies in fold orientations are present, perhaps due to strain partitioning in very small areas, or interference by later deformation events. Immediately below the shear zones (i.e. less than about 1 metre), the S_2 cleavage is more or less consistently orientated (dips about 20-25° to the south), although the cleavage intensity decreases significantly away from the shear zone.

The marked difference in S_2 cleavage intensity towards the bedding sub-parallel shear zones indicates a large strain gradient from within the shear zones to immediately adjacent to them. This relationship suggests, first, that the shear strain was highly concentrated into narrow zones, and second, that cleavage development is spatially and temporally related to the bedding sub-parallel shear zones, and is thus a function of the same deformation event.

3.3.2 Folds

a) Black Reef Quartzite Formation and Chuniespoort Group

An extensively developed set of asymmetric non-cylindrical folds is developed in the Black Reef Quartzite Formation (Fig. 3.4) and the lower units of the Chuniespoort Group (Fig. 3.5) in the study area. The folds in the Chuniespoort Group vary in wavelength from less than 0.5 m to in excess of 2 m, with amplitudes of up to 1 m. The folds in the Black Reef Quartzite Formation are, however, more consistent in their dimensions, having wavelengths of up to 3 m and amplitudes of up to 1,5 m. The fold structures in both the Black Reef Quartzite Formation and towards the base of the Chuniespoort Group are frequently exposed as a set of up to three of four north-verging folds, with steep northern limbs dipping in excess of 60° to the north, and possibly even overturned. Some of the smaller-scale folds in the Chuniespoort Group are recumbent. Fold hinges plunge by up to 20° to the east or west (Fig. 3.6). Folds in the Black Reef Quartzite Formation occasionally resemble E-W elongated domes, reflecting their non-cylindrical nature.

Fold axial planes strike east-west and dip up to 45° to the south, consistent with northward-verging shear. Comparison of the orientations of cleavage in the adjacent slate lithologies (Fig. 3.2) with the axial planes of these round-hinged folds reveals that S_2 cleavage strikes sub-parallel to fold axial planes, but the cleavage generally dips more shallowly to the south than the fold axial planes. The cleavage is thus not axial planar to the round-hinged folds.

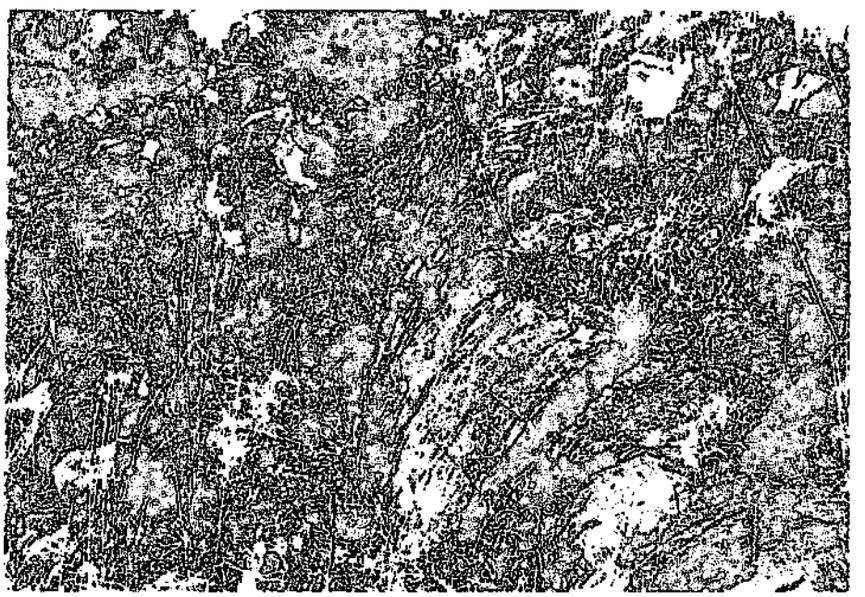

Fig. 3.4 North-verging D_3 round-hinged folds in the Black Reef Quartzite Formation. Looking east. Locality (2863,1 X; -97,1 Y).

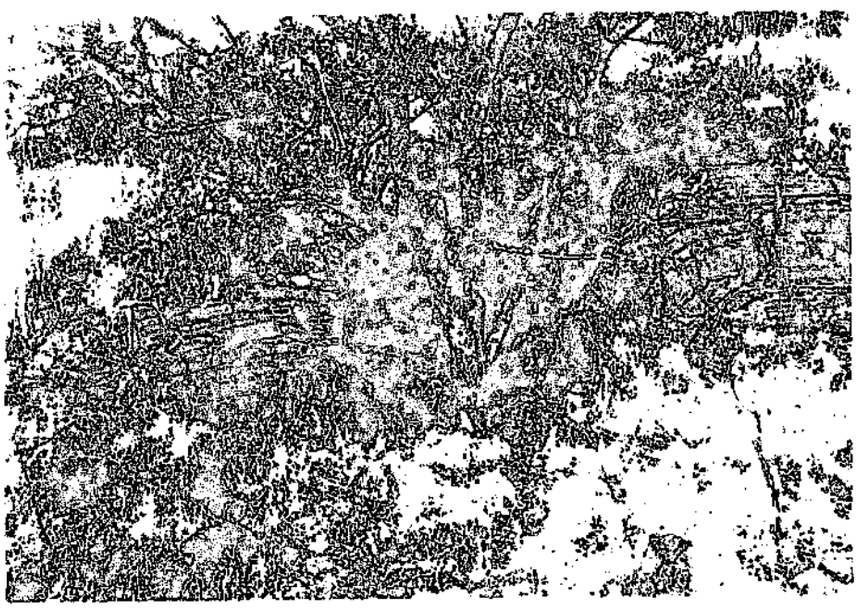

Fig. 3.5 North-verging D_3 round-hinged folds in the lower strata of the Chuniespoort Group. Looking east. Locality (2863,0 X; -95,0 Y).

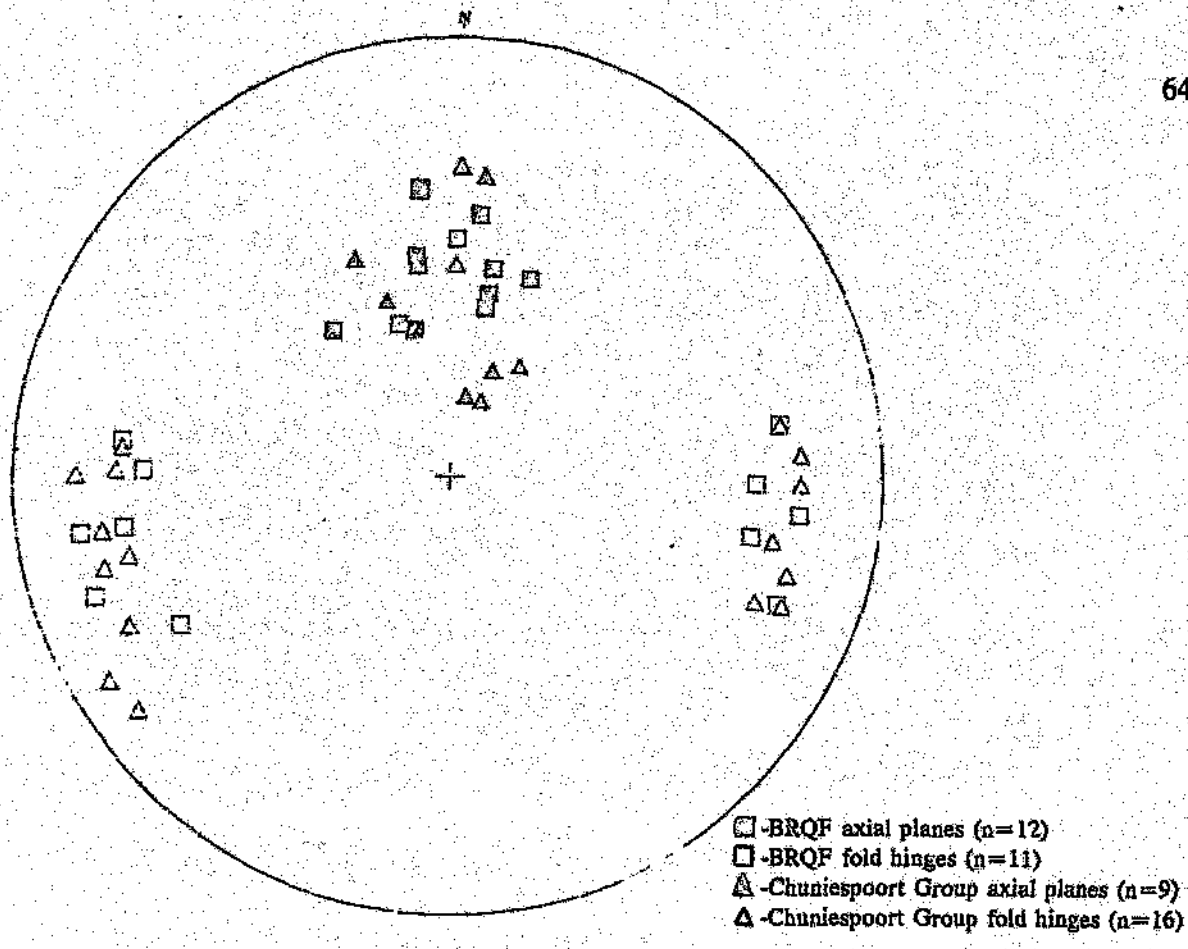

Fig. 3.6 Equal area (Schmidt) stereographic representation of D_2 round-hinged folds in the Black Reef Quartzite Formation (BRQF) and the Chuniespoort Group.

Chevron folds are locally developed in the slate units of the Black Reef Quartzite Formation (Fig. 3.7). These folds have wavelengths of approximately 2-6 cm, amplitudes of up to 5 cm and interlimb angles as small as 30°. Examination of thin sections of the chevron folds revealed the extreme intensity of the axial planar cleavage. The shallowly southward dipping axial planes of the chevron folds, which, on average, strike approximately east-west and dip approximately 25° south, are coincident with an axial planar cleavage (Fig. 3.8), which is consistent with northerly vergence.



Fig. 3.7 North-verging D_2 chevron folds in a slate unit of the Black Reef Quartzite Formation. Looking east. Locality (2862,8 X; -97,4 Y).

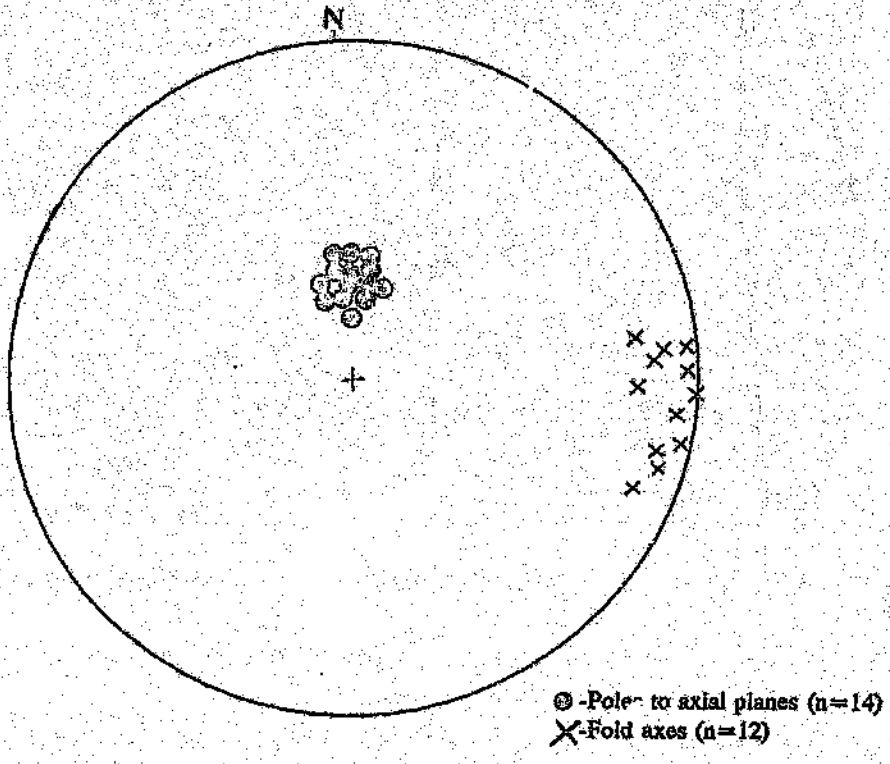

Fig. 3.8 Equal area (Schmidt) stereographic representation of the D_2 chevron folds in the Black Reef Quartzite Formation. Locality (2862,8 X; -97,4 Y).

b) Pretoria Group

A number of northward-verging monoclinal structures with fold hinges trending approximately east-west are developed in the Pretoria Group. The steep limbs of these structures dip up to 80° to the north (Fig. 3.9). Although 3-D exposure is limited, these folds have a similar morphology to the D_2 folds encountered in the Black Reef Quartzite Formation and the lower Chuniespoort Group (i.e. they are not intense folds, have steeply north-dipping northern limbs, verge in a northerly direction, and are generally of comparable scale, i.e metres to tens of metres), and may thus be a function of the same north-directed deformation.

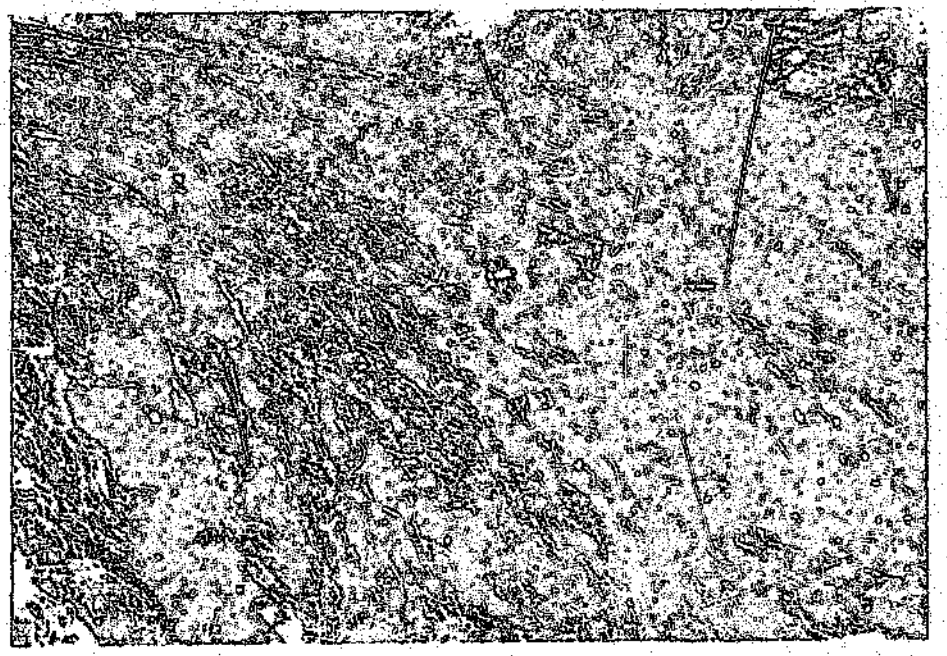

Fig. 3.9 Monoclinal structure with steep limb developed in the Pretoria Group. Locality (2854,7 X; -91,6 Y). Looking west.

A large-scale monocline with a wavelength of several hundred metres defines the northern flank of the Schurweberg hills (Map 2). Its hinge trends approximately 110°. The origin of this structure is uncertain, although its northward vergence suggests that it may also be related to the D_2 event.

3.3.3 Bedding sub-parallel shear zones

Zones of intense, predominantly non-coaxial deformation (simple shear) in the study area are usually defined by a mylonitic fabric. These shear zones are encountered in the dolomitic strata of the Chuniespoort Group as well as in the clastic sediments of the Pretoria Group. They are best exposed in cliff sections, and range in thickness from less than 0,5m to more than 3m. They generally strike east-west and dip shallowly to the north, except where they have been folded (Section 3.4.1 and cross-section, Map 1). The shear zones typically exploit pre-existing planes of weakness such as bedding and lithological contacts (notably dolomite-sill contacts), and thin shale layers within the dolomite. Sills are frequently sheared and brecciated at their contact with the country rock, and thus the bedding sub-parallel shear zones post-date sill emplacement.

No evidence has been found that the bedding sub-parallel shear zones significantly cross-cut bedding. Despite the absence of displaced markers, however, a northward-directed bulk sense of shear can be determined by the study of numerous shear-sense indicators within the shear zones. These include shear zone-hosted folds, S-C fabrics, porphyroclasts and porphyroblasts.

a) Shear zone hosted folds

Mylonites commonly display a heterogeneous deformation history, and local flow variations may evolve into asymmetric folds (micro- or meso-scale) with vergence consistent with the shear sense (Simpson and Schmidt, 1983). The mylonites of the bedding sub-parallel shear zones in the study area have abundantly developed tight to isoclinal recumbent folds, which range in scale from millimetres to several centimetres. Figure 3.10 shows typical small-scale folds developed in a bedding sub-parallel shear zone in dolomite, and Figure 3.11 shows an isoclinal recumbently folded quartz vein in a similar shear zone in the Pretoria Group slate.

The axial planes of folds within the bedding sub-parallel shear zones are discordant to the shear zones (Figs. 3.10 and 3.11). During progressive deformation, the axial planes of these folds have been rotated toward parallelism with the mylonitic fabric, consistent with the observations of other studies (e.g. Hamner and Passchier, 1991). The folds hosted in the D_2 shear zones have relatively variable fold hinge and axial plane orientations (Fig. 3.12), probably due to heterogeneous strain in the shear zones during deformation, or as the result of later deformation events (Section 3.4). The fold hinges plunge shallowly (10-20°) either easterly or westerly, while the fold axial planes dip moderately (approximately 30-40°) to the south. The northward vergence of the folds indicates the overall shear sense in the shear zones.

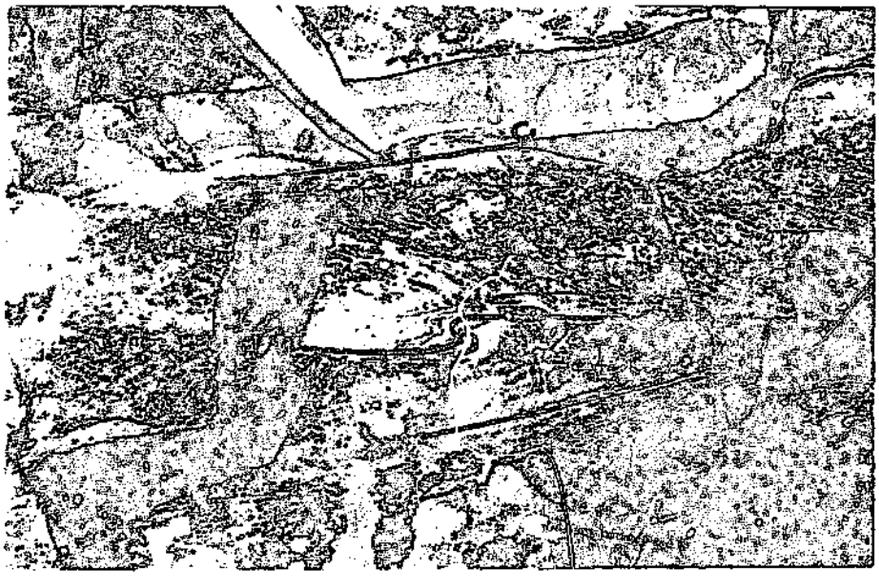

Fig. 3.10 Small-scale disharmonic recumbent folds verging northwards in a bedding sub-parallel shear zone hosted in Chuntespoort Group dolomite. Looking east. Locality (2861.7 X; -95.1 Y)

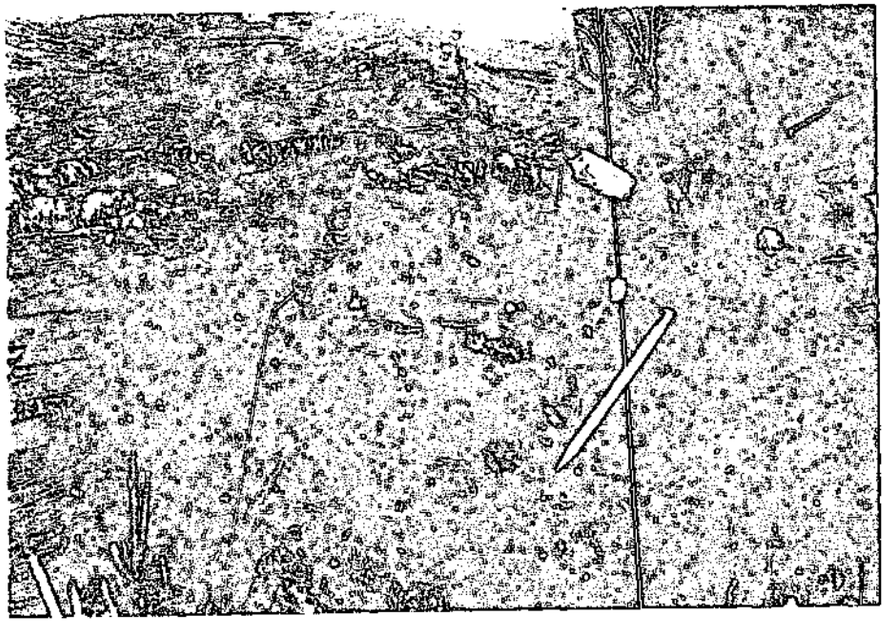

Fig. 3.11 North-verging, isoclinal, recumbently folded quartz vein in a bedding sub-parallel shear zone in Pretoria Group slate. Looking west. Locality (2857 X; -95.8 Y)

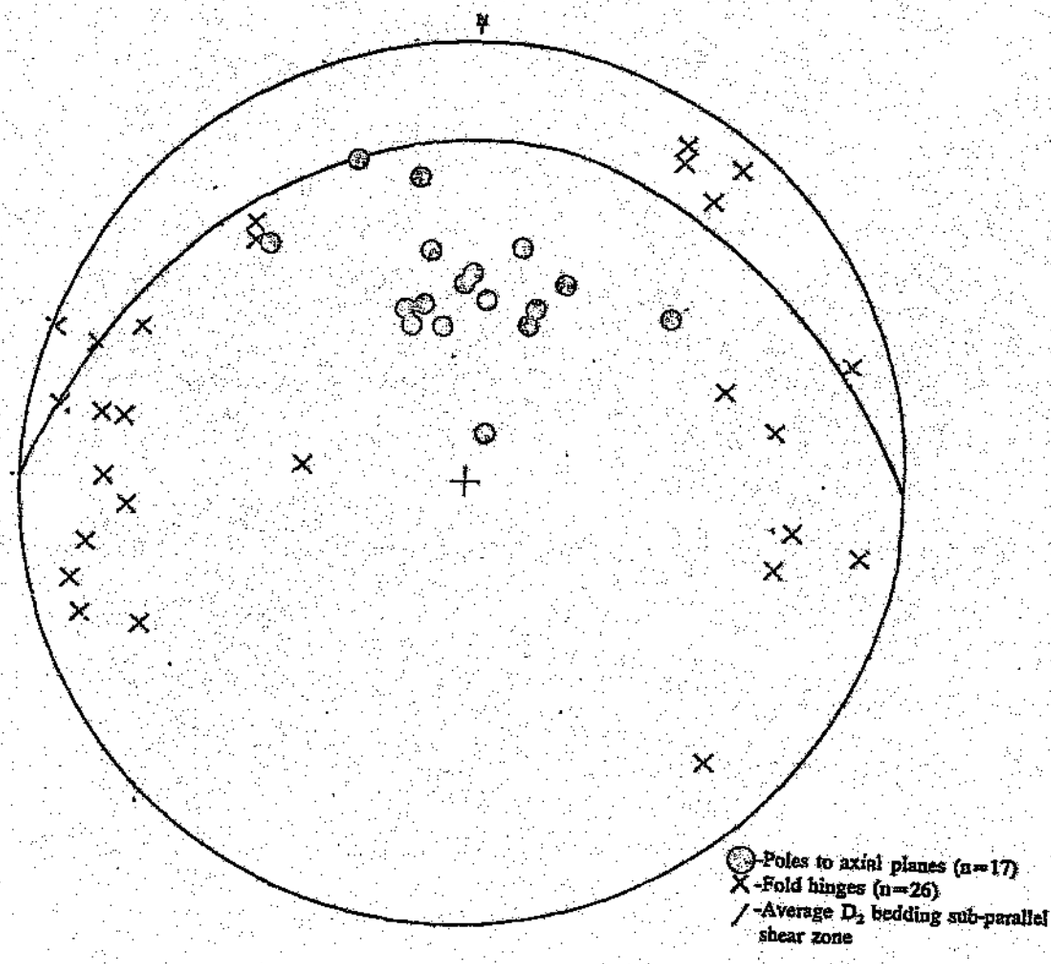

Fig. 3 12 Equal area stereonet plot of the orientations of fold hinges (n=26) and axial planes (n=15) hosted in bedding sub-parallel shear zones throughout the sequence studied. Note the consistent fold vergence, as shown by the grouping of axial plane plots.

Asymmetric, north-verging, micro-folds with fold axial planes sub-parallel to the S_2 south-dipping cleavage occur in several thin section samples from bedding sub-parallel shear zones. Samples from slate horizons and the slaty chert breccia (Section 2.2.3), which may represent zones of less intense shear, also display similar structures (Fig. 3.13).



Fig. 3.13 Micro-folded quartz vein with fold axial plane sub-parallel to S_2 cleavage in a slate horizon near the base of the Chuniespoort Group. Locality (286,3 X; -96,8 Y). Scale bar 0,5mm.

b) S-C fabrics

Mylonitic rocks commonly have two cleavages developed within them, namely S-surfaces (related to finite strain accumulation) and C-surfaces (related to displacement discontinuities or zones of high strain) (Lister and Snoke, 1984). Simpson and Schmidt (1983) state that C-surfaces develop parallel to the main shear zone boundary, and maintain this orientation during progressive deformation. The C-surfaces are spaced-slip surfaces with sense of shear coinciding with that of the overall shear zone, while the S-surfaces, initially orientated at approximately 45° to the shear zone (and hence the C-surfaces), curve into the C-surfaces

(Simpson and Schmidt, 1983). The presence of S-C relationships is an indication of intense non-coaxial laminar flow, where locally the orientation of the bulk shear plane and shear sense can be estimated (Lister and Snoke, 1983) by the angular relationship between the S- and C-surfaces (Simpson and Schmidt, 1983).

S-C structures, although not extensively developed, are encountered in the D_2 bedding sub-parallel shear zones in the study area. Figure 3.14 shows a well-developed example of these sigmoidal structures with the C-surfaces orientated approximately parallel to bedding (approximately 260°/15° N). The S-surfaces curve into the C-surfaces such that a top-to-the-north shear sense can be deduced. A similar scenario is developed in Fig. 3.15 where the S-surfaces are defined by deformed ooids. S-C fabrics are also developed where S-surfaces parallel small-scale fold axial planes (Fig. 3.10), and indicate top-to-the-north shear sense.



Fig. 3.14 S-C structures (a), small-scale duplexes (b) and asymmetric disharmonic folds (c) developed in a bedding sub-parallel shear zone in the Chuniespoort Group. The orientation of the S-C structure together with northward-verging folds developed within the shear zone confirm top-to-the-north shear sense. Locality (2861,0 X; -94,5 Y). Looking west.

Ooids in dolomite strata adjacent to the bedding sub-parallel shear zones provide excellent strain and movement sense indicators. They frequently show a progressive increase in non-coaxial strain (the ooids are increasingly elongated and rotated) towards the bedding sub-parallel shear zones. Figure 3.15 shows the relationship of deformed ooids to a bedding sub-parallel shear zone. This S-C structure shows a top-to-the-north sense of shear.

c) Porphyroclasts and porphyroblasts

During deformation, mylonites are formed by extensive dynamic recrystallisation of the precursor host-rock minerals, resulting in a more fine-grained rock. Large grains are commonly preserved as porphyroclasts (Hamner and Passchier, 1991). In the study area, porphyroclasts ranging from millimetres to centimetres in size occur within the bedding sub-parallel shear zones as well as in the thin slaty horizons intercalated with the carbonate strata of the Chuniespoort Group. The porphyroclasts identified in the study area are of the σ type, i.e. porphyroclasts with wedge-shaped tails of recrystallised material which develop when the dynamic recrystallisation rate is high with respect to the rate of rotation (Simpson, 1986). The porphyroclast tails are, however, often not well-developed, or their relationships are obscured by weathering. Their structural significance is, therefore, usually ambiguous. Nonetheless, they do all seem to give a consistent sense of top-to-the-north rotation.

The presence of small-scale, north verging folds in close proximity to a relatively large porphyroclast of chert within a shear zone in dolomite (Fig. 3.16) confirms that the σ structure reflects the top-to-the-north shearing. Hanmer and Passchier (1991) state that the kinematic significance of σ structures only becomes certain when many similar examples are present in a study area. The porphyroclasts in the study area consistently show top-to-the-

a



b

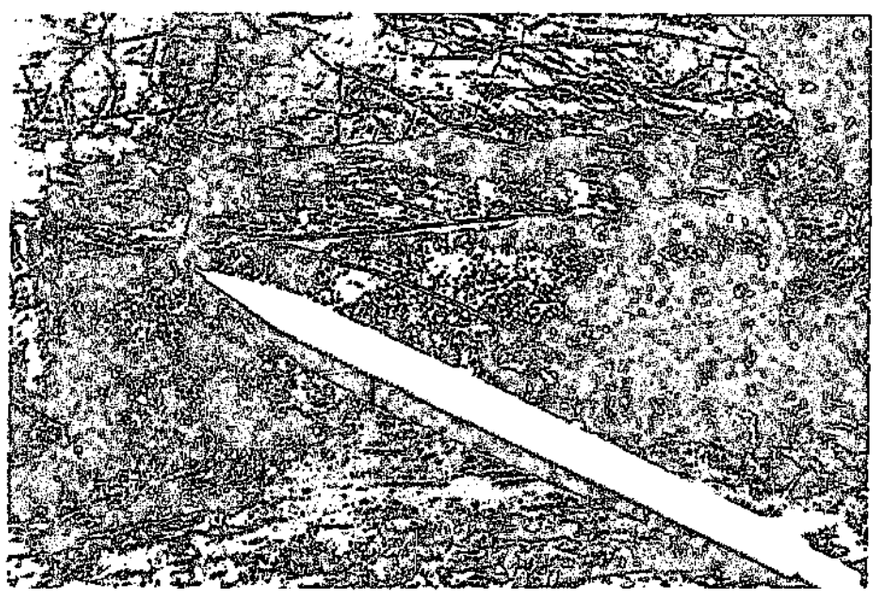

Fig. 3.15 Deformed ooids a) above and b) below a D_3 bedding sub-parallel shear zone in the Chuniespoort Group as a result of north-verging shear. Looking east. Locality (2861.7 X; 195.1 Y).

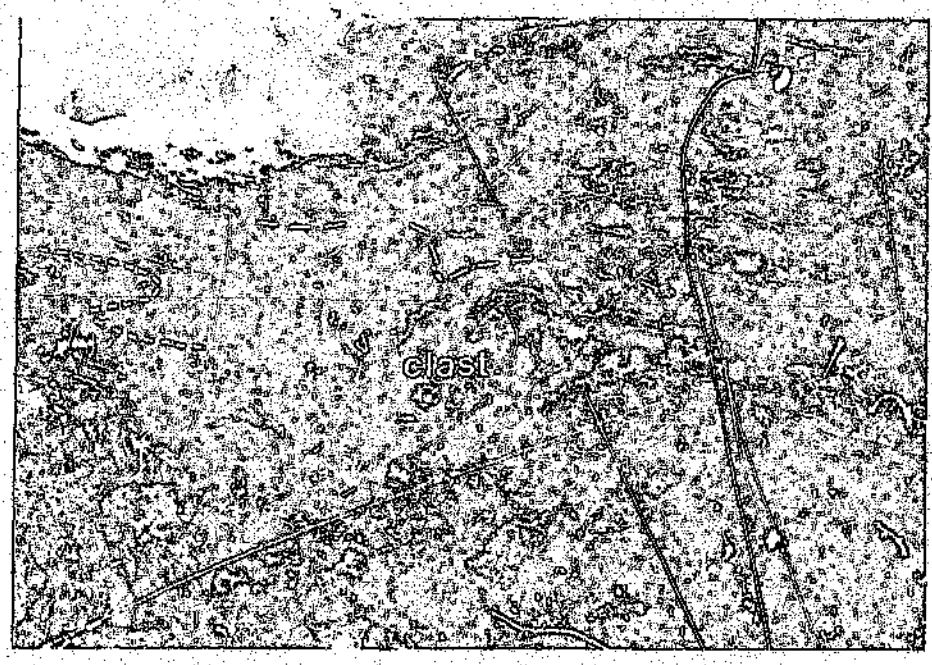

Fig. 3.16 Large-scale σ clast of chert showing top-to-the-north shear sense within a bedding sub-parallel shear zone in Chuniespoort Group dolomite. Locality (2861,8 X;-96,9 Y). Looking west.

All porphyroblasts seen in the bedding sub-parallel shear zones are altered, probably by oxidation processes (Fig. 3.17). Not only does this preclude identification of the original porphyroblast mineralogy, it also obliterates any traces of internal fabric (S_i), which is of vital importance if the kinematic significance of the porphyroblast is to be determined (Hanmer and Passchier, 1991). Strain shadows and S_2 cleavage anastomosing around the porphyroblasts do, however, indicate that their growth was pre- or syn-deformational (Fig. 3.17).

d) Other structures

Figure 3.18 shows a possible micro-scale thrust system displacing a quartz-layer in slate. Competent quartz micro-layers form duplex type structures, similar to those seen in Fig. 3.14, verging in a northerly direction (Fig. 3.18). This structure displays vergence sense consistent with that determined from other structures, and serves to reinforce other evidence of north-directed shearing for the D_2 event in the study area.

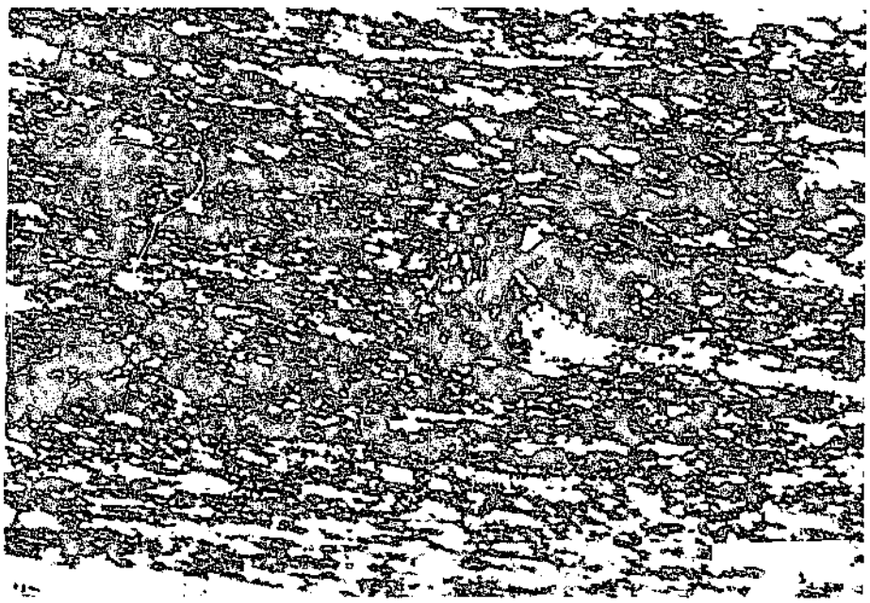

Fig. 3.17. Oxidised porphyroblast (arrowed) which grew pre- to syn-S_2 deformation. Sample from a slate horizon in the Chuniespoort Group. Locality (2863,2 X; -96,4 Y). Scale bar 0,5 mm.

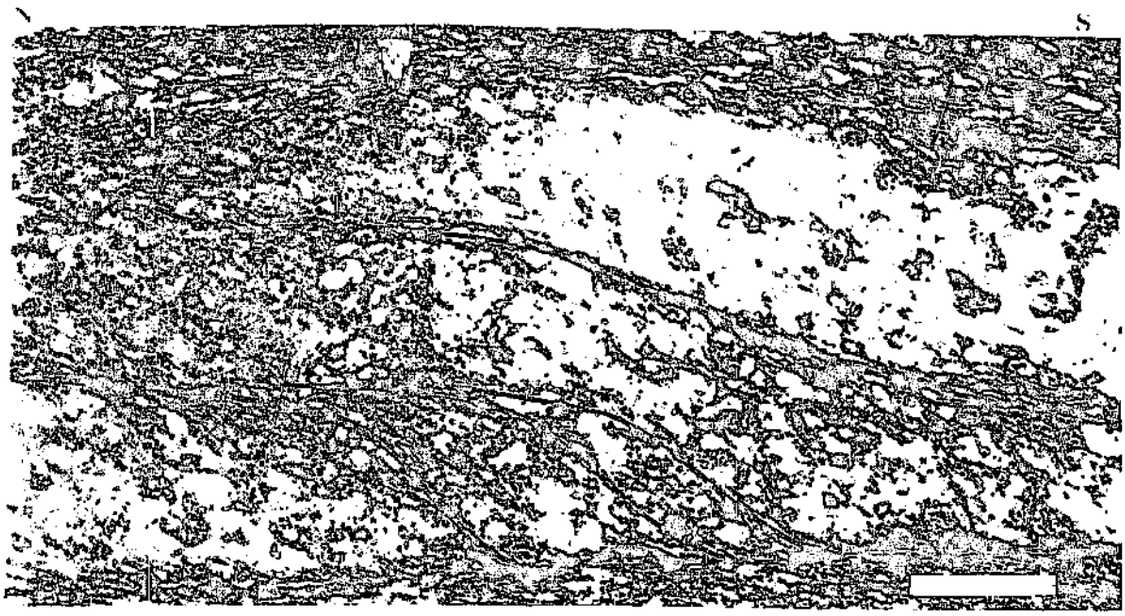

Fig. 3.18 Northerly verging micro-thrust system developed in a predominantly quartz layer. Scale bar 0,5 mm. Locality (2857,2 X; -92,5 Y).

e) Strain analysis

As the shear zones are bedding sub-parallel, there is no direct evidence of the amount of shortening. It is, however, possible to obtain some indication of the amount of strain using methods of strain analysis. In order to establish the state of strain in a body of rock, strain markers of some known original shape or size must be present, which includes (Ramsay and Huber, 1983; Price and Cosgrove, 1990):

a) originally spherical objects;

b) originally ellipsoidal objects;

c) objects with known original size or length;

d) objects with original bilateral symmetry.

Originally spherical inclusions in undeformed rock, such as carbonate concretions (ooids), are excellent strain markers once deformed. Spherical strain markers become ellipsoids once strained, and appear as ellipses on any surface intersecting the deformed rock. These ellipses depict the strain in a specific area of rock (Price and Cosgrove, 1990). The abundance of ooids (strained and unstrained) occurring in the dolomite horizons in the study area facilitates strain analysis, and as the shear zones have clearly undergone intense deformation, an attempt has been made to quantify the strain involved.

A Vernie. calliper was used to obtain accurate measurements of the principle strain axes (X, Y, and Z axes) of deformed ooids from a suitable 3-D exposure of dolomite adjacent to an approximately 1 m thick D_2 bedding sub-parallel shear zone at locality (2861,7 X; -95,1 Y). At this locality, ooids show an increase in strain as the shear zone is approached. Appendix 3 shows the dimensions of the X, Y and Z axes at A) approximately 10 cm above the shear zone, B) approximately 5 cm above the shear zone, and C) at the contact with the shear

zone. From the measurements at localities A, B and C, average lengths (in mm) for each of the axes was determined. The principle strain ratios (elipticity R) and the *k-values* were determined for localities A, B and C, and then plotted on a Flinn graph, as outlined in Ramsay and Huber (1983).

At locality A:

$X_{avg} = 2,57 \pm 0,08$

$Y_{avg} = 2,06 \pm 0,07$

$Z_{avg} = 1,56 \pm 0,07$

At locality B:

$X_{avg} = 2,11 \pm 0,06$

$Y_{avg} = 1,76 \pm 0,07$

$Z_{avg} = 1,21 \pm 0,05$

At locality C:

$X_{avg} = 1,59 \pm 0,05$

$Y_{avg} = 1,41 \pm 0,06$

$Z_{avg} = 0,71 \pm 0,04$

The principle plane strain ratios (R), presented in Table 3.1, were determined from the equations (Ramsay and Huber, 1983):

$R_{xz} = X_{avg}/Z_{avg}$

$R_{xy} = X_{avg}/Y_{avg}$

$R_{yz} = R_{xz}/R_{xy}$

Table 3.1 Principle plane strain ratios (R) of deformed ooids adjacent to a D_2 bedding sub-parallel shear zone. Locality (2861,7 X; -95,1 Y).

	Locality A	Locality B	Locality C
R_{xz}	1,65	1,74	2,23
R_{xy}	1,25	1,19	1,12
R_{yz}	1,32	1,46	1,99

A method of classifying 3-D strain ellipsoids (such as deformed ooids) in naturally deformed rocks uses independent values of elipticity of the principal plane-strain ellipses (R_{xy} and R_{yz}), and facilitat s a 2-D graphical plot of the 3-D ellipsoids in the form of a Flinn graph, using the parameter *k* to describe the general position of the ellipsoid plot (Ramsay and Huber, 1983). The *k-values* for ea.. of the localities A, B and C, presented in Table 3.2, were determined by the formula (Ramsay and Huber, 1983):

$$k = R_{xy} - 1 / R_{yz} - 1$$

Table 3.2 *K-values* determined from the principle plane strain ratios (R) of deformed ooids presented in Table 3.1.

	Locality A	Locality B	Locality C
k-value	0,78	0,41	0,12

These *k-values* plot in positions in field A of the Flinn Graph (Fig. 3.19), and depict increasing strain, from locality A to locality C, as the shear zone is approached. Field A

indicates that the post-deformation shape of ooids adjacent to the bedding sub-parallel shear zones is in the field of apparent flattening, i.e. the ooids are oblate. While this may give some indication of the strain state in the study area, it must be remembered that the deformation is heterogeneous, and so strain rates *within* the shear zones are conceivably orders of magnitude greater. Similarly, strain may affect carbonate matrix materials differently to the ooids, and thus the ooids alone probably do not reflect a complete strain history. Such calculations, therefore, probably indicate only the minimum strain state involved in the D_2 bedding sub-parallel shear zones.

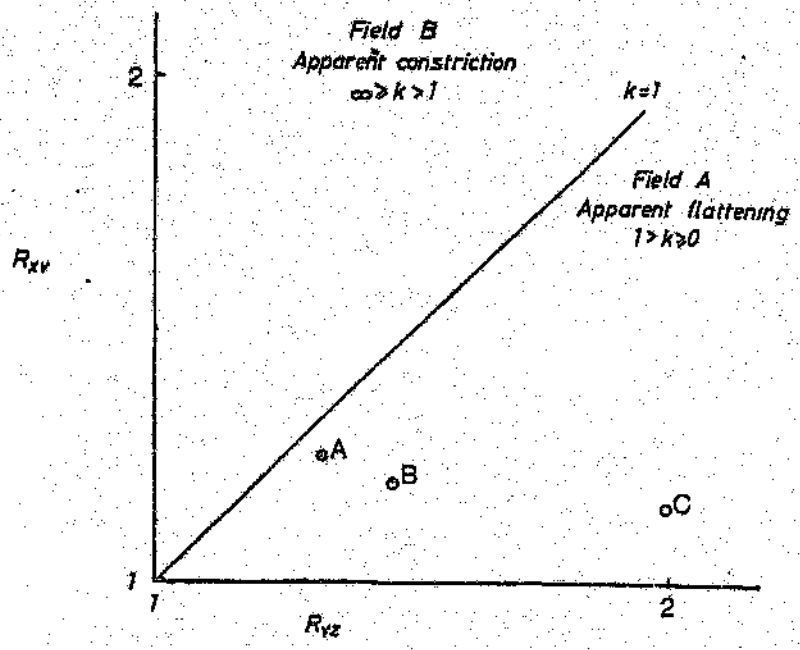

Fig. 3.19 Flinn graph with the plots of *k-values* for deformed ooids adjacent to a bedding sub-parallel shear zone in the Chuniespoort Group.

In ductile shear zones, such as those present in the study area, the angle between the plane of flattening and the shear plane can be used to determine the shear strain, gamma (γ), by employing the relationship

$$\gamma = 2 / \tan 2\Theta'$$

where Θ' is the angle between the maximum principal strain axis (X-axis) and the shear plane (Ramsay, 1980).

In the study area, the shear zones are assumed to be approximately bedding parallel. The angle of principal strain axes (as measured with a clinorule), relative to the shear planes, is, on average, approximately 30°. Using this value in the formula above gives the shear strain

$$\gamma = 2 / \tan 2\Theta'$$
$$= 2 / 1{,}73$$
$$= 1{,}15.$$

However, it is not uncommon for principal strain axes immediately adjacent to shear zones to be inclined 15° or less to the shear plane. In such cases, the shear strain (γ) approaches 3,5.

3.3.4 Lineations

Bedding-parallel quartz mineral rodding lineations (Fig. 3.20) are the most prominent lineations encountered in the study area. They are preferentially developed on thin chert laminae within the carbonate lithologies. Occasionally the lineations are curved (Fig. 3.21), either by inhomogeneities in shear intensity, or due to later deformation. The quartz rodding lineations occur sporadically throughout most of the Chuniespoort Group and are not necessarily spatially related to the major bedding sub-parallel shear zones. Those that occur within the D_2 shear zones plunge consistently on an approximately northerly bearing, roughly parallel to the dip direction of the shear zones (see Fig. 3.40).

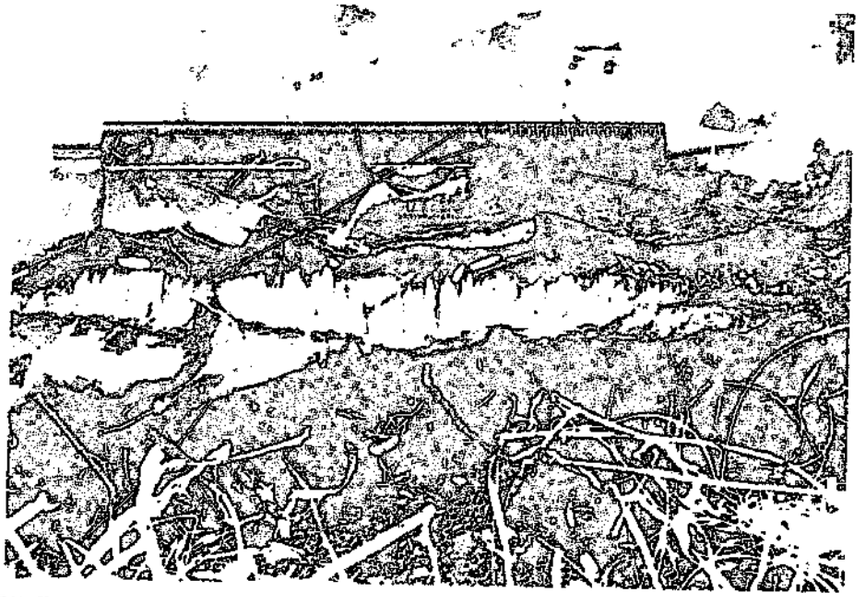

Fig. 5.20 Quartz rodding lineations developed on thin chert laminae in the dolomite strata. Locality (2862,7 X; -95,9 Y). Looking north.

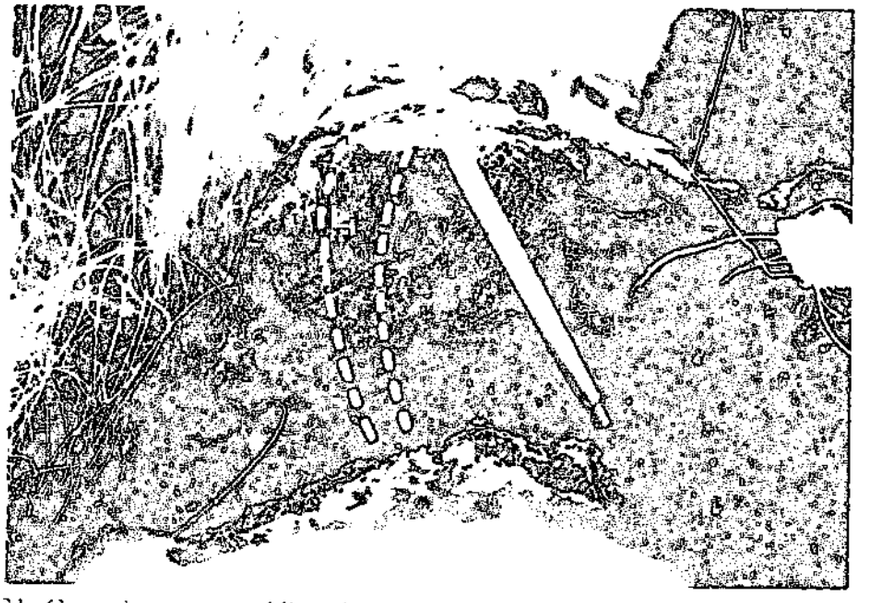

Fig. 5.21 Curved quartz rodding lineations on sub-horizontal bedding surface in the Chuniespoort Group. Pencil is pointing north. Locality (2856,2 X; -93,5Y).

Lineations developed outside the bedding sub-parallel shear zones have a wide variety of orientations (Fig. 3.22). The majority of these lineations, however, trend approximately north-south and plunge NNE, consistent with the trend of L_2 lineations. Stepping on lineated surfaces (Fig. 3.23) confirms that they developed in an environment of northerly-verging deformation. Lineations with orientations not consistent with a northerly plunge may have been a result of:

a) disturbance of the lineated surfaces by later periods of deformation (indicated by anomalous bedding orientations, Section 3.4);

b) localised inhomogeneities in strain during D_2; or

c) post-D_2 shearing episodes.

Lineations defined by crenulation microfold hinges are only rarely encountered on outcrop-scale in the study area. In the finely-laminated slate units of the Chuniespoort Group, the crenulation fold hinges encountered trend E-W and deform both the bedding and the S_2 cleavage. The wavelength of the crenulations is typically less than 1 mm. The upright nature of the folds in hand-specimen gives no indication of their vergence direction. Thin-section analysis, however, reveals slight overturning of the crenulations towards the north. The presence of crenulations provides evidence for deformation of the S_2 cleavage (Davis, 1984). Considering that the apparent northward vergence of the crenulations in the Chuniespoort Group slate units is consistent with the northward-verging cleavage-forming (D_2) event, it is possible that they represent a late D_2 feature, and may have been a result of progressive deformation during D_2. More data is, however, needed to confirm this.

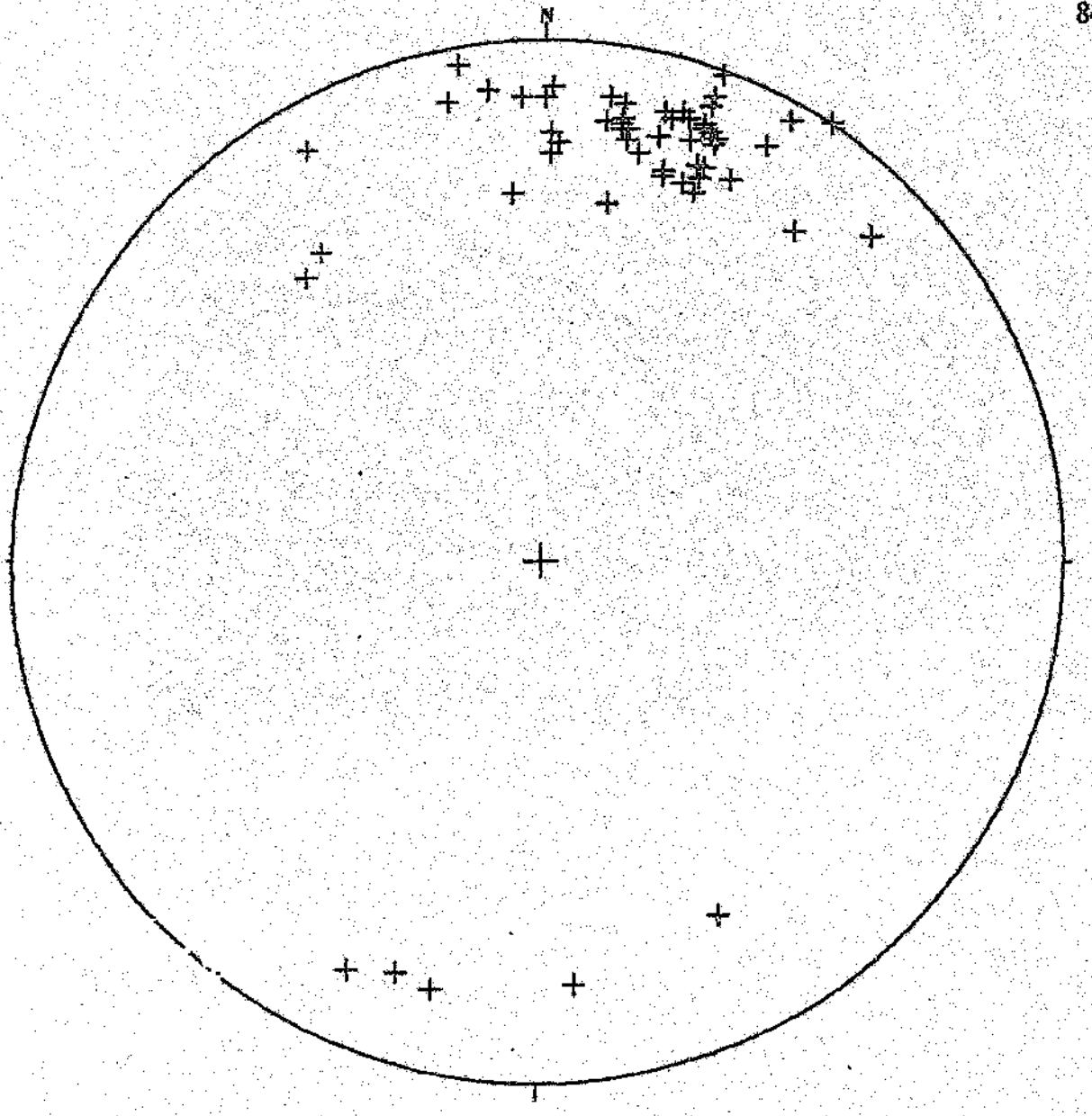

Fig. 3.22 Equal area (Schmidt) stereographic representation of the orientations of quartz rodding lineations (n=67) developed outside the bedding sub-parallel shear zones.

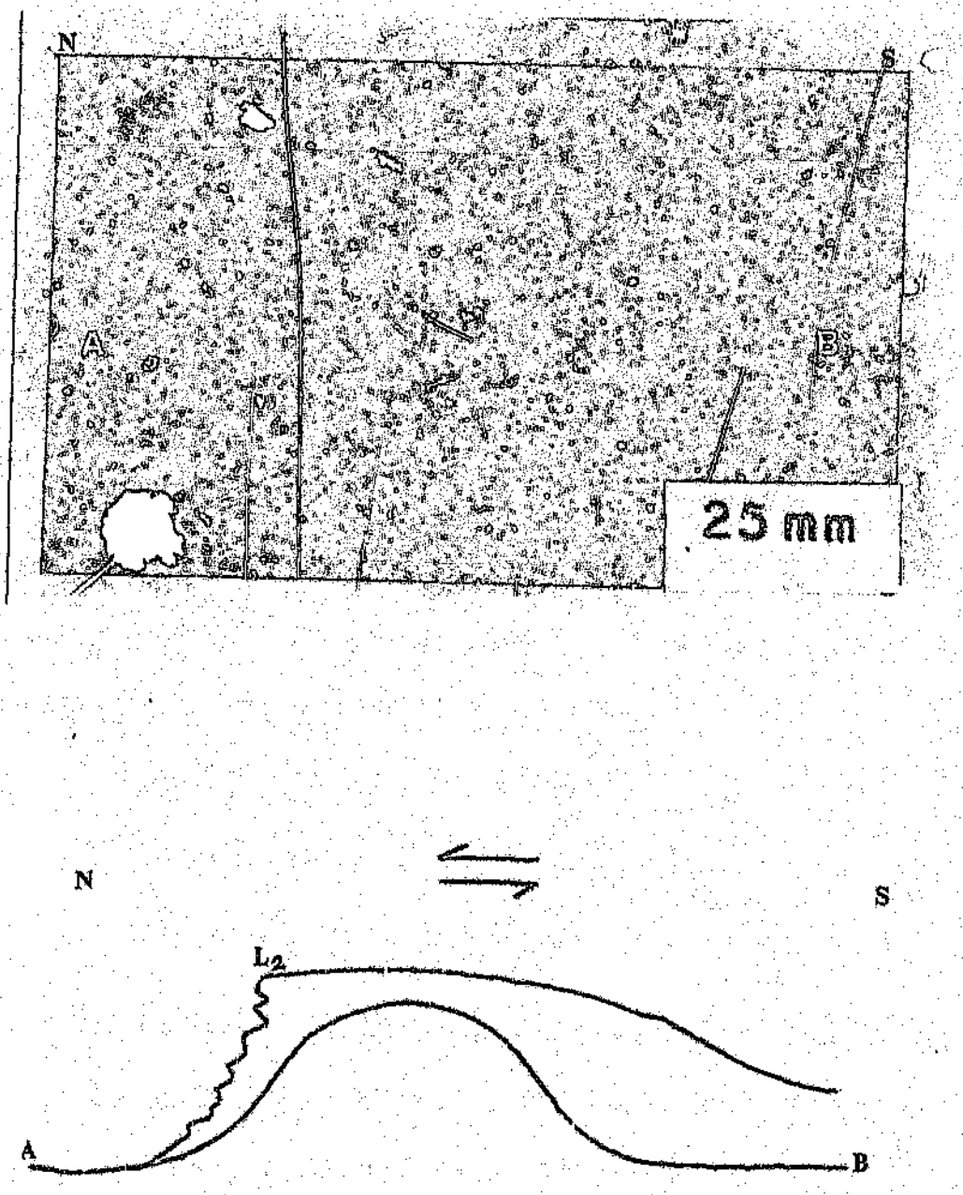

Fig. 3.23 a) Photograph showing a stepped lineated surface over a small stromatolite dome.

b) Cross-section from A-B showing top-to-the-north sense of shear.

In the Pretoria Group slate, approximately 20 km west of Magaliesburg along the R509, intense crenulations are abundantly developed, deforming both bedding and cleavage. Two sets of crenulation fold hinges are present (Fig. 3.24), trending approximately east-west and approximately north-south, respectively. The east-west trending crenulations have been correlated with the D_2 event. The north-south trending crenulation lineations may have resulted from east-west directed stresses.

Other lineations in the study area include poorly developed slickenside lineations in D_2 bedding sub-parallel shear zones, and elongated metamorphic minerals orientated in a north-south direction, plunging down the dip of bedding. Slickenside lineations are sporadically developed in the pelitic horizons and in certain sills. Those lineations in slate units show a similar orientation to the overall northerly trend of the other lineations. The lineations occurring in the sills have, unfortunately, not been encountered *in situ*, and thus their orientations could not be determined. If the lineations in the sills are related to the D_2 event, their presence would confirm that the sills intruded prior to the D_2 event.

3.3.5 Deformed ooids

Ooids are extensively, albeit irregularly, distributed in the Chuniespoort Group dolomites in the study area (Section 2.2.3). Ooids in the study area are not only deformed within, or immediately adjacent to, bedding-parallel shear zones (Section 3.3.3). Heterogeneous deformation of ooids also occurs within folded, as well as in undeformed, dolomite strata. The oblate ooids generally dip shallowly in a southerly direction, corresponding to the S_2 cleavage orientation in pelitic horizons, and are probably a result of the same stresses. Figure 3.25 shows extreme flattening and elongation of ooids, which defines a planar fabric dipping

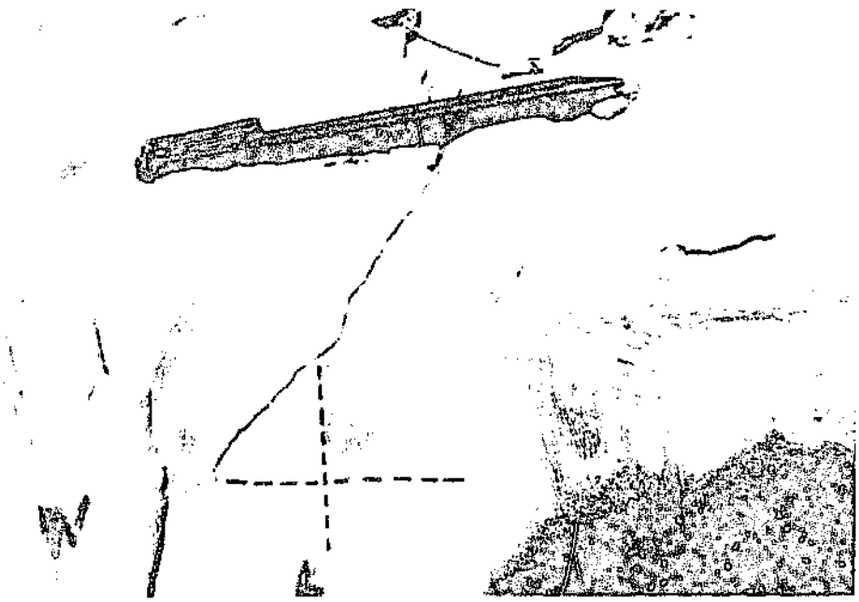

Fig. 3.24 Two sets of crenulation lineations detectable in slate horizons at the Magaliesberg locality. Looking down. South is to the top of the photograph.



Fig. 3.25 Extreme flattening of ooids, corresponding to the orientation of the south-dipping S_1 cleavage. Locality adjacent to a D_2 bedding sub-parallel shear zone in the Chuniespoort Group dolomite. Locality (2862,0 X; -95,0 Y). Looking west.

approximately 20° south. Closer inspection reveals the close relationship of this flattening to S_2 cleavage development in the rock (S_2 here is oriented 250°/20°S). The angular relationship of flattened ooids to bedding is consistent in the majority of cases examined. This relationship prevails even where the rocks are folded by F_3 (Section 3.4), leading to the conclusion that ooid flattening was a pre-folding, D_2 event.

Elsewhere in the study area, oblate deformed ooids display different attitudes to those described above (Fig. 3.26). The deformed ooids in Fig. 3.26 define a fabric oriented 335°/50°NE. This deformation is highly localised and does not correspond to any known major structures in the region.

3.4 The D_3 event

The D_3 event in the study area involved folding with associated sub-vertical shearing. The D_3 structures clearly deform D_2 bedding sub-parallel shear zones, cleavage and lineations.

3.4.1 Folds in the Chuniespoort Group

The dolomite units of the Chuniespoort Group reflect D_3 as large-scale open, upright folds with wavelengths ranging from tens to hundreds of metres (Fig. 3.27). These folds are concentrated in a broad zone roughly 1500 m wide, approximately mid-way through the Chuniespoort Group (Map 1). The D_3 fold hinges plunge approximately 10° on a bearing of about 300° (10 axes), or on approximately 120° (8 axes) (Fig. 3.28). This variation in fold hinge plunge is probably a function of the non-cylindrical nature of folds, and therefore the D_3 folds are probably periclinal in form.



Fig. 3.26 Highly localised deformation of ooids. The strained ooids define a fabric oriented 335°\50° NE. Looking northwest. Locality (2861,4 X; -94,3 Y).

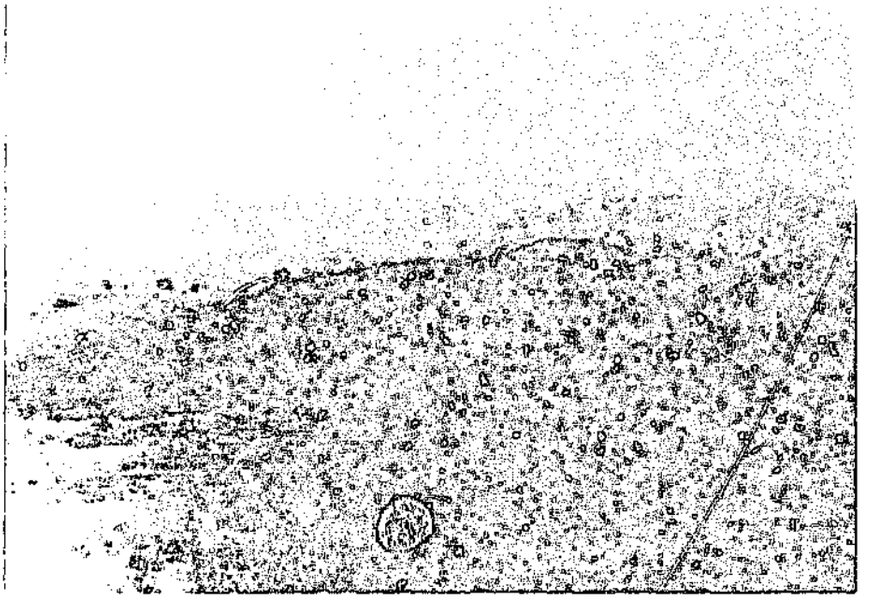

Fig. 3.27 Large-scale D_3 folding in the Chuniespoort dolomite. Looking north. Locality (2860,8 X; -95,2 Y).

An axial planar cleavage is only rarely associated with these folds but, where present, it dips steeply (70-80°) to the south (Fig. 3.28). Smaller-scale secondary folds are developed (Fig. 3.29), but their kinematic significance, as parasitic folds, for example, could not be ascertained.

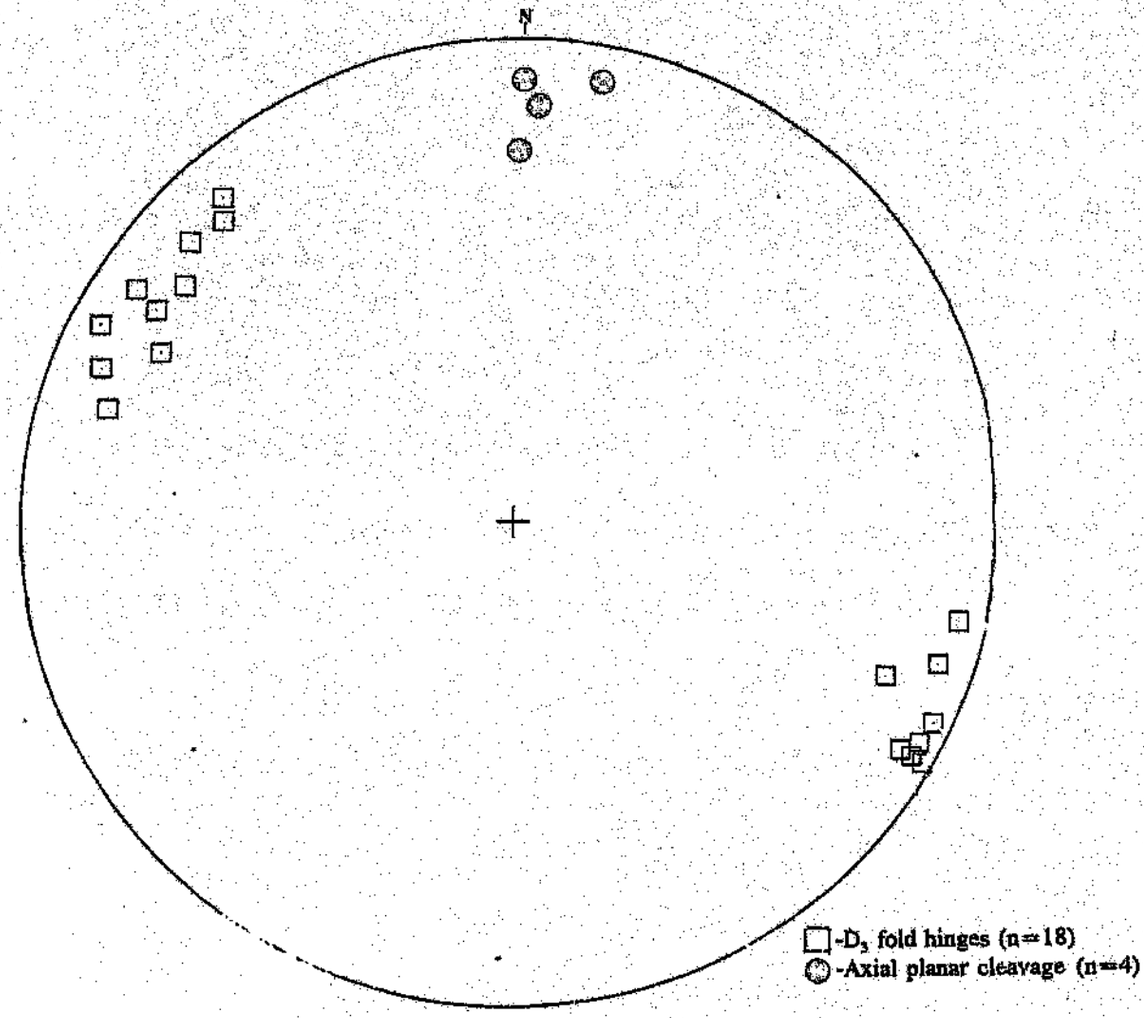

Fig. 3.28 Orientation of D_3 fold axes (n=18) and axial planar cleavage (n=4).



Fig. 3.29 Secondary fold in dolomite and chert layers associated with the D_3 folding event in the Chuniespoort Group. Looking east. Locality (2861,2 X; -95,6 Y).

Sub-vertical ductile shear zones are developed parallel to the D_3 fold axial planes in the Chuniespoort Group. These shear zones can usually be traced continuously for several kilometres (Map 1). The shear zones are subvertical, but dip measurements indicate that they anastomose. The shear zones all display down-to-the-south offset (cross-section, Map 1). The displacement across these shear-zones is, however, minor, and thus the D_3 folds do not appear to be ramp anticlines. Rather, the shear zones probably reflect ductile slip, parallel to the fold axial planes, as the intensity of deformation increased during D_3. Thin sections of oriented samples from within these shear zones show abundantly developed, fine-grained, recrystallised quartz with a prominent anastomosing shear fabric. Unfortunately, no definitive kinematic indicators, such as S-C fabrics or ooids deformed by the D_3 shear zones, were

encountered.

The D_2 bedding sub-parallel shear zones, as well as sills within the dolomite horizons, are folded by the D_3 folds (Map 1 and cross-section), indicating that D_3 occurred post-sill emplacement. Ooids deformed during D_2 maintain a consistent angular relationship with bedding around D_3 folds. D_3 folding thus conclusively post-dates D_2.

3.4.2 Folds in the Pretoria Group

In the Pretoria Group, the D_3 folding event manifests itself as non-cylindrical round-hinged folds in alternating slate and quartzite layers and, more commonly, as large-kink folds in argillaceous rocks (Fig. 3.30). The large scale kink folds have wavelengths up to 7 m, amplitudes up to 4 m and interlimb angles as small as 50°. The majority of the large-scale kink folds have axial planes which dip steeply to the southeast or the southwest (Fig. 3.31).



Fig. 3.30 Large-scale kink fold in Pretoria Group shales. Locality (2856,9 X; -94,5 Y). Looking southeast.

encountered.

The D_1 bedding sub-parallel shear zones, as well as sills within the dolomite horizons, are folded by the D_2 folds (Map 1 and cross-section), indicating that D_2 occurred post-sill emplacement. Ooids deformed during D_1 maintain a consistent angular relationship with bedding around D_2 folds. D_2 folding thus conclusively post dates D_1.

3.4.2 Folds in the Pretoria Group

In the Pretoria Group, the D_2 folding event manifests itself as non-cylindrical round-hinged folds in alternating slate and quartzite layers and, more commonly, as large-kink folds in [illegible] (Fig. 3.30). The large scale kink folds have wavelengths up to 7 m, amplitudes up to 4 m and interlimb angles as small as 50°. The majority of the large-scale kink folds have axial planes which dip steeply to the southeast or the southwest (Fig. 3.31).

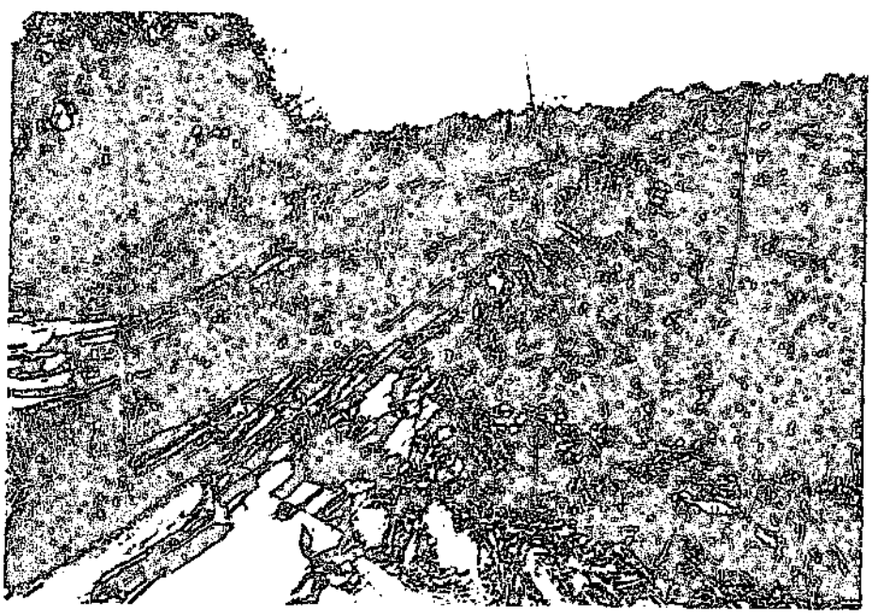

Fig. 3.30 Large-scale kink fold in Pretoria Group shales. Locality (2856,9 X; -94,5 Y). Looking southeast.

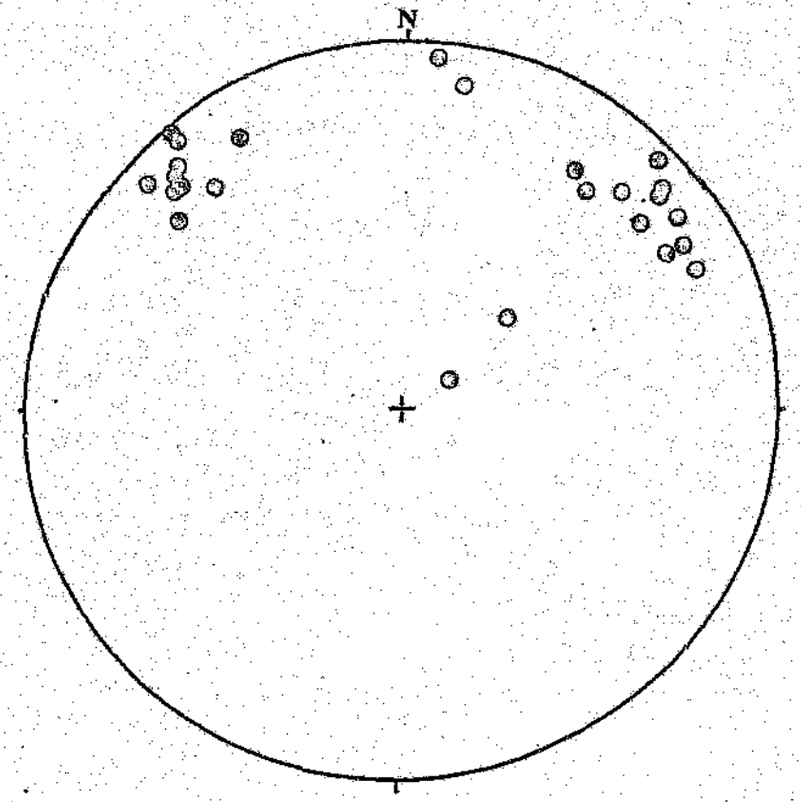

Fig. 3.31 Equal area stereonet plot of the poles to D_3 kink fold axial planes (n=25) in the Pretoria Group.

Analysis of thin sections from samples taken at appropriate localities within the D_3 kink folds shows that the folds deform the S_2 cleavage. The angular relationship between bedding and S_2 cleavage remains constant (approximately 30°) throughout the fold (Fig. 3.32). Restoring the orientations of cleavage at various localities in the fold was attained by applying multiple rotations. The first rotation accounted for the regional tilt (± 20° N) of the strata. Secondly, the fold hinge was rotated to the primitive circle. Finally, bedding was rotated to correct for folding. Although somewhat dispersed, the resultant pre-folding orientation of S_2 cleavage within this fold is shown in Fig. 3.33, which plots in the field of S_2 cleavage determined for undeformed rocks in the study area (compare with Fig. 3.2).

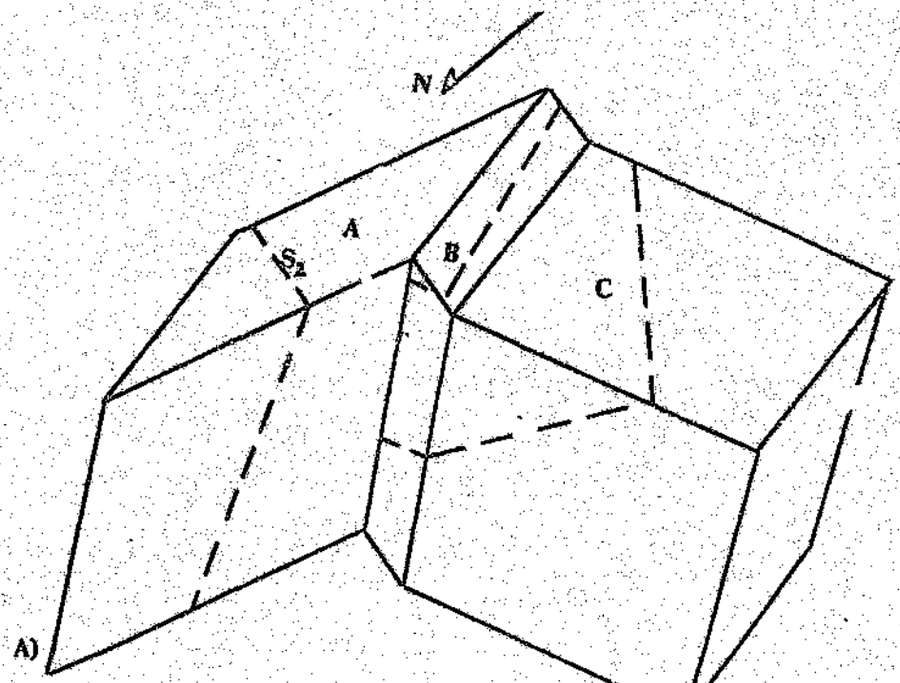

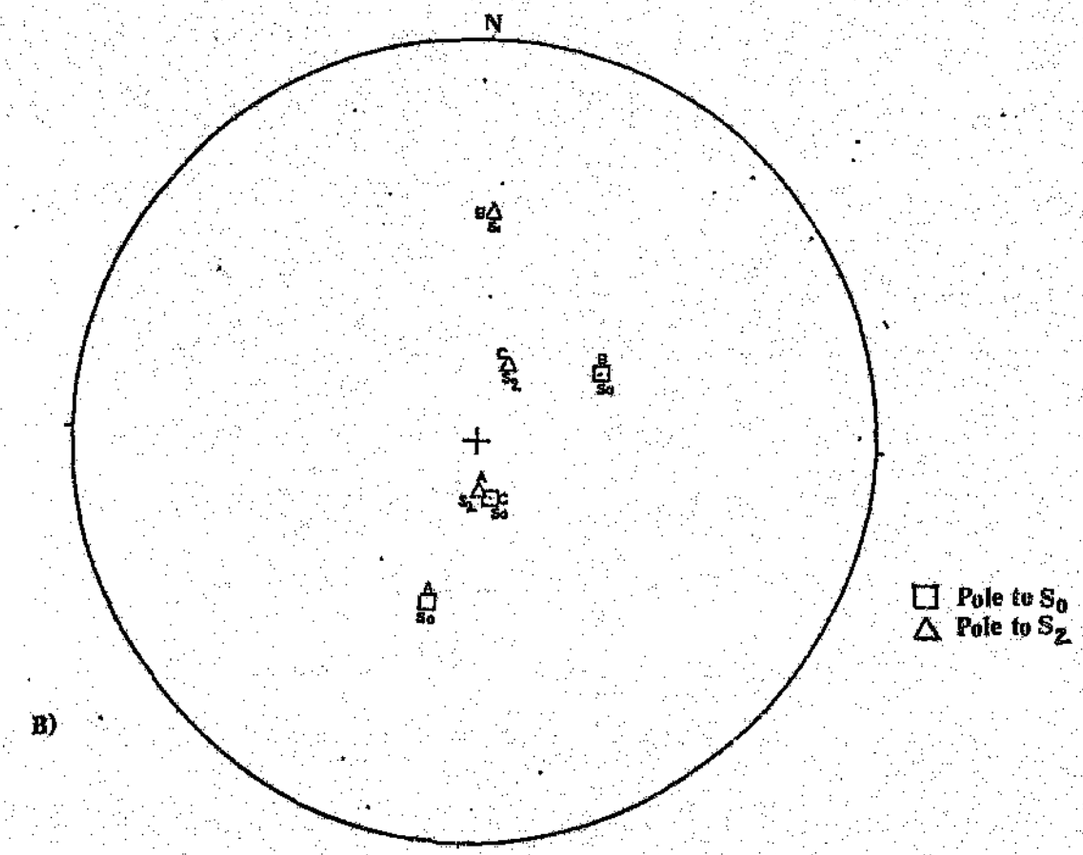

Fig. 3.32 Schematic representation (A) and stereonet (B) demonstrating how S_2 cleavage retains a constant angular relationship with bedding during kink folding.

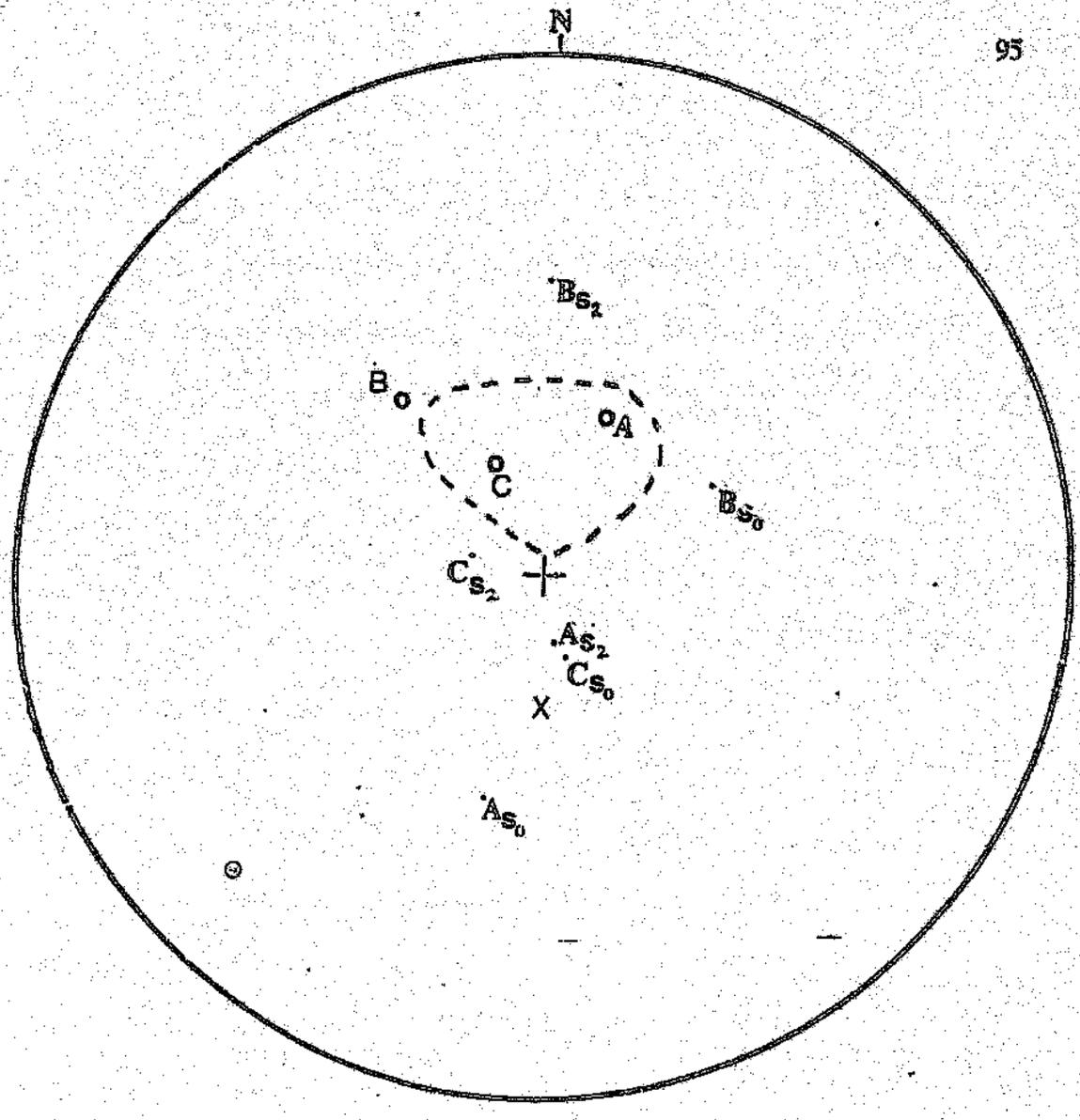

Fig. 3.33 Equal area (Schmidt) stereonet showing the rotation of S_2 cleavage and bedding in a kink fold to their original orientations. Dashed line indicates the field of S_2 poles in Fig. 3.2.

The contrasting styles of kink-folds in the Pretoria Group slate and round-hinged folds in the Chuniespoort Group dolomite can be explained in terms of experimental results. Kink-bands have been experimentally produced at the boundary of a multilayer during the initial stages of layer-parallel compression, due to local irregularities in layering (Cobbold *et al.*, 1971). These workers determined that kink-bands develop preferentially in materials with high mechanical anisotropy, while upright, sinusoidal, internal buckles develop in materials with low mechanical anisotropy. In the study area, the slate layers (which have high mechanical anisotropy due to their fine layering and abundant development of penetrative S_2 cleavage) produce kink-bands, while the less mechanically anisotropic [illegible] by virtue of their more massive nature, great layer thickness, and scarcity of [illegible] hinged folds.

Honea and Johnson (1976), however, contradict the model of Cobbold *et al.* (1971) by proposing that localised cohesion loss in the limbs of low amplitude buckles can produce conjugate kink-bands. Honea and Johnson (1976) therefore concluded that low mechanical anisotropy produces kink-bands, whereas high mechanical anisotropy produces sinusoidal folds, contrary to the deduction of Cobbold *et a.*. (1971).

The contradiction between the models of Cobbold *et al.* (1971) and Honea and Johnson (1976) can, however, be resolved. Latham (1985) determined that, at a particular strain, two moduli are defined: a) incremental strain due to incremental stress, and b) stress due to the total strain. When a "non-linear" material is deformed, the two moduli differ, and an induced anisotropy results. Following this, the greater the difference between the two moduli, the greater the induced anisotropy. Most natural materials conform to non-linear behaviour, and

thus when they are deformed, induced anisotropy is added to the material, which increases with the incremental response to deformation. Intrinsic anisotropy is the anisotropy inherent in a material due to any layering or fabric and, when combined with induced anisotropy, gives the total anisotropy of a material. Latham (1985) concluded that materials with high i. duced anisotropy are favourable for the development of kink-bands. Thus a multilayer with small intrinsic anisotropy could develop a high induced anisotropy during deformation, such as was the case with the multilayer experiment of Honea and Johnson (1976), where local loss of interlayer cohesion resulted in non-linear behaviour.

A material with pronounced intrinsic anisotropy (for example due to layering and/or cleavage) may, when subjected to deformation, exhibit instability as either reverse or normal kink-bands, depending on whether maximum compression was directed perpendicular to, or parallel with, the layering or fabric (Price and Cosgrove, 1990). An homogeneous material (such as sandstone or granite) has insignificant intrinsic anisotropy, but with deformation may obtain sufficient induced anisotropy to equal the total anisotropy of a rock with high intrinsic anisotropy (Price and Cosgrove, 1990). This rock may express instability as a shear zone, rather than as kink-bands (Price and Cosgrove, 1990).

The difference in fo. ! style resulting from the same deformation event in Chuniespoort Group dolomite and Pretoria Group slate units can, therefore, be attributed to competency and anisotropy contrasts between the two lithologies. The slate in the study area has very fine layering and widespread presence of S_2 cleavage, and thus has high intrinsic anisotropy (Latham, 1985). Lack of fine layering and cleavage in the dolomite, as well as its more massive, competent nature dictates that these strata have low intrinsic anisotropy (Latham,

1985). Thus, when exposed to stress, the slate units would tend to develop kink-folds while the dolomite would not (Price and Cosgrove, 1990).

Round-hinged folds (Fig. 3.34) are occasionally encountered in the Pretoria Group where slate and quartzite are intercalated. The folds have wavelengths of up to 5 m, and amplitudes of up to 1,5 m. Their interlimb angles seldom exceed 120°. The orientation of fold axial planes varies, although they are typically oriented approximately 320°/80°S or 050°/80°S. The non-cylindrical nature of the round-hinged folds is reflected in the variation of fold hinge orientations (Fig. 3.35). The geometry of these round-hinged, non-cylindrical folds is probably controlled by the relatively high competence contrast between the competent quartzite units intercalated with incompetent slate. The S_2 cleavage is rotated by the D_3 round-hinged folding.

In the Pretoria Group slates, the area around locality (2855,0 X; -92,7 Y) is folded by two sets of open folds with wavelengths of one to five metres. Exposure at this locality is poor, and the fold closures have been eroded, therefore no fold superposition or fold interference structures were seen. Fold limb orientation data does, nonetheless, reveal two distinct sets of fold axes which plunge approximately ↓ NE and approximately WSW respectively (Fig. 3.36). S_2 cleavage is, unfortunately, not homogeneously developed, and the relationship of bedding to cleavage within the folds is unclear. As the structural relationship of these folds is highly ambiguous, their origin can only be speculated upon. These folds may be a result of interference of minor easterly- or westerly-verging deformation events with D_3 folding.

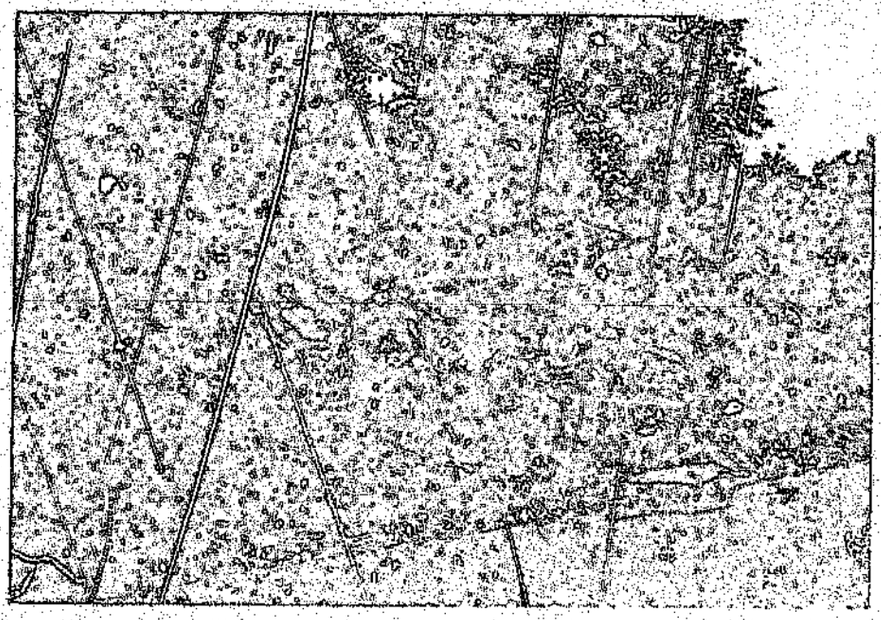

Fig. 3.34 Round-hinged fold in intercalated slate and quartzite layers in the Pretoria Group. Locality (2854,8 X; -95,1 Y). View to the west.

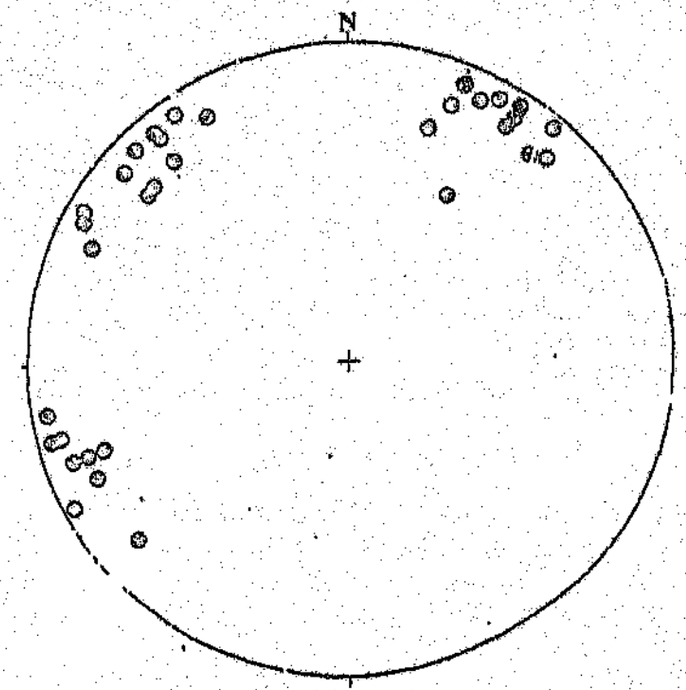

Fig. 3.35 Stereonet plot of the hinges of D_3 round-hinged folds (n=33) in the Pretoria Group showing their non-cylindrical nature.

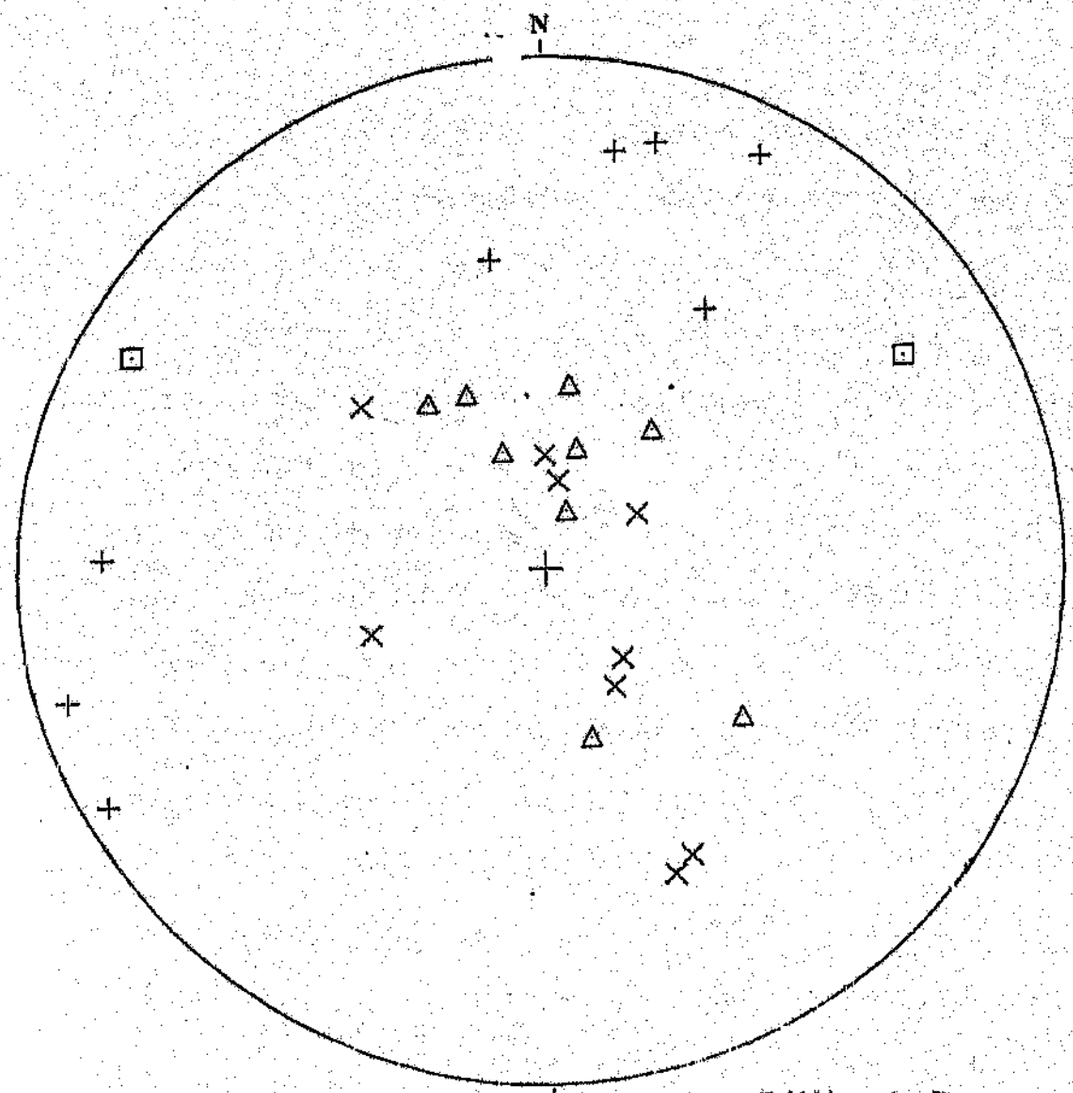

Fig. 3.36 Stereonet plot of the interference fold sets at locality (2855,0 X; -92,7 Y).

3.5 D_4 event

This deformation event gave rise to the development of northerly and ENE trending sub-vertical faults and, possibly, to some of the enigmatic lineaments encountered in the study area. Only a few of the fault zones are exposed in the field, and, as a result, very little fault-plane and lineation orientation data was obtained. A large proportion of the faults can, however, be clearly traced as negative relief features and on aerial photographs, some for several kilometres. Offset of markers across some of the more prominent faults suggests apparent strike-slip separation varying from metres to hundreds of metres. Sinistral offsets across these faults are most commonly associated with the larger-scale faults. Dextral offsets are, however, also prevalent, but more commonly associated with smaller-scale faults. The movement-sense along these sub-vertical faults could not be directly determined due to the lack of fault-plane and lineation data. However, similar offset of both sub-vertical quartz-veins (Fig. 3.37) and bedding (which dips approximately 20° from the horizontal) in a strike-slip fashion suggests that this is the movement sense across these sub-vertical faults. The occurrence of both apparent sinistral and dextral strike-slip fault movement in the study area suggests either that there was more than one episode of fault activity giving rise to the different offsets, or they may be part of a conjugate set of faults. Some faults in the Chuniespoort Group dolomite are infilled with quartz from fluids migrating along the fault zones (Fig. 3.38).

D_2 bedding sub-parallel shear zones, D_3 upright folds and the sills in the study area are offset and truncated by the D_4 sub-vertical faults (Map 1). A prominent strike-slip fault orientated approximately 170°, which occurs near the western border of the study area, is fairly well-exposed by excavations at one locality in the Pretoria Group. A highly weathered dyke is

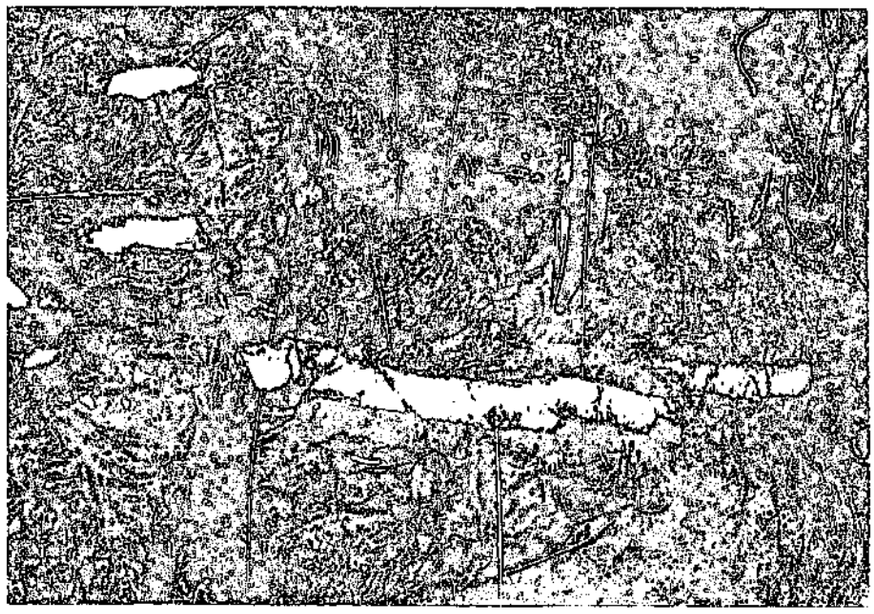

Fig. 3.37 Dextral strike-slip offset of sub-vertical quartz vein adjacent to a major northerly-trending D_6 fault. Locality (2862,5 X; -97,0 Y).

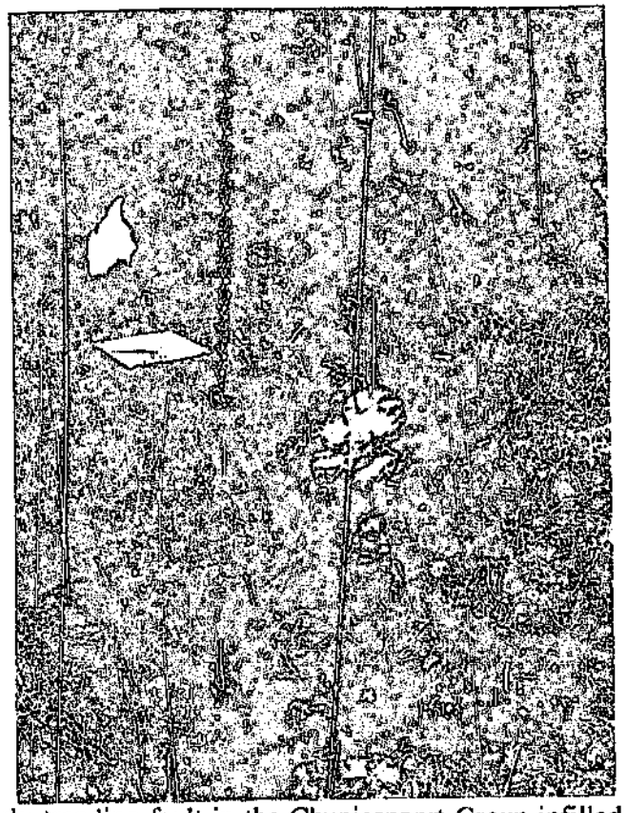

Fig. 3.38 Northerly trending fault in the Chuniespoort Group infilled with quartz. Locality (2856,4 X; -91,5 Y). Looking north.

associated with this fault (Map 1). Fault breccias encountered in this fault zone comprise clasts of chert, marble and dyke material of the above-mentioned dyke (Fig. 3.39). Fault breccia with dyke- and other clasts in strike-slip faults suggests that the fault may have exploited the zone of weakness created by the emplacement of the dyke. Alternatively, the fault may have pre-dated the dyke controlling its emplacement, the fault having been subsequently reactivated. Therefore, a period of strike-slip fault activity in the Transvaal basin occurred post-dyke emplacement. The highly weathered nature of this dyke unfortunately precludes identification of its origin and any attempt at age determination. A prominent syenite dyke, which is probably related to the Pilanesberg Complex (Section 2.2.6), trends approximately south-easterly, cross-cutting the dolomite units. It is slightly offset by northerly orientated strike-slip faulting (Map 1).



Fig. 3.39 Fault breccia comprising clasts of chert (C), marble (M) and dyke material (D).

Locality (2856.2 X, 97.2 Y)

associated with this fault (Map 1). Fault breccias encountered in this fault zone comprise clasts of chert, marble and dyke material of the above mentioned dyke (Fig. 3.39). Fault breccia with dyke- and other clasts in strike-slip faults suggests that the fault may have exploited the zone of weakness created by the emplacement of the dyke. Alternatively, the fault may have pre-dated the dyke, controlling its emplacement, the fault having been subsequently reactivated. Therefore, a period of strike-slip fault activity in the Transvaal basin occurred post-dyke emplacement. The highly weathered nature of this dyke unfortunately precludes identification of its origin and any attempt at age determination. A prominent syenite dyke, which is probably related to the Pilanesberg Complex (Section 2.2.6), trends approximately south-easterly, cross-cutting the dolomite units. It is slightly offset by northerly orientated strike-slip faulting (Map 1).



[illegible] comprising clasts of chert (C), marble (M) and dyke material (D).

[illegible]

Sub-vertical, east-west trending, faults are encountered in the dolomite units towards the southern boundary of the study area. These faults can be traced for hundreds of metres along strike. No displacement was detected across the faults. The fault zones are generally several metres wide and are infilled with vein quartz. Occasionally, small pods of massive sulphide (mainly pyrite) occur in the vein quartz. Adits have been dug into these fault zones in the past, indicating mining activity and the presence of mineralization. The Pretoria Group shales are also affected by similarly orientated faults, although these are not extensively developed. These faults are narrow fracture zones, usually of the order of a few centimetres in width, and are not infilled with chert or other material. Offsets of markers have not been observed across these fractures.

Aerial photograph analysis has revealed the existence of linear features several kilometres in extent trending approximately 070° (Map 2). Field investigations, however, failed to establish their structural significance. A lack of dyke outcrop or surface rubble in the area suggests that is unlikely that these lineaments represent dykes. The possibility that these linear features represent faults cannot be excluded. They may be related to similarly trending faults near Pretoria, east of the study area, described originally by Temperly (1977).

3.6 Effects of the Johannesburg Dome

According to Eriksson (1977), uplift of the Johannesburg Dome may have occurred periodically during the Proterozoic. The tilt of the Black Reef Quartzite Formation, the Chuniespoort Group, and the Pretoria Group off the Johannesburg Dome may have been a result of the emplacement of the dome, which constrains the doming event to post-Transvaal times (McCarthy *et al.*, 1986; Hilliard, 1994). According to McCarthy *et al.* (1986), uplift

of the Johannesburg Dome dispersed cleavages and reactivated structures attributed to the formation of the Vredefort Dome. Uplift of the Johannesburg Dome thus post-dated the Vredefort event. It will be shown in Section 6.3.2 that D_2 structures in the study may have resulted from the emplacement of the Vredefort Structure, and thus northerly tilting of strata in the study area probably post-dated D_2.

The emplacement of the Johannesburg Dome may have been responsible for the formation of D_4 structures in the study area (Section 6.3), and thus doming may have post-dated D_3. This relationship could not, however, be conclusively established in the study area. Nonetheless, if the doming event did post-date D_3, then rotations to compensate for the northerly tilt of the strata are necessary to determine the orientation of D and D_3 structures at the time of their formation.

The rotation undertaken in Fig. 3.40 shows that L_2 lineations (Section 3.3.4) originally had a horizontal to southerly plunge. Similarly, rotation of axial planar cleavage associated with D_3 folds in the dolomite lithologies (Section 3.4.1) indicates that the axial planes of the D_3 folds were originally sub-vertical to north dipping (Fig. 3.41) and, thus, the folds may originally have been slightly overturned to the south. Rotation of D_3 shear zones, which are oriented approximately parallel to D_3 axial planar cleavage, suggests that they originally dipped steeply to the north. This, together with their down-to-the-south offset, suggests that th D_3 shear zones are southerly-verging, high-angle, thrust faults. Restoring the orientation of D_3 kink fold axial planes in the Pretoria Group slates (Section 3.4.2) reveals their original average strike to be $\sim 300°$ and $\sim 045°$, dipping sub-vertically (Fig. 3.42).

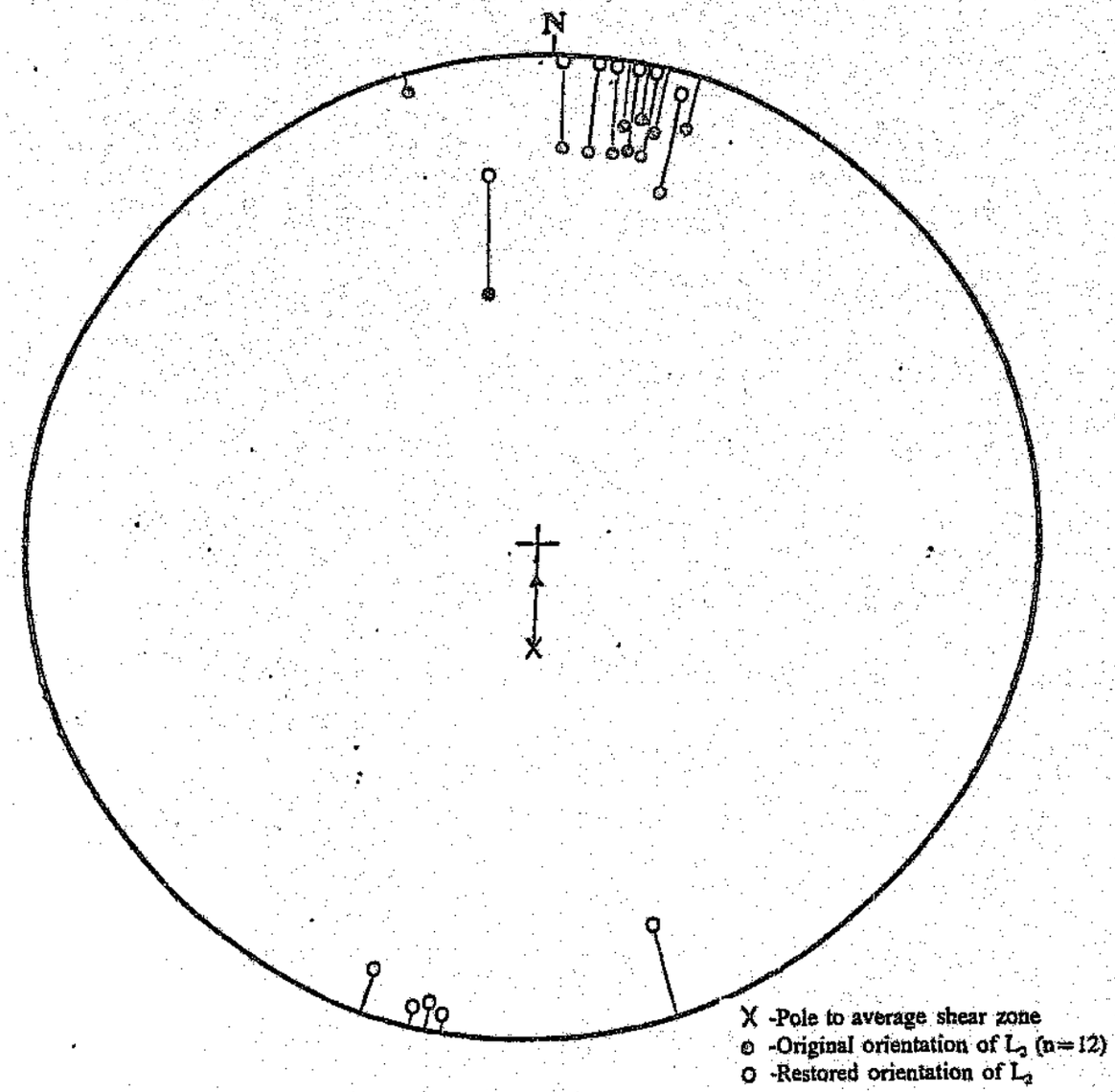

Fig. 3.40 Orientation of L_2 lineations. Restoration of bedding to the horizontal suggests that they plunged horizontally or slightly south at the time of their formation.

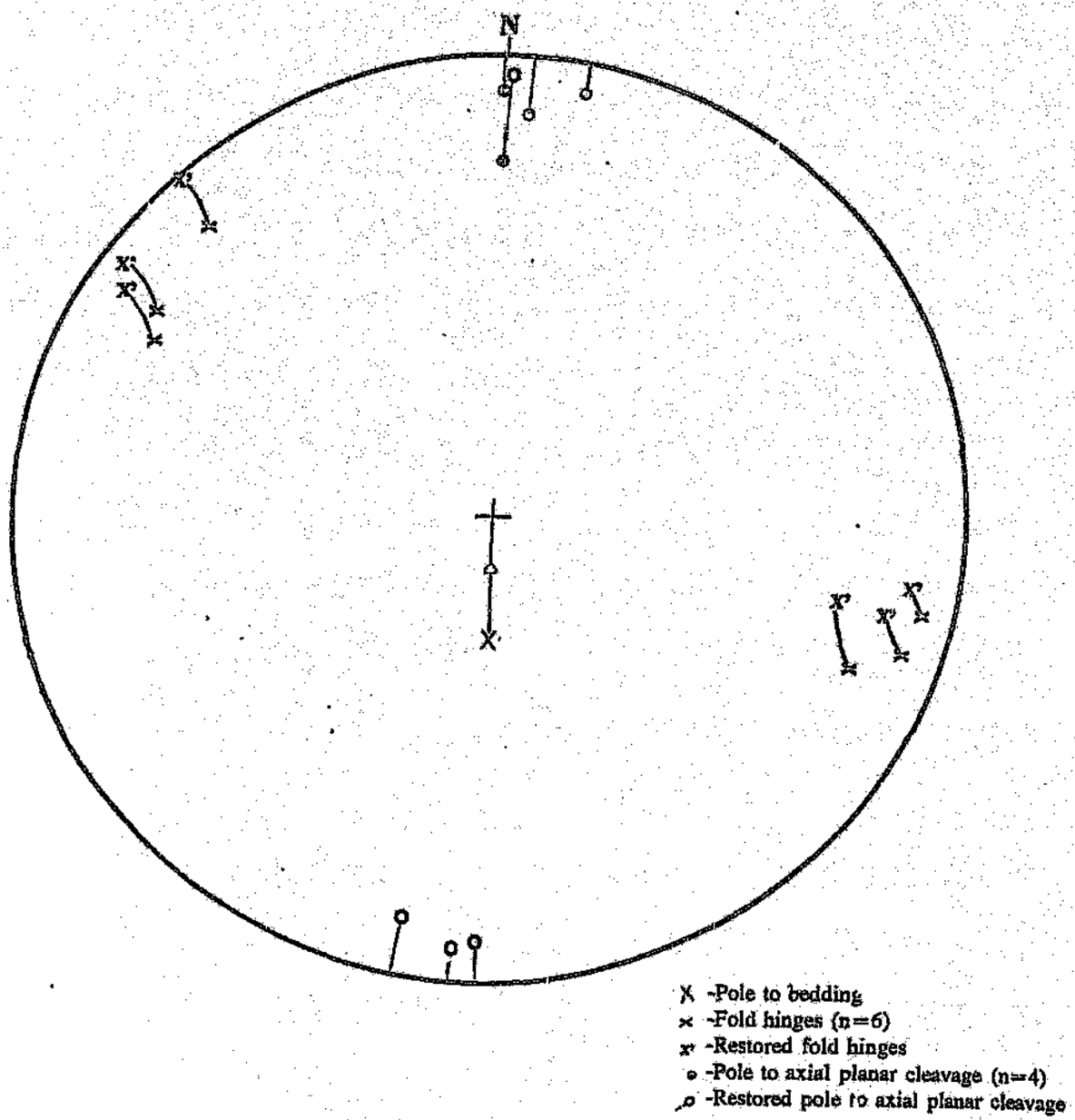

Fig. 3.41 Rotation of D_3 folds and associated shear zones to their original orientations to account for the regional tilt of strata. Orientation of bedding is 090°/20°N.

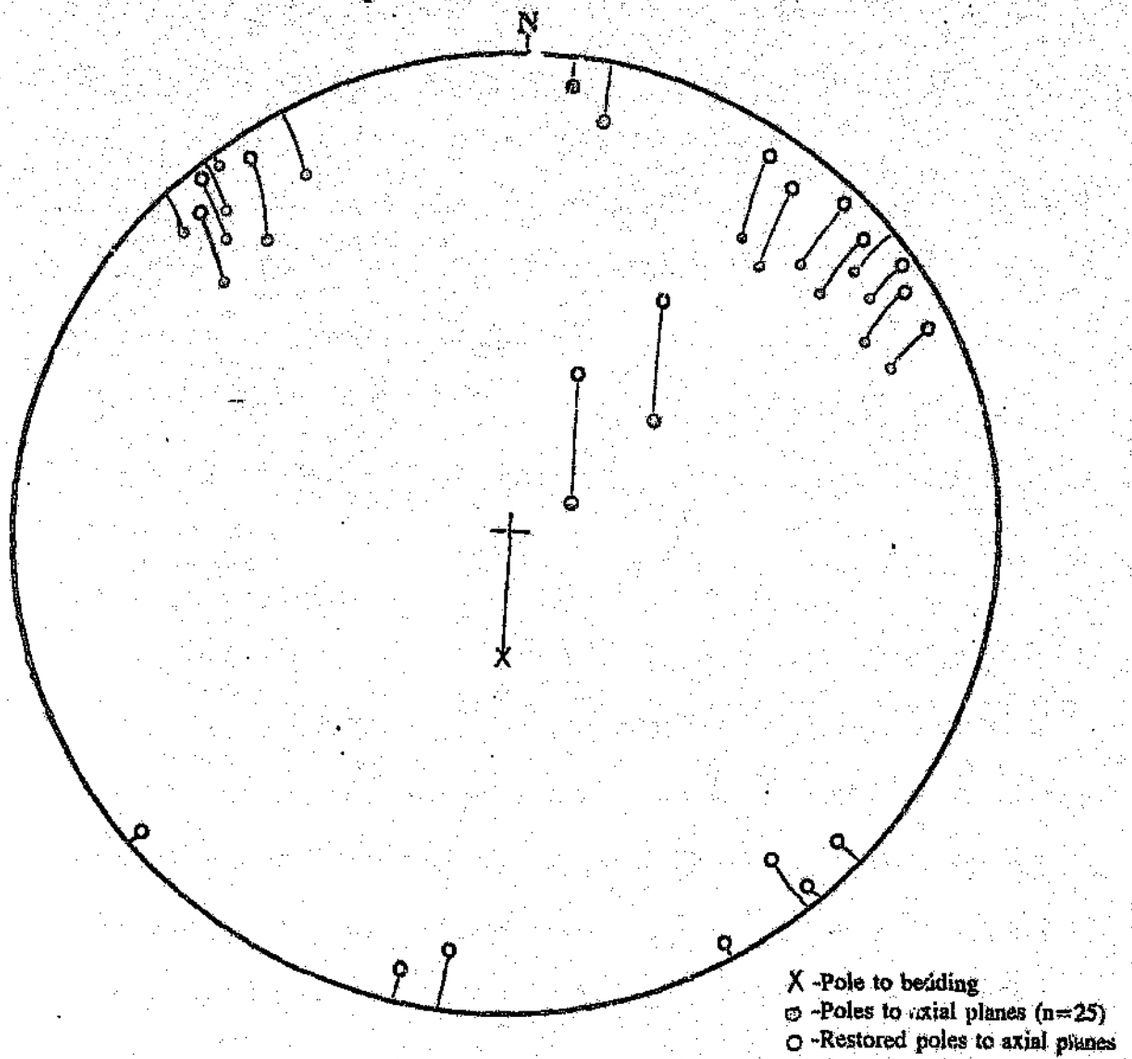

Fig. 7.42 Rotation of D_3 kink-fold axial planes in the Pretoria Group to account for the regional tilt of strata.

3.7 Other ductile deformation

The D_2 cleavage, bedding sub-parallel shear zones and lineations have all been significantly deformed by later structural events. Evidence for other shearing events which exploited and reactivated the planes of weakness which define the D_2 bedding sub-parallel shear zones, as well as adjacent lithologies, includes both westerly-verging duplex structures and easterly-verging kink folds. These structures are, however, extremely localised, and it is not possible to determine their relative timing or their relationship with other (D_3 and D_4) structures. Heterogeneously developed small- to medium-scale folds with fold axes oriented approximately N-S deform the Pretoria Group slates, possibly as a result of the same E-W oriented stresses responsible for the reactivation of the D_2 shear zones.

3.7.1 West-verging structures

a) Reactivated shear zones

The most convincing macro-scale example of different components of shearing in the D_2 bedding sub-parallel shear zones occurs in the basal slates of the Pretoria Group near the Crocodile River (locality 2857,5 X; -94,0 Y). At this locality, a well-exposed D_2 bedding sub-parallel shear zone occurs near the base of a cliff. A duplex structure, which owes its origin to approximately westerly directed deformation, has deformed this bedding sub-parallel shear zone (Fig. 3.43). Oriented samples were examined from various localities above, below and within this structure in order to obtain a structural profile across the shear zone.

Approximately 4 m above the shear zone, a pronounced shear fabric is seen in thin section, with matrix quartz and phyllosilicate (including biotite) grains aligned approximately parallel to compositional layering. Porphyroblasts with hourglass zoning, characteristic of chloritoid,

are developed discordantly to the overall fabric. An easterly dipping cleavage is only weakly developed in these samples. As the shear zone is approached, the cleavage becomes more intense, dipping 13-15° eastwards, and is prominent in thin section. Numerous porphyroblasts are preserved in samples from this area (Fig. 3.44). They are, however, all oxidised, and thus their original composition is indeterminable. The presence of internal cleavages (S_i), which are critical for determining the kinematic significance of the porphyroblasts (Hanmer and Passchier, 1991), is largely obscured by oxidation (Fig. 3.44). Therefore, traces of possible internal cleavage observed at the margins of some porphyroblasts (Fig. 3.44) cannot be followed through the porphyroblast cores. As a result, no conclusive kinematic interpretations can be made from these porphyroblasts. Easterly-dipping cleavage anastomosing around these altered porphyroblasts (Fig. 3.44) does, however, suggest pre- to syn-deformation growth of the porphyroblasts.

Immediately above the duplex structure, zonal to discrete crenulation cleavage is heterogeneously developed (Fig. 3.45). This crenulation cleavage dips steeply (approximately 65°) towards the east, and deforms the earlier, subhorizontal, S_2 cleavage.

Immediately below the bedding sub-parallel shear zone, in an area of less pronounced strain, an intense, heterogeneous cleavage which dips 20-25° to the east, has crenulated the pre-existing shear fabric (S_2). No other east-west oriented kinematic indicators were found within or adjacent to the bedding sub-parallel shear zone, except a recumbently folded quartz vein indicating top-to-the west shear.

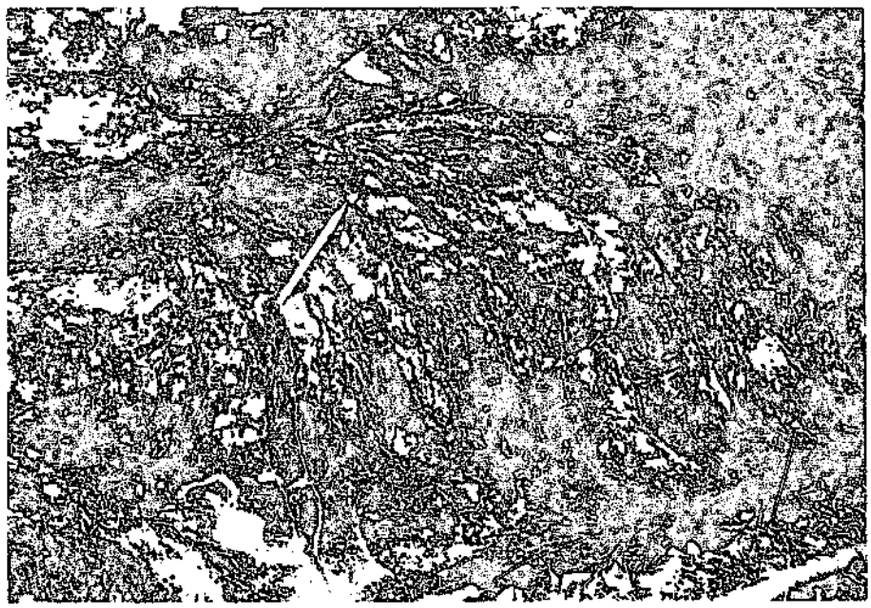

Fig. 3.43 Duplex structure in a bedding sub-parallel shear zone. Locality (2857,5 X; -94,0 Y). Looking north.

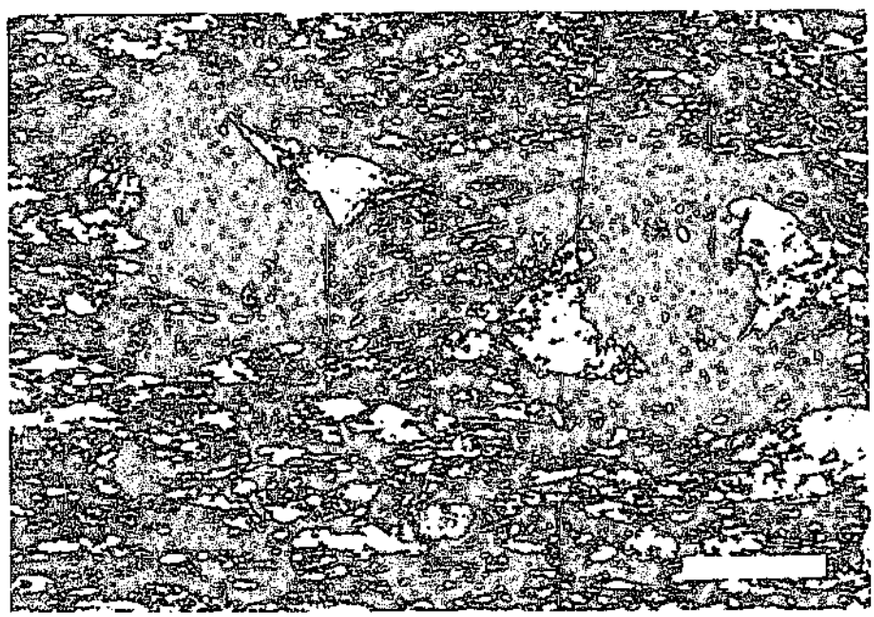

Fig. 3.44 Oxidised porphyroblasts adjacent to the duplex structure shown in Fig 3.43 above. Scale bar 0,5mm

Westerly-verging structures with similar morphology and intensity to the duplex at locality (2857,5 X; -94,0 Y) in the study area have been encountered superimposed upon a bedding s...-parallel shear zone (Fig. 3.46) in a road cutting approximately 20 km west of the town Magaliesburg (Fig. 1.1), along the R509. Also encountered at this locality were small-scale, westerly-verging fold sets and associated cleavage hosted in the strata adjacent to the shear zones.

Based on the observations in the study area and near Magaliesburg, the westerly-verging deformation may be more widely developed in the Transvaal Supergroup, however, additional regional mapping would have to be undertaken to establish this.

b) Lineations

Lineations defined by crenulation fold hinges are only occasionally seen in hand specimen. They plunge shallowly (up to 20°) on a northerly bearing. Their wavelengths are similar to the wavelengths of crenulations in the Chuniespoort Group (i.e. approximately 1 mm), although their fold intensity may be greater. Analysis of thin-sections cut perpendicular to the crenulation lineation confirms the westerly vergence of these structures.

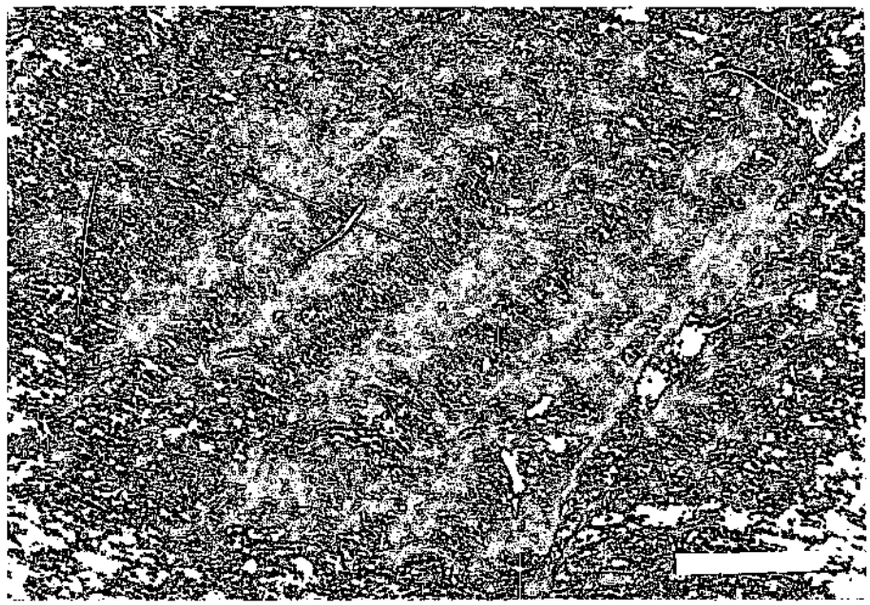

Fig. 3.45 Easterly-dipping cleavage deforms the earlier S_2 cleavage adjacent to a reactivated D_2 bedding sub-parallel shear zone in the Pretoria Group. Scale bar 0,5 mm.

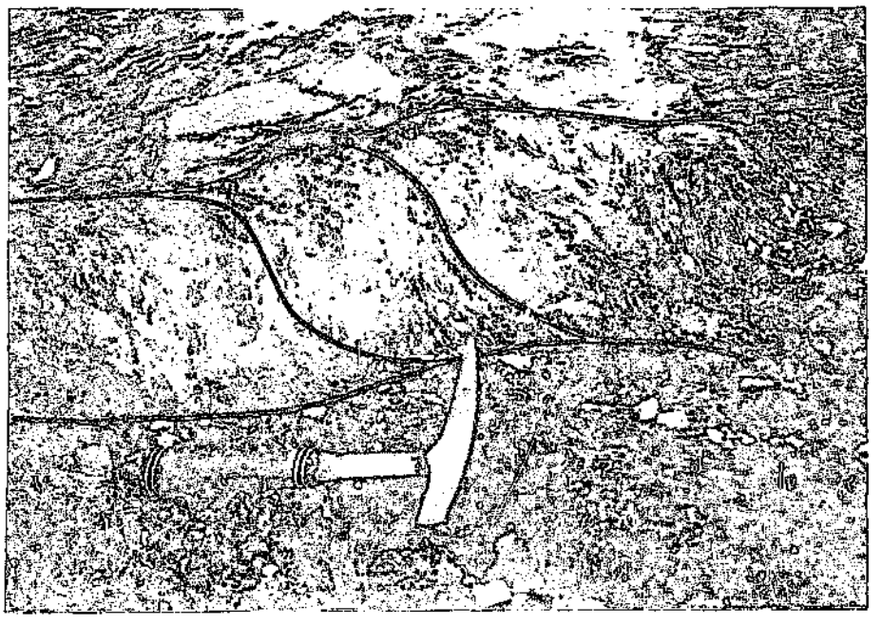

Fig. 3.46 Duplex structure similar to that in Fig. 3.43 in a slate-hosted shear zone. Locality 20 km west of Magaliesburg, along the R509. Looking north.

c) Folds

Sinusoidal, small- to medium-scale, gentle to open folds with wavelengths which range from < 0,5 m to approximately 3 m have deformed the Pretoria Group slates outside the shear zones. Their fold-axes plunge shallowly to moderately on either northerly or southerly orientations (Fig. 3.47) and, although the majority of these folds are upright, some axial planes dip to the east (Fig. 3.47), indicating westward vergence. Due to limited outcrop and isolation of the folds with respect to other structures, the relative timing of these folds could not be accurately determined. S_2 cleavage is very poorly developed in the majority of these folded slates, and thus whether or not these folds rotate S_2 cleavage could not be determined. Their relative timing with respect to D_2 structures therefore remains uncertain.

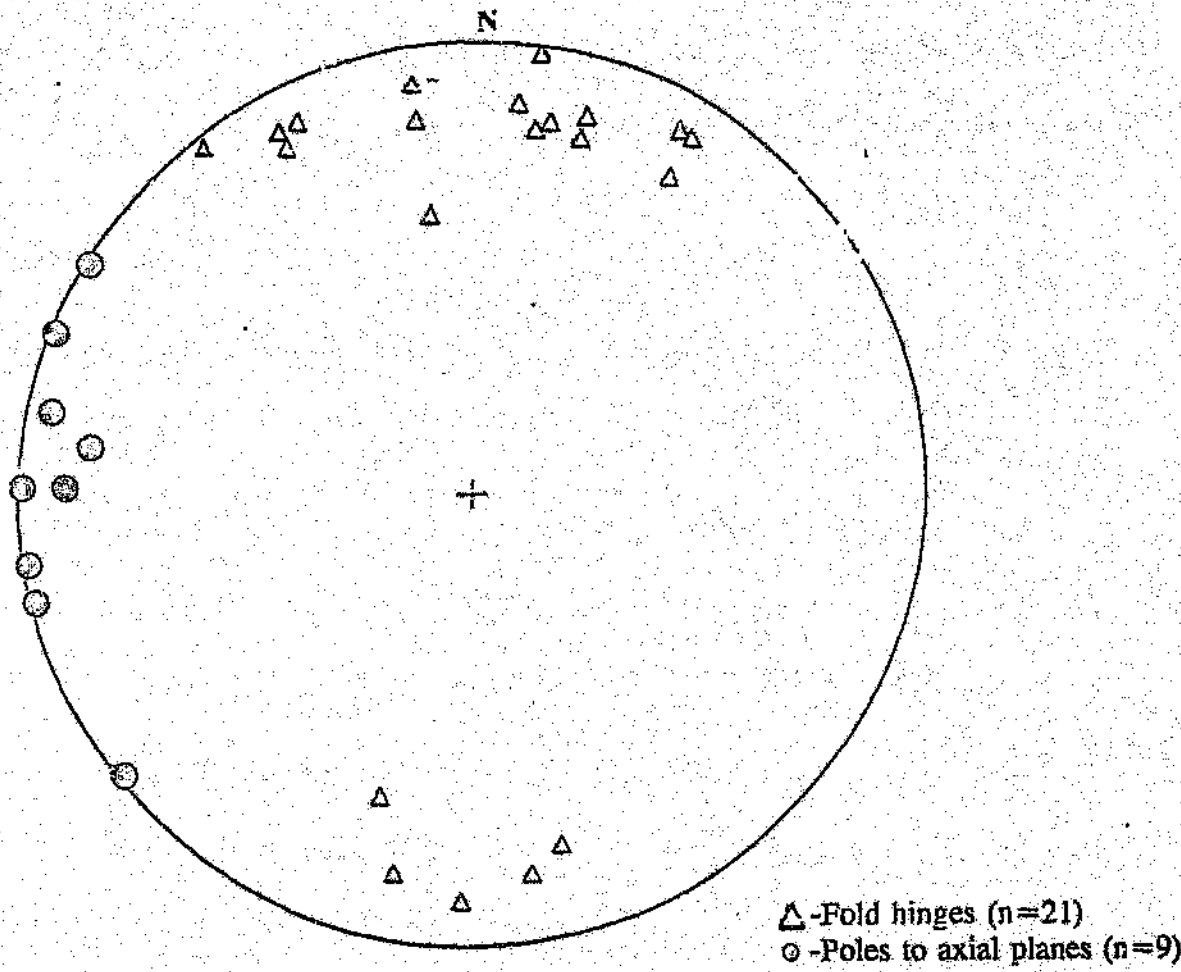

Fig. 3.47 Stereographic representation of west-verging folds outside of bedding sub-parallel shear zones in the Pretoria Group.

3.6.2 East-verging structures

East-verging structures are not as intense or as widespread as the west-verging structures in the study area. The east-verging deformation expresses itself mainly as isolated small-scale east-verging folds which rotate the pre-existing fabric in the D_2 shear zones (Fig. 3.48). These eastward-verging folds are seldom found outside the shear zones, except at locality (2855,0X; -92,7Y). This suggests that stress giving rise to these structures was preferentially located along pre-existing D_2 bedding sub-parallel shear zones.

Within the bedding sub-parallel shear zones, the matrix cleavage, which is asymmetrically arranged around porphyroclasts or altered porphyroblasts (Fig. 3.49), is tentatively interpreted as being a function of top-to-the-east sense of shear. However, the paucity of structures reflecting similar shear sense in these shear zones makes micro-scale shear sense interpretations inconclusive.

Easterly verging fold structures have been observed within bedding sub-parallel shear zones in the road cutting 20 km west of Magaliesburg along the R509 (Fig. 1.1), indicating that the stresses responsible for this deformation may have affected bedding sub-parallel shear zones and adjacent lithologies on a regional scale.

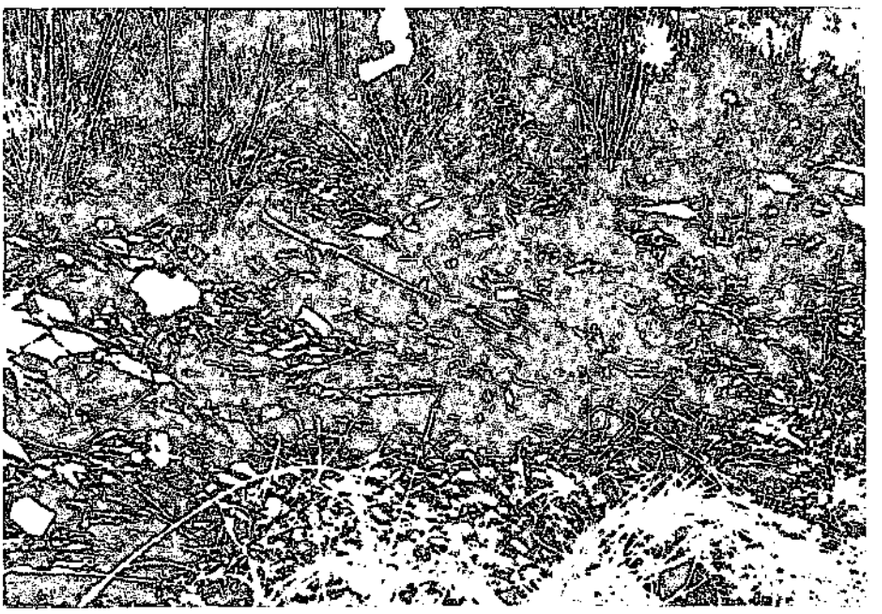

Fig. 3.48 Easterly verging fold deforming the cleavage of a D_3 bedding sub-parallel shear zone. Looking north. Locality (2857.3 X; -94.9 Y).

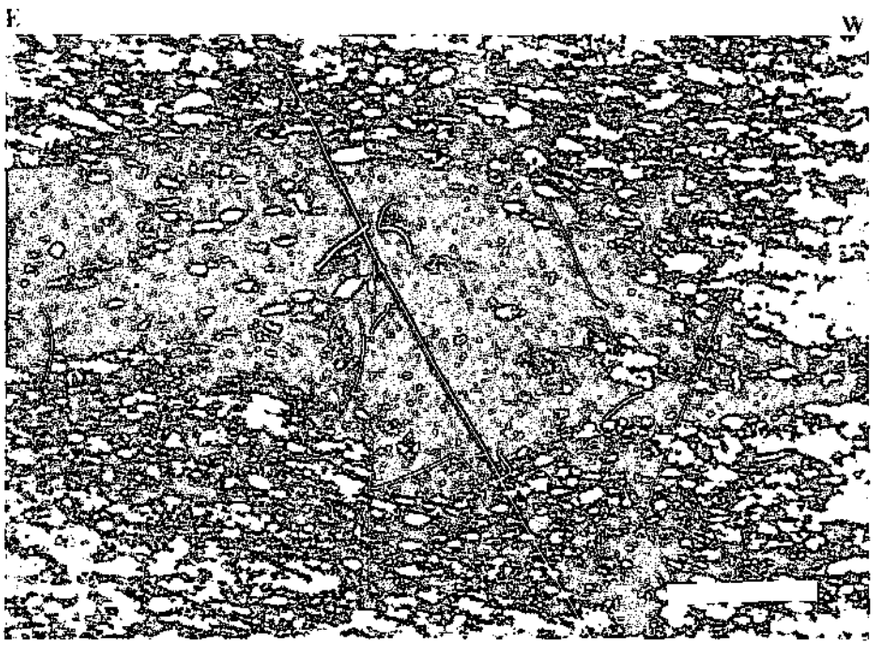

Fig. 3.49 Altered porphyroblast within a D_3 bedding sub-parallel shear zone displaying possible top-to-the-east shear sense. Locality (2857.5 X; 94.0 Y). Scale bar 0.5 mm.

3.7 Jointing and neotectonic activity

The development of joint sets in the study area cannot be attributed with any confidence to a single deformation event, and is therefore discussed separately. Brittle structures in Recent soil and tufa deposits, while not associated with strike-slip fault activity, may be related to certain joint sets.

3.7.1 Joints

Joints are most obviously developed in the slate units of the Pretoria Group, although they are also ubiquitous in the Chuniespoort Group dolomites. The relatively competent carbonate rocks of the Chuniespoort Group, however, do not display the jointing as well as the slate horizons due to chemical weathering widening and obliterating joint surfaces. The individual joints encountered in the slates of the study area are planar, with generally featureless joint surfaces. Plumose markings are, nevertheless, occasionally developed on joint surfaces.

Joints are widely considered to be particularly unreliable in determining deformation history, as they can be formed in various ways, and are activated and reactivated during subsequent deformation events (Davis, 1984). Nonetheless, several observations were made in order to establish whether or not the joint sets in the study area are related to any major recognisable structural features. Analysis of jointed slate outcrops adjacent to a major northerly trending fault with apparent strike-slip displacement was undertaken in order to determine whether this faulting had any influence on the development of joints. Figure 3.50 is a stereographic representation of joint sets on opposite sides of this fault. From this stereonet it is clear that the orientations of the joints do not coincide with the orientation of the main fault. Secondary shear features are, however, often associated with strike-slip faults. Two sets of Riedel

shears, one set oriented approximately 75°-80° and the other set oriented approximately 10°-15° to the fault plane, characteristically develop adjacent to strike-slip faults (Ramsay and Huber, 1987). Some of the joint sets analyzed on either side of this strike-slip fault lie in the angular domains typically reserved for Riedel shears, but do not display any detectable sinistral or dextral offset.

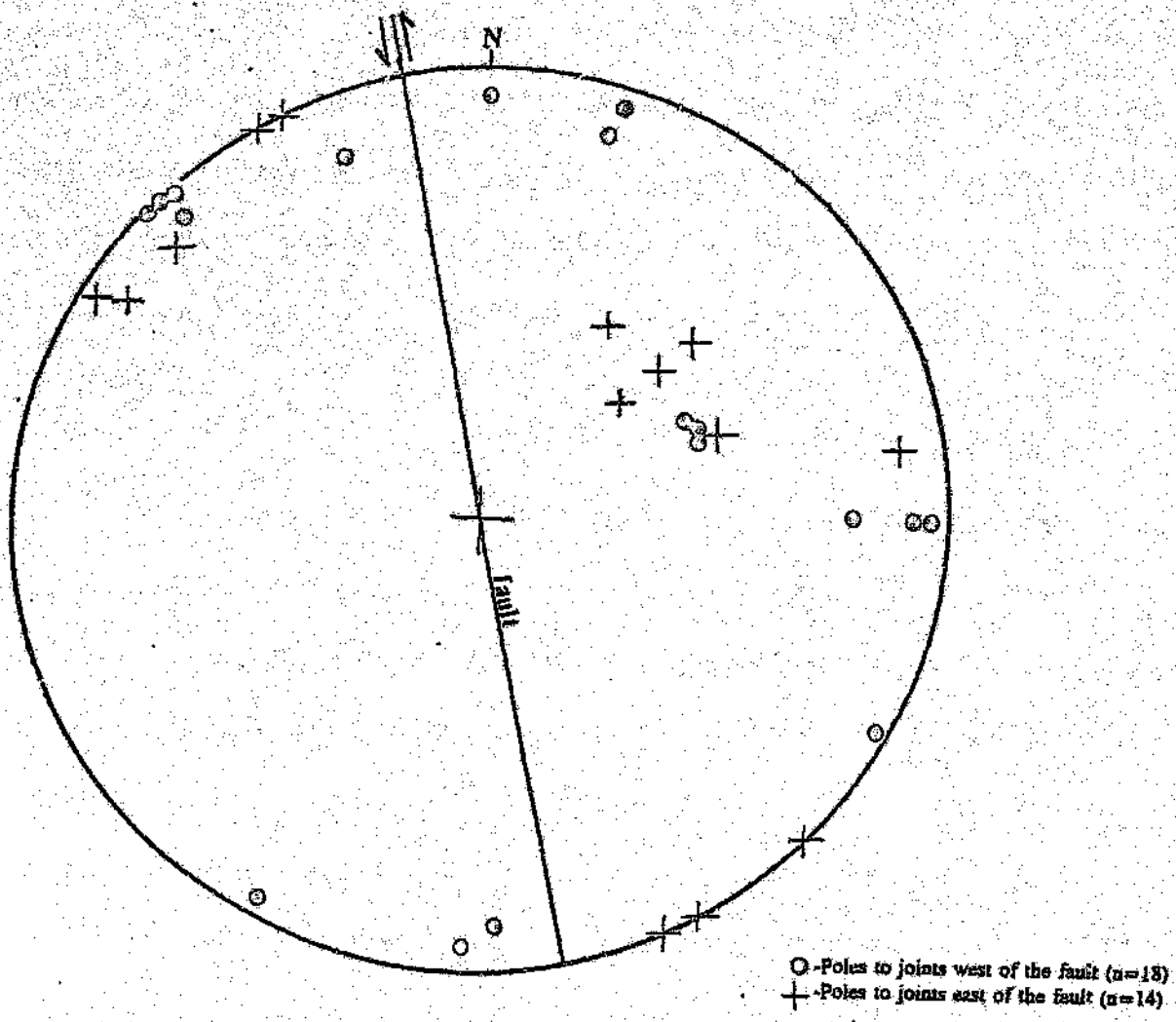

Fig. 3.50 Stereographic representation of joint orientations on opposite sides of a major sinistral strike-slip fault trending approximately 170°. Locality in th ni" of (2857,2X; -92,0Y).

To determine the regional significance of the joint sets in the study area, comparisons were made between the orientations of joint sets in the study area and joint sets developed regionally. Joint sets in the study area were determined from field observations as well as from aerial photograph analysis, whereas regional joint sets were determined solely from aerial photographs. Aerial photograph analysis does, unfortunately, have inherent disadvantages as only the strike trends of joints can be determined. Also, only steeply dipping joints are distinctly visible on aerial photographs, while shallowly dipping joints are concealed from view, with the result that not all joint set trends are recorded. Joint density, therefore, could not be determined. Nonetheless, joint sets were traced onto an overlay from selected 1:50 000 aerial photographs of Job 603 using a stereoscope, and their orientations measured.

The quartzite ridges in the vicinity of the Hartebeespoort Dam were selected as suitable sites for the aerial photographic study as they are well-jointed, the joints are well represented on the aerial photographs, and they are in relatively close proximity to the study area. The photograph numbers of Job 603 studied were 646-651 (north of the study area), 6940-6943 (northwest of the study area) and 7020-7031 (west-northwest of the study area). These areas were further subdivided into smaller sections of approximately equal size. The data are presented as trend orientations on rose diagrams, with populations grouped in 15° domains (Fig. 3.51).

Comparison of regional joint set data with the data from the study area shows that there is a wider distribution of joint orientations in the study area than in any one of the areas of the regional aerial photographic study (Fig. 3.51). This is most likely due to greater detail

obtained for the study area (since it was more intensively studied, and thus a more representative spread of data was obtained), and the limited data available from aerial photographs, due to the inherent disadvantages discussed above. Joints observed on aerial photographs near to the study area have a predominant 90-105° orientation, which is not seen in the study area (Fig. 3.51). The predominant 330-360° joint trend seen west of the study area is also not especially significant in the study area (Fig. 3.51). The lack of coincidence between joint-set orientation domains determined for the study area and those determined regionally does not, however, imply that the region has been affected by multiple deformation events, since joints are questionable tectonic indicators. Therefore, no conclusive deductions could be made from aerial photograph analysis of the regional implications for the joint sets encountered in the study area.

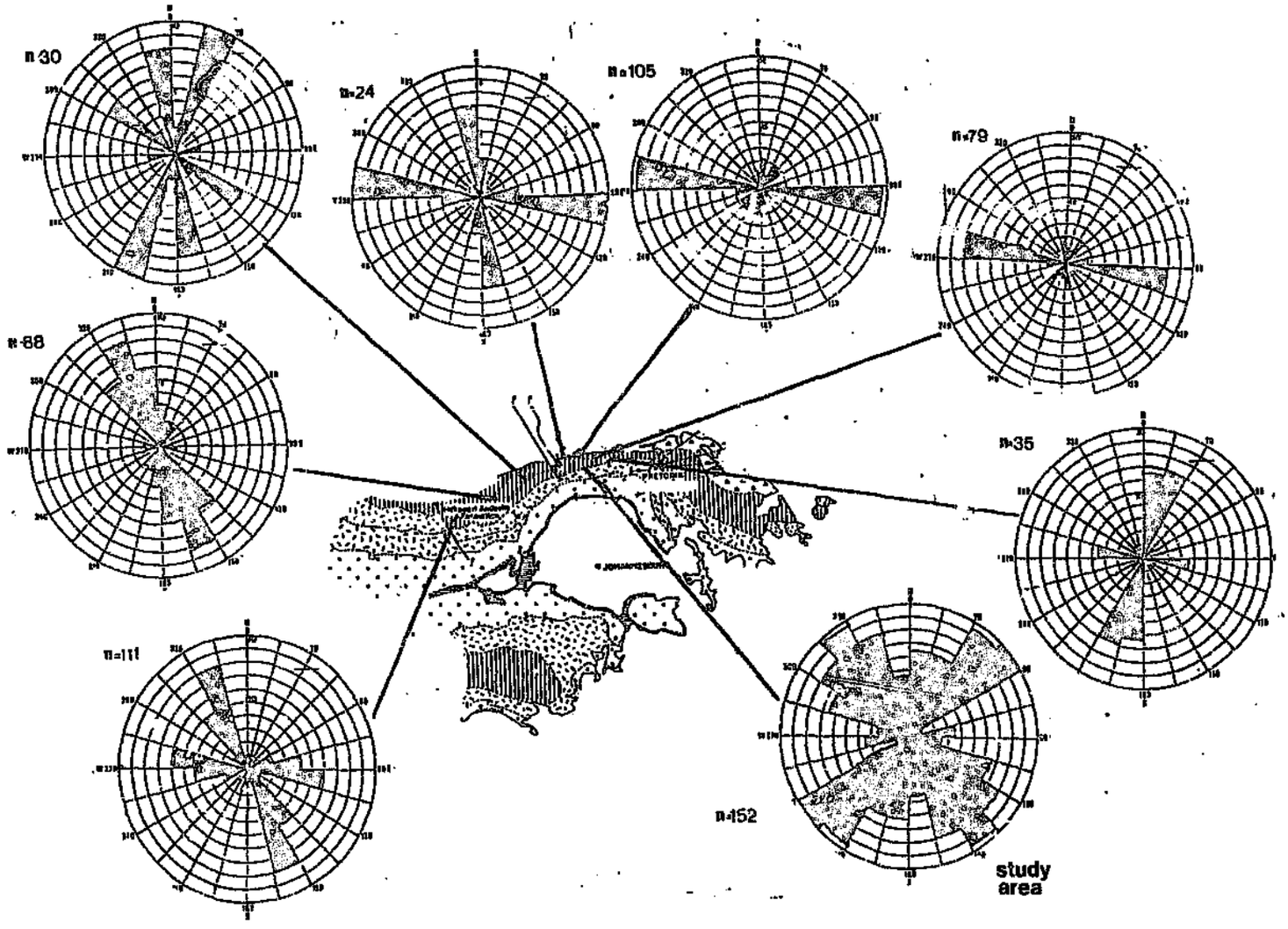

Fig. 3.51 Rose diagrams representing regional joint set orientations (as determined from aerial photographs) compared with the orientation of joint sets measured from the study area.

3.8.2 Neotectonic activity

In addition to the obvious jointing in slate horizons, brittle structural features are developed in Recent unconsolidated sediments and tufas.

a) Structures in unconsolidated soils

Regular sets of sub-vertical cracks, up to 10 m in length, are developed in unconsolidated soils which occupy a valley in the Pretoria Group shale (locality 2856,0 X; -95,6 Y). These cracks can be divided into three sets on the basis of their orientation, i.e. those striking approximately 060°, 100°, and 130° (Fig. 3.52). The orientation of these sets appears to be too consistent to be a consequence of the effects of rootlets or rivulets. The regular orientation, characteristic penetrative nature, and the fact that they are often continuous throughout the entire thickness of the sediment suggests that they are probably not related to slump or collapse features. Comparison of the orientations of the Recent sediment cracks with joint sets in the slate units (Fig. 3.53) suggests that the soil cracks may be a function of an event which gave rise to some of the jointing.

The non-perennial stream that flows in the valley at locality (2856,0 X; -95,6 Y) has produced an approximately 10 m waterfall in the unconsolidated soil sediments (Fig. 3.54). The unconsolidated nature of the sediments suggests that this waterfall is a Recent feature. "Basement" slates of the Pretoria Group, which dip south at this locality, are encountered at the base of the cliff formed by this waterfall, as well as in the stream bed upstream of the waterfall. It thus appears likely that an easterly striking normal fault, with downthrow of at least 10 m to the north, is responsible for the development of this waterfall (Fig. 3.55).

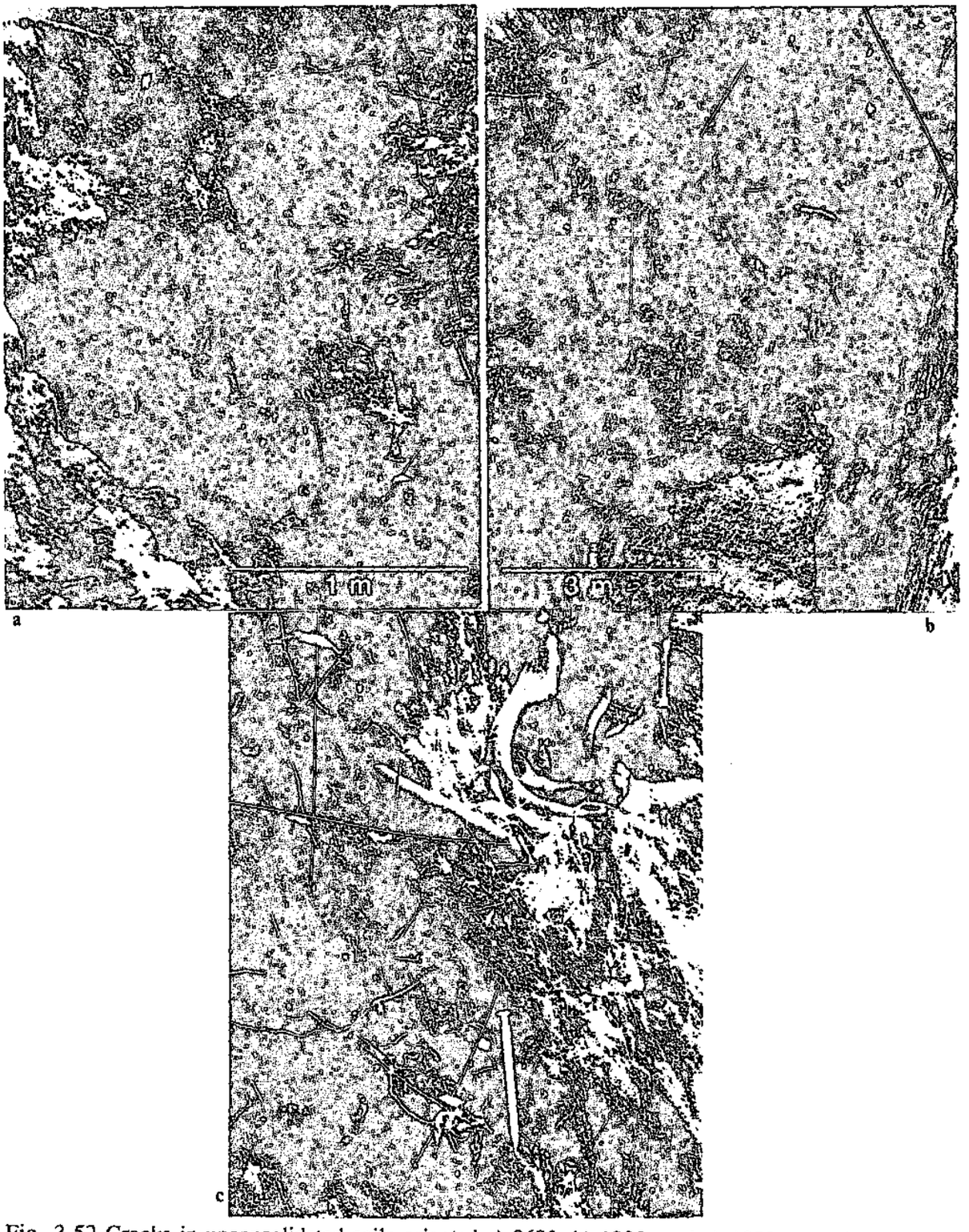

Fig. 3.52 Cracks in unconsolidated soils oriented a) 060°. b) 100°, and c) 130°. Locality (2856,0 X; -95,6 Y).

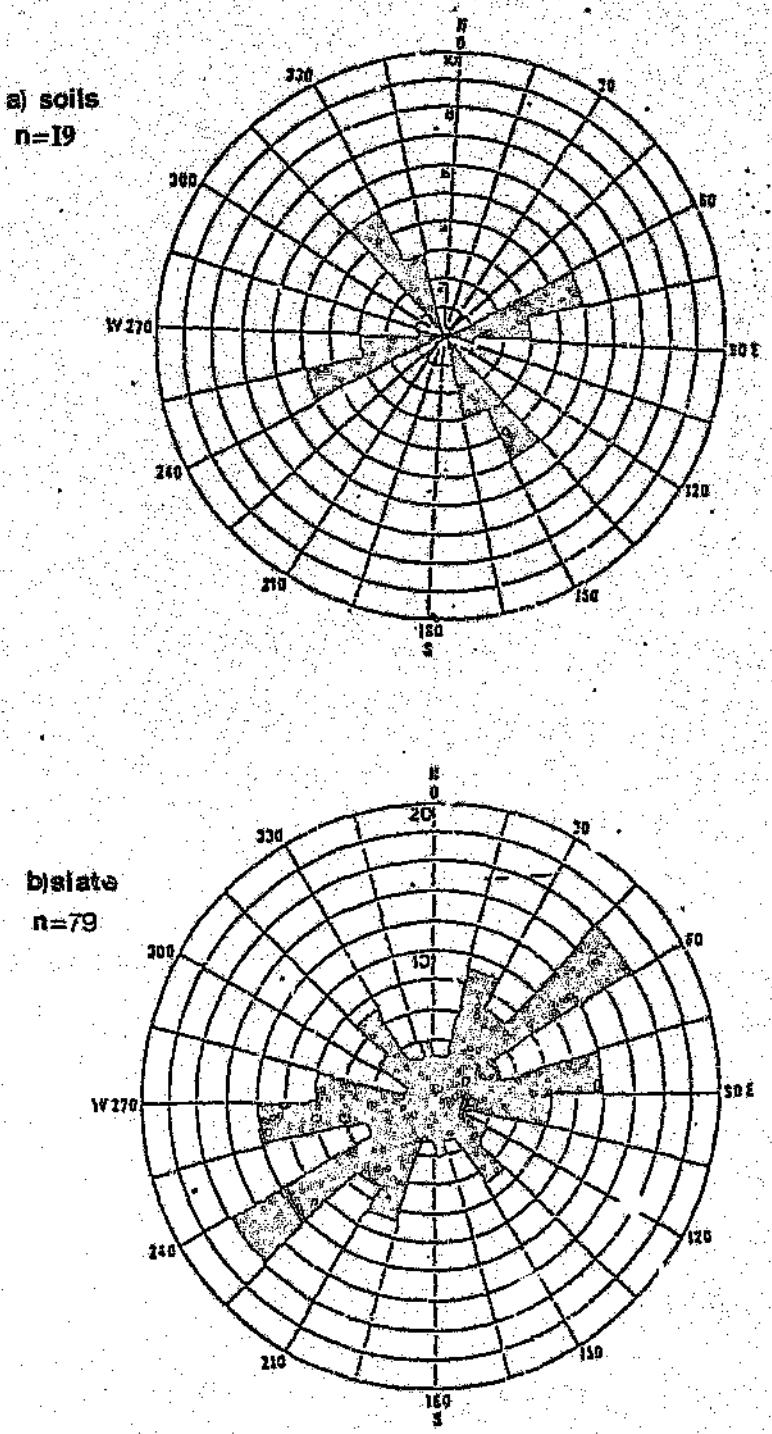

Fig. 3.53 Comparison of the orientations of cracks in the unconsolidated soils (a) with orientations of joint sets in the adjacent slate (b), showing some correlation of orientations.

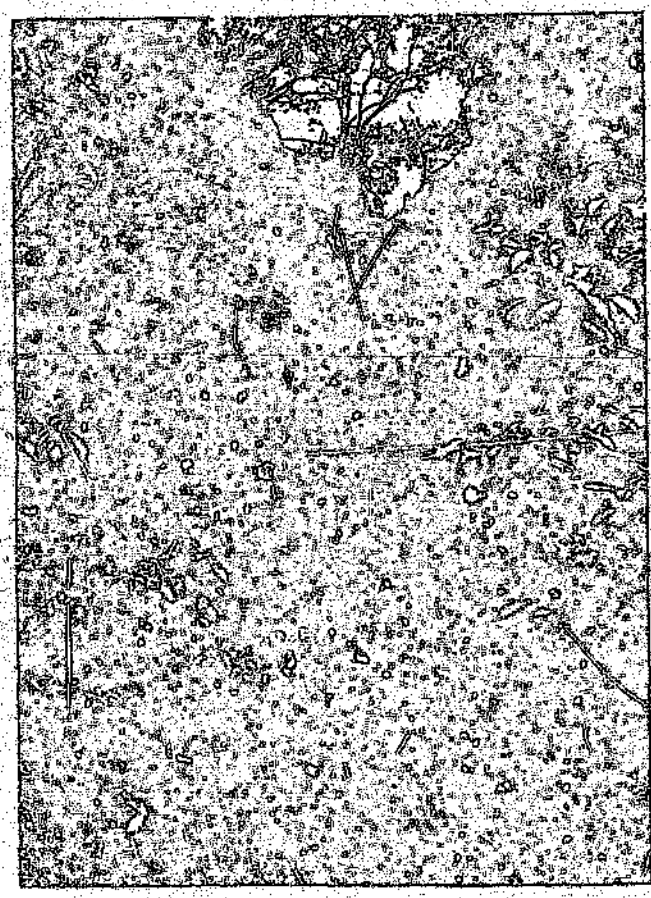

Fig. 3.54 Waterfall in more than 10 m thick unconsolidated sediments. Looking south.

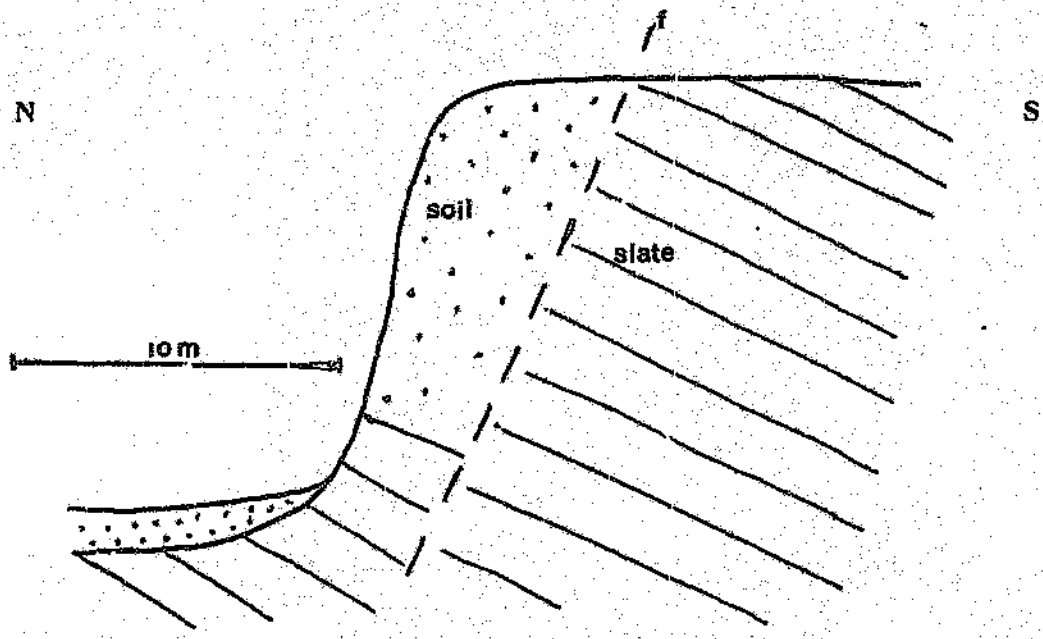

Fig. 3.55 Cross-section of the waterfall in Fig. 3.54 showing the position of an inferred normal fault with downthrow to the north.

b) Structures in tufa

An isolated pod of tufa is developed in a stream near the contact of the Chuniespoort Group with the Pretoria Group at locality (2857,6 X; -91,8 Y). This tufa deposit is deformed by a number of consistently trending, planar penetrative fractures (Fig. 3.56). These fractures closely resemble joints. Comparison of joint data in the adjacent area with these fractures shows some correlation (Fig. 3.57). The tufa cracks may thus be related to the east-west striking joints in the area. The stream that hosts the tufa is also linear, orientated east-west, and is possibly fault related (Map 2). Some joint sets in the slate units, as well as the planar fractures in the tufa, may therefore be a result of east-west faulting. Horizontal fractures developed in the tufa are of uncertain origin.



Fig. 3.56 Linear fractures in tufa trending 100°. Looking west. Locality (2857,6 X; -91,8Y).

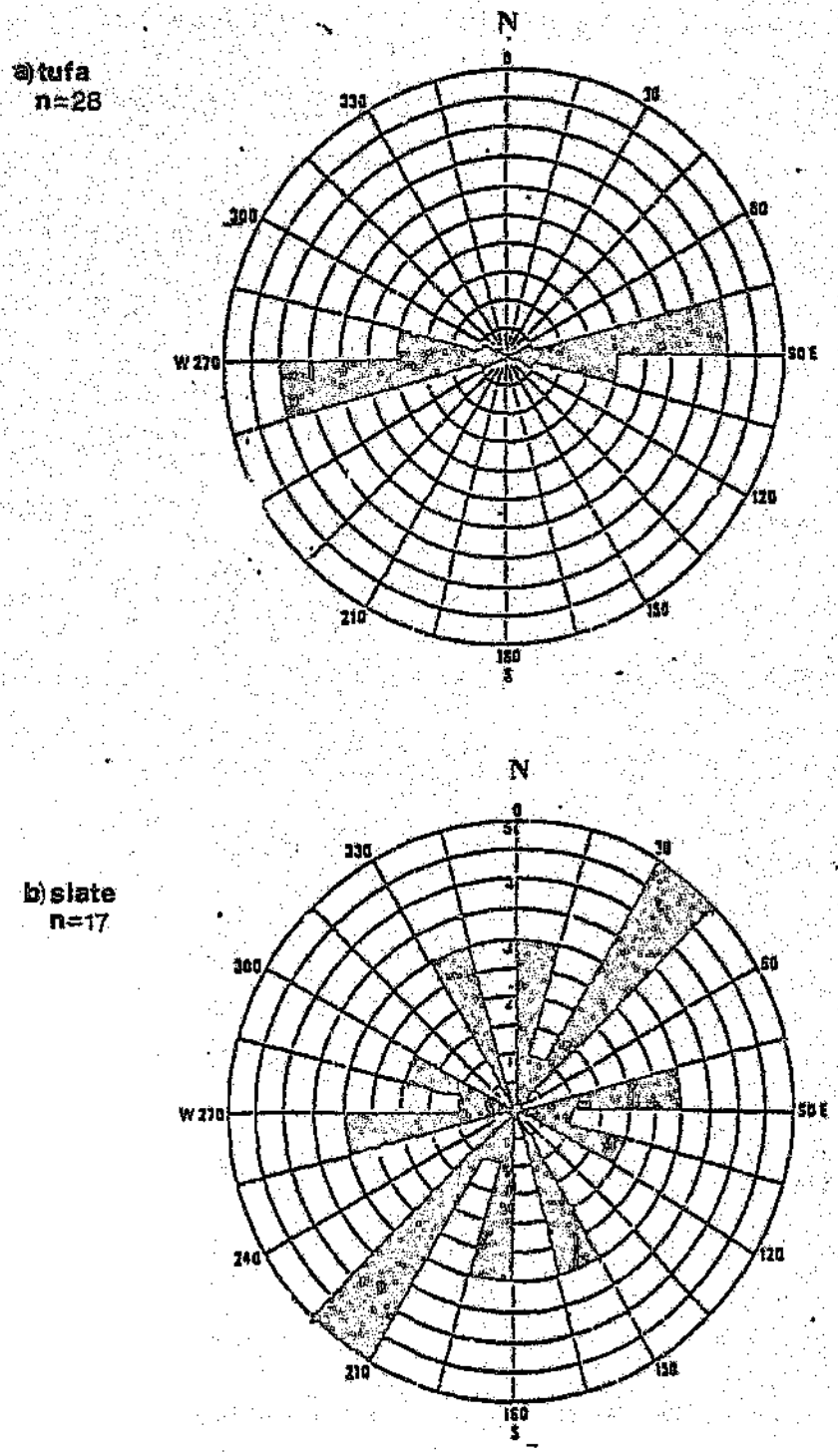

Fig. 3.57 Comparison of joint set data with the tufa fractures, showing some degree of coincidence. a) Prominent E-W trend of tufa "joints". b) Joints in slate adjacent to the tufa. Locality (2857,6 X; -91,8 Y).

A small waterfall in this stream is defined by a series of three steps, each approximately 0,5-1 m high, developed in the tufa (Fig. 3.58). The stepping is down to the north and is defined by the same fractures as described above. This waterfall, as with the waterfall in the unconsolidated sediments (Fig. 3.54), is possibly related to east-west trending normal faulting, with downthrow to the north.



Fig. 3.58 Waterfall defined by tufa fractures trending 100°. Looking west. Locality (2857,6 X; -91,8 Y).

3.9 Summary

Field investigations, aerial photograph studies and microstructural analysis has revealed the complex deformation history of the study area. The earliest recognisable deformation event (D_1) in the study area resulted in a locally-developed, southerly-verging cleavage (S_1). Northerly-verging bedding sub-parallel shear zones, folds, lineations & cleavage (S_2) of the D_2 event are extensively developed throughout the study area. In the Chuniespoort Group, D_3 resulted in large-scale, southerly verging folds, associated with steep thrusts, which deform D_2 bedding sub-parallel shear zones. The D_3 deformation event in the Pretoria Group resulted in large-scale, southerly-verging kink folds, and minor round-hinged folds, which rotate S_2. Northerly trending strike-slip faults (D_4) truncate the earlier structures. Isolated easterly- and westerly-verging ductile structures tend to exploit D_2 bedding sub-parallel shear zones. However, the relative timing of these deformation events with respect to D_3 and D_4 could not be determined. Brittle deformation in the study area resulted in joints in the slate and dolomite units, and fractures in Recent tufa and unconsolidated soils.

CHAPTER 4

PORPHYROBLAST MICROSTRUCTURAL RELATIONSHIPS

4.1 Introduction

The slates of the Chuniespoort and Pretoria Groups in the study area have been metamorphosed to the greenschist facies, and it will be shown in Chapter 5 that this metamorphism, and hence porphyroblast growth, most likely originated from the thermal effects of the Bushveld Complex. The importance of considering the metamorphic history of the area is that textural relationships can be used to determine the relative timing between porphyroblast growth (metamorphism) and cleavage development (e.g. Zwart, 1962; Vernon, 1978, 1989). For this study, an attempt has been made to constrain the timing of the porphyroblast-forming event with respect to deformation (in particular, the S_1 and S_2 cleavage-forming events), by examining oriented thin-sections from samples containing cleavage and porphyroblasts.

Several critical problems were encountered which hampered accurate and definitive interpretation of structural-metamorphic relationships. First, outcrop is not continuous from south to north throughout the study area, due to deep weathering of the Hekpoort Andesite Formation in the Pretoria Group (Fig. 1.2). The S_2 cleavage, therefore, could not be traced throughout the Transvaal Supergroup to the contact aureole of the Bushveld Complex. Secondly, porphyroblasts are developed in hornfelses in the contact aureole of the Bushveld Complex, which are devoid of penetrative cleavage. In addition to these problems, internal cleavages (S_i) - which are crucial for porphyroblast-matrix relationship interpretations (Vernon, 1978, 1989; Hanmer and Passchier, 1991) - are either absent or obscured in the

majority of porphyroblasts studied.

4.2 Porphyroblast growth and cleavage relationships

Porphyroblasts from the study area frequently display ambiguous relationships to matrix cleavage. They do, however, display certain relationships to cleavage similar to those described by previous workers. Therefore, an overview of the relevant literature is followed by descriptions of porphyroblasts occurring in the study area. The literature can be divided into: 1) considerations of the mechanical effects of porphyroblast growth under hydrostatic stress conditions; and 2) the relationships between prophyroblast growth and cleavage formation under directed stress conditions.

4.2.1 Porphyroblast growth under hydrostatic stress conditions

Saggerson (1974) described the "bowing" or deflection of S-surfaces around porphyroblasts in the argillaceous rocks of the Timeball Hill Formation in the eastern Transvaal. The shales that Saggerson (1974) studied are porphyroblastic hornfelses, containing andalusite, staurolite, garnet, cordierite and chloritoid, which form part of the thermally metamorphosed contact aureole of the Bushveld Complex. According to Saggerson (1974), the primary sedimentary layering of the shales was deflected by growing porphyroblasts. Finer layers are preferentially deflected, and deflection decreases with distance from the porphyroblasts. Some examples show the sedimentary layers both deflected around, and truncated by, a porphyroblast. Saggerson (1974) interpreted these relationships as expressing porphyroblast growth by both displacement and replacement of matrix, similar to conclusions drawn by Misch (1971), with the replacement mechanism being more prevalent than displacement. Central to Saggerson's (1974) interpretation is that the porphyroblasts grew in a deformation-

free environment in the aureole of the Bushveld Complex, and thus the "tightening" of matrix layering around porphyroblasts was not a result of microfolding or flattening, but rather due to the growth of porphyroblasts. Saggerson (1974) thus suggested that surfaces within the matrix become more intensely deflected as porphyroblasts grow, since growing porphyroblasts are able to create local pressure differences that disturb pre-existing banding.

Yardley (1974) showed experimentally that porphyroblast growth involves no bulk volume increase, although a local volume increase at the growth site could cause local deflection, such as dislocation of the matrix. He showed that stress is transmitted through rocks in the presence of intercrystalline pore fluids. Minerals dissolve into the pore fluid, which becomes saturated with respect to all adjacent minerals. Some minerals (e.g. quartz and feldspar), however, go into solution preferentially, since they are more soluble than micas and other minerals (e.g. graphite) (Yardley, 1974). Thus micas remain in close proximity to a growing porphyroblast, while quartz and feldspars are preferentially removed, even if these soluble minerals are not in direct contact with the growing prophyroblast. Yardley (1974) concluded (similarly to Saggerson, 1974) that it is likely that a growing porphyroblast could push aside its matrix, and the porphyroblast would preferentially include insoluble minerals (such as ilmenite) rather than soluble minerals (such as quartz).

In their study of the mechanical interaction between growing porphyroblasts and the adjacent matrix in quartz-biotite-muscovite hornfelses, Ferguson *et al.* (1980) encountered dome-shaped accumulations of muscovite and minor graphite attached to the crystal faces of garnet porphyroblasts. They noticed that these cleavage domes (Ferguson *et al.*, 1980) are attached to, and concave towards, the porphyroblast faces, and do not seem to be controlled by any

preferred crystal-face direction. The samples studied by Ferguson *et al.* (1980) are devoid of cleavage, which implies that there was no significant deviatoric stress component during porphyroblast growth, and thus only hydrostatic stress conditions prevailed. They postulated a model for the growth of mica-domes where porphyroblasts (garnet) nucleate in a normal matrix. Biotite, muscovite and graphite are insoluble under bulk hydrostatic conditions, and none of these matrix minerals are included in the porphyroblast as it grows. Rather they are swept ahead of, and accumulated onto, the advancing porphyroblast margins. Dissolution of quartz at matrix-mica and porphyroblast interfaces occurs, and simultaneously small amounts of garnet are added to the porphyroblast as it grows. As quartz is dissolved, micas are brought into parallelism with the advancing porphyroblast face. Further dissolution of quartz and porphyroblast growth leads to displacement of micas in the direction of growth, and hence the formation of cleavage domes. Rice and Mitchell (1991) confirm that cleavage domes are good evidence for displacement of matrix during porphyroblast growth.

The model of Ferguson *et al.* (1980) is based on two mechanical processes existing in a metamorphic rock during porphyroblast growth:

a) A growing porphyroblast makes room for itself by dissolution, and then occupies the volume previously occupied by matrix minerals. Some of the dissolved matrix minerals may either be assimilated by porphyroblast growth, or may form new minerals. Other matrix minerals may be insoluble and either form inclusions within the porphyroblast, or are displaced and/or deformed by the growing porphyroblast.

b) The second mechanical process originates because porphyroblasts generally have a different compressibility to the surrounding matrix. Even in bulk hydrostatic stress environments, compositional heterogeneities between porphyroblasts and matrix

minerals induce local deviatoric stress fields in close proximity to porphyroblast-matrix boundaries. In the presence of "some form of creep mechanism...stored elastic strain energy can be dissipated through permanent creep deformation" (p 340), and thus this "creep" will move with a growing porphyroblast boundary. The "creep mechanism" essentially involves "matrix grain translation and rotation due to transport ahead of the advancing porphyroblast margin, and further rotations and minor translations in response to the local deviatoric stress field" (p 340).

Thus, Ferguson *et al.* (1980) concluded that porphyroblasts growing in a bulk hydrostatic stress field may displace previously aligned matrix grains. Slight deviations from bulk hydrostatic stress would, however, overwhelm mineral growth-related stresses, and augen textures in the matrix would ensue.

4.2.2 Porphyroblast growth under directed stress conditions

Hanmer (1979) studied porphyroblastic pelitic rocks which had undergone heterogeneous deformation. Syntectonic growth of biotite, andalusite and staurolite porphyroblasts was initiated by the emplacement of adjacent granite. Heterogeneous deformation results in the development of separate layer-normal and layer-parallel compression domains, as well as incipient microshears and kink-bands. The kink-bands are plainly seen to have initiated on some porphyroblast edges. With progressive deformation, the relationship of microfolding to the spatial distribution of porphyroblasts is maintained, and two microstructural domains, i.e. quartz (Q) and mica (M) domains, develop. The M-domains occupy microshear zones and the long limbs of asymmetrical microfolds, while the Q-domains are developed on microfold hinges, short limbs of folds, or the zones between adjacent microshears. The Q-domains are generally located on porphyroblasts, while the M-domains are developed

tangentially between them.

Bell (1981) postulated that heterogeneous deformation in a rock mass is partitioned into discrete coaxial and non-coaxial strain fields. Non-coaxial strain occurs in the M-domains, while low-intensity coaxial deformation occurs in the Q-domains (Bell, 1981, 1985). Bell *et al.* (1986) proposed that fluids saturated with suitable components for the formation of porphyroblasts migrated to microfractures in the coaxially strained Q-domains, while in the adjacent non-coaxially strained M-domains, intense deformation resulted in the dissolution of minerals, notably quartz, but not micas or graphite. Micas and graphite thus accumulate in the non-coaxial strain M-domains, while most porphyroblast minerals are dissolved in these areas. Growth of porphyroblasts can, therefore, only occur in the low-strain, coaxial Q-domains. Should the porphyroblast encroach on an active M-domain, Bell *et al.* (1986) indicate that growth will terminate and dissolution may occur. In this way, partitioning of deformation controls the size and location of porphyroblasts. In certain cases, however, it is possible that M-domains become inactive due to partitioning of the strain on a larger scale during the later stages of progressive deformation. In this scenario, porphyroblasts may overgrow inactive M-domains and not experience dissolution.

Vernon (1989), in contrast to Bell *et al.* (1986), concluded that porphyroblasts themselves

might cause the initial partitioning of matrix cleavage during progressive deformation, and that non-coaxially strained M-domains may nucleate on porphyroblasts. Thus cleavages anastomose around porphyroblasts. Vernon (1989) observed that only one porphyroblast occurs in any one Q-domain. He maintained that if the hypothesis of Bell *et al.* (1986) is valid, several porphyroblast nuclei would develop in the coaxial strain Q-domains, instead of just one. This observation could, however, be explained by cleavage anastomosing around a growing porphyroblast (e.g. Hanmer, 1979). Both hypotheses are, nonetheless consistent with syn-deformational porphyroblast growth.

Prior (1987) considered porphyroblastic phyllites containing chloritoid, biotite, chlorite, ilmenite and garnet, all of which show essentially the same textures. In nearly all cases, cleavage crenulations are associated with porphyroblasts. The cleavage intensifies around the porphyroblasts by dissolution of quartz, feldspar and calcite, thus leaving mica and opaque-mineral rich seams. The intensity of cleavage decreases away from porphyroblasts, and porphyroblasts may be truncated by intensified cleavage. Prior (1987) concluded that one of three mechanisms may be responsible for deflection and intensification of cleavage around the porphyroblasts:

a) deformation partitioning around rigid porphyroblasts, where the porphyroblasts are present during cleavage development. Further deformation is accommodated by the surrounding matrix since porphyroblasts deform at a slower rate than the surrounding matrix. Intense cleavages develop parallel to the crystal-end faces;

b) heterogeneous deformation prior to porphyroblast growth; or

c) deformation of cleavage by porphyroblast growth, where the deflection and intensification of cleavage is a function of the porphyroblast "pushing aside" the

earlier-formed cleavage.

Prior (1987) contended that once a porphyroblast has nucleated in a site created by deformation partitioning, it continues to grow and fulfil the role of a strain inhomogeneity around which deformation is further partitioned. Cleavage thus intensifies and deflects around the porphyroblast during and after its growth.

4.3 Porphyroblasts in the study area

Porphyroblasts are present in many of the slate and hornfels samples in the area studied. These include chloritoid and andalusite (chiastolite), which are the most prominent, mica (biotite and muscovite) and opaque porphyroblasts. All of the porphyroblasts encountered are altered to varying degrees. The surrounding matrix mineralogy is generally fine-grained, and comprises predominantly quartz, chlorite and micas (biotite, muscovite).

4.3.1 Chloritoid

A sample from near the D_2 bedding sub-parallel shear zone in Pretoria Group slate, described in Section 3.3.3, contains porphyroblasts of altered chloritoid and minor chloritised biotite. The chloritoid crystals commonly display characteristic hourglass zoning (Fig. 4.1), and are commonly replaced by opaque minerals, probably iron oxides. The penetrative cleavage (S_2) in this area dips consistently shallowly to the south, and is defined on the microscale by the alignment of matrix phyllosilicate grains. Internal cleavage (S_1) is not detectable in these porphyroblasts, as they are very small and usually altered. The chloritoid porphyroblasts show slight preferred alignment, the majority oriented approximately 60°-90° to the overall cleavage orientation. Cleavage is deflected adjacent to the chloritoid porphyroblasts and, where the cleavage wraps around the crystal ends, it is most intense (Fig. 4.2). The intensity

of the cleavage increases in close proximity to these porphyroblasts, but decreases away from them, leaving on each side a wedge-shaped strain shadow of equidimensional quartz, often with a weakly developed grain-shape alignment (Fig. 4.2). The quartz-rich zones have grain-sizes that are similar to those in the surrounding matrix. Therefore, the quartz grains may be remnants of a pre-S_2 cleavage preserved in the strain shadow provided by the porphyroblast, similar to the features described by Prior (1987). However, the possibility exists that the quartz-rich strain-shadows may represent the soluble mineral phase lost due to intensified cleavage enveloping the porphyroblast, by a process of solution transfer, consistent with the model of Bell *et al.* (1986). Originally idioblastic chloritoid porphyroblasts are commonly rounded or truncated (Fig. 4.3). This may be attributed to strain-related dissolution at those localities where cleavage is wrapped around the porphyroblast (Prior, 1987). The porphyroblasts of chloritoid occasionally interfere with one another, having a cleavage layer preserved and "squeezed" between them (Fig. 4.3). Cleavage is possibly truncated by the chloritoid porphyroblasts in some examples (Fig. 4.2), and, occasionally, the porphyroblasts may indent one another. This may be consistent with a process in which displacement and replacement of the matrix contribute to porphyroblast growth (Saggerson, 1974; Yardley, 1974).

Rounding of porphyroblast ends adjacent to the cleavage (Figs. 4.2 and 4.3) implies dissolution, which suggests that the porphyroblast may have grown prior to the cleavage-forming event (Prior, 1987). Similarly, cleavage deflection around porphyroblasts may imply pre-cleavage growth of the porphyroblasts (e.g. Hanmer, 1979; Oleson, 1982). However, the chloritoid porphyroblasts in the study area truncate cleavage, cleavage may anastomose naturally (Bell *et al.*, 1986), and porphyroblast growth is probably rapid with respect to

cleavage development (Knipe and Wintch, 1985). Therefore, the possibility that the chloritoid porphyroblasts grew syntectonically cannot be disregarded. In such a scenario, the porphyroblast may have grown entirely within a deformation event, and, once it had completed its growth, may have been affected by the same strain episode, giving the impression that its growth was both pre- and syn tectonic (Prior, 1987).

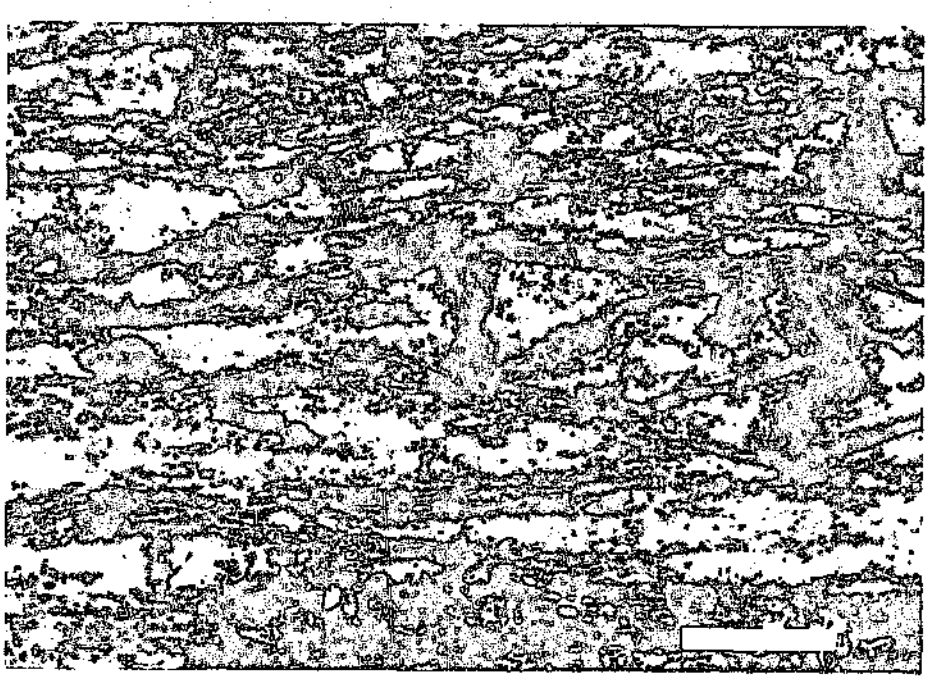

Fig. 4.1 Chloritoid porphyroblast at a high angle to S_2 cleavage, displaying hour-glass zoning. Locality (2857,5 X;-94,1 Y). Scale bar 0,25 mm.

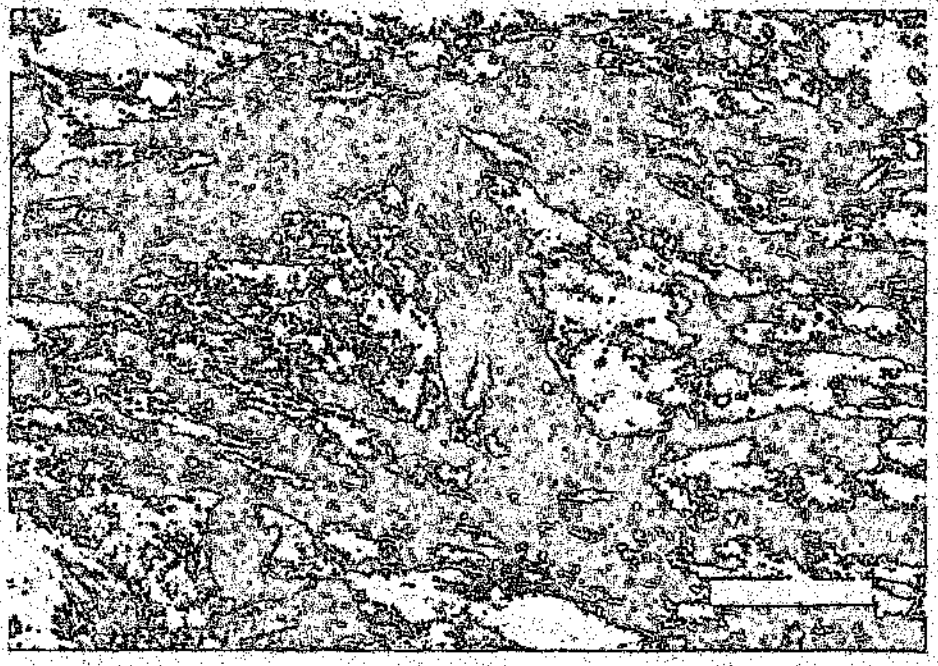

a

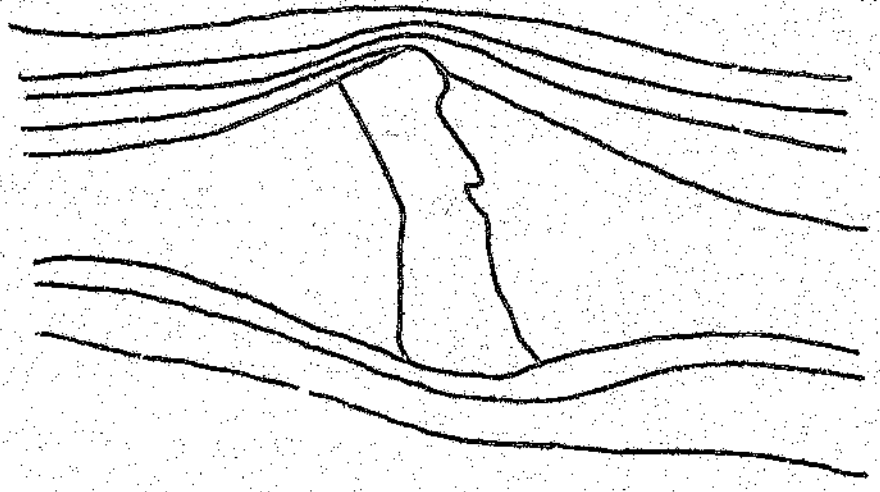

b

Fig. 4.2 Photomicrograph (a) and schematic representation (b) showing the intensity of cleavage increasing in close proximity to a chloritoid porphyroblast, and enveloping a wedge-shaped strain shadow of quartz on either side of it. Locality (2857,5 X;-94,1 Y). Scale bar 0,125 mm.

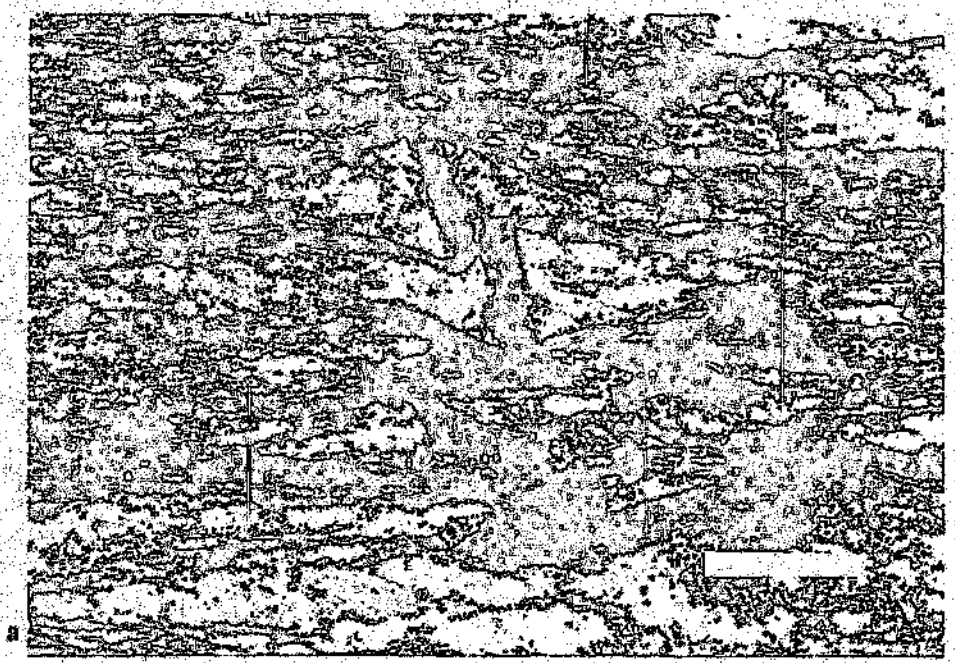

a

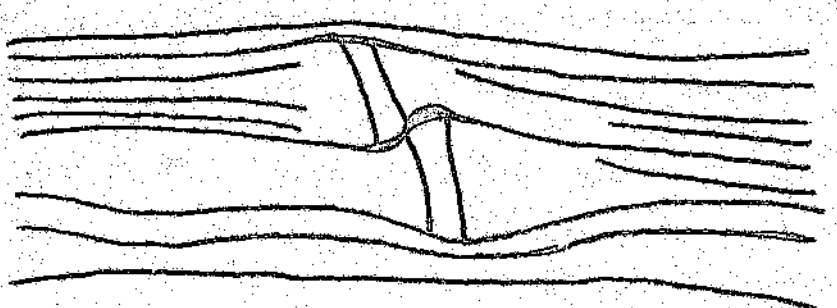

b

Fig. 4.3 Photomicrograph (a) and schematic representation (b) showing the ends of chloritoid porphyroblasts rounded and truncated by dissolution. Locality (2857,5 X;-94,1 Y). Scale bar 0,25 mm.

The evidence presented demonstrates that growth of chloritoid porphyroblasts in the study area can be constrained with certainty as either pre- or syn-D_2.

4.3.2 Chiastolite

Samples from a traverse west of the Bekker Schools, approximately 20 km northeast of Magaliesburg town (Fig. 1.1) contain andalusite (chiastolite) in a slate unit in close proximity to hornfelses in the Pretoria Group. In thin-section, the porphyroblasts clearly show crosses characteristic of chiastolite. The chiastolite occurs as idioblastic rods up to 1 cm long, with their long axes randomly arranged in the plane of compositional layering. A moderately well-developed, bedding-parallel, penetrative cleavage (S_1) is present (see also Section 3.2). Some of the chiastolite porphyroblasts, however, display equivocal growth and timing relationships with respect to cleavage development.

The cleavage typically wraps itself partially around the chiastolite porphyroblasts, but is also truncated by them (Fig. 4.4). Internal cleavage (S_i) is, however, absent in the majority of chiastolite crystals, although inclusions comprising fine rods of quartz do occur. The only control on the orientation of the quartz rods, however, is due to the crystallographic structure of the porphyroblast itself. The quartz rod inclusions are thus unrelated to the external cleavage.

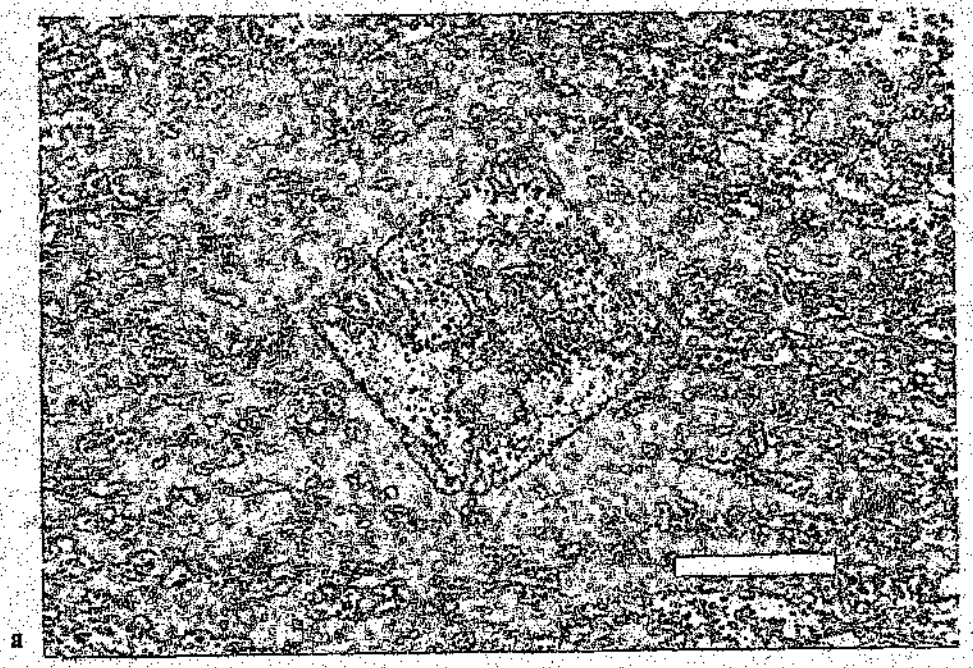

a

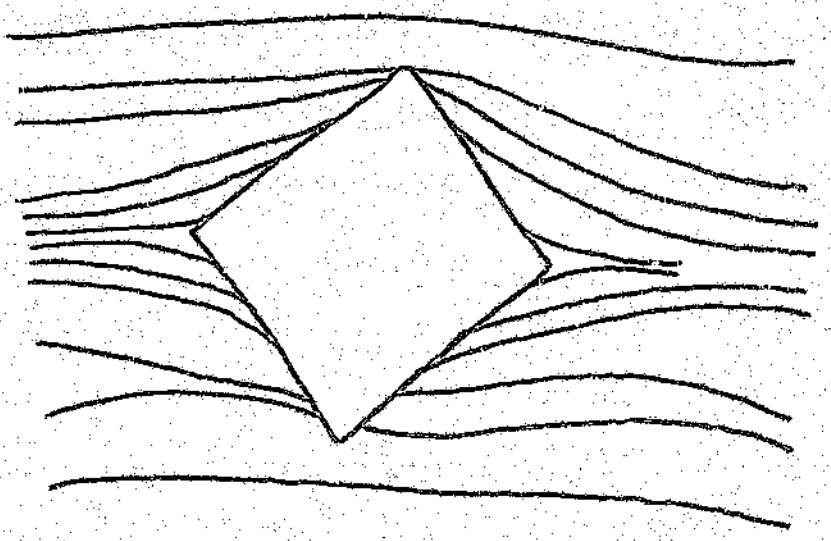

b

Fig. 4.4 Photomicrograph (a) and schematic representation (b) showing idioblastic chiastolite porphyroblast in a foliated matrix. The cleavage partially wraps, and is truncated by, the crystal. Bekker Schools locality (Fig. 1.1). Scale bar 0,5 mm.

Figure 4.5 shows two idioblastic chiastolite crystals in close proximity with cleavage anastomosing around, and being truncated by, the grains. The cleavage is more intense, and "squeezed", between the porphyroblasts. Cleavage anastomoses less with increased distance from the porphyroblasts. There is no evidence for continuation of the external matrix cleavage (S_e) within the porphyroblast. The porphyroblast-cleavage relationship resembles that discussed by Misch (1971) and Saggerson (1974), and experimentally determined by Yardley (1974). They concluded that the cleavage anastomosing around, and truncated by, the porphyroblasts was produced by a post-"s-surface" episode of metamorphism, in which porphyroblasts pushed aside, and overgrew, the earlier cleavage by displacement and replacement mechanisms. Bell *et al.* (1986), on the other hand, have suggested that a similar relationship may have occurred syn-deformationally within coaxial low-strain zones (Q-domains) which originated from strain partitioning during heterogeneous deformation. With subsequent increase of strain partitioning, the porphyroblast overgrew and included the inactive cleavages (M-domains) (Bell *et al.*, 1986). The latter alternative is, however, less likely, as there are no remnants of Q-domains (such as strain shadows) around the porphyroblasts. Post-deformation growth for these porphyroblasts is thus preferred.

The majority of chiastolite porphyroblasts observed are prismatic, and all lack pressure shadows. Porphyroblasts growing in a strain-free environment would have no pressure shadows, intimating post-deformational porphyroblast growth.

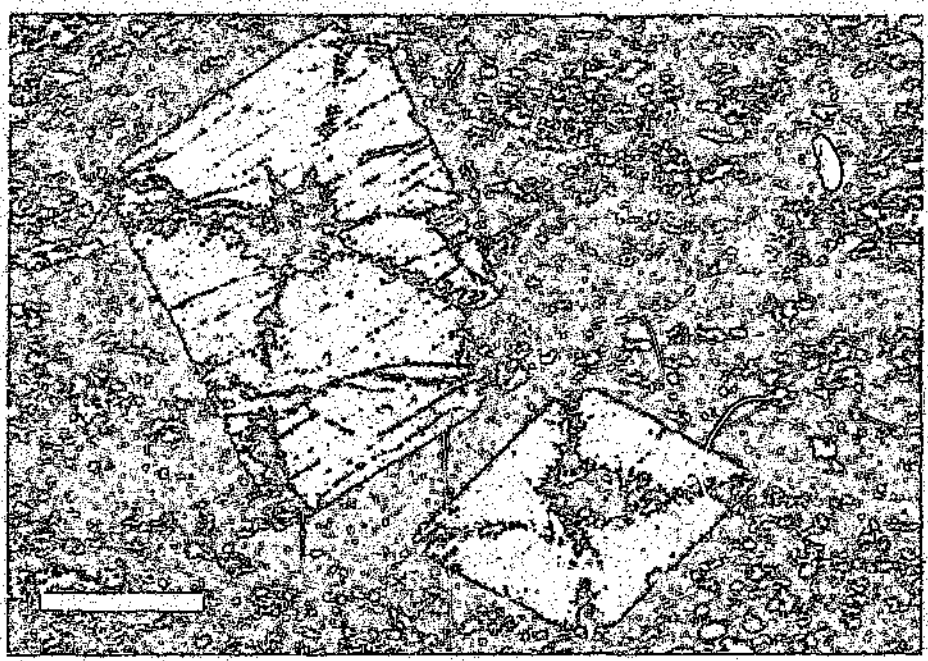

a

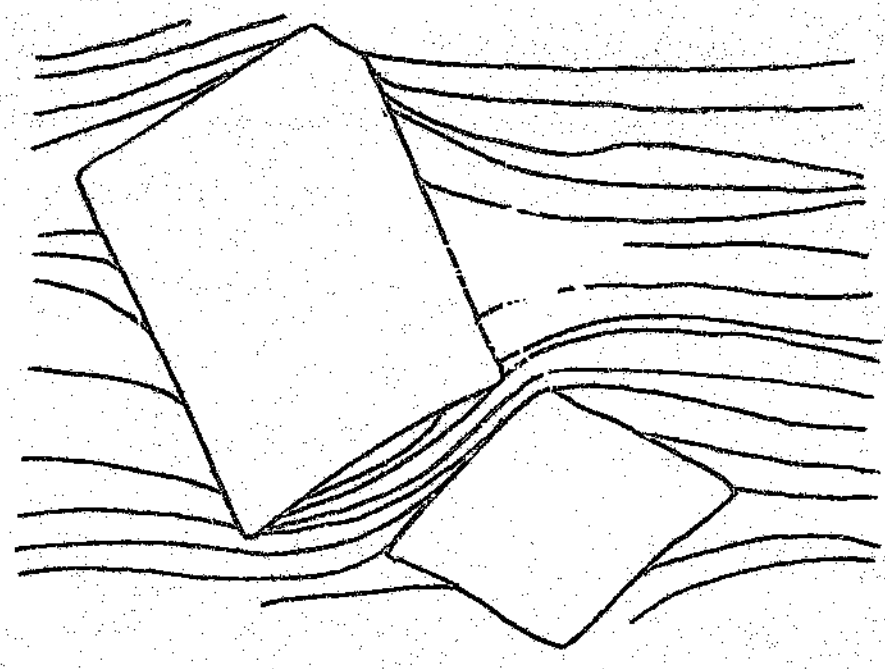

b

Fig. 4.5 Photomicrograph (a) and schematic representation (b) showing two idioblastic chiastolite porphyroblasts with cleavage anastomosing, truncated and squeezed between them. Bekker Schools locality. Scale bar 0,5 mm.

The cleavage "squeezed" between porphyroblasts in Fig. 4.5 may be accounted for by a component of deformation (possibly reactivation) once growth was completed. Alternatively, the "squeezed" cleavage on the lower face of the larger crystal in Fig. 4.5 may be similar to the so-called cleavage-domes ("mica-domes") described by Ferguson *et al.* (1980) and and Mitchell (1991). Cleavage-domes are interpreted to develop only in the presence of bulk hydrostatic stress by pushing aside pre-existing matrix cleavage. Applying the cleavage-dome model to the porphyroblast-cleavage relationship in Fig. 4.5 thus suggests post-deformation growth of the chiastolite porphyroblast under conditions of bulk hydrostatic stress. Figure 4.6 shows traces of similar cleavage-dome features, although they are not as clearly developed. The cleavage-domes are, however, not developed on all crystal faces of a particular porphyroblast, as would be expected from the model of Ferguson *et al.* (1980).

Occasionally, chiastolite crystals interfere with one another (Fig. 4.6). In Fig. 4.6, the crystal on the left appears to have the cleavage abruptly truncated against it, while the crystal on the right has cleavage slightly wrapped around it, although it also truncates cleavage.

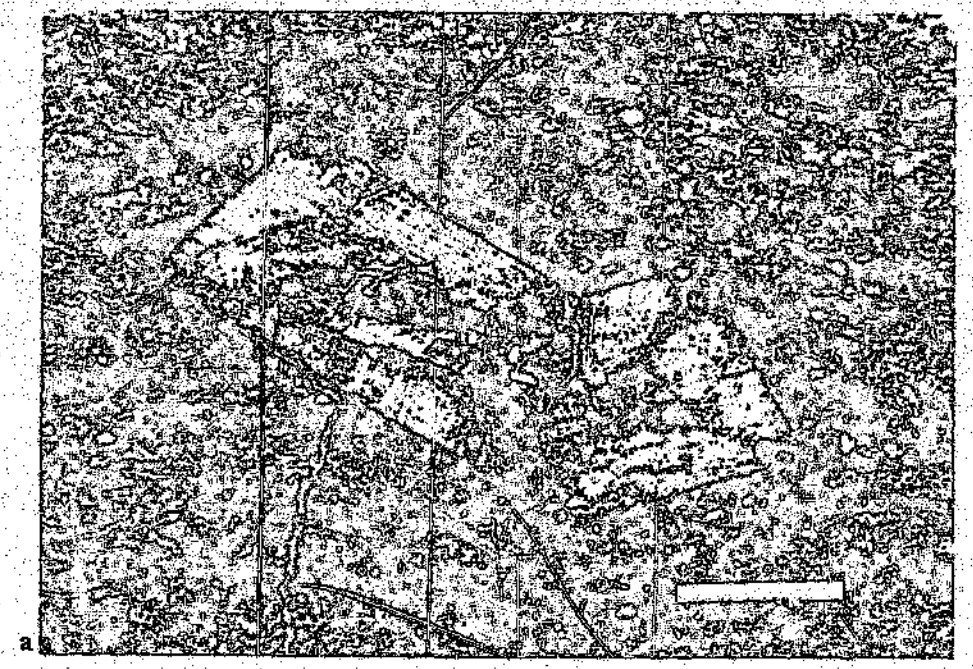

a

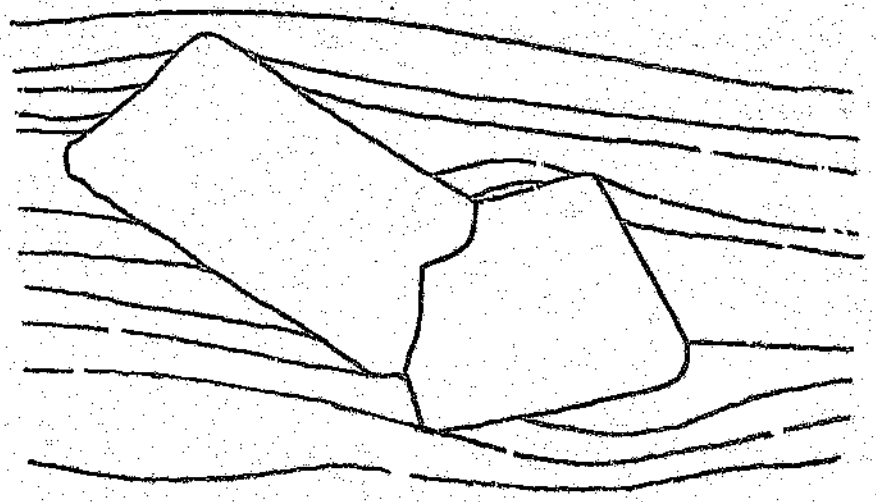

b

Fig. 4.6 Photomicrograph (a) and schematic representation (b) showing interfering chiastolite crystals, and variably truncated and anastomosing cleavage. Bekker Schools locality. Scale bar 0,5 mm.

4.3.3 Other Porphyroblasts

The majority of porphyroblasts occurring within shear zones in the study area are, unfortunately, highly altered (Figs. 3.44 and 3.49), and are not conclusive in determining timing relationships between metamorphism and deformation.

A thin spotted slate unit within the Black Reef Quartzite Formation at the base of the Transvaal Supergroup (locality 2863,1 X; -94,7 Y) contains deformed porphyroblasts. Although these porphyroblasts are altered and replaced in part by chlorite, quartz and white mica, they contain crosses (Fig. 4.7a) which suggests that they may originally have been chiastolite. They are wrapped by the S_2 cleavage, and are deformed to lozenge shapes (Fig. 4.7b), suggesting that they grew prior to D_2, and therefore that D_2 postdated the peak of metamorphism.

Phyllosilicate porphyroblasts, are widespread throughout the study area. Thin-sections reveal biotite, often altered to chlorite, and muscovite. Undulose extinction patterns under crossed nicols, as well as their tapered shapes, indicate that these porphyroblasts have been strained, and are therefore likely to have grown pre- or syn-D_2.

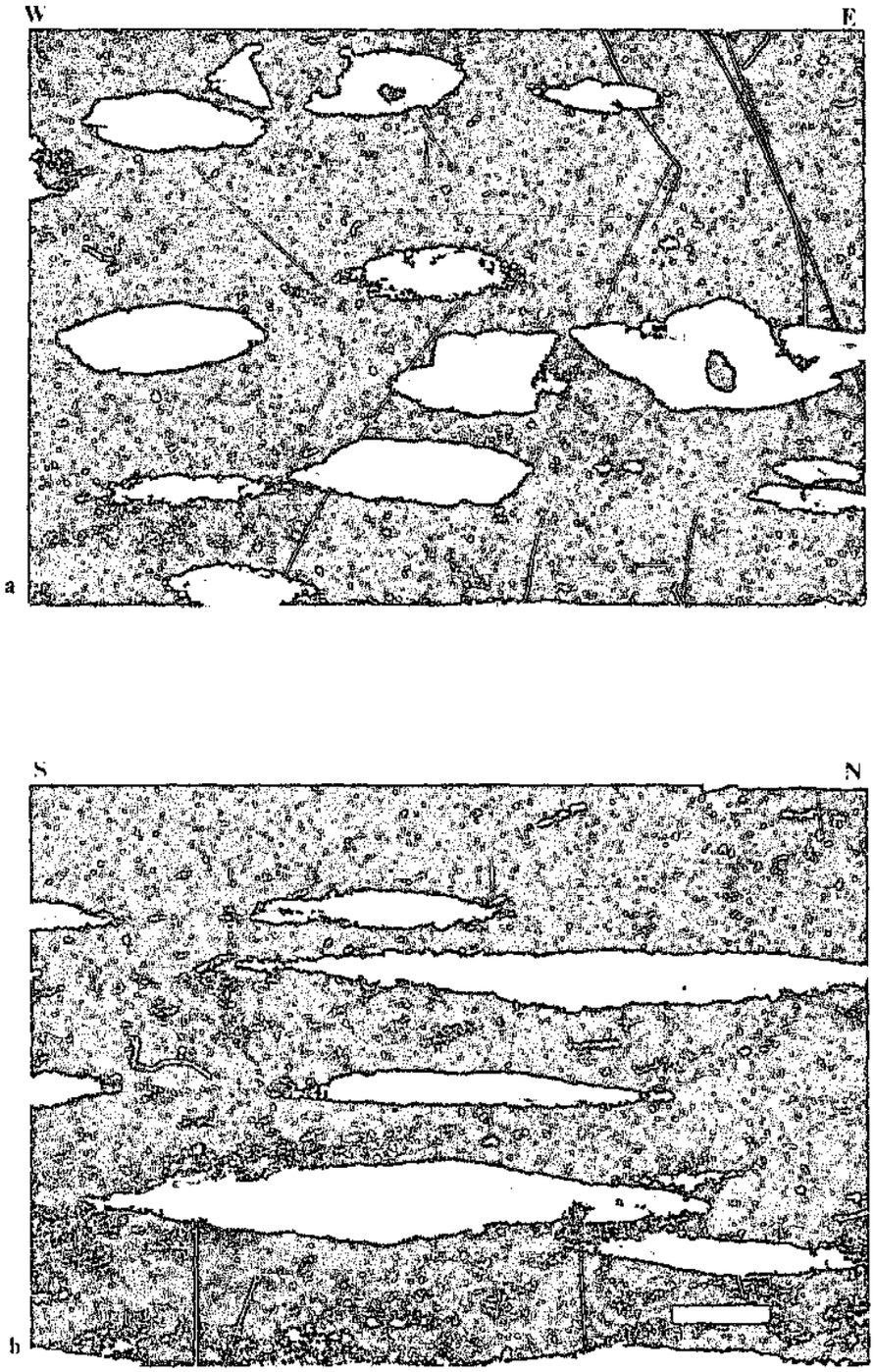

Fig. 4.7 Altered and deformed porphyroblasts from within a spotted slate, Black Reef Quartzite Formation. a) East-west section showing crosses probably indicating chiastolite. b) North-south section showing the porphyroblasts deformed to lozenge shapes. Scale bar 0.5 mm. Locality (2863.1 X; -95.0 Y).

4.4 Summary

Investigation of porphyroblast-cleavage relationships in the study area has revealed the relative timing of deformation events with respect to metamorphism. Chiastolite hosted in slates close to the metamorphic aureole of the Bushveld Complex displays relationships with cleavage which suggest that D_1 occurred prior to, or synchronously with, metamorphism. Chloritoid porphyroblasts from near a D_2 bedding sub-parallel shear zone in Pretoria Group slates, altered chiastolite from the Black Reef Quartzite Formation, as well as widely distributed phyllosilicate porphyroblasts, indicate that D_2 deformation post-dated, or was synchronous with metamorphism.

CHAPTER 5

METAMORPHISM

5.1 Introduction

Widespread metamorphism related to Bushveld Complex magmatism has been documented in the sedimentary rocks of the Transvaal Supergroup (e.g. Hall, 1908; 1909), as well as in the rocks of the Witwatersrand Supergroup (e.g. Gibson and Wallmach, 1995). In this chapter mathematical modelling is used to determine the likely extent of the thermal metamorphic effects of the Bushveld Complex in the study area. The aim of the exercise is to demonstrate that Bushveld Complex-related metamorphism was the most likely cause of porphyroblast growth in the study area, which places important constraints on the relative timing of deformation and metamorphism (Chapter 4).

5.2 Metamorphism of the Witwatersrand basin

Basin-wide studies of the Witwatersrand Supergroup have revealed that lower greenschist facies metamorphic assemblages are consistently developed in pelitic horizons throughout the goldfields, indicative of a regional metamorphic event (Phillips, 1987; Wallmach and Meyer, 1990) which may have occurred at approximately 2,0 Ga ago (e.g. Layer *et al.*, 1988). Greenschist facies metamorphism in the Witwatersrand goldfields is widely believed to have occurred at pressures of approximately 2-3 kbar (e.g. Phillips, 1987; Wallmach and Meyer, 1990; Phillips and Law, 1994; Frimmel, 1994b), which indicates burial depths of 7-11 km, and thus most, or all, of the Transvaal Supergroup sediments must have been deposited prior to the onset of metamorphism (Gibson and Wallmach, 1995). Temperature conditions during Witwatersrand basin metamorphism were in the order of 350 $\pm$ 50°C, as indicated by the

formation of kyanite and the composition of chlorite in aluminous shales (Wallmach and Meyer, 1990) and the presence of coexisting pyrophyllite-chloritoid assemblages, commonly in foliated zones (Phillips, 1988; Phillips and Law, 1994). Evidence for syn-tectonic growth of chloritoid porphyroblasts in the Witwatersrand basin given by Phillips and Law (1994) includes:

a) the fact that chloritoid is in chemical equilibrium with the matrix minerals, including those that define the cleavage; and

b) the development of quartz pressure shadows and textures around the crystals.

Metamorphic assemblages and strain are heterogeneously developed in the Central Rand Group, although they are spatially and genetically related to one another (Phillips, 1987). Phillips and Myers (1989) proposed that the metamorphism in the Witwatersrand basin was related to a high strain cleavage-forming event, initially documented by McCarthy *et al.* (1986), that affected the Witwatersrand, Ventersdorp and Transvaal Supergroup lithologies. Phillips and Myers (1989) suggested that the Vredefort Dome may have been a response to the same thermal event that caused the regional metamorphism, and thus that a close relationship existed between the Vredefort Dome and the metamorphism. Phillips *et al.* (1989) claimed that the deformation, which post-dated the deposition of the Transvaal Supergroup (McCarthy *et al.* 1986), occurred before the emplacement of the Bushveld Complex, although they do not give specific reasons for this conclusion. Their claim, therefore, is that the Bushveld Complex was emplaced after the deformation and metamorphism that affected the Witwatersrand, Ventersdorp and Transvaal Supergroups. These relationships are, however, invalidated by recent chronological data obtained for the Bushveld Complex (Walraven *et al.*, 1990) and the Vredefort Dome (Kamo *et al.*, 1995) which place the Vredefort Dome approximately 30-40 Ma after the Bushveld Complex.

Peak metamorphic temperatures in the Witwatersrand basin are consistent regionally, but increase towards the Johannesburg and Vredefort Domes (Phillips and Law, 1994). The collar rocks of the Vredefort Dome show concentric metamorphic zonation (Bisschoff, 1982), with evidence of greenschist and amphibolite facies grades (e.g. Phillips and Law, 1994). This higher metamorphic grade had previously been considered unrelated to the regional metamorphism in the remainder of the Witwatersrand basin, and was rather considered as representing the effect of a localised heat-source, integral with the formation of the Vredefort Dome (e.g. Phillips and Law, 1994; Frimmel, 1994). The Vredefort Dome was, however, almost certainly the result of an exogenous, rather than endogenous, event (e.g. Therriault *et al.*, 1995), which led Gibson and Wallmach (1995) to formulate a model for the relationship between the Vredefort event and metamorphism in the Witwatersrand basin. These authors derived an anticlockwise P-T path for the collar rocks of the Vredefort Dome, which indicated the existence of a regional, approximately 40°C/km geothermal gradient metamorphic event associated with thickening of the overlying crust. They attributed this regional metamorphism to the emplacement of substantial quantities of mafic magmas below, and into, the lower crust. These magmas were part of the same magmatic event that gave rise to the Bushveld Complex. Metamorphism of the Vredefort Dome collar rocks overlaps with the regional metamorphism in the main Witwatersrand basin, and was accompanied by strain, as seen by the development of synmetamorphic cleavages (Gibson, 1993). Following regional metamorphism and initial crustal cooling, a younger metamorphic paragenesis, consistent with rapid, Vredefort Dome-related exhumation and a geothermal gradient of approximately 30°/km, overprinted the regional metamorphic event (Gibson and Wallmach, 1995).

Gibson and Wallmach (1995) thus concluded that the regional greenschist facies

metamorphism in the Witwatersrand basin was a result of major syn-Bushveld Complex magmatism.

5.3 Bushveld Complex related metamorphism

The Bushveld Complex is transgressive and cuts progressively lower down into the Transvaal Supergroup rocks. The thermal aureole thus affects many rock types, and, in places, the metamorphism related to the main mass of the Bushveld Complex overprints contact metamorphism related to earlier sills (Button, 1976). The limits of the contact metamorphic aureole related to the Bushveld Complex have been well-defined in the eastern Transvaal (Hall, 1908) and the western Transvaal (Hall, 1909) since the beginning of this century.

Saggerson and Turner (1986) maintained that the extent of the contact metamorphic aureole of the Bushveld Complex is highly variable around its margins. The limit of the metamorphic aureole of the Bushveld Complex according to Saggerson and Turner (1986) is shown in Fig 5.1. The metamorphic effects of the emplacement of the Bushveld Complex resulted in the widespread, approximately zonal, development of cordierite-sillimanite, andalusite (chiastolite) and biotite-chlorite hornfelses and slates (Hammerbeck, 1986). The pelitic rocks of the Pretoria Group were subjected to varying degrees of metamorphism and, although contact metamorphism was the most prominent process, dynamic metamorphism also occurred in some areas adjacent to the Bushveld Complex (Hammerbeck, 1986; Uken and Watkeys, 1995).

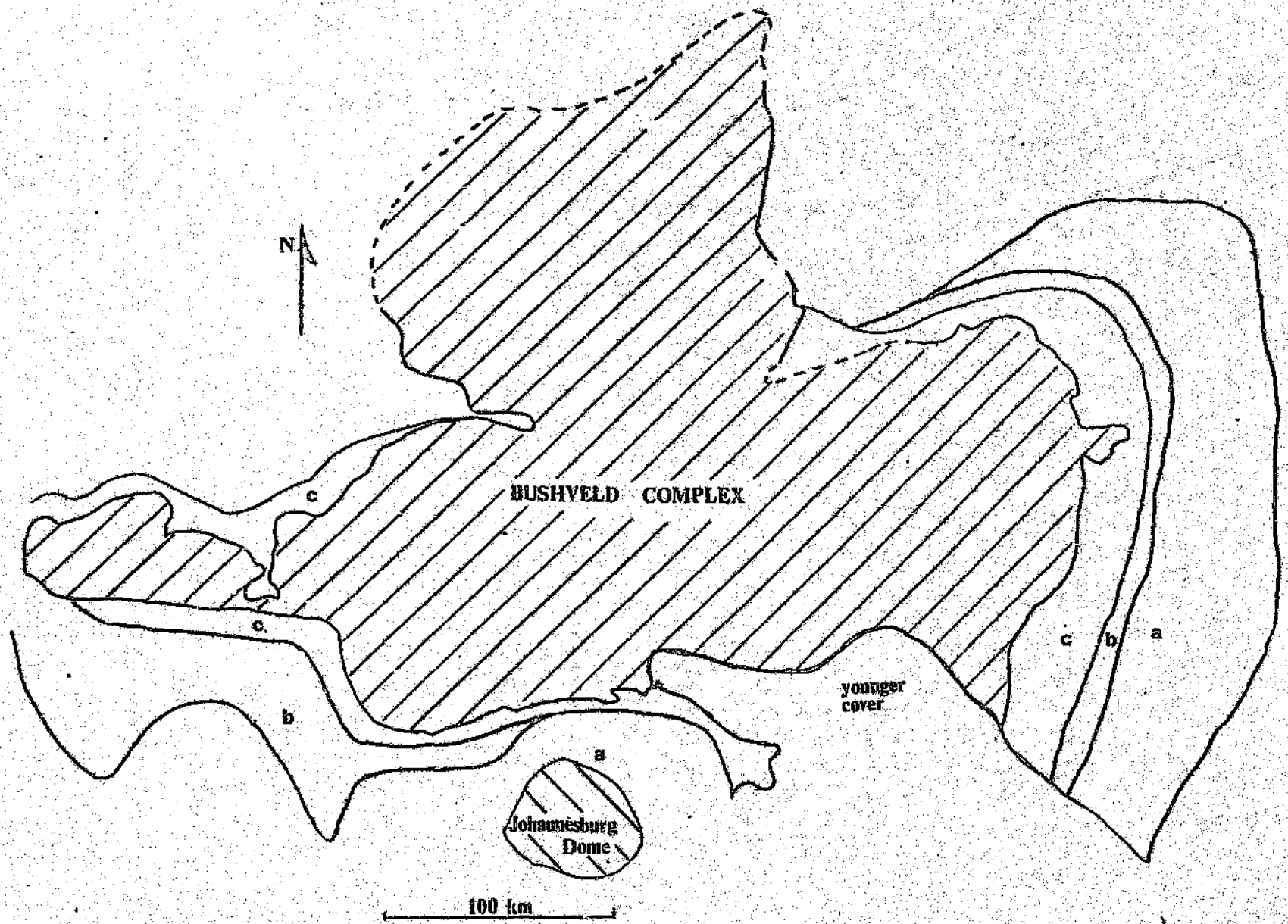

Fig. 5.1 Bushveld Complex aureole metamorphism map (modified from Saggerson and Turner, 1986). a) Unmetamorphosed lithologies. b) Albite-epidote hornfels. c)Hornblende hornfels

5.3.1 Eastern lobe

In the eastern Transvaal, Hall (1908) recorded two types of metamorphism, namely the Groothoek and Longsight types. The Groothoek type metamorphism owed its origin to the thermal effects related to the Bushveld Complex, and occurred between the Magaliesburg Quartzite and the contact with the Bushveld Complex. This contact metamorphism predominantly gave rise to cordierite hornfels, with all original textures obliterated. The second (Longsight) type of metamorphism, caused by sills intrusive into the Pretoria Group, produced chiastolite and staurolite slates, with original textures still mostly discernable (Hall, 1908).

The argillaceous rocks of the Pretoria Group in the eastern Transvaal are metamorphosed to at least greenschist facies (Button, 1976). This metamorphism is directly related to the Bushveld Complex (Button, 1976), and corresponds to the Groothoek type metamorphism documented by Hall (1908). Scattered biotite and andalusite are present in greenschist facies shales. At slightly higher grades, lydianites (fine-grained hornfelses (Bates and Jackson, 1987)) and hornfelses alternate. At even higher grades, only crystalline hornfels (with macroscopic biotite, cordierite and andalusite) is developed; partial melting and remobilisation of hornfels is not uncommon at some localities in the eastern Transvaal (Button, 1976).

Nell (1985) divided the metamorphic evolution in the floor rocks of the Bushveld Complex in the Potgietersrus area in the northern Transvaal into two stages, one at pressures of 1,5 kbar and temperatures up to 750°C, and the other at 4-5 kbar pressure and 850-900°C. Nell (1985) proposed a model where the first metamorphic stage was related to the older, Lower

Zone magmas of the Bushveld Complex which intruded as a sheet-like body, while the second stage of metamorphism was synchronous with the (gabbroic) magma intrusion (intruded at a higher stratigraphic level) from which the Critical-, Main- and Upper Zones crystallized. The pressures of 4-5 kbar associated with the second metamorphic event cannot be justified for the lithostatic pressure due to overburden at the time of intrusion, which has been calculated at no more than 2,5 kbar. Nell (1985) thus attributed the difference of roughly 2 kbar to one, or a combination of,

a) gas overpressure;

b) tectonic overpressure; or

c) an underestimation of lithostatic pressure during this metamorphic event.

Nell (1985) asserted that directed stress (tectonic overpressure) is indicated by a large fold in the Dwaalheuwel Formation with a roughly N-S fold axis, parallel to the contact of the Bushveld Complex and the floor rocks in this region, and 010° trending lineaments identified by Sharpe and Chadwick (1982). Polymetamorphism in the eastern lobe of the Bushveld Complex has been attributed to an initial dynamothermal event in addition to contact metamorphism (Hammerbeck, 1986). The dynamic event manifests itself as narrow shear zones, often with the cleavage parallel to the original bedding (Hammerbeck, 1986). Hornfelses, owing their origin to the thermal effects of the Bushveld Complex, have in some areas been deformed by later stresses. Sharpe and Snyman (1980) suggested temperatures of about 700°C and pressures of more than 4 kbar with some deviatoric stress influence (although this is likely to contribute less than 10% to total pressure (Bell and Cuff, 1989) whereas Wallmach *et al.* (1989) calculated pressures of 3-4 kbar in the floor rocks, and 1,1-2,4 kbar from calc-silicate xenoliths in the overlying Bushveld Complex.

Metamorphic zonation adjacent to the Bushveld Complex in the northeastern Transvaal is defined by pelitic porphyroblasts (chloritoid, staurolite, cordierite, garnet, orthoamphibole, andalusite, fibrolite and K-feldspar) (e.g. Uken and Watkeys, 1995). The metamorphism here was accompanied by intense deformation, which gave rise to schistose contact-metamorphic rocks, due to a combination of magma emplacement mechanisms, gravitational instability and reactivation of the Thabazimbi Murchison Lineament (Uken and Watkeys, 1994; 1995). Metamorphism in this area associated with the intrusion of the Bushveld Complex was thus accompanied by intense deformation, as a result of either one or a combination of emplacement mechanisms and contemporaneous regional deformation episodes.

Saggerson and Turner (1986) claim that, in the eastern Transvaal, the metamorphic effects are evident up to 4 km below the contact with the Bushveld Complex, whereas north of Pretoria, the metamorphism affected rocks only a few metres from the contact. This claim is, however, questionable, considering temperature estimates calculated from the thickness of Bushveld Complex magmas intruded (Section 5.4.1), and may possibly be explained in terms of subsequent displacement of metamorphosed lithologies by faulting.

5.3.2 Western lobe

Longsight and Groothoek types of metamorphism were also prevalent in the Transvaal Supergroup rocks in the western Transvaal (Hall, 1909). However, the metamorphism is more extensive adjacent to the eastern lobe than adjacent to the western lobe of the Bushveld Complex (Hammerbeck, 1986). Metamorphism in the western Transvaal was attributed mostly to the Bushveld Complex (Groothoek type) and, to a lesser extent, to sill intrusion (Longsight type). In the Zeerust area, Hall (1909) recognised that most of the pelitic Pretoria

Group rocks, as well as the uppermost dolomite units of the Chuniespoort Group, have been affected by contact metamorphism due to the Bushveld Complex. Hall (1909) observed that the extent of the contact metamorphic aureole of the Bushveld Complex increased from Pretoria westwards, and included the entire thickness of the Pretoria Group in the western Transvaal.

Garnet-hypersthene-cordierite assemblages have been reported in hornfelses adjacent to mafic sills in the western Bushveld Complex (Vermaak, 1970), and andalusite-biotite-cordierite and andalusite-almandine (garnet)-biotite assemblages occur 2,2 km stratigraphically below the Bushveld Complex (Engelbrecht, 1976). These assemblages confirm country rock temperatures of over 600°C in the high-grade areas (Cawthorn *et al.* 1981). According to Engelbrecht (1990b), the contact metamorphic aureole in this region extends up to 40 km from the contact of the Bushveld Complex with the Pretoria Group, which corresponds to approximately 7-10 km of stratigraphic thickness.

Chiastolite slates with andalusite-muscovite-biotite assemblages are encountered in the Bushveld Complex margin in the Marico district (Engelbrecht, 1976). The development of chiastolite in the region is restricted mainly to the Timeball Hill Formation (Hammerbeck, 1986). There is no evidence for any directed stress component associated with this metamorphism (Hammerbeck, 1986). These rocks have been classified into three distinct metamorphic zones (Engelbrecht, 1988):

1) an outer, low-grade chiastolite zone;

2) an intermediate cordierite zone;

3) an inner, high-grade orthopyroxene zone;

Beyond the chiastolite zone, the rocks were subjected to burial metamorphism to lower greenschist facies, assisted by the emplacement of Marico Hypabyssal Suite (MHS) sills (Engelbrecht, 1988; Engelbrecht, 1990b). The outer limit of the chiastolite zone is considered to be the maximum extent of the contact aureole of the Rustenburg Layered Suite in the western Transvaal (Engelbrecht, 1988). Thermobarometric calculations from the orthopyroxene zone of the metamorphic aureole in the western Transvaal yield pressures of 4,2 - 4,3 kbar (consistent with results from other lobes of the Bushveld Complex, e.g. Sharpe and Snyman, 1963; [illegible] temperatures of 610°C, but field and petrographic evidence reveal pressures [illegible] (based on 5,4 km overburden and petrogenetic grid observations) (Engelbrecht, 1988). Subsequently, a metamorphic model has been proposed by Engelbrecht (1988, 1990b) in which metamorphism was a continuous event that commenced with the intrusion of the Marico Hypabyssal Suite (MHS) sills, and terminated with the crystallisation of the Upper Zone of the Bushveld Complex. In this model, the intrusion of the MHS sills elevated floor rock temperatures and, as a consequence, initiated regional burial metamorphism. Intrusion of the marginal zone of the Rustenburg Layered Suite (RLS) initiated contact metamorphism that attained a maximum temperature of 610°C, which remained more or less constant during the intrusion of the Lower-, Critical- and Lower Main-zones. Prior to the intrusion of additional magmas, the Marginal, Lower and Critical zones may have been partially solidified and would have acted as thermal barriers between the floor rocks and the later intrusions. The bulk of the heat would consequently have been dispersed through the roof. The model thus accounts for the increased pressure, to approximately 4,2 kbar, by the emplacement of additional magmas while temperatures remained at approximately 610°C.

Cawthorn *et al.* (1981), however, identified two stages of metamorphism in the Transvaal Supergroup southeast of Rustenburg. The first metamorphic stage gave rise to a biotite-cordierite-quartz-alkali feldspar assemblage in hornfelses, part of the intermediate cordierite zone (Engelbrecht, 1976), which formed due to the effects of the metamorphic aureole of the Bushveld Complex. The second stage of metamorphism documented by Cawthorn *et al.* (1981) was related to later intrusion of mafic sills, and produced needles of sillimanite which grew through biotite grains of the precursor assemblage. The sillimanite may, however, have grown epitaxially during prograde metamorphic conditions (Cawthorn *et al.*, 1981).

5.4 Intrusion-related metamorphism in the study area

A rise in the temperature of rocks adjacent to magmatic intrusions of local extent results in contact metamorphism, and if the volume of intrusion is sufficiently large, the temperature rise in the surrounding country rocks will last long enough to initiate mineral reactions (Winkler, 1979). Small dykes and sills would tend to metamorphose adjacent country rock to a lesser extent (Winkler, 1979). However, if the ambient temperature of the country rock was already elevated by some other means, a small intrusion may increase the country rock temperature sufficiently to allow the commencement of metamorphic reactions.

5.4.1 Thermal modelling

For the study of metamorphic reactions and the growth of metamorphic index minerals, it is important to be able to calculate the maximum temperature to which the rocks at a specific distance from the contact of an intrusion have been raised (Jaeger, 1959a). Jaeger (1959b), in determining the temperatures in the neighbourhood of an intrusive sheet, outlined several assumptions which are made, namely:

a) That the intrusion assumes the form of a flat sheet, with thickness (D) in one direction, which extends indefinitely.

b) That intrusion is rapid, and that the country rock is at a constant temperature (zero). If the ambient temperature of the rock is not zero, then the resulting temperature is simply the sum of the ambient temperature and the induced temperature of the rock.

c) That the thermal properties of the rocks are taken to be the same, independent of the temperature of the rock.

d) That heat loss due to escaping volatiles is neglected.

e) That cooling is by conduction only, and that the effects of convection are not considered.

The greatest rise in country rock temperature occurs in direct contact with the intrusion, while away from it there are zones of lower temperature (Winkler, 1979). The extent to which the country rock is heated depends on the heat content, i.e. the size and composition of the intrusion. Thus the temperature rise of the country rock is a function of the temperature of the intruded magma, which has been estimated at 700-800°C for granitic magmas, approximately 900°C for syenitic magmas, and approximately 1200°C for gabbroic magmas (Winkler, 1979). The intrusion temperatures of the Bushveld Complex magmas have been experimentally determined at between 1200 and 1300°C (Irvine and Sharpe, 1982). Based on gravity profiles, the thickness of the mafic portion of the western lobe of the Bushveld Complex has been estimated at approximately 5000 m (Walraven and Darracott, 1976).

Thermal models assume that heating is by conduction only, and that intrusion is rapid or instantaneous. Realistically, factors such as:

a) the presence of metamorphic fluids;

b) under- or over-estimation of the original thickness of the Bushveld Complex;

c) progressive, rather than instantaneous, intrusion of the Bushveld Complex; and

d) the thermal effects of sills;

will influence the rate of heat transfer and the extent of the metamorphism. Since many simplifications and assumptions are applied to thermal modelling, the results should only be used as a broad estimate for the temperature conditions arising from the emplacement of an intrusion.

Two thermal models pertaining to the effects of the Bushveld Complex in the study area are presented below. The first model follows the method outlined by Winkler (1979) in which the thickness of the Bushveld Complex is used to determine temperature estimates on a given graph. The second model is based on the mathematical equations derived by Jaeger (1959a,b) and summarised by Yardley (1989).

a) Model 1

Winkler (1979) considers that the temperature in the country rock in immediate contact with an intrusion will be $> 0{,}6\ (T_i) + (T_n)$, where T_i is the temperature of the intrusion, and T_n is the ambient temperature of the country rock. At a distance equivalent to 10% of the thickness of the intrusion (D), the final temperature of the country rock would be $0{,}5\ (T_i) + (T_n)$. At a distance equivalent to 50% of D, the temperature of the country rock would be

approximately 0,33 (T_l) + (T_n).

Winkler (1979) has presented data concerning the temperatures of the country rocks adjacent to different intrusions at different depths as a function of the distance from the intrusion (Fig. 5.2). The essentially gabbroic magmas of the Bushveld Complex would have intruded at a temperature of at least 1200°C (Irvine and Sharpe, 1982). From Fig. 5.2, considering a depth of intrusion in the order of several kilometres, the temperature of the floor rocks at the contact with the Bushveld Complex would be approximately 875°C. The stratigraphic thickness of the Transvaal Supergroup rocks in the region of the study area is no more than approximately 5100 m (S.A.C.S., 1980), which is similar to the thickness estimated for the mafic portion of Bushveld Complex in this area (Walraven and Darracott, 1976). Table 5.1 shows the temperature at various levels in the Transvaal Supergroup induced by the emplacement of the Bushveld Complex. At the base of the Transvaal Supergroup, the temperature of the rocks due to the intrusion of the Bushveld Complex, derived by extrapolation from Fig. 5.2, would be in the order of 400°C. An inverted temperature gradient from the base to the top of the Transvaal Supergroup with a range of more than 400°C has consequently been established.

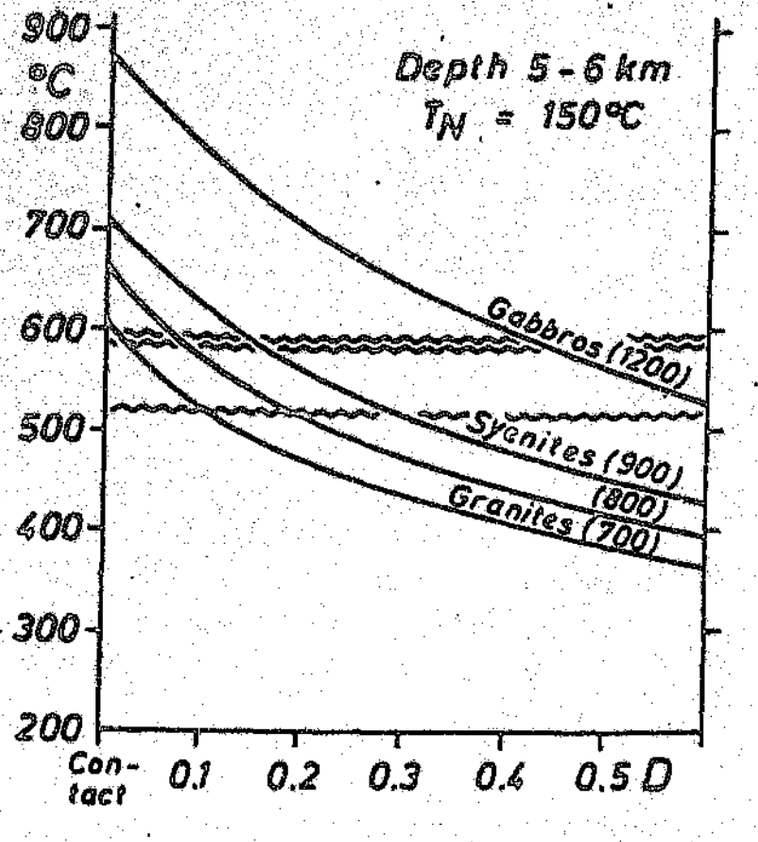

Fig. 5.2 Heating of the country rock adjacent to different intrusions at different depths. D=thickness of intrusion. Distance from the contact on the x-axis given as fractions of D (after Winkler, 1979).

Table 5.1 Temperatures attained at various levels in the Transvaal Supergroup due to the intrusion of the Bushveld Complex, based on the model of Winkler (1979). See Fig. 5.2. D=5000m.

Depth	Temp.
Contact	875°C
0,1D=500m	800°C
0,2D=1000m	710°C
0,3D=1500m	680°C
0,4D=2000m	610°C
0,5D=2500m	585°C
1D=base of Transvaal	400°C

The maximum temperature at any point in the country rock away from the contact with the Bushveld Complex would be sustained for a period of time (in years) which is given by $0,01\ D^2$ (Winkler, 1979). In the case of the approximately 5 km thick Bushveld Complex, the temperature of the country rock at a given point will be sustained for the period $0,01(5000)^2$, which is in excess of 250 000 years.

b) Model 2

As with the first model, there is a simple relationship between the size of the intrusion, and the size and duration of the thermal aureole that it produces. The equations can, therefore, be applied equally to an intrusion of any size (Yardley, 1989).

The quantities necessary for mathematical thermal modelling are outlined below (in Yardley, 1989, simplified after Jaeger, 1959a,b):

y - half-thickness of the intrusion

x - distance from the centre of the intrusive sheet to the point under discussion

T - temperature at point and time under discussion

T_o - initial temperature of the magma

k - thermal diffusivity of the rock

t - time in years

The quantity k varies very little over most rock types, and a constant 31,5 m^2/yr may be used for all calculations (Yardley, 1989).

The dimensionless ratios

$d = x/y$ and

$r = kt/y^2$

are used as the mathematical functions to determine temperature from the equation

$T/T_o = \Phi\ (d,r)$

The values of Φ for values of d and r are given in Table 2 (Jaeger, 1968). For simplicity of the calculations, the thickness of the Transvaal Supergroup in the region of the study area

is assumed to be 5000 m, and the thickness of the Bushveld Complex, also 5000 m. Thus $y = 2500$ m. Temperature estimates have been made at 1000 m intervals from the base to the top of the Transvaal Supergroup, at time intervals of 10^4, 10^5, 10^6 and 2×10^6 years after the (instantaneous) intrusion of the Bushveld Complex.

Table 5.2 The values of d and r for thermal modelling, after Jaeger (1968).

d \ r	0.01	0.02	0.04	0.1	0.2	0.4	1	2	4	10
0	1.000	1.000	1.000	0.975	0.886	0.736	0.520	0.383	0.276	0.177
0.2	1.000	1.000	0.998	0.960	0.868	0.725	0.516	0.381	0.276	0.177
0.4	1.000	0.999	0.983	0.909	0.815	0.690	0.503	0.376	0.274	0.176
0.6	0.998	0.977	0.921	0.814	0.731	0.636	0.482	0.367	0.270	0.175
0.8	0.981	0.941	0.780	0.673	0.622	0.566	0.455	0.356	0.266	0.174
1.0	0.500	0.500	0.500	0.500	0.499	0.487	0.421	0.341	0.260	0.173
1.2	0.079	0.160	0.240	0.327	0.376	0.405	0.384	0.325	0.253	0.171
1.4	0.002	0.023	0.079	0.186	0.264	0.324	0.344	0.306	0.246	0.169
1.6		0.001	0.017	0.090	0.171	0.249	0.303	0.285	0.237	0.166
1.8			0.002	0.037	0.103	0.185	0.262	0.264	0.228	0.163
2				0.013	0.057	0.131	0.222	0.242	0.217	0.160
3				0.000	0.001	0.013	0.076	0.136	0.161	0.142
4							0.017	0.061	0.106	0.119
5							0.002	0.021	0.061	0.096
6								0.006	0.032	0.073

For the determination of $d = x/y$:

At the base of the

Transvaal Supergroup: $d = 7500/2500 = 3,0$

At 4000 m depth: $d = 6500/2500 = 2,6$

At 3000 m depth: $d = 5500/2500 = 2,2$

At 2000 m depth: $d = 4500/2500 = 1,8$

At 1000 m depth: $d = 3500/2500 = 1,4$

At the contact with

the Bushveld Complex: $d = 2500/2500 = 1,0$

For the determination of $r = kt/y^2$

$= 31{,}5.t/2500^2$

At 10^4 yrs: $r \sim 0{,}05$

At 10^5 yrs: $r \sim 0{,}5$

At 10^6 yrs: $r \sim 5$

At $2x10^6$ yrs: $r \sim 10$

So, for example, the value of Φ at a distance of 1000 m from the contact, 10^6 years after intrusion would be Φ *(1,4; 5)*, which corresponds to a proportional value between $r = 4$ and $r = 10$. Thus Φ would be approximately 0,226. The temperatures of the country rock at certain times after intrusion is given by $T = T_o.\Phi$ *(d,r)* where Φ is determined from Table 5.2, $T_o = 1200°C$, and the temperature of the country rocks is assumed to be 0°C. The calculated temperatures of the country rocks at various depths and times after intrusion are presented in Table 5.3.

From Table 5.3 it can be seen that temperatures tend to become homogeneous throughout the entire country rock sequence as time progresses, and while the country rocks at the contact are cooling down, the rocks further from the contact are still increasing in temperature. The maximum temperature range determined from this model is between 187°C at the base to 600°C at the contact (assuming initial country rock temperatures of 0°C).

Table 5.3 Temperatures attained in the Transvaal Supergroup due to the intrusion of the Bushveld Complex at various positions in space and time, based on the mathematical model of Jaeger (1959a). Initial country rock temperature assumed to be 0°C.

Time(Ma)	Base	4000m	3000m	2000m	1000m	Contact
10^4				12°C	126°C	600°C
10^5	34°C	89°C	145°C	244°C	395°C	564°C
10^6	187°C	200°C	228°C	253°C	271°C	286°C
2.10^6	170°C	178°C	185°C	196°C	203°C	207°C

In a realistic situation, the influence of a geothermal gradient must be considered when determining the actual temperature of the country rock at a particular point in space and time. Jaeger (1959a,b) asserts that the temperature induced in the country rock by the intrusion of a magma body is simply added to the initial temperature (as determined by the local geothermal gradient) of the country rock. A geothermal gradient has not as yet (as far as can be established) been determined for the Transvaal Supergroup in this region. Thus the effects of various geothermal gradients are discussed in terms of the thermal modelling results due to the emplacement of the Bushveld Complex. Low, medium and high geothermal gradients (20°C/km, 30°C/km and 40°C/km respectively) are applied to the maximum temperatures attained by thermal modelling at various positions in the Transvaal Supergroup presented in Table 5.3. Peak metamorphic conditions through most of the Transvaal Supergroup were, according to Table 5.3, attained approximately 10^6 years after the (instantaneous) intrusion

of the Bushveld Complex. Table 5.4 is a representation of the maximum temperatures attained during peak metamorphic conditions when added to various geothermal gradients.

Table 5.4 Maximum modelled temperatures (from Table 5.3) when various geothermal gradients are taken into account.

Depth (m)	Modelled Temperature	+20°C/km Geotherm	+30°C/km Geotherm	+40°C/km Geotherm
0 (contact)	600°C	+0=600°C	+0=600°C	+0=600°C
1000	395°C	+20=415°C	+30=425°C	+40=435°C
2000	253°C	+40=293°C	+60=313°C	+80=333°C
3000	228°C	+60=288°C	+90=318°C	+120=348°C
4000	200°C	+80=280°C	+120=320°C	+160=360°C
5000 (base)	187°C	+100=287°C	+150=337°C	+200=387°C

c) Relevance of the thermal models to the study area

Biotite, commonly associated with muscovite and chloritoid, is present in the slate units of the Black Reef Quartzite Formation at the Base of the Transvaal Supergroup in the study area. In the light of current knowledge, the formation of biotite requires conditions of P > 3 kbar, and T ~ 400°C to form (Wang *et al.*, 1986). The appearance of biotite + muscovite in the same pelitic rock is thought to occur at temperatures between 300 and 400°C (Spear, 1993). Hence the minimum temperature attained at the base of the Transvaal Supergroup at peak metamorphic conditions should be in the region of 400°C. This corresponds with the

theoretically determined temperature at the base of the Transvaal Supergroup from Model 1, and is most consistent with a geothermal gradient of at least 40°C/km in Model 2. A higher geothermal gradient for Model 2 cannot, however, be ruled out. This figure corresponds well with the 40°C/km geothermal gradient proposed by Gibson and Wallmach (1995), 35°C/km by Walimach and Meyer (1990), and 39°C/km by Schreyer and Bisschoff (1982), and is less than the 50°C/km suggested by Phillips (1987), for the region in the vicinity of the Witwatersrand basin.

5.5 Metamorphism of carbonate rocks

Carbonate rocks (siliceous dolomite) are present in the Black Reef Quartzite Formation (S.A.C.S, 1980), and dominate the Chuniespoort Group (S.A.C.S., 1980) in the study area. Carbonate-quartz rocks do not show any visible mineralogical changes until they are affected by low-grade metamorphism, however, at higher grades of metamorphism, numerous mineral reactions occur, initially forming talc, then tremolite, diopside and forsterite (Winkler, 1979). Sporadic tremolite occurrences are only found within 2m of the contacts of sills intrusive into the Chuniespoort Group in the study area may be a result of localised temperature increases induced by pre-Bushveld sills (Section 2.2).

5.6 Metamorphism of pelitic rocks

The Pretoria Group in the study area constitutes slate, quartzite, and minor sills (Section 2.2.4). Closer to the Bushveld Complex, the slate units are metamorphosed to hornfelses. Hornfelses (*sensu stricto*) are fine grained granoblastic metamorphic rocks (Whitten and Brookes, 1979; Bates and Jackson, 1987), that commonly preserve relict bedding, and form in the contact aureole around an intrusion (Lapidus, 1987). Preferred mineral alignment in

hornfelses is typically absent due to lack of deformation during metamorphic mineral growth.

During a traverse approximately 20 km northeast of the town of Magaliesburg, west of the Bekker Schools (Fig. 1.1), numerous rock samples were taken in order to establish structural-metamorphic relationships. On the outcrop scale, many of the samples resembled hornfels. These "hornfelses" are typically fine-grained, commonly preserve bedding, and fracture conchoidally when struck with a hammer. Macroscopically, there is no evidence for any fabric development in the samples. Thin sections of some of the samples do, however, expose the development of a penetrative shear cleavage (S_1) oriented sub-parallel to bedding, which strikes approximately east-west and dips approximately 20° to the north (Section 3.2). The cleavage was not developed in the sediments due to lithostatic pressure, but was rather the result of ductile deformation, and therefore the samples collected from this area are not true hornfelses. Uncertainties arising from the question as to whether the deformation resulting in these fabrics occurred pre-, syn- or post-metamorphism may be resolved by the microscale examination of metamorphic index minerals and their relationships with the fabrics (Chapter 4).

In slate samples from the study area, chloritoid and andalusite (chiastolite) porphyroblasts are developed on microscopic and, in the case of chiastolite, macroscopic scales. Chloritoid is present in many of the slates sampled, but is best developed in close proximity to D_2 bedding sub-parallel shear zones. Chloritoid forms under low-grade metamorphic conditions (T ~ 350 - 530°C), and persists throughout the whole range of low-grade metamorphism (Winkler, 1979).

Chiastolite is relatively rare in the study area. The first occurrence is highly altered, near the base of the Transvaal Supergroup, where it occurs in a thin unit of spotted slate. Another occurrence of chiastolite, higher up in the Transvaal Supergroup stratigraphy in relatively close proximity to the contact with the Bushveld Complex, displays interesting relationships with the penetrative fabric (Section 4.3.2). There were, however, no other chiastolite occurrences encountered in any other lithologies. The presence of chiastolite is an indication of medium-grade metamorphism (Winkler, 1979).

5.7 Metamorphism of sills

The sills encountered in the Chuniespoort Group in the study area have been metamorphosed (Chapter 2), and can be correlated with metadolerite (amphibolite) sills documented in other areas adjacent to the Bushveld Complex (e.g. Willemse, 1959; Engelbrecht, 1976; Sharpe, 1981) (Section 2.2.5). The minerals constituting the sills, as determined by thin-section petrographic studies, include hornblende, plagioclase, actinolite, quartz, micas, minor talc, carbonate and chlorite. The presence of chlorite in the metamorphic mineral paragenesis is diagnostic of low-grade metamorphism (Winkler, 1979). The chlorite may, however, be a feature of retrograde metamorphism. Actinolite and hornblende coexist in the sills. As actinolite gives way to hornblende from greenschist to amphibolite facies, which indicates temperatures in the order of 500°C (Winkler, 1979; Spear, 1993), it is probable that metamorphism occurred at temperatures slightly lower than 500°C.

5.8 Summary

The emplacement of the Bushveld Complex resulted in regional metamorphism in the Transvaal (e.g. Hall, 1908, 1909) and Witwatersrand Supergroups (e.g. Gibson and Wallmach, 1995). Thermal modelling has demonstrated that Bushveld Complex metamorphism, superimposed on a geothermal gradient of approximately 40°C/km, was probably prevalent throughout the Transvaal Supergroup in the study area. The emplacement of the Bushveld Complex was, therefore, probably responsible for the regional, low-grade, metamorphism, as well as the development of porphyroblasts in the study area. This conclusion is important for the relative timing of deformation events with respect to the emplacement of the Bushveld Complex (Chapter 4).

CHAPTER 6

DISCUSSION

6.1 Introduction

The objective of this study has been to identify, and constrain the relative timing of, the deformation events affecting an area of the Transvaal Supergroup north of the Johannesburg Dome. An important aspect of the study was to establish the interrelationship between deformation and (a) the metamorphism associated with the 2065-2054 Ma Bushveld Complex (Walraven *et al.*, 1990; Walraven and Hattingh, 1993) and (b) the 2025 $\pm$ 4 Ma Vredefort Dome (W.U. Reimold, pers. comm.). The Vredefort Dome is widely believed to have been the result of a catastrophic impact event (Therriault *et al.*, 1995) which had far-reaching effects on the rocks of the Kaapvaal Craton (e.g. McCarthy *et al.*, 1986).

Evidence from field mapping indicates that the area has undergone a complex deformation history, which resulted in heterogeneously developed ductile and brittle structures. The study also revealed that mid- to upper-greenschist facies metamorphism affected the rocks.

6.2 Metamorphism

Evidence for both single and multiple metamorphic events adjacent to the eastern and western lobes of the Bushveld Complex have been proposed by earlier workers (e.g. Engelbrecht, 1976; Cawthorn, 1981; Nell, 1985). Gibson and Wallmach (1995) have proposed, however, that syn-Bushveld Complex metamorphism was considerably more extensive than the contact aureole in the floor rocks of the Complex. They attribute greenschist to amphibolite facies metamorphism in the Witwatersrand basin, and granulite facies metamorphism in the

underlying Archaean basement, to regional intraplating of magmas into the lower and mid-crust accompanying the Bushveld Complex. Similarly, thermal modelling undertaken for this study has shown that the most likely origin of the metamorphism (and, thus, porphyroblast growth) in the study area is the Bushveld Complex (Section 5.4.1). Porphyroblast growth and metamorphism associated with the Bushveld Complex can, therefore, be used as an important time-line for determining the relative timing of ductile deformation events in the study area.

6.3 Deformation

Field relationships have established the relative timing of the main deformation events in the study area. Uncertainties do, however, remain regarding the relative timing of structures associated with the less deformation events.

6.3.1 D_1 event

The Pretoria Group slates at the Magaliesburg locality (Fig. 1.1) have two sets of intensely developed penetrative cleavage. The southerly-dipping cleavage, which has been correlated with S_2 cleavage in the main study area, crenulates the northerly-dipping cleavage (S_1) (Fig. 3.1).

Chiastolite porphyroblast-cleavage relationships at the Bekker Schools locality, approximately 20 km ENE of Magaliesburg (Fig. 1.1), aid in determining the relative timing of the S_1 cleavage-forming event. At this locality, only a single, bedding-parallel, cleavage, of indeterminate vergence, is developed in chiastolite slates. Porphyroblast-cleavage relationships indicate that the cleavage either predated, or occurred synchronous with, porphyroblast growth (Section 4.3.2). The slightly ambiguous nature of the porphyroblast-

cleavage timing relationships could conceivably have been the result of either:

a) multi-stage growth of porphyroblasts during more than one metamorphic event. Heterogeneous deformation could have accompanied the earlier metamorphism, whereas the later metamorphism proceeded in the absence of strain; or

b) a single prolonged metamorphic event during which a heterogeneous deformation event proceeded for a relatively short time. Initial porphyroblast growth could, thus, have occurred synchronous with cleavage development, and continued once deformation terminated.

Multiple metamorphic events related to the Bushveld Complex have been proposed (Section 5.3). However, it has been established that the metamorphism in the study area can probably be attributed to a single, prolonged, Bushveld Complex-related event (Section 5.4.1). Despite the uncertainty of the timing relationships, it is clear that the cleavage at the Bekker Schools locality did not post-date the porphyroblast-forming event. A D_2 origin for the cleavage (Section 6.3.2) can thus be discounted. It is concluded that this cleavage is S_1. This is supported by evidence from other samples in the immediate vicinity which contain north-dipping S_1. The chiastolite porphyroblast-cleavage relationships thus suggest that the S_1 cleavage was initiated prior to, or synchronous with, thermal activity associated with the emplacement of the Bushveld Complex. Metamorphism may have continued for a longer period than did deformation, thus explaining the post-deformation growth characteristics seen in some of the chiastolite porphyroblasts.

The earliest recognisable deformation (D_1) in the study area, therefore, produced a heterogeneously-developed, southerly-verging, S_1 cleavage, which formed in pre- to syn-Bushveld Complex times. This cleavage is preferentially developed in the pelitic units of the

Pretoria Group within the contact metamorphic aureole of the Bushveld Complex.

Origin of the D_1 deformation

Several workers (e.g. De Waal (1970), Coertze (1971), Walraven (1974) and Sharpe and Snyman (1980)) have proposed that stresses of uncertain origin may have been present prior to, or contemporaneous with, emplacement of the main plutonic phase of the Bushveld Complex. Deformation of the Transvaal Supergroup floor rocks is likely to have been facilitated by thermal weakening caused by the emplacement of the Bushveld Complex. This deformation may have culminated prior to the crystallisation of upper-zone rocks and the Nebo Granite (Sharpe and Chadwick, 1982) at approximately 2054 $\pm$ 4 Ma (Walraven and Hattingh, 1993). Shear-folding radial to the Bushveld Complex margins (De Waal, 1970) suggests that southerly-directed stresses may have been prevalent in the current study area in pre- to syn-Bushveld Complex times, which may have been the source of S_1. The style of D_1 deformation in the study area, however, differs from the NW trending folds near the Pilanesberg Complex (Walraven, 1974), the shallow south-dipping cleavages and north-verging folds north of the Bushveld Complex (Visser *et al.*, 1984; Uken and Watkeys, 1994) and the folds and fabrics in the eastern Transvaal (De Waal, 1970; Sharpe and Chadwick, 1982; Hartzer, 1995). Regional heating of the rocks of the Transvaal Supergroup during the emplacement of the Bushveld Complex would readily facilitate their deformation when subjected to regional compressional stresses or gravitational collapse. The S_1 cleavage may, thus, be a gravitational collapse structure triggered by thermal weakening of the floor rocks of the Bushveld Complex, or the product of south-directed shearing of uncertain origin.

6.3.2 D_2 event

The most intense and widely-developed deformation in the study area gave rise to the north-verging structures of the D_2 event, which affected the entire thickness of the Transvaal Supergroup in the study area. The combination of northward verging folds, strained ooids, S-C fabrics, lineations and porphyroclasts within the bedding sub-parallel shear zones strongly suggests that they formed from non-coaxial ductile deformation with top-to-the-north shear sense. Shear strain was preferentially partitioned into narrow zones and tended to exploit bedding and sill contacts in ooth the lower carbonate and the upper pelitic units. The strikes of bedding sub-parallel shear zones, S_2 cleavage, folds and deformed ooids in the study area are approximately parallel, and their vergence directions similar, which suggests that these structures are all a result of a single deformation event which originated south of the study area.

Timing of the D_2 deformation in the study area has been determined by the interrelationship between S_2 cleavage development and porphyroblast growth. In the study area, chloritoid, andalusite and phyllosilicate porphyroblasts display pre- to syn-S_2 cleavage growth characteristics. D_2, therefore, probably commenced after the onset of peak metamorphism, and thus post-dated the Bushveld Complex.

Origin of the D_2 deformation

The D_2 structures and their orientations in the study area are similar to those recorded in a study of the Black Reef Quartzite Formation adjacent to the northern portion of the Witwatersrand basin by McCarthy *et al.* (1986). Their study revealed a regional, post-Transvaal, period of deformation in the form of folds, cleavage and faults.

Large- and small-scale folds in the Black Reef Quartzite Formation trend sub-parallel to one another, and are concentrically arranged around the Vredefort Dome (McCarthy *et al.*, 1986) (Fig. 6.1), which is located at the approximate centre of the Witwatersrand basin. The folds verge outwards from the Witwatersrand basin (McCarthy *et al.*, 1986; McCarthy *et al.*, 1990). The northerly vergence of the D_2 folds seen in the study area is consistent with this pattern. A closely spaced, penetrative, heterogeneously-developed, cleavage was also documented in the mudstones of the Black Reef Quartzite Formation by McCarthy *et al.*, (1986). This cleavage strikes parallel to the axial planes of folds in the region, but is not axial planar to them. Rather, the cleavage dips towards the centre of the Witwatersrand basin at a shallower angle than do the fold axial planes (McCarthy *et al.*, 1986). S_2 cleavage and the axial planes of D_2 folds observed in this study show a similar relationship (Section 3.3.2 *a*). According to McCarthy *et al.* (1986), the cleavage is locally developed in a Bushveld-age sill, which constrains the timing of the deformation to post-Bushveld times. The relative timing of the deformation is further confirmed as altered pyrophyllite porphyroblasts are deformed by the cleavage (McCarthy *et al.*, 1986), similar to the S_2 cleavage-prophyroblast relationships in the current study area.

McCarthy *et al.* (1986) also recorded significant faults, some of which are bedding sub-parallel, which strike parallel to the fold axes and cleavage. These faults are correlatives of the D_2 bedding sub-parallel shear zones in the current study area. McCarthy *et al.* (1986) concluded that a single tectonic event, which acted radially to the Witwatersrand basin, gave rise to northerly verging folds, bedding parallel faults and cleavage in the vicinity of the

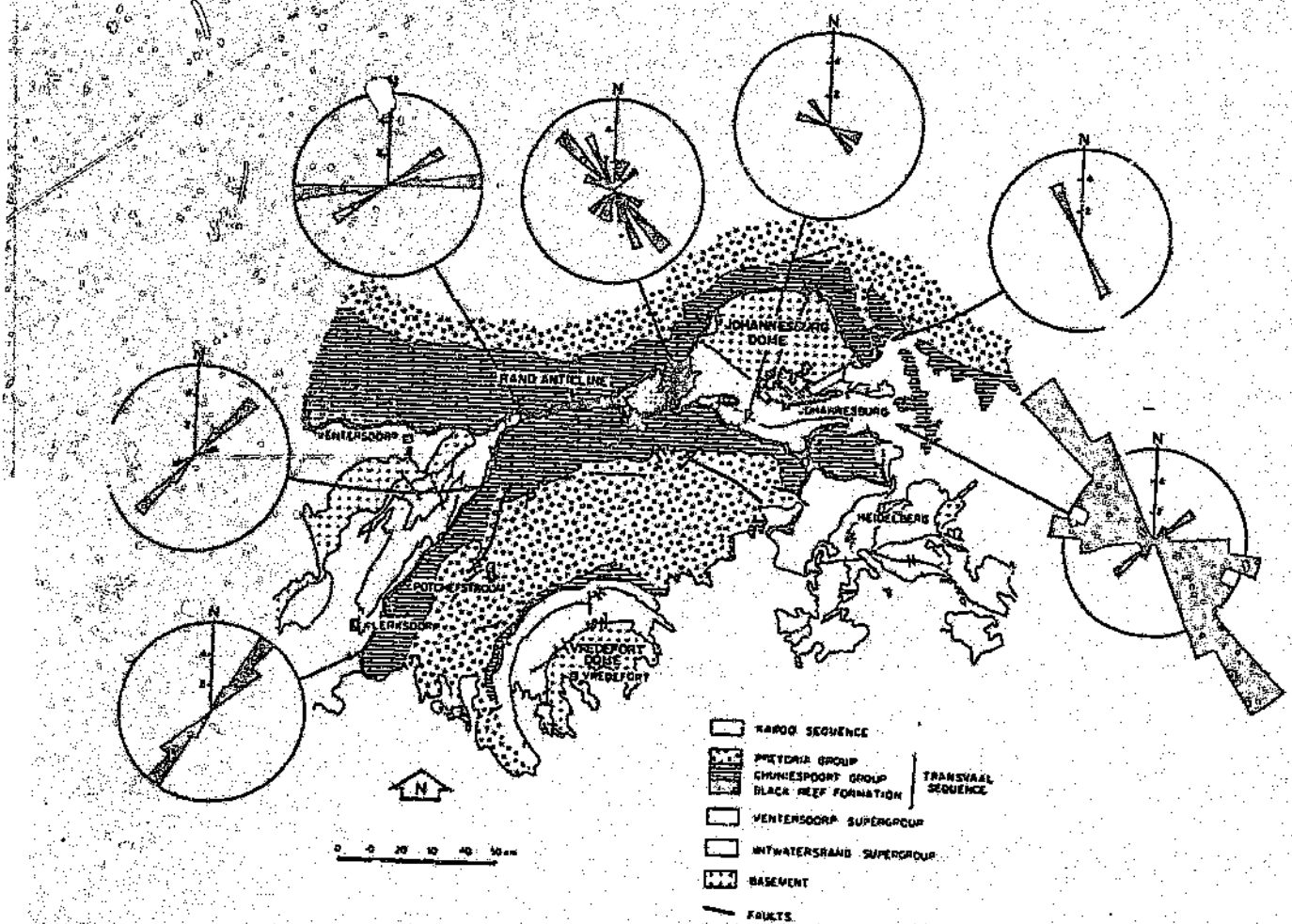

Fig. 6.1 Concentric arrangement of fold axes around the Vredefort Structure, from McCarthy *et al.* (1986).

study area. The deformation has been attributed to the formation of the Vredefort Structure (McCarthy *et al.*, 1986) (Fig. 6.1). This Structure, with an original diameter in the order of 190-300 km (Therriault *et al.*, 1995), encompasses the known limits of the Witwatersrand basin.

In contrast to the study of McCarthy *et al.* (1986), fewer folds and brittle structures appear to be developed in the present study area, whereas cleavage and bedding sub-parallel shear zones are more abundantly developed. This can probably be explained by rheological differences between the different rock-types in the respective study areas, as McCarthy *et al.* (1986) studied only the Black Reef Quartzite Formation, whereas the present study also included the Chuniespoort and Pretoria Groups. The similarity of timing, vergence and style of deformation of the structures arising from the D_2 event in the study area with those of McCarthy *et al.* (1986) suggest that D_2 originated in response to the formation of the Vredefort Structure. The Vredefort Structure is generally accepted as the product of an impact event (Therriault *et al.*, 1995) which occurred approximately 2025 Ma ago (W.U. Reimold, pers. comm.). This study suggests that deformation arising from this event was more extensively developed than was previously believed.

Northerly-verging deformation documented during this study may be related to other structures in the region. Specifically, bedding sub-parallel shear zones in the study area may be associated with the "Black Reef Decollement Zone" (BRDZ), which occurs near the base of the Transvaal Supergroup along the northern rim of the Witwatersrand basin (Fletcher and Reimold, 1989). The decollement zone may attain a maximum thickness of 130 m and displacement along it may be up to 5 km (Fletcher and Reimold, 1989). It is associated wi

two generations of pseudotachylite, tectonic breccias and folding. The BRDZ dips gently to the south or to the southeast, and verges northwards. Fletcher and Reimold (1989) suggested that the formation of the BRDZ was synchronous with folding in the Transvaal Supergroup, and the later generation of breccia was associated with uplift of the Vredefort Dome. The similarity of timing and vergence of the BRDZ and the D_2 structures in the study area suggests that they are related. Northerly-verging (020°) thrusts have also been observed in all the granitoids exposed in the Johannesburg Dome (Hilliard, 1994). Hilliard (1994) related widespread northerly-verging thrusts in the basement rocks of the Johannesburg Dome (including the Jukskei River shear zone along the northern rim of the Dome) and in the adjacent Witwatersrand Supergroup sediments to the same deformation event that resulted in similar structures on the southern, western and northern margins of the Johannesburg Dome described by Roering (1984) and McCarthy *et al.* (1986). Hilliard (1994) postulated that reactivation (of uncertain age and origin) of northerly-verging thrusts in the basement granitoids and along the rim of the Johannesburg Dome occurred in post-Black Reef Quartzite Formation times. This Early Proterozoic contraction event may have been responsible for the deformation of the Black Reef Quartzite Formation (Hilliard, 1994). Therefore, the northerly-verging deformation event may have had a prolonged history spanning pre- and post-Black Reef Quartzite Formation times, or was the result of multiple deformation events. The Jukskei River shear zone, however, currently strikes E-W and dips moderately in a southerly direction (Roering, 1986). Rotating the shear zone to account for the regional uplift-related northerly tilt of strata reveals the originally sub-vertical nature of the fabric, which is in contrast to the sub-horizontal nature of D_2 shear zones in the region. Also, the gently-folded Black Reef Quartzite Formation truncates the Jukskei River shear zone, and thus post-dates the deformation (Roering, 1986). Therefore, it is unlikely that this

deformation was associated with D_2 in the study area as the timing and the style of the deformation are dissimilar.

6.3.3 D_3 event

The D_2 north-verging bedding sub-parallel shear zones, as well as pre-Bushveld Complex sills in the study area, have been deformed by large-scale round-hinged D_3 folds in the Chuniespoort Group, thus unequivocally constraining the relative timing of this deformation. Large-scale D_3 folds in the Chuniespoort Group dolomites are not very intense, and the axial planes dip steeply to the south. Correcting for regional northward dip of the strata in the area (Section 3.6) shows that the axial planes may originally have dipped steeply north, i.e. the folds may originally have been slightly overturned to the south. The apparent contradiction of highly localised ductile shear zones forming synchronously with relatively low-intensity open, upright D_3 folds in the Chuniespoort Group carbonate lithologies can probably be explained in terms of the relatively homogeneous nature of the dolomite units. When homogeneous rocks are deformed, the induced anisotropy of the rock will increase (Section 3.4.2), and instability may be expressed as shear zones (Price and Cosgrove, 1990). The north-northeast - south-southwest orientated compression responsible for D_3 affected strata several kilometres thick. These massive strata are not conducive to tight folding and, therefore, failure along fold hinges, which resulted in the development of sub-vertical shear zones, accommodated some of the strain, rather than the folds becoming more intense. The shear zones associated with D_3 folds, at the time of their formation, may have dipped steeply to the north (Section 3.6) and involved down-to-the-south offset. They are interpreted as southerly-verging, high-angle thrusts.

Large-scale kink-folds in the Pretoria Group slates rotate S_2 cleavage, and have thus also been attributed to the D_3 event. The apparent difference in fold style developed in the Pretoria Group and the Chuniespoort Group may be explained in terms of competency differences between the finely laminated slates of the Pretoria Group, and the massively layered Chuniespoort Group dolomites (Section 3.4.2). Rotation of the axial planes of the kink-folds to account for regional tilting shows that they may originally have had a steep northerly dip (Section 3.6), which suggests that they may have been the result of the same southerly-verging deformation responsible for the round-hinged folds in the Chuniespoort Group. The possibility does, however, exist that kink-folding was a later, more brittle event which post-dated the development of round-hinged folds. In this case, kink folds may not have developed in the dolomite because of lithological competency and low anisotropy, as discussed in Section 3.4.2. The lack of conclusive field relationships does, however, make this interpretation highly speculative.

Origin of the D_3 deformation

Extrapolating a model proposed by Harley and Charlesworth (1991) for eastward-verging structures adjacent to the eastern lobe of the Bushveld Complex may provide insight into the origin of D_3 south-verging structures in the study area.

During the Bushveld event, the Transvaal Supergroup was subjected, in places, to rapid loading of 4 km of Rooiberg felsites, 2,5 km of basic sills (Sharpe and Snyman, 1980) and approximately 9 km of Bushveld intrusive rocks (S.A.C.S., 1980), and subsequently folded into a broad synform (Harley and Charlesworth, 1991). According to the model of Harley and Charlesworth (1991), "space problems" created by this folding, and by displacement of

sediments by Bushveld mafic intrusions, resulted in a directional stress field with σ_1 subhorizontal, and σ_2 tangential to the Bushveld Complex rim. Subsidence of the sedimentary floor rocks, in response to gravitational loading, and resulting flexure may have resulted in two main strain domains within the Transvaal Supergroup strata. Subvertical pure shear (co-axial) strain would be established beneath the Bushveld Complex. Assuming no significant loss of mass, the vertical compression should be compensated for by horizontal extension radial to the Bushveld Complex margins, in the form of sub-horizontal compressive stress surrounding the Bushveld Complex. In addition to this, the centre of the basin beneath the Bushveld Complex would be depressed relative to the basin margins, and accompanying folding of the Transvaal Supergroup strata might have induced rotational strain peripheral to the Bushveld Complex, aligned parallel to bedding. Adjacent to the eastern lobe of the Bushveld Complex, this deformation takes the form of bedding-parallel thrusts, which verge away from the Bushveld Complex, originating from flexural slip between sedimentary layers (Harley and Charlesworth, 1991). Thus the maximum compressive stress was oriented subhorizontally, radial to the Bushveld Complex margins (Harley, 1993). Extrapolating the model proposed by Harley and Charlesworth (1991) to the remainder of the Bushveld Complex would imply that in the study area, adjacent to the southern margin of the Bushveld Complex, gravitational loading subsequent to emplacement of the intrusive mass would have induced approximately southward directed shear stress. This could account for D_3 round-hinged folds and associated steep thrusts in the dolomite strata, and the kink-folds in the slate layers, which have been interpreted as southerly-verging structures.

Structures arising from southerly-verging deformation in close proximity to the study area have been reported by several earlier workers. North-to-south directed compression near

Pretoria, east of the study area, gave rise to south-verging folds, which may involve the entire thickness of the Timeball Hill Formation (Temperley, 1977), as well as reverse faulting, overthrusting and subsidiary folding (Purnell, 1994). Contemporaneous south-verging thrusts strike parallel to the folds (Temperley, 1977). The origin and timing of these stresses are not considered by these authors. However, the similarity of these structures to the D_3 structures in the study area suggests that they may be related.

Geophysical profiles from west of the study area revealed folding of the Transvaal Supergroup and the Bushveld Complex, and pre-Bushveld faults (Du Plessis and Levitt, 1987). A vibroseismic profile NNW of Pretoria (Fig. 6.2), in close proximity to the study area, indicates significant tectonic duplication of the Transvaal Supergroup by southward-verging thrusts in post-Bushveld Complex times (Andreoli, 1990). The origin of this deformation is, however, not considered by these workers. The post-Bushveld Complex timing of the deformation, and the vergence of the structures outward from the Bushveld Complex, suggests that they may be related to the D_3 event in the study area. It is possible that the shear zones associated with the D_3 round-hinged folds in the Chuniespoort Group are extensions of south-verging thrust faults identified in geophysical profiles (Du Plessis and Levitt, 1987; Andreoli, 1990), and are simply steeper expressions of, or rather splays from, these thrusts (Fig. 6.2). Similarly, these D_3 shear zones may be correlatives of steep thrusts with downthrow to the south in the Pretoria area (Jansen, 1977; Temperley, 1977).

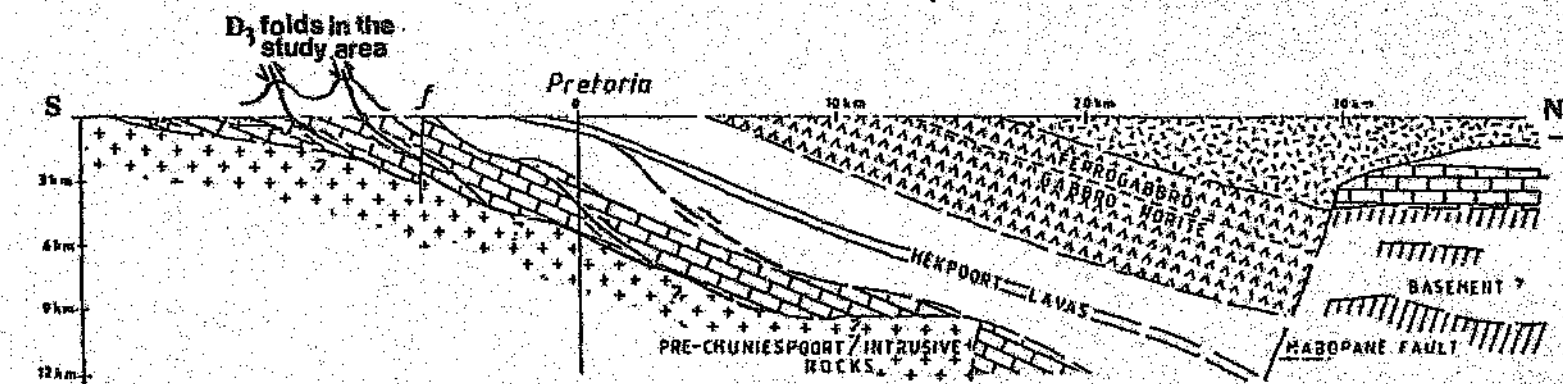

Fig. 6.2 Possible extensions of D_3 fold-related shears as splays of thrusts identified from geophysical profiles (modified after Du Plessis and Levitt, 1987; and Andreoli, 1990).

The effects of Bushveld Complex emplacement may have taken a long time to abate, especially considering subsidence following cooling and subsequent isostatic adjustment. It is possible that catastrophic emplacement of the Vredefort Structure, with an estimated diameter which originally would have penetrated well into the Bushveld Complex (Therriault *et al.*, 1995) and which involved major disturbance of the crust, may have initiated instability caused by the mass of the Bushveld Complex. The effects of the Bushveld Complex on its floor rocks may, therefore, have been present before (D_1) and after (D_3) the emplacement of the Vredefort Structure.

6.3.4 Uplift of the Johannesburg Dome

Along the northern rim of the Johannesburg Dome, the orientation of south-dipping cleavage in the Black Reef Quartzite Formation (S_2 in the current study area) is dispersed around the Johannesburg Dome, indicating that the formation of the Dome followed the cleavage-forming event (McCarthy *et al.*, 1986). As this cleavage probably owes its origin to the Vredefort event (Section 6.3.2), uplift of the Johannesburg Dome must have occurred after the emplacement of the Vredefort Dome (McCarthy *et al.*, 1986). Thus, northerly tilting of the rocks in the study area can be constrained to post-Vredefort times. Hilliard (1994) noted that northerly-verging, pre-Black Reef Quartzite Formation shear zones were rotated to their present attitude by uplift of the Johannesburg Dome. He postulated that doming of the Transvaal Supergroup rocks over the Johannesburg Dome may have been a result of crustal arching due to rising magmas i.e. thermal ("plume ?") activity, which may, in some way, be associated with the development, and possibly the emplacement, of the Bushveld Complex.

The combined effect of loading of the Transvaal Supergroup by intrusion of the Bushveld Complex, and the uplift of the Johannesburg Dome adjacent to the study area, may have resulted in the current northward dip of the strata in this region. This, however, creates very tight constraints on the timing of doming as the S_2 event post-dated the actual Bushveld Complex emplacement by 30 - 40 Ma. It may thus be that the catastrophic Vredefort event triggered the uplift of the Johannesburg Dome during large-scale tectonic readjustments on the Kaapvaal Craton. This raises the question of the nature of the relationship between the uplift of the Dome and the D_3 folds. Additional studies around the entire Johannesburg Dome would, therefore, have to be undertaken to establish the exact relationship of the doming to folding.

Regional tilting of the Kaapvaal Craton in a northerly and northwesterly direction occurred at some stage after the emplacement of the Vredefort Structure (McCarthy *et al.*, 1990). The northerly dip of strata in the region may, thus, consist of two components. Northerly tilting of the Transvaal Supergroup in the study area thus occurred after the emplacement of the Bushveld Complex.

6.3.5 D_4 event

Northerly and east-northeasterly trending, subvertical, brittle faults truncate and offset D_2 and D_3 structures, as well as a syenite dyke of Pilanesberg origin, constraining the minimum age of this deformation. The faults of the D_4 event have apparent sinistral and dextral offsets. Enigmatic, approximately ENE photolineaments may also be related to this deformation event.

Earlier workers in, and around, the Johannesburg Dome have documented faults which trend similarly to the D_4 faults in the study area (e.g. Anhaeusser, 1973; Jansen, 1977; Temperley, 1977). Faults in the Pretoria area are tangential to the Johannesburg Dome, although, on its eastern flank, some are radial to it, trending approximately east-west (Jansen, 1977). Post-Transvaal faults in the Pretoria area commonly parallel post-Transvaal dykes, while other faults trend parallel to pre-Transvaal dykes and displace the Black Reef Quartzite Formation, and thus post-Transvaal faults may be reactivated pre-Transvaal faults (Jansen, 1977). West-northwest trending faults post-date those faults oriented NNE (Jansen, 1977). Lineaments which trend 070° in the study area are interpreted as poorly exposed westward extensions of the faults observed in the vicinity of Pretoria (Jansen, 1977) and depicted on the 1: 1 000 000 geological map of southern Africa. According to Jansen (1977), the NNE and WNW trending faults in the Pretoria area are possibly related in some way to uplift of the Johannesburg Dome, which occurred in post-Vredefort, and thus post-Bushveld Complex, times (McCarthy *et al.*, 1986).

Temperley (1977) described NNW trending faults with large displacements north of the study area. These faults can be traced through the study area (Enclosure, Maps 1 and 2). The faults are traceable through lithologies of the Bushveld Complex as well as those of the Transvaal Supergroup, and define a graben near Brits, which is probably a reactivated pre-existing structure (Temperley, 1977). These post-Bushveld faults may also be related to uplift of the Johannesburg Dome.

Conjugate sets of strike-slip shear zones, which trend similarly to the D_4 faults in the study area, are heterogeneously developed in all granitoids exposed in the Johannesburg Dome.

They indicate a maximum principal compressive stress oriented approximately 010°-190° (Hilliard, 1994). Sinistral, NNE trending, strike-slip faults displace the Black Reef Quartzite Formation and the Chuniespoort Group north of the Johannesburg Dome (Anhaeusser, 1973; Hilliard, 1994), and may be brittle reactivations of the strike-slip shear zones in post-Black Reef Quartzite Formation times (Hilliard, 1994). Thus the D_4 faults seen in the study area are probably related to regional scale deformation which affected the basement rocks in the Johannesburg Dome, the Transvaal Supergroup and the Bushveld Complex.

Jansen (1977) claimed that Pilanesberg dykes near Pretoria are not offset by this faulting episode (D_4 in the study area), and that faulting occurred syn- or post-Bushveld emplacement, but before the onset of the post-Waterberg intrusive phase. Temperley (1977), however, recorded faulted Waterberg strata, which indicates that fault activity did continue to post-Waterberg times. Offset of a Pilanesberg Complex-related dyke in the study area by northerly oriented D_4 faulting may, therefore, suggest a post-Pilanesberg age for this deformation. Thus it is likely that the stresses responsible for D_4 structures may have had a prolonged history of repeated reactivation from pre-Transvaal to post-Pilanesberg times.

6.3.6 Other ductile deformation

Eastward-verging folds, small-scale westward-verging thrust duplexes and heterogeneous cleavage deform D_2 bedding sub-parallel thrusts, and thus post-date D_2. Their absolute timing, however, could not be determined as they are isolated and are seldom associated with other structures. This style of deformation is encountered in the main study area as well as in the vicinity of Magaliesburg. The deformation may thus be of regional extent, although additional regional mapping needs to be undertaken to confirm this.

a) East-verging structures

Easterly-verging deformation in the study area occurs in the form of isolated, small-scale folds which rotate the pre-existing cleavage in D_2 bedding sub-parallel shear zones. The east-verging structures thus post-date D_2 and, hence the Vredefort event.

Easterly-verging structures are known from the western extent of the Transvaal Supergroup which was deformed during the early stages of the 2100-1900 Ma Kheis orogeny (Stowe, 1986; Duane and Kruger, 1991). The easterly-verging structures include recumbent folds and west-to-east directed thrust faults which are traceable eastwards (Stowe, 1986). The Kheis orogeny is a thin-skinned fold and thrust belt (Roering *et al.*, 1990) which resulted in crustal shortening of 35-55 km (Beukes and Smit, 1987). The intensity of deformation of the Transvaal Supergroup rocks due to the Kheis orogeny decreases towards the east (Duane and Kruger, 1991). Although the Kheis belt is more than 500 km west of the study area its effects may still have been felt in the region, especially since tectonic events related to active plate margins may severely affect continental areas more than 1000 km away from those margins (e.g. Tapponier *et al.*, 1982). Consequently, the Kheis orogeny may have been the cause of easterly-verging deformation in the study area.

b) West-verging structures

Easterly dipping cleavage and duplex structures superimposed on D_2 bedding sub-parallel thrusts, and, to a lesser extent, porphyroclasts and porphyroblasts, indicate a westerly-verging period of deformation.

Westerly-verging structures have been recorded east of the Johannesburg Dome (Jansen,

1977; Temperley, 1977; Roering *et al.*, 1990). In this area, Transvaal and/or post-Transvaal faulting and folding, partly due to compression east of the Witwatersrand basin, reactivated pre-existing structures within the Witwatersrand basin (Jansen, 1977). This deformation may have had an effect on the Transvaal Supergroup rocks in the study area. Southeast of Pretoria, adjacent to the Johannesburg Dome, Transvaal Supergroup strata were thrust from east to west along a shallow easterly dipping fault plane (Temperley, 1977; Roering *et al.*, 1990) onto the Johannesburg Dome, and Chuniespoort Group dolomite was thrust onto Timeball Hill Formation quartzites along a northerly trending thrust fault which is terminated northeast of the Johannesburg Dome by NE trending lateral ramps (Roering *et al.* 1990). This westerly-verging thrusting, along with N to NW trending folds, has been attributed by Roering *et al.* (1990) to compression related to the emplacement of the eastern lobe of the Bushveld Complex. However, westerly-verging deformation in the study area unequivocally post-dated the Vredefort-related D_2 event, and emplacement of the Vredefort Dome post-dated the emplacement of the Bushveld Complex by approximately 30-40 Ma (Walraven *et al,* 1990; Walraven and Hattingh, 1993; Kamo *et al,* 1995). Therefore, it is unlikely that the westerly-verging deformation in the study area is related to the actual emplacement of the eastern lobe of the Bushveld Complex, as was suggested by Roering *et al.* (1990), and may rather have been the result of post-Vredefort subsidence of the intrusive mass. Temperley (1977) and Purnell (1994), however, claim that the basic phase of the Bushveld Complex is not developed in this area, and consequently could not have generated any deformation. Rather, they suggest that the ENE to WSW thrusting, which is directed from the centre of the Middleburg basin (of Waterberg age) towards the Johannesburg Dome, may be related to subsidence of the Cullinan-Middelburg basin during Waterberg times. This interpretation is, however, erroneous, as geophysical profiles (Tweedie, 1986) suggest that the Bushveld

Complex was intruded into the Evander basin, east of the Johannesburg Dome.

6.3.7 Jointing and neotectonic activity

Other brittle structures in the study area occur in the form of joints in slate, and planar structures in unconsolidated sediments and tufa. Although there is no coincidence of D_4 strike-slip fault and joint set orientations, it is possible that the strike-slip faults were responsible for the development of some joint sets as secondary fractures. East-west striking normal faults, with downthrow to the north, may be responsible for the development of offsets which caused waterfalls in tufa and unconsolidated soils. The orientation of the E-W trending normal faults coincides with the orientation of cracks in Recent sediments, tufa, a fault-controlled stream, and a joint set in the slate. These structures may, therefore, be synchronous, and the result of the same stresses. Normal faulting may thus have controlled the development of some joint sets. A time constraint for this deformation may be provided by the age of tufa deposition, which has been dated at between 43 ka and the present (Marker, 1973; 1974) elsewhere in the Transvaal Supergroup.

East-west striking normal faults affect Recent sediments and tufas, whereas the north-south strike-slip faults do not. Normal faulting thus post-dates the strike-slip faulting. The origin of the east-west striking normal faults is uncertain, although their very young age may suggest that they are related to tectonism associated with the East African Rift. This interpretation is, however, speculative.

CHAPTER 7

CONCLUSIONS

The main conclusions of the present study are as follows:

i) The Transvaal Supergroup between the Johannesburg Dome and the Bushveld Complex has been severely affected by multiple deformation events.

ii) Southerly-verging deformation (D_1) resulted in a locally-developed, penetrative, S_1 cleavage.

iii) Pervasive northerly-verging deformation (D_2), in the form of bedding sub-parallel thrusts, cleavage and folds, is developed throughout most of the Transvaal Supergroup in the study area. The most likely origin of this deformation was the emplacement of the Vredefort Dome at approximately 2025 Ma.

iv) Southerly-verging folds and associated thrusts (D_3) deform the D_2 structures. Although the origin of this deformation cannot be specifically identified, late-stage isostatic adjustment, possibly triggered by the emplacement of the Vredefort Dome following emplacement of the Bushveld Complex, may have been responsible.

v) Northerly trending strike-slip faults (D_4) offset earlier structures. Easterly trending photolineaments may be related to this deformation episode.

vi) Easterly- and westerly-verging deformation gave rise to isolated structures which post-date D_2, although the absolute timing of these deformation events is uncertain.

vii) The rocks of the study area have been metamorphosed to the greenschist facies. Thermal modelling suggests that the Bushveld Complex is the most likely cause of the metamorphism, and hence porphyroblast growth, in the region.

viii) Porphyroblast microstructural relationships confirm the post-Bushveld Complex timing of the D_2 event (and thus the emplacement of the Vredefort Dome), and the pre- to syn-Bushveld Complex timing of the S_1 cleavage.

ix) Brittle deformation, in the form of planar structures in unconsolidated sediments and tufa, as well as joints, occurred in the Holocene.

REFERENCES

Allen, P.A., Homewood, P., and Willaims, G.D. (1986). Foreland basins: an introduction. In: Allen, P.A., Homewood, P. (eds.), *Foreland Basins.* Int. Assoc. Sediment. Spec. Publ. 8: 3-12.

Andreoli, M.A.G. (1988). The discovery of a strange and hidden African orogeny: the Transvaalide fold belt. *4th annual conference, Tecs. div. Geol. Soc. S. Afr.*

Andreoli, M.A.G. (1990). Evidence for thrust tectonics in the Transvaal Sequence based on geophysical profiles. *Extended Abstracts, Geocongress '90, Geol. Soc. S. Afr.*: 3-6.

Anhaeusser, C.R., (1973). The geology and geochemistry of the Archaean granites and gneisses of the Johannesburg-Pretoria Dome: In Lister, L.A. ed: *Symposium on granites, gneisses and related rocks.* Spec. Publ. 3, Geol. Soc. S. Afr.: 361-385.

Anhaeusser, C.R., and Burger, A.J. (1982). An interpretation of U-Pb zircon ages for Archaean tonalite gneisses from the Johannesburg-Pretoria granite dome. *Trans. Geol. Soc. S. Afr.*, 85: 111-116.

Armstrong, R.A. (1987). *Geochronological studies on Archaean and Proterozoic formations of the foreland of the Namaqualand Front and possible correlations on the Kaapvaal Craton.* Unpub Ph.D. thesis. Univ. Witwatersrand. 274 pp.

Armstrong, R.A., Compston, W., Retief, E.A., Williams, I.S., and Welke, H.J. (1991). Zircon ion microprobe studies bearing on the age and evolution of the Witwatersrand triad. *Precambrian Res.* 53: 243-266.

Barton, J.M. Jnr, and van Reenen, D.D. (1992a). When was the Limpopo Orogeny? *Precambrian Res.* 55: 7-16.

Barton, J.M. Jnr and van Reenen, D.D. (1992b). The significance of Rb-Sr ages of biotite and phlogopite for the thermal history of the Central and Southern Marginal Zones of the Limpopo Belt of southern Africa and the adjacent portions of the Kaapvaal Craton. *Precambrian Res.* 55: 17-31.

Barton. J.M. Jnr, Ryan, B., Fripp, R.E.P., and Horrocks, P. (1979). Effects of metamorphism on the Rb-Sr and Pb-Pb systematics of the Singelele and Bulai Gneisses, Limpopo Mobile Belt, southern Africa. *Trans. Geol. Soc. S. Afr.* 82: 259-269.

Bates, R.L., and Jackson, J.A. (1987). *Glossary of Geology.* 3rd edition. Amer. Geol. Inst. 788pp.

Bell, T.H. (1981). Foliation development: the contribution, geometry and significance of progressive bulk inhomogeneous shortening. *Tectonophys.* 75: 273-296.

Bell, T.H. (1985). Deformation partitioning and porphyroblast rotation in metamorphic rocks: a radical reinterpretation. *J. Meta. Geol.* 3: 109-118.

Bell, T.H. and Cuff, C. (1989). Dissolution, solution transfer, diffusion versus fluid flow and volume loss during deformation/metamorphism. *J. Meta. Geol.* 7: 425-447.

Bell, T.H., Rubenach, M.J., and Fleming, P.D. (1986). Porphyroblast nucleation, growth and dissolution in regional metamorphic rocks as a function of deformation partitioning during foliation development. *J. Meta. Geol.* 4: 37-67.

Beukes, N.J. and Smit, C.A. (1987). New evidence for thrusting of Transvaal strata in Griqualand West: nature of the thrusts and geological implications with specific reference to the age of red beds and palaeooxidation profiles in the area. *S. Afr. J. Geol.* 90: 304-378.

Bisschoff, A.A. (1982). Thermal metamorphism in the Vredefort Dome. *Trans. Geol. Soc. S. Afr.* 85: 43-57.

Bowen, T.B., Marsh, J.S., Bowen, M.P.,and Eales, H.V. (1986). Volcanic rocks of the Witwatersrand triad, South Africa. 1; Description, classification and geochemical stratigraphy. *Precambrian Res.* 31: 297-324.

Brock, B.B. and Pretorius, D.A. (1964). Rand basin sedimentation and tectonics. In: S.H. Haughton (ed.). The geology of some ore deposits in Southern Africa. *Geol. Soc. S. Afr.* 1: 549-599.

Burger, A.J. and Coertze, F.J. (1973). Radiometric age determinations on rocks from southern Africa up to the end of 1971. *Bull. Geol. Surv. S. Afr.* 58: 46pp.

Burger, A.J., and Coertze, F.J. (1975). Age determinations: April 1972 - March 1974. *Ann. Geol. Surv. S. Afr.* 10: 135-141.

Button, A. (1976). Stratigraphy and relationships of the Bushveld floor in the eastern Transvaal. *Trans. Geol. Soc. S. Afr.* 79: 3-12.

Cadle, A.B., Cairncross, B., Christie, A.D.M., and Roberts, D.L. (1990). The Permo-Triassic coal-bearing deposits of the Karoo basin, southern Africa. *E.G.R.U. inf. circ. 218.* Univ. Witwatersrand. 38pp.

Cawthorn, R.G., Davies, G., Clubley-Armstrong, A., and McCarthy, T.S. (1981). Sills associated with the Bushveld Complex, South Africa: an estimate of the parental magma composition. *Lithos* 14: 1-16.

Cheney, E.S., Barton Jnr, J.M., and Brandl, G. (1990). Extent and age of the Soutpansberg of southern Africa. *S. Afr. J. Geol.* 93: 664-675.

Clendenin, C.W. (1989). *Tectonic influence on the evolution of the Early Proterozoic Transvaal Sea, southern Africa.* Unpubl. PhD. thesis. Univ. Witwatersrand. 367pp.

Clendenin, C.W. and Maske, S. (1986). Identification of syndepositional tectonics within the Transvaal sedimentary basin. *Extended Abstracts, Geocongress '86, Geol. Soc. S. Afr.*: 501-504.

Clendenin, C.W., Charlesworth, E.G., and Maske, S. (1988a). An early Proterozoic three-stage rift system, Kaapvaal Craton, South Africa. *Tectonophys.* 145: 73-86.

Clendenin, C.W., Charlesworth, E.G., and Maske, S. (1988b). Tectonic style and mechanism of early Proterozoic successor basin development, southern Africa. *Tectonophys.* 156: 275-291.

Clifford, T.N., Barton, E.S., Retief, E.A. and Rex, D.C. (1990). The Koperberg Suite, Okiep Copper District, Namaqualand, South Africa: new isotopic data. In: *Recent data in African Earth Sciences. International centre for training and exchanges in the geosciences.* G. Rocci and M. Deschamps (eds.), 22, Orleans, 415pp.

Cobbold, P.R., Cosgrove, J.W.,and Summers, J.M. (1971). Development of internal structures in deformed anisotropic rocks. *Tectonophys.* 12: 223-253.

Coertze, F.J. (1971). *The geology of the basic portion of the western Bushveld Igneous Complex.* D.Sc. thesis. Potchefstroom Univ. C.H.E., 114pp.

Coetzee, H. and Kruger, F.J. (1989). The geochronology and Sr- and Pb-isotope geochemistry of the Losberg Complex, and the southern limit of Bushveld Complex magmatism. *S. Afr. J. Geol.* 92: 37-41.

Colliston, W.P. and Reimold, W.U. (1992). Structural review of the Vredefort Dome. *Sudbury '92 conference, Lunar and Planetary Institute, Houston,* contribution no. 790: 16-17.

Cornell, D.H., Humphreys, H., Theart, H.F.J., and Scheepers, D.J. (1992). A collision related pressure-temperature-time path for the Prieska Copper Mine, Namaqua-Natal Metamorhic Province, South Africa. *Precambrian Res.* 59: 43-71.

Coward, M. P. (1976). Archaean deformation patterns in southern Africa. *Phil. Trans. R. Soc. London, A.* 313-331.

Cox, K.G., Johnnson, R.L., Monkman, L.J., Stillman, C.J., Vail, J.R., and Wood, D.N. (1965). The geology of the Nuanetsi igneous province. *Phil. Trans. R. Soc. Soc. London.* A257: 71-218.

Daly, M.C. (1988). Crustal shear zones in Central Africa: a kinematic approach to Proterozoic tectonics. *Episodes* 11: 5-11.

Davis, G.H. (1984). *Structural geology of rocks and regions.* J. Wiley, New York. 492pp

De Waal, S.A. (1970). Interference folding of Bushveld Igneous Complex age in the Transvaal System north of Marble Hall. 283-289. In: Visser, D.J.L. and Von Gruenewaldt, G. (eds.). *Symposium on the Bushveld Complex and other layered intrusions.* Spec. Publ. 1. Geol. Soc. S. Afr.

Dietz, R.S. (1961). Vredefort Ring structure: Meteorite impact scar?. *J. Geol.* 69: 499-516.

Duane, M. J. and Kruger, F.J. (1991). Geochronological evidence for tectonically driven brine migration during the early Proterozoic Kheis orogeny of southern Africa. *Geophys. res. letters* 18, no. 5: 975-978.

Du Plessis, A. and Levitt, J.G. (1987). On the structure of the Rustenberg Layered Suite - insight from seismic reflection data. *Indaba on the tectonic setting of layered intrusions.* Univ. Pretoria.

Du Plessis, C.P. (1987). New perspectives on early Waterberg Group sedimentation from the Gatkop area, northwestern Transvaal. *S. Afr. J. Geol.* 90: 394-408.

Du Plessis, C. P. (1991). *Tectonics along the Thabazimbi-Murchison Lineament.* Unpubl. PhD. thesis. Univ. Witwatersrand. 307pp.

Du Toit, A. L. (1954). *The Geology of South Africa.* Oliver and Boyd, Edinburgh. 611pp.

Eales, H.V., Marsh, J.S., and Cox, K.G. (1984). *The Karoo igneous province: and introduction.* Spec. Publ. 13. Geol. Soc. S. Afr.: 1-26.

Eglington, B.M., Harmer, R.E., and Kerr, A. (1989). Isotope and geochemical constraints on Proterozoic crustal evolution in southeastern Africa. *Precambrian Res.* 45: 159-174.

Elston, W.E. (1995). Bushveld Complex and Vredefort Dome: the case for multiple impact origin. *Extended Abstracts, Geocongress '95, Geol. Soc. S. Africa*: 504-507.

Engelbrecht, J.P. (1976). Meta-sediments of the Pretoria Group in the Enzelburg area, Marico District. *Trans. Geol. Soc. S. Afr.* 79: 61-75.

Engelbrecht, J.P. (1988). The metamorphic aureole of the Bushveld Complex in the Marico District, Western Transvaal, South Africa. *Inst. Geol. Res. Bushveld Complex Res.* Rep. 77.

Engelbrecht, J. P. (1990a). The Marico hypabyssal suite and the marginal zone of the Bushveld Complex in the Marico district, western Transvaal, South Africa. *S. Afr. J. Geol.* 93 (4): 318-328.

Engelbrecht, J.P. (1990b). Contact metamorphic processes related to the aureole of the Bushveld Complex in the Marico District, Western Transvaal, South Africa. *S. Afr. J. Geol.* 93: 339-349.

Eriksson, K.A. (1977). Tidal flat and sub-tidal sedimentation in the 2250 My Malmani Dolomite, Transvaal. *Sed. Geol.*, 18: 223-244.

Eriksson K.A., and Truswell J.F. (1974). Stratotypes from the Malmani Subgroup northwest of Johannesburg, South Africa. *Trans. Geol. Soc. S. Afr.*, 77: 211-222.

Eriksson, P.G. (1986). Sedimentological aspects of the Pretoria Group in the Pretoria-Rustenburg area. *Extended Abstracts, Geocongress '86, Geol. Soc. S. Afr.*

Eriksson, P.G. (1988). A palaeoenvironmental review of the Pretoria Group, Transvaal Sequence. *Extended Abstracts, Geocongress '88, Geol. Soc. S. Afr.* 187-190.

Eriksson, P.G., and Clendenin, C.W. (1990). A review of the Transvaal Sequence, South Africa. *J. Afr. Ea. Sc.* 10: 101-116.

Eriksson, P.G., and Reczko, B.F.F. (1995). Tectonic setting of the Pretoria Group, Transvaal Supergroup. *Extended Abstracts, Geocongress '95, Geol. Soc. S. Afr.*: 508-511.

Ferguson, C.C., Harvey, P.K. and Lloyd, G.E. (1980). On the mechanical interaction between a growing porphyroblast and its surrounding matrix. *Contrib. Min. Petr.* 75: 339-352.

Ferguson, J. (1973). The Pilanesberg alkaline province, southern Africa. *Trans. Geol. Soc. S. Afr.* 76: 249-270.

Fletcher, P and Reimold, W.U. (1989). Some notes and speculations on the pseudotachylites in the Witwatersrand basin and Vredefort Dome, South Africa. *S. Afr. J. Geol.* 92 (3): 223-234.

Frick, C. (1973). The sill Phase and the "chill-zone" of the Bushveld Igneous Complex. *Trans. Geol. Soc. S. Afr.* 76: 7-14.

Frimmel, H.E. (1994a). Metamorphism of Witwatersrand gold. Univ. Cape Town Dept. *Geol. Sci. Inf. Circ.* 13

Frimmel, H.E. (1994b). Metamorphism of Witwatersrand gold. *Expl. Min. Geol.*3: 357-370.

Gibson, R.L. (1993). When is a hornfels not a hornfels? Metapelitic rocks from the lower Witwatersrand Supergroup, Vredefort Dome , South Africa. *S. Afr. J. Geol.* 96: 42-48.

Gibson, R.L. and Wallmach, T. (1995). Metamorphism in the Witwatersrand Basin: A perspective from the Vredefort Dome. *E.G.R.U. Inf. circ. 288.* Univ. Witwatersrand. 30pp.

Grantham, G.H., Moyes, A.B., and Hunter, D.R. (1991). The age, petrogenesis, and emplacement of the Dalmation Granite, H.U. Svedrupfjella, Dronning Maud Land, East Antarctica. *Antarctic Science,* 2: 197-204.

Gray, D.R. (1977). Morphological classification of crenulation cleavage. *J. Geol.* 85: 229-235.

Hall, A.L. (1908). On contact metamorphism in the Pretoria Series of the Lydenberg and Zoutpansberg districts. *Trans. Geol. Soc. S. Afr.* 11: 1-24.

Hall, A.L. (1909). On contact metamorphism in the western Transvaal. *Trans. Geol. Soc. S. Afr.* 12: 119-138.

Hammerbeck, E.C.I. (1986). Andalusite in the metamorphic aureole of the Bushveld Complex, 993-1004. In: Anhaeusser, C.R. and Maske, S., (Eds.). *Mineral Deposits of Southern Africa,* 1. Geol. Soc. S. Afr. 1020pp

Hanmer, S.K. (1979).The role of discrete heterogeneities and linear fabrics in the formation of crenulations. *J. Struct. Geol.* 1(1): 81-91.

Hanmer, S. and Passchier, C. (1991). *Shear-sense indicators: a review.* Geol. Surv. Canada. Paper 90-17.

Hansen, V.L. (1990). Collection and preparation of thin sections of oriented samples. *J. Geol. Ed.* 38: p294.

Harley, M. (1993). *The geology of the Sable-Pilgrim's Rest goldfield, with special reference to the E andshoogte mine.* Unpubl. PhD. thesis. Univ. Witwatersrand. 271pp.

Harley, M. and Charlesworth, E.G. (1991). The mineralization and structure of the Elandshoogte gold mine, Sabie-Pilgrim's Rest goldfield, South Africa. In E.A. Ladeira (ed.). *Brazil Gold '91. The economics, geology, geochemistry and genesis of gold deposits* Balkema, Rotterdam. 823pp.

Hartnady, C., Joubert, P., and Stowe, C. (1985). Proterozoic crustal evolution in southwestern Africa. *Episodes* 8(4): 236-244

Hartzer, F.J. (1995). Transvaal inliers: Geology, tectonic development and relationship with the Bushveld Complex. *Extended Abstracts, Geocongress '95, Geol. Soc. S. Afr.*: 516-519.

Haughton, S.H. (1969). *Geological history of southern Africa. Geological Society of South Africa.* Cape Town. 535pp.

Hilliard, P. (1994). *The structural evolution of the Johannesburg Dome, Kaapvaal Craton, South Africa.* Unpubl. MSc. thesis. Univ. Pretoria. 99pp.

Honea, E., and Johnson,A.M. (1976). A theory of concentric, kink and sinusoidal folding and of monoclinal flexuring of compressible, elastic multilayers. IV. Development of sinusoidal and kink folds in multilayers confined by rigid boundaries. *Tectonophys.* 30: 197-239.

Hunter, D.R. (1974). Crustal development in the Kaapvaal Craton. Part 2: The Proterozoic. *E.G.R.U. Inf. circ. 89.* Univ. Witwatersrand.

Irvine, T.N. and Sharpe, M.R. (1982). Source-rock compositions and depth of origin of Bushveld and Stillwater magmas. *Carnegie Inst. Washington Year Book* 81: 294-303.

Jackson, M.C. (1991). The Dominion Group: A review of the late Archaean volcano-sedimentary sequence and implications for the tectonic setting of the Witwatersrand Supergroup, South Africa. *E.G.R.U. inf circ. 240.* Univ. Witwatersrand. 40pp.

Jacobs, J., Thomas, R.J., and Weber, K. (1993). Accretion and indentation tectonics at the southern edge of the Kaapvaal Craton during the Kibaran (Grenville) orogeny. *Geol.* 21: 203-206.

Jaeger, J.C. (1959a). Temperatures outside a cooling intrusive sheet. *Am. J. Sci.* 257: 44-54

Jaeger, J.C. (1959b). The temperature in the neighbourhood of a cooling intrusive sheet. *Am. J. Sci.* 255: 306-318.

Jaeger, J.C. (1968). Cooling and solidification of igneous rocks. In: H.H. Hess and A. Poldervaart (Eds.). *Basalts. The Poldervaart treatise on rocks of basaltic composition*, Vol. 2. John Wiley and Sons, New York. p 503-536.

Jansen, H. (1977). *The geology of the area around Pretoria.* Geol. Surv. S. Afr. expl. sheet 2527 DA, DB, DC, DB and 2528 CA, CB, CC, CD.

Kamo, S.L., Reimold, W.U., Krogh, T.E., and Colliston, W.P. (1995). Shocked zircons in Vredefort pseudotachylite and the U-Pb zircon age of the Vredefort impact event. *Extended Abstracts, Geocongress '95, Geol. Soc. S. Afr.*: 566-569.

Kent, P.E. (1974). The continental margin of East Africa - a region of vertical movements. 313-320. In: Burke, C.C., and Drake, C. L (eds). *The geology of continent margins.* Springer Verlag, Berlin. 1009pp.

Knipe, R.J., and Wintch, R.P. (1985). Heterogeneous deformation, foliation development and metamorphic processes in a polyphase mylonite. In: Metamorphic reactions, kinetics, textures and deformation. A.B. Thompson and D.C, Rubie (eds.). *Advances in physical geochemistry 4:* 180-210. Springer-Verlag, New York.

Lapidus, D.F. (1987). *Collins dictionary of Geology.* Collins, Glasgow. 565pp.

Latham, J.P. (1985). The influence of non-linear material properties and resistance to bending on the development of internal structures. *J. Struct. Geol.*, 7 (2): 237-249.

Layer, P.W., Kroner, A., McWilliams, M. and Clauer, N. (1988). Regonal magnetic overprinting of Witwatersrand Supergroup sediments, South Africa. *J. Geophys. Res.* 93: 2191-2200.

Light, M.P.R. (1982). The Limpopo Belt: a result of continental collision. *Tectonics* 1(4): 325-342.

Linton, P.L., McCarthy, T.S., and Brown, C.A. (1993). The sequential eruption and tectonic history of the Klipriviersberg Group as illustrated by the distribution of chemical units. *E.G.R.U. Inf. circ. 271.* Univ. Witwatersrand.

Lister, G.S. and Snoke, A.W. (1984). S-C mylonites. *J. Struct. Geol.* Vol.6 No.6: 617-638.

Marker, M.E. (1973). Tufa formation in the Transvaal, South Africa. *Zeit. fur Geomorph.* 17: 461-473.

Marker, M.E. (1974). Dating Quaternary climatic oscillations using cave and tufa deposits. *S. Afr. Arch. Soc.* Goodwin Series 2: 13-19.

Martin, A.K. and Hartnady, C.J.H. (1986). Plate tectonic development of the southeastern Indian ocean: a revised reconstruction of east Antarctica and Africa. *J. Geophys. Res.* 91: 4767-4780.

Martin, D.McB., Charlesworth, E.G. and Clendenin, C.W. (1990). Episodic reactivation of the Thabazimbi-Murchison Line as determined from slump breccia and rhythmite deposition within the Chuniespoort Group, Transvaal Sequence. *S. Afr. J. Geol.*, 93: 835-844.

Martin, D. Mc B., Charlesworth. E.G., Clendenin, C.W., Maske, S., and De Gasparis, A.A. (1988). The nature and influences of the Thabazimbi-Murchison Line, west of Thabazimbi, on a number of Early Proterozoic basins. *Extended Abstracts, Geocongress '88, Geol. Soc. S. Afr.*: 383-386.

Matthews, P.E. (1972). Possible precambrian obduction and plate tectonics in southeastern Africa. *Nature*, 240: 37-39

Matthews, P.E. (1981). Eastern or Natal sector of the Namaqua-Natal mobile belt in southern Africa. *In:* Hunter, D.R. (ed). *Precambrian of the southern hemisphere*: 705-714. Elsevier, Amsterdam.

McCarthy, T.S., Charlesworth, E.G., and Stanistreet, I.G. (1986). Post-Transvaal structural features of the northern portion of the Witwatersrand Basin. *Trans. Geol. Soc. S. Afr.* 89: 311-323.

McCarthy, T.S., Stanistreet, I.G., and Robb, L.J. (1990). Geological studies related to the origin of the Witwatersrand Basin and its mineralization - an introduction and strategy for research and exploration. *S. Afr. J. Geol.* 93 (1): 1-4.

McCourt, S. (1983). *Archaean lithologies in the Koedoesrand area, northwestern Transvaal.* Spec. Publ. 8. Geol. Soc. S. Afr.: 113-119.

Misch, P. (1971). Porphyroblasts and "crystallization force": some textural criteria. *Geol. Soc. Am. Bull.* 82: 245-252

Nell, J. (1985). The Bushveld metamorphic aureole in the Potgietersrus area: evidence for a two-stage metamorphic event. *Econ. Geol.* 80: 1129-1152.

Nicolaysen, L.O. (1972). North American cryptoexplosion structures: interpreted as diapirs which obtain releasefrom strong lateral confinement. *Geol. Soc. America, Memoir.* 132: 605-620.

Nicolaysen, L.O. and Burger A.J. (1965). Note on an extensive area of 1000 million year old metamorphic and igneous rocks in southern Africa. *Sciences Terres* 10: 497-518.

Norton, I.O., and Sclater, J.G. (1979). A model for the evolution of the Indian Ocean and the breakup of Gondwanaland. *J. Geophys. Res.* 84: 6803-6830.

Oleson, N.O. (1982). Heterogeneous strain of a phyllite as revealed by porphyroblast matrix relationships. *J. Struct. Geol.* 4: 481-490.

Papenfus, J.A. (1964). The Black Reef Series within the Witwatersrand Basin with special reference to its occurrence on Government Gold Mining Areas, 191-218. In: Haughton, S.H. Ed., *The geology of some ore deposits in southern Africa 1.* Geol. Soc. S. Afr., 625 pp.

Phillips, G.N. (1987). Metamorphism of the Witwatersrand gold fields: conditions during peak metamorphism. *J. Meta. Geol.* 5: 307-322.

Phillips, G.N. (1988). Widespread fluid infiltration during metamorphism of the Witwatersrand Gold fields: Generation of chloritoid and pyrophyllite. *J. Meta. Geol.*, 6: 311-322.

Phillips, G.N., and Law, J.D.M. (1994). Metamorphism of the Witwatersrand gold fields: A review. *Ore Geol. Reviews* 9: 1-31.

Phillips, G.N. and Myers, R.E. (1989). The Witwatersrand gold fields: Part II. An origin for Witwatersrand gold during metamorphism and associated alteration. *Monogr. Econ. Geol.* 6: 598-608.

Phillips, G.N., Myers, R.E., Law, J.D.M., Bailey, A.C., Cadle, A.B., Beneke, S.D., and Guisti, L. (1989). The Witwatersrand gold fields: Part 1. Postdepositional history, synsedimentary processes and gold distribution. *Monogr. Econ. Geol.* 6: 585-597.

Price, N.J. and Cosgrove, J.W. (1990). *Analysis of geological structures.* Cambridge University Press, Great Britain. 502pp.

Prior, D.J. (1987). Syntectonic porphyroblast growth in phyllites: textures and processes. *J. Meta. Geol.*, 5: 27-39.

Purnell, D.G. (1994). The engineering geology of central Pretoria. *Bull. Geol. Surv. S. Afr.* 106.

Ramsay, J.G. (1980). Shear zone geometry: a review. *J. Struct Geol.* 2: 83-99.

Ramsay, J.G. and Huber, M.I. (1983). *Techniques of modern structural geology, volume 1: strain analysis.* Academic Press Ltd. London.

Ramsay, J.G. and Huber, M.I. (1987). *Techniques of modern structural geology, volume 2: folds and fractures.* Academic Press Ltd. London.

Reimold, W.U. (1993). A review of the geology and deformation related to the Vredefort Structure, South Africa. *J.Geol. Ed.* 41: p106.

Rice, A.N.H. and Mitchell, J.I. (1991). Porphyroblast textural sector zoning and matrix displacement. *Min. Mag.* 55: 379-396.

Robb, L.J. and Meyer, F.M. (1995). The Witwatersrand basin, South Africa: geological processes and mineralization processes. *Inf. Circ. No. 293.* Univ. Witwatersrand. 37pp.

Robb, L.J., Davis, D.W., and Kamo, S.L. (1990). U-Pb ages on single detrital zircon grains from the Witwatersrand Basin, South Africa: constraints on the age of sedimentation and on the evolution of granites adjacent to the basin. *J. Geol.* 98: 311-328.

Roering, C. (1984). The Witwatersrand Group at Swartkops: a re-examination of the structural geology. *Trans. Geol. Soc. S. Afr.*, 87: 87-99.

Roering, C. (1986). Aspects of thrust faulting on the northern margin of the Witwatersrand Basin. *Extended Abstracts, Geocongress '86. Geol. Soc. S. Afr.*: 59-62.

Roering, C., Barton Jr, J.M., and Winter, H. de la R. (1990).The Vredefort Structure: A perspective with regard to new tectonic data from adjoining terranes. *Tectonophys.* 171: 7-22.

Roering, C., Van Reenen, D.D., Smit, C.A., Barton, J.M., De Beer, J.H., De Wit, M.J., Stettler, E.H., Van Schalkwyk, F.J., Stevens, G. and Pretorius, S. (1992). Tectonic model for the evolution of the Limpopo Belt. *Precam. Res.* 55: 539-552.

Rollinson, H.R. (1993). A terrane interpretation of the Archaean Limpopo Belt. *Geol. Mag.* 130 (6): 755-765.

SACS (South African Committee for Stratigraphy) (1980). *The Stratigraphy of South Africa. Part 1.* (Compiler: Kent, L.E.). Handbk. Geol. Surv. S. Afr., 8, 690 pp.

Sacchi, R., Marques, J., Costa, M. and Castoti, C. (1984). Kibaran events in the southern most Mozambique belt. *Precam. Res.* 25: 141-159.

Saggerson, E.P. (1974).Porphyroblastesis and displacement: some new textural criteria from pelitic hornfelses. *Min. Mag.* 39: 793-797.

Saggerson, E.P. and Turner, L.M. (1986). The metamorphic map of the republics of South Africa, Transkei, Boputhatswana, Venda, Ciskei, and the kingdoms of Lesotho and Swaziland. *Extended Abstracts, Geocongress '86, Geol. Soc. S. Afr.*: 855-859.

Schreyer, W. and Bisschoff, A.A. (1982). Kyanite as a metamorphic mineral in Witwatersrand sediments at Johannesburg and Krugersdorp, South Africa. *Trans. Geol. Soc. S. Afr.* 85: 211-214.

Schweitzer, J.K., and Hatton, C.J. (1995). Synchronous emplacement of the felsites, granophyres, granites and mafic intrusives of the Bushveld Complex. *Extended Abstracts, Geocongress '95, Geol. Soc. S. Afr:* 532-535.

Shackleton, R. (1986). Precambrian collision tectonics in Africa. In M.P. Coward and A.C. Ries (eds). Collision tectonics. *Spec. Publ. 19. Geol. Soc. London*: 329-349.

Sharpe, M.R. (1981). Petrology and geochemistry of pre-Bushveld and Waterberg mafic sills. *Trans. Geol. Soc. S. Afr.* 84: 75-83.

Sharpe, M.R. (1982). *Petrography, classification and chronology of intrusion of mafic sills beneath the eastern Bushveld Complex.* Inst. Geol. Res. Bushveld Complex 37.

Sharpe, M.R. (1984). *Petrography, classification and chronology of mafic sill intrusions beneath the eastern Bushveld Complex.* Geol. Surv. S. Afr. Bull. 77: 40pp.

Sharpe, M.R. and Chadwick, B. (1982). Structure in Transvaal Sequence rocks within and adjacent to the eastern Bushveld Complex. *Trans. Geol. Soc. S. Afr.* 85: 29-41.

Sharpe, M.R. and Snyman, J.A. (1980). A model for the emplacement of the eastern compartment of the Bushveld Complex. *Tectonoph* 85-110.

Sharpe, M.R., Bahat, D., and von Grunewaldt, G. (1981). The concentric elliptical structure of feeder sites to the Bushveld Complex and possible economic implications. *Trans. Geol. Soc. S. Afr.* 86: 239-244.

Simpson, C. (1977). *A structural analysis of the rim synclinorium of the Vredefort Dome.* Unpubl. MSc. thesis. Univ. Witwatersrand. 257pp.

Simpson, C. (1986). Determination of movement sense in mylonites. *J. Geol. Ed.* 34: 246-261.

Simpson, C. and Schmidt, S.M. (1983). An evaluation of criteria to deduce the sense of movement in sheared rocks. *Geol. Soc. Am. Bull. 94*: 1281-1288.

Spear, F.S. (1993). Metamorphic phase equilibria and pressure-temperature-time paths. *Min. Soc. America Monograph.* Michigan. 798pp.

Stanistreet, I.G. and Mc Carthy, T.S. (1991). Changing tectono-sedimentary scenarios relevant to the development of the Late Archaean Witwatersrand basin. *E.G.R.U. Inf. Circ. 233. Univ. Witwatersrand.*

Stanistreet, I.G., McCarthy, T.S., Charlesworth, E.G., Myers, R.E. and Armstrong, R.A. (1986). Pre-Transvaal wrench tectonics along the northern margin of the Witwatersrand basin, South Africa. *Tectonophys.* 131: 53-74.

Stear, W.M. (1977). The stratigraphy and sedimentation of the Pretoria Group at Rooiberg, Transvaal. *Trans. Geol. Soc. S. Afr.*, 80: 53-65.

Stepto, D. (1990). The geology and gravity structure in the central core of the Vredefort structure. *Tectonophys.* 171: 75-103.

Stowe, C.W. (1986). Synthesis and interpretation of structures along the northeastern boundary of the Namaqua Tectonic Province, South Africa. *Trans. Geol. Soc. S. Afr.* 89: 185-198.

Stowe, C.W. (1989). Discussion on "The Proterozoic Magondi Mobile Belt in Zimbabwe". *S. Afr. J. Geol.* 92(1): 69-71.

Stowe, C.W. (1990). The Kheis and Magondi belts - rift, drift and collisional events at an Early-Proterozoic continental margin. *Extended Abstracts, Geocongress '90, Geol. Soc. S. Afr*: 538-541.

Tankard, A.J., Jackson, M.P.A., Eriksson, K.A., Hobday,D.K., Hunter, D.R., and Minter, W.E.C. (1982). *Crustal evolution of southern Africa: 3,8 billion years of earth history*. Springer-Verlag New York, Inc. 523 pp.

Tapponier, P., Peltzer, G., Le Dain, A.Y., Armijo, R., and Cobbold, P. (1982). Propagating extrusion tectonics in Asia: new insights from simple experiments with plasticine. *Geol.* 10: 611-616.

Temperly, B.N. (1977). Detailed structures in the Transvaal System. In: Jansen, H. (1977). *The geology of the country around Pretoria.* Geol. Surv. expl. sheet 2527DA, DB, DC, DD and 2528 CA, CB, CC, CD.

Therriault, A.M., Reimold, W.U., and Reid, A.M. (1995). The Vredefort Granophyre and the Vredefort Impact Structure. *Extended Abstracts, Geocongress '95, Geol. Soc. S. Afr.*: 589-592.

Thomas, R.J. (1989). A tale of two tectonic terranes. *S. Afr. J. Geol.* 92 (4): 301-305.

Thomas, R.J., Eglington, B.M., and Bowring, S.A. (1993). Dating the cessation of Kibaran magmatism in Natal, South Africa. *J. Afr. Ea. Sci.* 16: 247-252

Thomas, R.J., Walraven, F., and Eglington, B.M. (1995). Zircon evaporation geochronology of granitoids from southern Natal, South Africa. *Extended Abstracts, Geocongress '95, S. Afr. Geol. Soc.* 418-421.

Trieloff, M., Reimold, W.U., Kunz, J., Boer, R.H., and Jessenberger, E.K. (1994). ^{40}Ar-^{39}Ar thermochronology of pseudotachylite at the Ventersdorp Contact Reef, Witwatersrand basin. *S. Afr. J. Geol.* 97 (3): 365-384.

Tweedie, E.B. (1986). The Evander goldfield. In: C.R. Annhaeusser and S. Maske (eds.). *Mineral Deposits of Southern Africa*: 705-730.

Uken, R. and Watkeys, M.K. (1994). Deformation, timing and emplacement mechanisms for the eastern Bushveld Complex. *Tecs. Div. Geol. Soc. S. Afr.*

Uken, R. and Watkeys, M.K. (1995). Structural processes in a low pressure, high temperature contact metamorphic terrane. *Extended Abstracts, Geocongress 1995, Geol. Soc. S. Afr.*: 688-692.

Vermaak, C.F. (1970). *The geology of the lower portion of the Bushveld Complex and its relationships to the floor rocks in the area west of the Pilanesberg, western Transvaal.* Spec. Publ. 1. Geol Soc. S. Afr: 242-265.

Vernon, R.H. (1977). Relationships between microstructures and metamorphic assemblages. *Tectonophys.* 39: 439-452.

Vernon, R.H. (1978). Porphyroblast-matrix microstructural relationships in deformed metamorphic rocks. *Geol. Rundschau* 67: 288-304.

Vernon, R.H. (1989). Porphyroblast-matrix microstructural relationships: recent approaches and problems. In: Daly, J.S., Cliff, R.A., and Yardley, B.W.D. (Eds.), *Evolution of metamorphic belts.* Spec. Publ. Geol. Soc., 43, 83-102.

Visser, J.N.J. (1969). *n Sedimentologiese studie van die Serie Pretoria in die Transvaal.* D.Sc. thesis (unpubl.), Univ. O.F.S., Bloemfontein.

Visser, D.J.L., Coertzee, F.J., Walraven, F., Hammerbeck, E.C.I., Martini, E.C.I. and Kleywecht, R.J. (1984). *Explanation of the 1:1 000 000 geological map, fourth edition.* Geol. Surv. 491pp.

Wallmach, T. and Meyer, F.M. (1990). A petrogenetic grid for metamorphosed aluminous Witwatersrand shales. *S.Afr. J. Geol.* 93: 93-102.

Wallmach, T. Hatton, C.J. and Droop, G.T.R. (1989). Extreme facies of contact metamorphism developed in calc-silicate xenoliths in the Eastern Bushveld Complex. *Canadian Mineralogist* 27: 509-523.

Walraven, F. (1974). Tectonism during the emplacement of the Bushveld Complex and the resulting fold structures. *Trans. Geol. Soc. S. Afr.* 77: 323-328.

Walraven, F. (1981). *Geology of the Rustenburg area.* Geol. Surv. Expl: Sheet 2526.

Walraven, F. (1995, in press) Geochronology of the Rooiberg Group, Transvaal Supergroup, South Africa. Accepted for publication in *Chem. Geol.*

Walraven, F. and Darracott, D.W. (1976). Quantitative interpretation of a gravity profile across the western Bushveld Complex. *Trans. Geol. Soc. S. Afr.* 79: 22-26.

Walraven, F. and Hattingh, H. (1993). Geochronology of the Nebo Granite, Bushveld Complex. *S. Afr. J. Geol.* 96: 31-41.

Walraven, F., Armstrong, R.A., and Kruger, F.J. (1990). A chronostratigraphic framework for the north-central Kaapvaal Craton, the Bushveld Complex, and the Vredefort structure. *Tectonophys.* 171: 23-48.

Wang, G., Banno, S, and Takeuchi, K. (1986). Reactions to define the biotite isograd in the Ryoke metamorphic belt, Kii Peninsula, Japan. *Contrib. Min. Pet.* 93: 9-17.

Watkeys, M.K. (1983). *Brief explanatory notes on the provisional geological map of the Limpopo Belt and environs.* Spec. Publ. 8. Geol. Soc. S. Afr.: 5-8.

Whitten, D.G.A., and Brookes, J.R.V. (1979). *The Penguin Dictionary of Geology.* Penguin Books. 495pp.

Willemse, J. (1959). The "floor" of the Bushveld Complex and its relationships, with special reference to the eastern Transvaal. *Proc. Geol. Soc. S. Afr.* 58: 21-74.

Winkler, H.G.F. (1979). *Petrogenesis of metamorphic rocks* (5th ed.). Springer-Verlag, New York. 348 pp.

Winter, H. de la R. (1987). A cratonic foreland model for Witwatersrand Basin development in a continental back-arc, plate-tectonic setting. *S. Afr. J. Geol.* 90 (4): 409-427.

Yardley, B.W.D. (1974). Porphyroblasts and "crystallization force": discussion of some theoretical considerations. *Geol. Soc. Am. Bull.* 85: 61-62.

Yardley, B.W.D., Mac Kenzie, W.S., and Guilford, C. (1990). *Atlas of metamorphic rocks and their textures*. Longman Gp. U.K. Ltd. 120 pp.

Zwart, H.J. (1962). On the determination of polymetamorphic mineral associations, and its application to the Bosost area (Central Pyrenees). *Geol. Rundschau*. 52: 38-65.

Appendix 1

The localities are represented by the co-ordinates appearing on the 1:10 000 orthophotographs and indicated on the enclosures (Maps 1 and 2). Longitude appears first, followed by latitude, e.g. (2855,5 X; -91,0 Y). The numerals following the comma refer to further subdivisions of the co-ordinate grid.

Appendix 2
Major element compositions of the sills in the study area. Average composition derived from these analyses is presented in Table 2.2.

	S20	S18	S11	S19	S21bx	S23	S12
SiO2	52,89	52,55	58,18	57,15	55,86	38,87	49,36
TiO2	1,77	0,83	1,87	1,36	0,97	1,85	2,21
Al2O3	12,84	14,32	14,38	10,64	13,61	16,33	9,94
Fe2O3	12,46	10,43	10,18	10.95	10,02	10,77	17,41
FeO							
MnO	0,12	0,17	0,05	0,16	0,15	0,11	0,17
MgO	3,49	6,53	5,83	6,65	5,04	20,78	6,00
CaO	4,71	8,17	0,49	7,19	6,42	1,80	6,85
Na2O	4,70	2,04	2,41	2,71	2,31	0,00	3,94
K2O	0,35	2,55	0,82	0,51	2,89	0,33	1,08
P2O5	0,33	0,11	0,22	0,17	0,19	0,31	0,21
L.O.I	5,27	1,36	4,47	1,59	1,60	9,01	1,54
Total	98,73	99,06	98,90	99,08	98,99	100,16	98,71

	S25	S6	S17	S7	S26	S22	S21b
SiO2	52,118	53,69	56,15	51,83	49,85	50,69	55,69
TiO2	2,14	1,91	1,32	1,78	1,23	1,07	0,93
Al2O3	11,48	11,39	11,06	12,33	9,97	14,64	13,66
Fe2O3	16,28	15,08	10,96	12,24	9,64	12,31	10,03
FeO							
MnO	0,19	0,18	0,16	0,13	0,15	0,19	0,15
MgO	4,71	5,19	6,15	3,55	6,08	6,53	5,05
CaO	4,80	5,89	6,78	5,65	6,99	10,55	6,35
Na2O	4,26	6,06	2,53	4,36	5,86	1,66	2,28
K2O	1,19	1,14	1,78	0,33	1,57	0,71	2,85
P2O5	0,27	0,25	0,17	0,32	0,15	0,18	0,10
L.O.I	1,15	1,10	1,60	6,28	8,95	0,62	1,65
Total	98,588	102,88	98,66	98,80	100,44	99,15	98,74

Appendix 3
Principle axes (X, Y, Z) of strained ooids for strain analysis, Section 3.3.3.

Locality A

X	Y	Z
2.45	2.20	1.56
2.70	1.90	1.31
2.55	2.10	1.53
2.45	1.93	1.51
2.62	2.05	1.49
2.63	1.99	1.51
2.70	2.06	1.58
2.45	2.05	1.59
2.68	2.16	1.65
2.47	2.00	1.62
2.64	2.04	1.63
2.60	2.01	1.58
2.56	2.06	1.50
2.60	2.05	1.52
2.65	2.15	1.50
2.49	1.95	1.51
2.52	2.09	1.53
2.62	2.11	1.61
2.53	2.10	1.57
2.47	2.07	1.68
2.70	1.95	1.60
2.57	2.19	1.59
2.56	2.09	1.60
2.53	1.99	1.62
2.49	2.06	1.59
2.66	2.08	1.57

Locality B

X	Y	Z
2.26	1.68	1.16
2.16	1.73	1.16
2.00	1.70	1.16
2.06	1.83	1.23
2.08	1.81	1.28
2.11	1.76	1.26
2.07	1.67	1.26
2.08	1.84	1.18
2.17	1.63	1.20
2.16	1.69	1.23
2.08	1.80	1.19
2.10	1.81	1.15
2.14	1.68	1.28
2.18	1.88	1.28
2.05	1.77	1.19
2.10	1.86	1.14
2.12	1.79	1.20
2.13	1.75	1.24
2.18	1.68	1.30
2.06	1.83	1.18
2.12	1.79	1.25
2.05	1.73	1.17
2.03	1.77	1.20
2.13	1.79	1.21
2.10	1.68	1.18
2.08	1.70	1.17

Locality C

X	Y	Z
1.59	1.50	0.80
1.52	1.31	0.70
1.55	1.42	0.77
1.51	1.39	0.66
1.57	1.49	0.75
1.53	1.41	0.67
1.59	1.43	0.71
1.51	1.45	0.68
1.55	1.38	0.71
1.63	1.47	0.75
1.59	1.39	0.77
1.61	1.32	0.71
1.55	1.30	0.65
1.54	1.39	0.60
1.60	1.40	0.69
1.52	1.50	0.71
1.61	1.37	0.73
1.61	1.39	0.72
1.68	1.41	0.65
1.66	1.40	0.70
1.67	1.50	0.69
1.70	1.45	0.73
1.65	1.29	0.69
1.67	1.48	0.75
1.63	1.47	0.70
1.55	1.44	0.74


LOCALITY MAP SHOWING THE POSITION OF MAP 1
Pretoria
627
MAP 2
MAP 1
Hennops R.
Crocodile R.
5 km
25°55'
25°50'
28°00'
2858X
2859X
2860X
2861X
2862X
2863X
2864X
HENNOPS RIVER
CROCODILE RIVER
A
B
1362.7
1422.4
N
S
1400m
1200m
SECTION AB
horizontal scale = vertical scale 1:10 000
-93Y
-94Y
-95Y
-96Y
-97Y
-98Y
Map 1: Geolgical Map of a portion of the Kareebosrand Conservancy
Explanation
DOLERITE DYKE
SYENITE DYKE
SILL
DOLOMITE
MARKERS
CCDM
DCM
CDM
SCB
CCM
SLATE
QUARTZITE
LINEATION AZIMUTH AND PLUNGE
BEDDING STRIKE AND DIP
CLEAVAGE STRIKE AND DIP
D_2 SHEAR ZONE
D_2 SHEAR ZONE STRIKE AND DIP
D_3 SHEAR ZONE
D_3 SHEAR ZONE STRIKE AND DIP
FAULT
INFERRED FAULT
D_2 FOLD HINGE
D_3 FOLD HINGE
LITHOLOGICAL BOUNDARY
INFERRED LITHOLOGICAL BOUNDARY
PHOTOLINEAMENT
TRIG. BEACON
SCALE 1:10 000
0 200 400 600 800 1000
metres
COMPILED AND DRAUGHTED BY P.M. COURTNAGE

Map 2: Geological Map of the Pelindaba area

Explanation

- UNCONSOLIDATED SEDIMENTS
- TUFA
- DYKE
- MASSIVE CHERT BRECCIA
- Fe RICH BRECCIA
- QUARTZITE
- SLATE
- CHERT MARKER
- DOLOMITE
- LINEATION AZIMUTH AND PLUNGE
- BEDDING STRIKE AND DIP
- CLEAVAGE STRIKE AND DIP
- D_2 SHEAR ZONE
- D_2 SHEAR ZONE STRIKE AND DIP
- FAULT
- INFERRED FAULT
- FOLD HINGE
- LITHOLOGICAL BOUNDARY
- INFERRED LITHOLOGICAL BOUNDARY
- PHOTOLINEAMENT
- TRIG. BEACON 1433

SCALE 1:10 000

0 200 400 600 800 1000 metres

LOCALITY MAP SHOWING THE POSITION OF MAP 2

Pretoria

Map 2

Map 1

Crocodile R.

Hennops R.

5 km

SECTION A–B

horizontal scale: vertical scale = 1:10 000

1400 m

1200 m

COMPILED AND DRAUGHTED BY P.M. COURTNAGE

Author: Courtnage Paul Michael.
Name of thesis: Post-Transvaal deformation between the Johannesburg dome and the Bushveld complex.

PUBLISHER:
University of the Witwatersrand, Johannesburg
©2015

LEGALNOTICES:

Copyright Notice: All materials on the University of the Witwatersrand, Johannesburg Library website are protected by South African copyright law and may not be distributed, transmitted, displayed or otherwise published in any format, without the prior written permission of the copyright owner.

Disclaimer and Terms of Use: Provided that you maintain all copyright and other notices contained therein, you may download material (one machine readable copy and one print copy per page)for your personal and/or educational non-commercial use only.

The University of the Witwatersrand, Johannesburg, is not responsible for any errors or omissions and excludes any and all liability for any errors in or omissions from the information on the Library website.